UNIVERSITY OF LIVERPOOL

Culture Conditions Govern Mouse Embryonic Stem Cell Behaviour: Dependence on Heparan Sulfate and Optimisation of Synthetic Polymer Substrates

Thesis submitted in accordance with the requirements of the University of Liverpool for the degree of Doctor in Philosophy.

By

Chloe Jayne Williams

May 2013

For Mum, Dad, Ant and Matt

Acknowledgements

First I would like to thank my supervisors Prof. Jerry Turnbull, Dr. Patricia Murray and Prof. David Edgar for their support, motivation and patient guidance throughout. I feel extremely lucky to have had Jerry as my primary supervisor; at times when I felt like my only option was to give up, his kind words, compassion and encouragement kept me going – a brilliant role model.

Special thanks go to fellow students and staff at The University of Liverpool and specifically to all members of Lab B, past and present, for their technical know-how, especially Dr. Sophie Thompson and Dr. Scott Guimond. I accredit Sophie with keeping me sane as we regularly discussed the latest Eastenders storyline, and re-lived our teenage youth through Radio One's golden years in the hope of forgetting the frustrating lab problems!

Many thanks also go to the CASE partners SpheriTech Ltd, specifically Don Wellings and Andy Gallagher, not only for providing us with novel polymers but for their input regarding materials and methods for chapter 5. Dr. Victoria Kearns and Prof. Rachel Williams of the Clinical Engineering department at the University of Liverpool provided invaluable advice regarding materials analysis.

On a personal level, I would like to thank my mum, an inspiration to whom I owe my hardworking ethos. Selflessly, mum would listen to me ramble about my latest experiments during coffee breaks (sometimes cake if we were in non-diet mode!). Thanks go to my younger brother Matt (equally as inspirational as he completes his GCSEs at this time) for repeatedly asking those basic questions that could so easily have been lost; 'what is a stem cell? Where do they come from? Why are they so important?' My dad and brother Ant unfortunately can't read this thesis or witness my graduation, but I hope I have made them

both proud. I look back fondly on their constant Dr. jokes and light-hearted, unique sense of humour that so importantly kept me smiling.

Special thanks too, go to Alex. She constantly provided me with personal support, encouragement and laughs; a hug when I needed one and a kick-up the a** when I lost sight of the finish. Black coffee seemed in endless supply, and I hope one day I can repay the favour.

Finally, I would like to thank the BBSRC for the financial support and likewise, my CASE partner SpheriTech Ltd.

Contents

1. Introduction 14
1.1 Embryonic Stem Cells 14
1.1.1 Origins of ESCs 14
1.1.2. Early embryonic development 16
1.1.2 Human ESCs (hESCs) and mouse ESCs (mESCs) 17
1.1.3 ESC pluripotency 18
1.1.4 *In vitro* expansion of mESCs (maintenance of pluripotency) 23
1.1.5 Embryoid Body (EB) 24
1.1.7 Lineage commitment of mESCs 25
1.2 Heparan Sulfate 37
1.2.1 Glycosaminoglycans (GAGs) 37
1.2.2 HS structure 38
1.2.3 HS Biosynthesis 39
1.2.4 Core proteins 42
1.2.5 Heparin: a close relative of HS 44
1.3 Heparan sulfate in development 45
1.3.1 Early embryonic development 45
1.3.2 HS-protein interactions 46
1.4 Biomaterials 54
1.4.1 Overview of biomaterials 54
1.4.2. Optimising polymer surfaces to enhance polymer-cell interaction 60
1.5 Work leading to current studies 61
2. Materials and Methods 62
2.1 Materials 62
2.1.1 Solutions 62
2.1.2 Buffers 63
2.1.3 Cell lines 63
2.1.4 Biomaterials 64
2.2 Methods 65
2.2.1 Cell Culture 65
2.2.2 Immunochemistry and histology 71
2.2.3 Real Time Polymerase Chain Reaction 75
2.2.4 Compositional disaccharide analysis of HS 77
2.2.5 Sample (polymer) preparation for SEM analysis 81

2.2.6 Statistical Analysis 83
3. Variations in mESC culture condition influences behavior 84
3.1 General Introduction 84
3.2 mESCs maintained in the absence of feeders and/or serum, remain undifferentiated and display typical behaviour during 2D culture 86
3.3 mESC development in the EB model is dependent upon 2D culture conditions prior to EB formation 91
3.3.1 EB characterisitcs including morphology, size and cavitation all differ depending on 2D mESC culture conditions 91
3.3.2 mESC differentiation capacity is impaired in EBs generated from serum-free feeder-free conditions 97
3.3.3 Differentiation of extraembryonic endoderm and BM formation within EBs is influenced by mESC pre-culture conditions 101
3.4 Differentiation of mesendoderm and ectoderm within EBs is influenced by mESC pre-culture conditions 110
3.5 Discussion 113
4. Heparan Sulfate is crucial for normal mESC behaviour 125
4.1 General Introduction 125
4.2. Defective EB development attributed to a lack of serum, can be rescued with exogenous porcine mucosal heparin (PMH) 130
4.3 HS-deficient $EXT1^{-/-}$ mESCs require serum and feeders for normal behaviour 136
4.3.1 HS-deficient mESCs cannot be maintained in the absence of serum during 2D expansion 136
4.3.2 HS-deficient EBs do not display characteristic morphological development 141
4.3.3 HS-deficient EBs show restricted EEE differentiation 146
4.4 HS structure and abundance differs depending on mESC culture conditions 154
4.4.1 mESC culture condition influences the structure of cell-surface HS 155
4.4.2 Culture conditions influences the structure of HS synthesised by mESCs 159
4.4.3 Levels of HS biosynthetic enzyme expression in E14 mESCs differs depending on culture condition 167
4.5 Discussion 171
5. Optimisation of polymers for the expansion of mESCs and KSCs *in vitro* 179
5.1 General Introduction 179
5.2 Hydrogels for cell attachment or viability 188
5.3 Poly-Ɛ-lysine based polymers support mESC viability and self renewal 198
5.4. Growth of kidney stem cells on poly-Ɛ-lysine 203
5.4.1. Poly-Ɛ-lysine-based polymers +/- RGD support KSCs-GFP 203
5.5 Poly-Ɛ-lysine-based polymers modified with HS analogues 208

5.6 Discussion 216
6. General Discussion and Future Directions 224
References 234
Appendices 264

Table of Figures

1.1. Early embryonic development 16
1.2. mESC pluripotency 19
1.3. EB development 26
1.4. Laminin 33
1.5. GAG repeating unit 38
1.6. HS biosynthesis. 40
Table 1.1 HS biosynthetic enzymes and their respective roles 41
1.7 HS master regulator ..... **Error! Bookmark not defined.**
Table 1.2 Classifications of biomaterials 55
Figure 1.8. Polystyrene application in cell culture. 58
Table 1.3 Uses of common polymers in medical applications and corresponding monomers 59
Table 2.1 Synthetic SpheriTech hydrogels and corresponding compositional ratios. 64
Figure 2.1 Schematic outlining the three distinct 2D culture conditions employed during E14 mESC expansion 66
Figure 2.2 Schematic diagram depicting the trans-well set-up 70
Table 2.4 HS compounds adsorbed to surface of poly-Ɛ-lysine macroporous. 71
Figure 2.3 Diagram outlining the quantification of a Nanog immunostain. 75
Figure 2.4 Diagram outlining the quantification of differentiating EBs with regard to laminin expression. 75
Table 2.5 Heparitinase enzymes for HS digestion to aid disaccharide analysis 79
Table 2.6 Order of disaccharide standards elution during HPLC-SAX analysis with time 81
Figure 2.6 Schematic of CPD set-up. 82
Figure 3.1. E14 mESC display typical morphology in the absence of feeders and/or FBS. 88
Figure 3.2 E14 mESCs express Oct4 and Nanog in the absence of feeders and/or FBS. 89
Figure 3.3 The proportion of Oct4 and Nanog positive E14 mESCs was comparable in all three culture conditions. 89
Figure 3.4 E14 mESC proliferation rate is dependent on culture condition. 90
Figure 3.5 Serum-free feeder-free EBs are significantly smaller than EBs derived from mESCs cultured with serum +/- feeders.. 93
Figure 3.6 Serum-free EBs are smaller than EBs conditioned with serum. 93
Figure 3.7 E14 mESCs EB development and morphology is different and dependent on 2D growth conditions prior to EB formation. 94
Figure 3.8 EB development is influenced by 2D growth conditions prior to EB formation. 96
Figure 3.9 Percentage of Oct4+ and Nanog+ cells within 7d EBs depends on prior 2D culture conditions.. 98
Figure 3.10 Localisation of Oct4 positive mESCs EBs changes with different mESC culture conditions. .. 99
Figure 3.11 *Oct4* mRNA levels are significantly higher for serum-free feeder-free conditioned day 7 EBs.. 99
Figure 3.12 Localisation of Nanog differs depending on culture condition.. 100
Figure 3.14 *Gata6* mRNA levels differ depending on culture condition. 104
Figure 3.13 Gata6 positive cell numbers vary depending on culture condition. 104
Figure 3.15 Primitive endoderm marker, AFP levels vary depending on culture condition.. 105
Figure 3.16 *AFP* mRNA levels do not change between conditions. 105
Figure 3.17 2D mESC culture conditions affect laminin distribution in EBs. 106
Figure 3.18 2D ESC culture conditions affect laminin distribution in EBs. 107
Figure 3.20 *LamA1* expression levels differ depending on culture conditions.. 109
Figure 3.21 Levels of nascent mesoderm marker, *Bry* are significantly different for day 7 EBs depending on 2D culture conditions. 112
Figure 3.22 Levels of paraxial mesoderm makers *Foxc1* and *Tbx6* in day 7 EBs significantly differ depending on 2D culture pre-condition. 112
Figure 3.23 Levels of early ectoderm marker, *Pax6* are significantly different between culture conditions. 112

Table 3 Summary of 2D culture conditions prior to EB formation and the effects they have on subsequent EB development. 115
Figure 4.1 Exogenous PMH affects the distribution of Oct4 positive cells within EBs. 131
Figure 4.2 Exogenous PMH induces Gata6 expression in peripheral EB cells.. 132
Figure 4.3 Effect of exogenous PMH on laminin expression. 134
Figure 4.4 Exogenous PMH was shown to rescue a typical EB differentiation marker pattern expression in 7 day serum-free conditioned EBs. [..... 135
Figure 4.5 HS-deficient EXT1$^{-/-}$ mESC expansion was not supported in serum-free and feeder-free 2D culture conditions.. 138
Figure 4.6 HS-deficient EXT1$^{-/-}$ mESC maintained in serum-free 2D conditions are not viable by 48 h. 139
Figure 4.7 Oct4 and Nanog expression in HS-deficient EXT1$^{-/-}$ mESCs cultured in the presence or absence of feeder cells.. 139
Figure 4.8 The percentage of Nanog positive mESCs is higher in HS-deficient EXT1$^{-/-}$ mESCs compared to E14 mESCs but only in the absence of feeders. 140
Figure 4.9 HS-deficient EBs are significantly smaller compared to E14 EBs. 142
Figure 4.10 HS-deficient EXT1$^{-/-}$ EBs display some signs of normal development but lack cavitation, despite culture condition. 143
Figure 4.11 HS-deficient EBS lack cavitation and a complete BM. 145
Figure 4.12 The distribution of Oct4 positive cells is more extensive throughout HS-deficient EBs compared to E14 EBs and a lack of feeders enhances this effect. 148
Figure 4.13 The percentage of Oct4 positive cells within HS-deficient EBs is higher than in E14 EBs. 149
Figure 4.14 *Oct4* expression in day 7 EBs is significantly higher in HS-deficient EXT1$^{-/-}$ EBs compared to E14 EBs. 149
Figure 4.15 HS-deficient EBs display abnormal localisation of Gata6 positive cells. 150
Figure 4.16 HS-deficient EBs display significantly lower Gata6+ cells in day 7 EBs compared to E14 EBs.. 150
Figure 4.17 Laminin is abnormally localised in HS-deficient EBs. 151
Figure 4.18 Abnormal intracellular LamA1 expression in HS-deficient EBs. 152
Figure 4.19 HS-deficient EBs display significantly lower LamA1 expression compared to day 7 E14 EBs derived from the same culture conditions. 153
Figure 4.20 Expression of 10E4 HS epitope was detected in all three conditions but localisation differed and primary expression was by feeder cells. 156
Figure 4.21 Levels of HSPGs on the surface of mESCs, identified by an antibody specific to the 3G10 HS-epitope, differed in three different culture conditions.. 157
Figure 4.22 10E4 and 3G10 epitope expression levels and localisation differs depending on the mESC culture condition. 158
Figure 4.23 Quantitation of HS detected from equal volumes of starting material demonstrates differences in HS levels depending on source or culture condition. 161
Figure 4.25 HPLC-SAX analysis of soluble HS purified from media components, Advanced DMEM and serum (FBS), demonstrates the abundance of HS and disaccharide compositional make-up. 163
Table 4.1 HPLC-SAX analysis demonstrated differences in soluble HS purified from conditioned media, from different culture conditions. 165
Figure 4.27 EBs generated from mESCs cultured in the absence of serum express higher levels of *EXT2* than EBs generated from mESCs cultured in the presence of serum. 168
Figure 4.28 Levels of the HS biosynthetic enzyme *NDST1* are significantly different depending on mESC 2D culture condition. 169
Figure 4.29 Levels of the HS modification sulfatase enzyme *Sulf1* are different depending on mESC culture condition but *Sulf2* levels are unchanged. 170
Table 5.1 Outlining some common hydrogels successfully employed as biomaterials 183
Figure 5.1 Poly-E-lysine polymer, showing the monomer subunit, n = 25 - 30. 184
Table 5.2 Ratios of hydrogel components. 189
Figure 5.2 Methacrylic-based hydrogels 1, 3 and 5 do not support fibroblast attachment or proliferation. 192

Figure 5.3 Methacrylic-based hydrogels 6, 15 and 16 do not support fibroblast attachment or proliferation. 193
Figure 5.4 Acrylic-based hydrogels 7, 9 and 11 display little evidence of supporting fibroblast attachment and spread..... 194
Figure 5.5 Acrylic-based hydrogels 12, 13 and 14 display little evidence of supporting fibroblast attachment and spread..... 195
Figure 5.6 Fibroblast morphology varies according to ability to spread. STO fibroblasts were seeded onto two different control conditions, one to encourage cell attachment and spread (fibronectin-coated cover slip) and another to discourage cell attachment (uncoated glass cover slip). Cell morphology was assessed accordingly, 48 h post seeding. 196
Figure 5.7 Fibroblast viability was completely lost in all but three hydrogels. 197
Figure 5.8 mESCs seeded onto poly-Ɛ-lysine polymers, attach, proliferate and retain alkaline phosphatase expression up to 10 days.. 200
Figure 5.9 E14 mESCs maintain Nanog expression when seeded onto poly-Ɛ-lysine-based macroporous polymers and topography of polymer directs location of mESCs. 201
Figure 5.10 Poly-Ɛ-lysine topography and architecture. 202
Figure 5.11 Poly-Ɛ-lysine macroporous polymers (+/- RGD) support KSCs-GFP attachment and proliferation up to 10 days..... 205
Figure 5.12 Synthetic poly-Ɛ-lysine coupled with RGD, supports KSCs-GFP proliferation at a higher rate than poly-Ɛ-lysine not coupled with RGD. 206
Figure 5.13 KSCs-GFP populate the pores of the poly-Ɛ-lysine or on the surface of the spheres, and fibroblast-like processes appear to be lost compared to standard tissue culture plastic. 207
Figure 5.14 Tissue culture plastic coated with per-sulfated heparin, outperforms other heparin analogue coatings, in supporting KSC-GFP attachment and spreading..... 209
Figure 5.15 PMH and per-sulfated heparin structures absorbed to the surface of tissue culture plastic best support KSC-GFP proliferation compared to tissue culture plastic coated with 6-O and 2-O desulfated heparin or NAc heparin structures. 212
Figure 5.16 Surface topography of poly-Ɛ-lysine macroporous polymers is affected by coating with different HS-mimetic structures. 213
Figure 5.17 KSC-GFP proliferation on poly-Ɛ-lysine macroporous polymers altered depending on heparin structure.. 214
Figure 5.18 KSC-GFP-polymer interaction alters depending on the level/pattern of sulfation exhibited by the coating material; per-sulfated heparin-coated polymers support elongated KSC-GFP morphology.. 215

Abstract

Human embryonic stem cell (hESC)-based therapies will only become viable once we eliminate the use of animal-derived material during ESC scale-up. Some groups have demonstrated the expansion of hESCs in xeno-free systems but the effect on downstream self-renewal and differentiation is poorly understood. Heparan sulfate (HS) is a master regulator of cellular behavior but the role of HS during ESC expansion is unclear, as is the exogenous source of HS in cultures. It has been shown that mESCs synthesise low levels of low-sulfated HS, but it is unclear if culture condition has any impact.

In the studies here, three discrete culture conditions were employed for E14 mESC expansion along with immunostaining and RT-qPCR to study marker expression for differentiation to the three lineages and corresponding BM synthesis. SAX-HPLC was used to characterise soluble HS from cells/medium/serum. A varierty of polymers were tested as synthetic alternatives for ESC expansion.

It was found that HS-deficient embryoid bodies (EBs) (derived from $EXT1^{-/-}$ mESCs in normal culture conditions) remained in a pluripotent state and lacked a typical differentiation pattern. Furthermore, HS-deficient mESCs could not be maintained in the absence of serum, highlighting a link between serum and HS. EBs derived from E14 mESCs cultured in the absence of serum displayed unusual differentiation patterns, which were rescued by exogenous porcine mucosal heparin (PMH). Feeder cells displayed cell-surface HS but feeder-cell conditioned medium (CM) was predominantly an unsulfated structure. An array of low and highly sulfated HS structures were identified in serum-alone. 10-fold more HS was purified from serum-free feeder-free (-F –FBS) CM compared to the other mESC CM (with/without feeders but in the presence of serum; +/-F +FBS). Furthermore, unlike +/-F +FBS conditions, highly sulfated HS disaccharide UA2S–GlcNS6S was the major constituent in –F-FBS and *Sulf2* levels were significantly reduced. Poly-Ɛ-lysine macroporous substrates supported mESC and kidney-derived stem cells (KSCs-GFP) adherence and proliferation, further enhanced by adsorbing RGD or per-sulfated HS structures to the surface of the poly-Ɛ-lysine.

The key conclusions from these studies were that serum is a source of HS, without which, mESCs behave uncharacteristically; that synthetic HS-mimetic structures could represent an alternative to serum; and poly-Ɛ-lysine shows great promise to replace current animal-derived coating materials for ESC expansion.

Abbreviations

Adv DMEM	Advance Dulbecco's Modified Eagle Medium
BM	Basement membrane
BMP	Bone morphogenic protein
BODIPY	Boron-dipyrromethene
Bry	Brachyury
cDNA	Complimentary deoxyribonucleic acid
CEE	Columnar epiblast epithelium
CM	Conditioned media
CNS	Central nervous system
DAPI	4',6-diamidino-2-phenylindole
DMEM	Dulbecco's Modified Eagle Medium
DNA	Deoxyribonucleic acid
DNAse	Deoxyribonucleic acid enzyme
EB	Embryoid body
EC	Embryonic carcinoma
ECM	Extracellular matrix
EDTA	Ethylenediaminetetraacetic acid
EEE	Extraembryonic endoderm
EG	Embryonic germ
EMT	Epithelia-mesechymal transition
ESC	Embryonic stem cell
EXT1	Exostosin-1
EXT2	Exostosin-2
F	Feeder layer
FBS	Fetal bovine serum
FGF	Fibroblast growth factor
GAPDH	Glyceraldehyde-3-phosphate dehydrogenase
GAG	Glycosaminoglycan
HPLC	High performance liquid chromatography
HS	Heparan sulfate
HS2OST	Heparan sulfate 2-O Sulfatransferase
ICM	Inner cell mass

Klf	Kruppel-like factor
LIF	Leukaemia inhibitory factor
LIFR	Leukaemia inhibitory factor receptor
Min	Minutes
NA	N-Acetyl
NDST	N-Decetyl Sulftransferase
NS	N-Sulfatase
PBS	Phosphate buffered saline
PCR	Polymerase chain reaction
PE	Primitive endoderm
PƐL	Poly-Ɛ-lysine
PFA	Paraformaldehyde
PGC	Primordial germ cell
PMH	Porcine muscosal heparin
PMHS	Porcine mucosal heparan sulfate
Rpm	Revolutions per minute
RT	Room temperature
RT-qPCR	Real-time quantitative polymerase chain reaction
RNA	Ribonucleic acid
SAX	Strong anion exchange
SEM	Secondary electron microscopy
SSEA	Stage-specific embryonic antigen
STAT	Signal transducer and activator of transcription
Su1f1	Sulfatase enzyme 1
Sulf2	Sulfatase enzyme 2
TLC	Thin film liquid chromatography

1. Introduction

1.1 Embryonic Stem Cells

Embryonic stem cells are pluripotent cells that can differentiate to become any cell type whilst maintaining the ability to replicate indefinitely. As a result, embryonic stem cells have massive potential in medicine, both therapeutically in repairing damaged/diseased tissue, for example, in Parkinson's disease or diabetes, and for implementation in drug screening. However, before stem cell-based therapies can be developed or employed clinically, it is necessary to understand how embryonic stem cells are regulated, both in maintenance of their pluripotency and direction of their differentiation.

1.1.1 Origins of ESCs

Since 1970, four different classes of pluripotent cells have been isolated; embryonic stem cells (ESCs), embryonic germ (EG) and epiblast stem cells (EpiSCs) from the embryo, and embryonic carcinoma (EC) cells isolated from adults. All three have the capacity for self-renewal and differentiation but discrete differences underpin their respective therapeutic potential.

Embryonic stem cells (ESCs)

Embryonic stem cells (ESCs) are derived from the inner cell mass (ICM) of a pre-implanted blastocyst (Evans and Kaufman 1981; Martin 1981) and represent pluripotent cells with the ability to replicate indefinitely in an undifferentiated state, whilst maintaining the ability to give rise to all cell lineages once stimulated correctly, such is the ability of ESCs to generate high cell numbers.

Embryonic germ (EG) cells

Embryonic germ (EG) cells are derived from primordial germ cells (PGC) of the post-implanted embryo, destined to form eggs or sperm. In the human, EG cells can be isolated from the gonadal ridge of the fetus post-fertilisation (5 – 10 week), analogous to derivation

from PGCs in the mouse embryo at 8.5 day post-coitum (Labosky, Barlow et al. 1994; Donovan and de Miguel 2003).

Epiblast Stem Cells (EpiSCs)

Epiblast-derived stem cells (EpiSCs) are derived from the very early (pre-implanted blastocyst stage) embryo but pre-gastrulation.

Embryonal carcinoma (EC) cells

A teratoma represents an encapsulated tumour composed of various tissues foreign to their site of origin, of which there are two classifications; malignant and benign. Benign teratomas have limited growth ability and are represented by well-differentiated somatic tissues. Malignant teratomas (t*eratocarcinomas)* in contrast, contain undifferentiated stem cells with an unlimited proliferative ability and tendency to metastasize. Teratocarcinomas, first formed experimentally in adult mice by grafts of early mouse embryonic tissues, represent the origin of EC cells. Most EC cell lines, despite retaining some capacity to differentiate, display poor differentiation *in vivo* and typically form tumours (Stevens 1970; Damjanov, Damjanov et al. 1987).

Consequently, EC cells do not present much potential in any clinical capacity, largely owing to their tumourigenic nature. Furthermore, EC cells are aneuploid and cannot proceed through meiosis to produce mature gametes, unlike ESCs which stably retain euploid chromosome constitution, crucial for meiosis and underpins genetic manipulation technology. Although EG cells form chimeras following injection into the blastocyst and give rise to the three germ layers (Stewart, Gadi et al. 1994), their genomic imprint can be erased, therefore negating the ability to employ them as therapeutic agents (Smith 2001). Subsequently, ESCs represent the class of embryonic stem cell isolated from the embryo with real potential.

1.1.2. Early embryonic development

ESCs, owing to their defining pluripotent characteristic, theoretically can mimic *in vivo* development in an *in vitro* model. Embryonic development is a complex, highly sequential process whereby the zygote diversifies into every cell type, as a consequence of differentiation, proliferation and growth, which begins with cleavage (mitotic divisions after fertilisation) and gastrulation (polarisation of the embryo), outlined in Figure. 1.1.

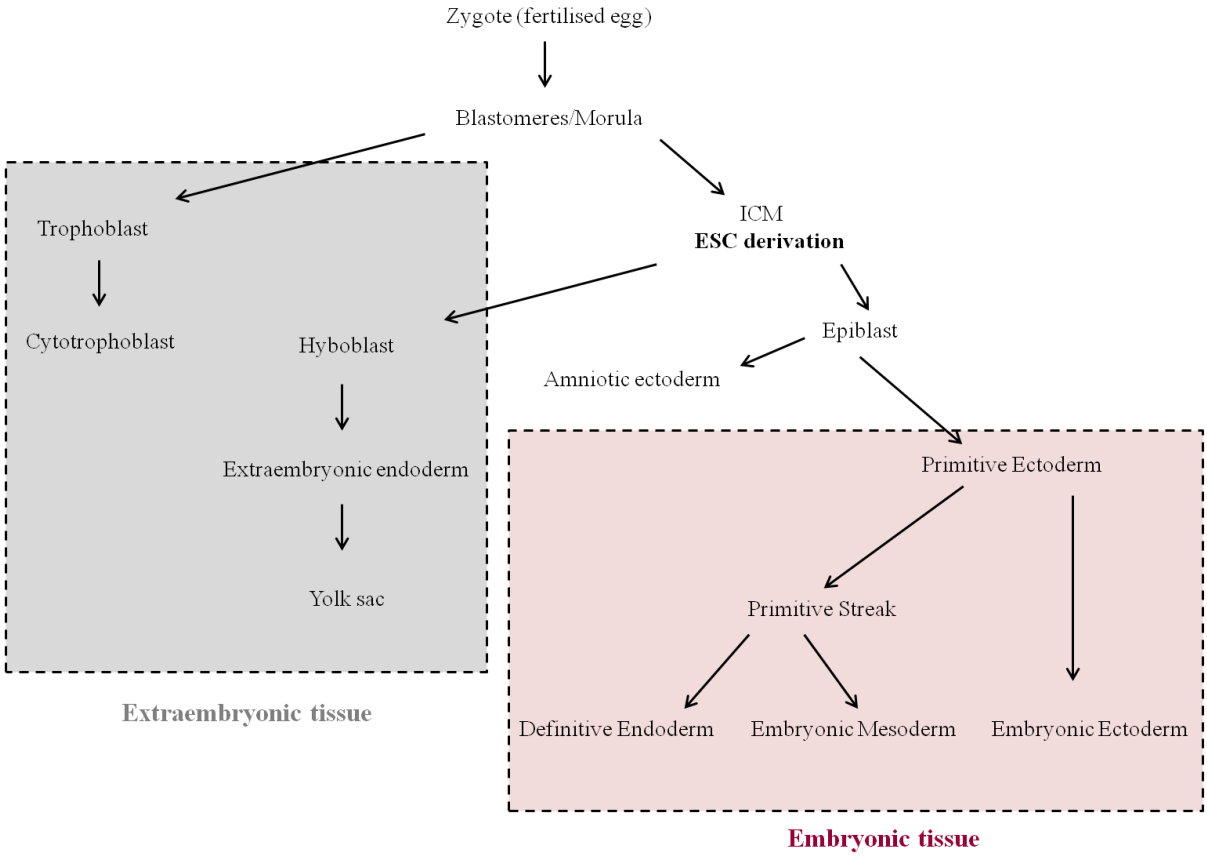

1.1. Early embryonic development Schematic outlining the early embryonic development cascade which gives rise to extraembryonic and embryonic tissues **(from stemcells.nih.gov)**

Given that ESCs are isolated at the ICM stage of embryonic development, they possess the ability to give rise to all three germ layers; endoderm, ectoderm and mesoderm, underpinning the massive clinical potential, since every cell type in the adult human originates from one of three primary germ layers.

Ectoderm (outer layer):

- Outer surface - epidermal (skin)
- CNS - neuron of brain
- Neural crest - pigment cell

Mesoderm (middle layer):

- Dorsal - notochord
- Paraxial - bone tissue
- Intermediate - tubule cell of kidney
- Lateral - red blood cells
- Head - facial muscle

Endoderm (inner layer):

- Digestive tube - stomach cell
- Pharynx - thyroid cells
- Respiratory tube - lung cell

Consequently, any population of ESCs theoretically can be directed to differentiate and become a specific cell type to suit specific clinical applications; for example, ESCs stimulated to become neurons for a Parkinson's disease-based application (Marchetto, Brennand et al.; Zhang, Duan et al.) or ESCs stimulated to become insulin-producing cells for diabetes treatment (Soria, Roche et al. 2000).

However, any clinical application will initially require the expansion of ESCs to suitably high cell numbers, therefore, understanding and foremost exploiting pluripotency is crucial.

1.1.2 Human ESCs (hESCs) and mouse ESCs (mESCs)

Any embryonic stem cell-based clinical application requires human-derived embryonic stem cells at its origin, however, owing to the ethics and limitations surrounding human embryonic

stem cell (hESC) research, mouse embryonic stem cells (mESCs) are often used as a model (de Wert and Mummery 2003).

hESCs were isolated as recently as 1998 from the ICM of a pre-implanted blastocyst at the 4-5 day stage (Thomson, Itskovitz-Eldor et al. 1998), almost 20 years after the derivation of mESCs from 3.5-4 day embryo (Stevens 1970). Consequently, much of the research, speculation and prospects of hESCs is founded on the well defined and deeply investigated, murine model. Furthermore, the difference in timing of ESC isolation in the embryo (4-5 day for hESCs compared to 7.5day for mESCs) is likely to underpin some of the major differences in ESC behaviour. Nonetheless, many similarities are apparent, justifying the usage of mESCs throughout this project.

In culture, like mESCs, hESCs express the pluripotency marker and transcription factor, Oct4 (Smith 2001) and similar antigens, SSEA-1 for example (Ginis, Luo et al. 2004; Zeng, Miura et al. 2004), although hESCs display a relatively slow proliferation rate compared to that of mESCs. hESCs do not respond to the leukaemia inhibitory factor (LIF), the major factor maintaining mESC pluripotency *in vitro*, and furthermore, it is unclear if the STAT pathway, so crucial in mESCs pluripotency, governs any part of hESC pluripotency. In the developing embryo, trophectoderm cells, which give rise to the placenta, do not differentiate in the mouse model, as identified in the human model.

1.1.3 ESC pluripotency

As mentioned, ESCs are characterised by their ability to self-renew, a property governed by extracellular signals coupled to a complex, timely activated intracellular signalling cascade, to activate transcription programs (summarised in Fig. 1.2.).

1.1.4.1 Transcriptional regulators of ESC pluripotency

Oct4

Oct-4, a 352 amino acid protein belonging to class V of POU transcriptional factors, is initially expressed in all blastomeres of the developing embryo, constantly expressed in ICM cells and maintained throughout the epiblast (Pesce and Scholer 2001; Sterneckert, Hoing et al. 2012). Targeted disruption of Oct4 was shown to result in an ICM lacking pluripotent properties (Nichols, Zevnik et al. 1998) therefore Oct4 has long been identified as a marker of ESC pluirpotency. Steady-state expression of Oct4 is shown to be crucial; high-expressing Oct4 ESCs are driven towards mesoderm and endoderm differentiation, whilst low-level Oct4 expressing ESCs become trophectoderm (Niwa, Miyazaki et al. 2000; Niwa 2001).

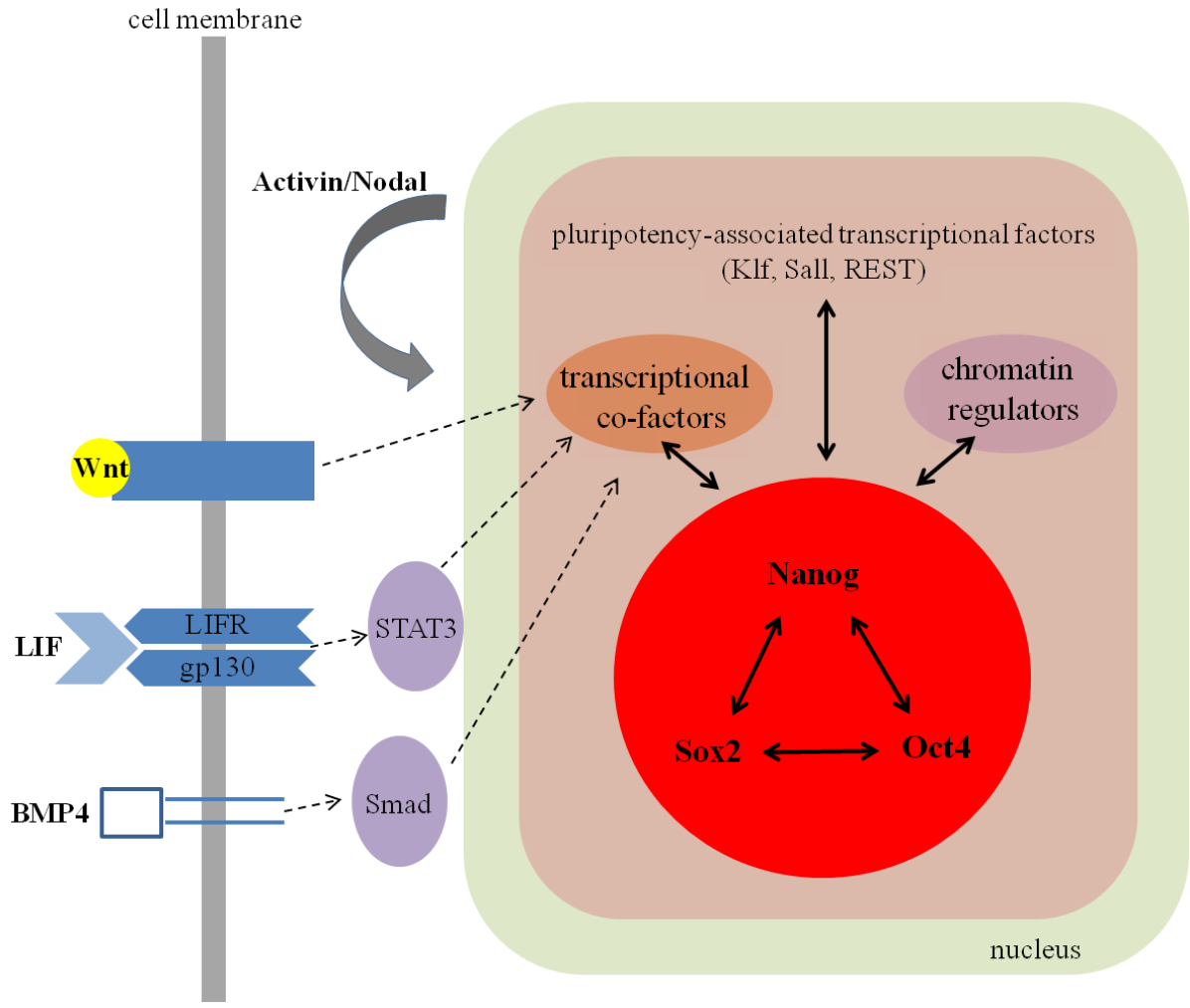

1.2. mESC pluripotency Schematic representing extracellular and intracellular factors governing mESC pluripotency

Nanog

Nanog, a homeobox-containing protein has more recently been identified as a marker of pluripotency (Chambers, Colby et al. 2003; Mitsui, Tokuzawa et al. 2003) expressed in mESCs and hESCs and EC and EG cells (Yamaguchi, Kimura et al. 2005). Nanog-null embryos fail to survive beyond implantation due to failure to specify the pluripotent epiblast and Nanog deletion in mESCs was shown to result in ESC differentiation (Mitsui, Tokuzawa et al. 2003; Ivanova, Dobrin et al. 2006), highlighting the importance of Nanog in mESC pluripotency. Interestingly, unlike Oct4, Nanog functions independently of the LIF-STAT3 pathway since over-expression of mESCs renders ESCs independent from STAT3 stimulation, but cannot abrogate the requirement for Oct4 (Orkin, Wang et al. 2008; Silva, Nichols et al. 2009).

Sox2, Klfs and other regulators of ESC pluripotency

Genome-wide studies have highlighted co-localisation of Sox2 with Oct4 and Nanog in ESC chromatin (Chambers and Tomlinson 2009) in an organised transcriptional network to maintain pluripotency. Sox2 (SRY (sex determining region-Y)-box 2) is another transcription factor thought to regulate pluripotency, largely attributed to its interaction with Oct4 (Masui, Nakatake et al. 2007; Kashyap, Rezende et al. 2009).

Krüppel-like factors (Klfs) are evolutionarily conserved zinc finger-containing transcription factors, shown to participate in the maintenance of mESC pluripotency (Bourillot and Savatier). Klf2, Klf4 and Klf5 have more recently been particularly highlighted as influential, since triple knockdown of Klf2/Klf4/Klf5 was shown to induce ESC differentiation (Jiang, Chan et al. 2008; Parisi, Passaro et al. 2008; Hall, Guo et al. 2009). Klf2 and Klf4 are more efficient at reprogramming cells into iPS cells than Klf5 though, suggesting a hierarchical relationship (Guo, Yang et al. 2009). Interestingly, Klf2, Klf4 and Klf5 can activate the

expression of Oct4, Nanog and Sox2, however disparity occurs in activation of Klfs; Klf2 is activated by Oct4 whilst Klf4 and Klf5 are activated by Nanog (Bourillot, Aksoy et al. 2009) and furthermore Klf4 and Klf5 (not Klf2) are regulated by STAT3, suggesting these link extrinsic regulators to the core pluripotency nectwork (Schulz, Kolde et al. 2009).

Neural repressor REST and Sall4 are two more transcription factors shown to be of great importance in maintenance of ESC pluripotency. Deletion of REST results in loss of ESC pluripotency (Ballas, Grunseich et al. 2005; Singh, Kagalwala et al. 2008) and mutation in Sall4 leads ESCs to re-specify to trophoblast cells, since Sall4 is known to activate Oct4 (Elling, Klasen et al. 2006; Sakaki-Yumoto, Kobayashi et al. 2006).

1.1.4.2. Mechanisms and signalling pathways maintaining mESC pluripotency

LIF/STAT3 pathway

The leukaemia inhibitory factor (LIF) was the first purified factor shown to govern the undifferentiated state of mESCs *in vitro* (Moreau, Donaldson et al. 1988; Smith, Heath et al. 1988; Williams, Hilton et al. 1988), originally identified as a macrophage maturation-inducing factor during the inhibition of leukaemia (Patterson 1994), hence the name.

LIF is a glycoprotein, which belongs to the IL – 6 cytokine family shown to function via the binding to LIF receptors, gp190 (LIFR) and gp130. LIF binds LIFR and forms a heterodimeric complex with gp130, recruiting tyrokinase JAK on its cytoplasmic domain, in turn, upon phosphorylation, creating sites for signal transducer and activator of transcription (STAT) proteins (Boeuf, Hauss et al. 1997; Niwa, Burdon et al. 1998; Turkson, Ryan et al. 2001). The LIF-STAT3 pathway has specifically been identified as critical in mESC self-renewal (Niwa, Burdon et al. 1998; Niwa, Ogawa et al. 2009). Activation of STAT3 is shown to be sufficient in maintaining mESC self-renewal (Matsuda, Nakamura et al. 1999). However, as mentioned, even in the presence of LIF, mESCs can spontaneously differentiate

into primitive endoderm, although visceral and parietal endoderm is inhibited (Shen and Leder 1992; Murray and Edgar 2001). LIF could therefore facilitate mESC pluripotency via inhibition of visceral endoderm differentiation, supported by Mountford et al., who demonstrated that a lack of primitive endoderm, attributed to transfection with Oct4 promoter gene, results in maintained pluripotency, despite the lack of LIF (Mountford, Nichols et al. 1998).

Activin/Nodal pathway

The transforming growth factor beta (TGF-β) is a superfamily, including 30 proteins, with a broad array of biological functions, of which Activin and Nodal are members. They signal upon formation of heteromeric complexes of type I and II receptors; active type II receptor kinase, phosphorylates type I receptor, thus activating intracellular signalling cascades, SMAD being an important example (Miyazawa, Shinozaki et al. 2002).

It has been demonstrated that these signalling pathways are important in maintaining an mESC niche (Ramalho-Santos, Yoon et al. 2002; Chng, Vallier et al. 2011). Nodal-null mice result in limited Oct4 expression (Conlon, Lyons et al. 1994) and inhibition of Activin/Nodal signalling by Smad7 expression, resulted in decreased mESC propagation (Ogawa, Saito et al. 2007), emphasising the importance of Activin/Nodal signalling in ESC pluripotency.

Bone Morphogenic Protein (BMP)

The bone morphogenic proteins (BMPs) were originally identified as facilitators of ESC differentiation (discussed in greater detail later), initially discovered during bone and cartilage development. However, more recently, it has been reported that BMPs induce the expression of Id (Inhibition of differentiation) genes via the Smad pathway to co-operate with

the LIF pathway to maintain the ESCs self-renewal (Ying, Nichols et al. 2003). In the absence of LIF however, BMPs function to facilitate ESC differentiation.

Wnt

Unlike LIF/STAT3 and BMP, Wnt signalling, thus far, is the only signalling pathway thought to be active in maintaining pluripotency in both human and mouse ESCs (Sato, Meijer et al. 2004; Sokol 2011). Wnt proteins were originally identified during wing development in *Drosphilia* studies, owing to the name. Wnts represent a group of secreted, lipid-modified proteins shown to function to maintain mESC pluripotency via inactivation of a serine kinase GSK-β (a consequence of activation of cytoplasmic signal protein, Disheveled) to stabilise β-catenin (cell-cell adhesion gene regulator) (Sato, Meijer et al. 2004; Miki, Yasuda et al. 2011).

1.1.4 *In vitro* expansion of mESCs (maintenance of pluripotency)

Since the 1960s, *in vitro* cell propagation has been achieved via expansion of certain cell populations on tissue culture plastic (polystyrene) dishes (Curtis, Forrester et al. 1983), corresponding to tailored culture conditions. Expansion of pluripotent mESCs and hESCs, has long been achieved using serum supplementation and a fibroblast feeder cell layer as substrate (Heath and Smith 1988; Smith, Heath et al. 1988; Brook and Gardner 1997) and more recently, leukaemia inhibitory factor (LIF) supplementation for the maintenance of mESCs pluripotency (Niwa, Burdon et al. 1998; Sun and Shi 1998).

mESCs typically form compact colonies, and display high nuclear:cytoplasmic ratio. However, despite the presence of LIF, mESCs positioned at the periphery of the colonies spontaneously differentiate. Furthermore, mESCs undergo spontaneous apoptosis if cell

density is low enough, furthermore highlighting the importance of a proper experimental niche for the maintenance and proliferation of ESCs.

1.1.5 Embryoid Body (EB)

An interesting feature of mESCs is that, once grown in suspension culture, they clump together to form aggregates known as embryoid bodies (EBs). EBs represent a well-established model system of early development (Robertson 1987), since the three-dimensional structure mimics a developing embryo at the egg cylinder stage *in vivo* (Denker 2004), demonstrating differentiation to all three primary germ layers; endoderm, ectoderm and mesoderm, as discussed previous.

EB development persists once ESCs aggregate to form clusters by day 2. This is followed by differentiation of extraembryonic primitive endoderm (PE) at the periphery of the EB by day 3 (Murray and Edgar 2000). At day 4, visceral and parietal endoderm cells are present, a result of differentiation from their PE precursors. PE cells deposit a BM at their basal surface, resembling that of the BM which is present between the primitive endoderm and epiblast in the early embryo. Parietal endoderm cells deposit a thick BM similar to Reichert's membrane, which is found between parietal endoderm and trophectoderm in the early embryo, although the BM in the blastocyst between the ICM and PE cells is much thinner (Inoue, Leblond et al. 1983) since the parietal endoderm cells cannot migrate away from core of the EB as they would normally do from the ICM. BM deposition initiates polarisation of inner cells forming primitive ectoderm epithelium, separating pluripotent inner cells from differentiated outer cells. Some inner ESCs differentiate to epiblast to form columnar epiblast epithelium (CEE), whilst other inner ESCs undergo programmed cell death (Coucouvanis and Martin 1995), representing the start of cavitation, a phenomenon typically seen by day 7. CEE cells then further differentiate to definitive endoderm, ectoderm and mesoderm, such as neuronal cells (summarised in Figure 1.3.).

1.1.7 Lineage commitment of mESCs

1.1.7.1 Transcriptional regulators of ESC differentiation during lineage commitment

ESC differentiation is dependent on silencing the self-renewing, highly complex signaling cascade described previously and the response of ESCs to specific environmental cues to make fate decisions. *In vitro*, ESCs can be directed to differentiate, instead of undergoing self renewal, via a combination of aggregation culture and the removal of LIF (Keller 1995; Smith 2001), the method employed throughout this study, although two other methods also exist both consistent with the removal of LIF. One involves expansion of ESCs on stromal cells (Nakano, Kodama et al. 1994), while the other entails expansion of ESCs on ECM proteins (Nishikawa, Nishikawa et al. 1998). Upon differentiation *in vitro*, analogous to ESC differentiation *in vivo*, a specific patterning exists correlating to a specific order of transcriptional networks. Throughout this project, key markers of these transcriptional networks operating, are monitored.

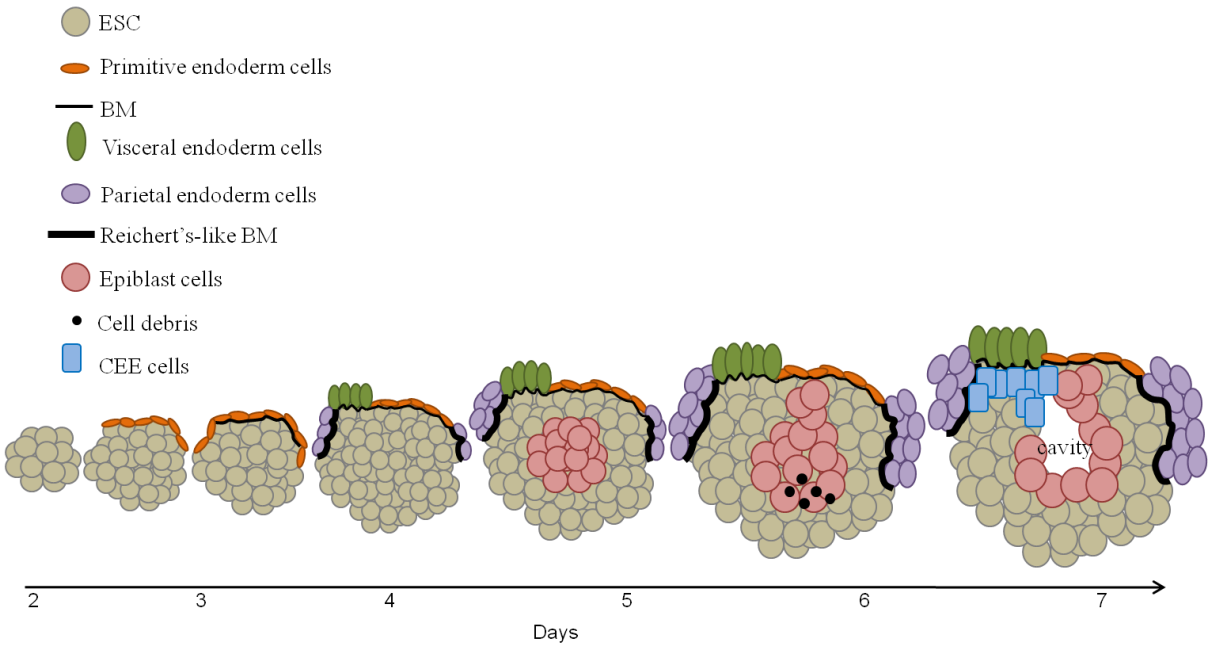

1.3. EB development Schematic diagram outlining the important stages of EB development once ESCs are grown in suspension. Aggregation of ESCs occurs at day 2, followed by differentiation of cells on the periphery of EB to extraembryonic primitive endoderm by day 3. Visceral and parietal endoderm develop from primitive endoderm precursors by day 4. Parietal endoderm cells contribute to thick BM deposition, specifically a Reichert's-like BM. Some inner ESCs differentiate to epiblast and upon contact with BM become polarised and become columnar primitive ectoderm (CEE), whilst epiblast cells that do not deposit BM undergo programmed cell death, resulting in cavitation of EB. Primitive ectoderm undergoes further differentiation to mesoderm, definitive endoderm and definitive ectoderm, although this process is chaotic.

Mesoderm differentiation

Mesoderm, as outlined briefly, forms all tissues of the adult human with the exception of the nervous system, skin epidermis and epithelia and can be categorized into paraxial, intermediate and lateral plate. Accordingly, a vast array of transcription factors and activated signaling cascades occur according to patterning stage, some of which are used in this project.

Mesoderm differentiation in the early developing embryo is initially identified by the epithelial to mesenchymal transition (EMT), a pivotal point during gastrulation and formation of the germ layers (Lehembre, Yilmaz et al. 2008), thought to be associated with a loss of E-

cadherin expression (Frame and Inman 2008). *Brachyury*, a T-box transcription factor (Inman and Downs 2006) marks the specification of mesoderm at the time of gastrulation and is transiently expressed from E7 to 8.5 in the mouse intermediate and axial mesoderm (Wilkinson, Bhatt et al. 1990; Kispert and Herrmann 1994), and is therefore a useful marker of mesoderm differentiation *in vitro*. Mutations in the *Bry* gene result in eventual embryonic lethality, owing to insufficient mesoderm and absence of the notochord, although development is normal up to the primitive streak (Herrmann 1992; Herrmann and Kispert 1994). Paraxial, intermediate and lateral plate mesoderm differentiation occurs as a consequence of successful patterning due to somite divisions into sclerotom, dermatome and myotome. In the mouse, the first genes known to be asymmetrically identified at this stage are members of the TGFβ family member *Nodal***,** around the node (Jones, Kuehn et al. 1995; Beddington and Robertson 1999; Gritsman, Talbot et al. 2000), followed by *Lefty2*, and *Pitx2* in the left LPM and *Lefty1* in the left floor plate of the neural tube (Lowe, Yamada et al. 2001; Brennan, Norris et al. 2002; Saijoh, Oki et al. 2003). The paraxial mesoderm develops via the formation of two cylinders of tissue either side of the notochord and after weeks 4 and 5, blocks of this tissue called somites bud off to the cranial end, to begin governing segmentation. The t-box transcription factor *Tbx-6* is known to work downstream of *Nodal* and has important roles in the presomitic mesoderm and formation of the somite borders (Chapman, Agulnik et al. 1996; Hadjantonakis, Pisano et al. 2008). Scleratome, which gives rise to vertebral body and arch surrounding neural tube is thought to be initiated and maintained by sonic hedgehog (*Shh*) and Noggin, molecules produced by the neural tube (Dockter and Ordahl 1998; Dockter 2000), functioning to antagonize BMP4 (Hirsinger, Duprez et al. 1997). Epithelial-mesenchymal conversion of the dermatome, which contributes to skin on the dorsal side of the body and the myotome, which develops to form skeletal musculature of the neck, trunk and limbs, is thought to depend on signals from the neural

tube (Brill, Kahane et al. 1995). The intermediate mesoderm gives rise to the gonads, kidneys and adrenal cortex (Evseenko, Zhu et al.); Pax-2 and Osr1 are important transcription factors first seen after gastrulation in the mediolateral mesoderm (James and Schultheiss 2005) and the forkhead transcription factors Foxc1 and Foxc2 are crucial (Wilm, James et al. 2004), demonstrated by Foxc1-deficient mice lacking mesoderm differentiation (Aitola, Carlsson et al. 2000).

Despite the complexity, mesoderm differentiation is the most well studied and well categorized of the three germ lineages, perhaps underpinned by some default mechanism, given the ease of differentiating mESCs to hematopoetic, vascular and cardiac lineages (Doetschman, Eistetter et al. 1985). Differentiation of ESCs to mesoderm in the EB model is often achieved using combinations of exogenous proteins (Liu, Wang et al.; Torres, Prieto et al.) and provides little information on positional information for cell types (Era); therefore much work is still needed to optimize for mesoderm-derived cells using this model.

Endoderm-differentiation

Endoderm is classically defined as the inner layer of the embryo, whose main derivative is the epithelia of the digestive tract, from which organs such as the liver and pancreas develop. Analogous to endoderm development in the EB model, *in vivo* endoderm develops in close association with mesoderm in vertebrates, and most endoderm cells are derived from the primitive streak (Lawson, Meneses et al. 1991; Wells and Melton 1999). Extraembryonic endoderm structures, referred to in this project, are defined as primitive endoderm, parietal endoderm and visceral endoderm and differ from definitive endoderm, although they do share many transcriptional markers.

Extraembryonic primitive endoderm cells give rise to endoderm-derived cell lineages in a precise spatial pattern, outlined in the murine model whereby cells within the ICM proliferate

and segregate to form an outer layer detected by E4.0 shortly before implantation (Gardner 1982). Likewise during EB development, endoderm differentiation persists via the differentiation of cells on the EB periphery to extraembryonic primitive endoderm (PE), as outlined previously.

GATA factors have been identified as key regulators of both extraembryonic and definitive endoderm differentiation, via regulation of primitive endoderm differentiation (Murakami, Okumura et al. 2005; Okumura, Matsumoto et al. 2005). GATA factors are evolutionarily conserved transcriptional regulators, comprised of six members (Gata1 - 6). Gata1-3 are generally expressed in hematopoietic lineages; for instance Gata2 and Gata3 have been suggested to play a role in early embryonic patterning in Xenopus and Zebrafish (Zon, Mather et al. 1991), specifically detected at the pre-primitive streak stage in the chick (Sheng and Stern 1999). Gata4-6 in contrast are mainly found in mesoderm and endoderm lineages (Molkentin 2000; Ralston and Rossant 2005) evidently crucial in early development (Simon 1995) and Gata6 specifically, is employed in this project.

Gata6 is a key regulator of endoderm differentiation, demonstrated neatly since Gata6-null embryos lack primitive endoderm differentiation, and visceral and parietal endoderm are consequently lacking also (Morrisey, Tang et al. 1998; Cai, Capo-Chichi et al. 2008). Moreover, ectopic Gata6 expression can bypass the requirement of Grb2, crucial in Nanog repression and primitive endoderm differentiation (Hamazaki, Kehoe et al. 2006; Wang, Smedberg et al. 2011), further highlighting the importance of Gata6 in primitive endoderm differentiation.

Alpha-fetoprotein (AFP), Sall4, Sox7, Sox17 and HNF-4 (Duncan, Manova et al. 1994) represent key factors also crucial in extraembryonic endoderm differentiation, many of which interact with GATA factors to stimulate endoderm differentiation. AFP is the most abundant

protein of the mammalian embryo identified in the embryonic yolk sac and fetal liver (Tomasi 1977; Spear and Tilghman 1990), although expression is shown to substantially decrease after birth. AFP is thought to be secreted by the visceral endoderm (Dziadek 1978), although it is proposed that synthesis and expression may depend on interactions of visceral endoderm with underlying ectoderm tissue. Hepatocyte nuclear factor 4 (HNF-4) is a transcription factor identified in liver extracts as a DNA binding protein (Sladek 1994), of which primitive endoderm differentiation is thought to depend, attributed to its interaction with Gata6 (Duncan, Nagy et al. 1997; Morrisey, Tang et al. 1998). Sall4, a component of the spalt-like zinc-finger family of transcription factors, is also demonstrated to be crucial in differentiation to primitive endoderm (Elling, Klasen et al. 2006), and proposed to be specifically important for the Nanog repression step of primitive endoderm differentiation (Frankenberg, Gerbe et al. 2011). Sox7 and Sox17 are thought to govern parietal endoderm differentiation through interactions with GATA factors (Futaki, Hayashi et al. 2004), and one proposed model is that Sox7 competes with Gata4 for FGF3 binding (Murakami, Shen et al. 2004). Interestingly Sox7 and Sox17 are thought to depend and affect BM formation, specifically attributed to Laminin alpha 1 (LamA1) interactions (Niimi, Hayashi et al. 2004).

Ectoderm

In vertebrates, ectoderm is dissected into the external (or surface) ectoderm, the neural crest, and the neural tube. Cell lineages derived from the ectoderm differentiate to form the epidermis; skin, hair, and nails, the brain, and the nervous systems. Formation of these neural tissues commence when the notochord, derived from the mesoderm, induce over-lapping areas of ectoderm to form the neural plate. The neural plate subsequently folds to form the neural tube and dorsal/lateral polarity is established. Within the neural tube, neuroepithelial cells proliferate and differentiate into a variety of ectodermal cell lineages. These cells will

form the adult nervous system. Specific ectodermal lineages include oligodendrocytes, type-1 and -2 astrocytes, and neuron progenitors.

The relationship and interactions between BMP4, Noggin and Chordin is thought to largely underpin ectoderm differentiation, specifically inhibition of BMP4-Noggin-Chordin interactions is thought to be required for folding of the neural plate (Piccolo, Sasai et al. 1996; Zimmerman, De Jesus-Escobar et al. 1996). *Pax2* and *Pax6* are transcription factors that contain paired box DNA binding domains, and are evolutionarily conserved in ectoderm development. Eye development is a classic demonstration of the importance of Pax6 for example; Pax6 mutants lose functionality of the eye, consistent with *Drosophila,* mice and humans (Hogan, Horsburgh et al. 1986; Quiring, Walldorf et al. 1994). Pax6 expression is detected in a number of regions of the developing mouse central nervous system, including the presumptive retina from the headfold stage onwards (Walther and Gruss 1991; Walther, Guenet et al. 1991; Stoykova and Gruss 1994; Grindley, Davidson et al. 1995) and therefore represents a useful marker of differentiation to ectoderm in the EB model.

1.1.7.2 Basement membrane

Basement membranes (BM) represent the earliest extracellular matrices produced during embryogenesis. In the early embryo, primitive endoderm cells deposit BM at their basal surface, present between the PE and epiblast. Parietal endoderm cells deposit a thick BM similar to Reichert's membrane, which is found between parietal endoderm and trophectoderm in the early embryo (Austria and Couchman 1991).

BMs are synthesised to provide structural support onto which epithelial tissues grow and for compartmentalisation, as a specialised type of extracellular matrix (ECM) localised between epithelial and mesenchymal tissues (Amenta, Clark et al. 1983; Martinez-Hernandez and Amenta 1983; Paulsson 1992; Engvall 1995; LeBleu, Macdonald et al. 2007). In many

instances, BMs function as semi-permeable membrane, controlling the passage of macromolecules by size and charge and more recently, it has been shown that BMs influence cell behaviour; certain BM components are shown to promote cell adhesion and proliferation in the early stages of blood vessel development (Navaratnam 1991) and direct definitive endoderm differentiation in mESCs (Higuchi, Shiraki et al. 2010).

Components of BM largely underpin their structure and function; laminin and collagen IV are major constituents (Kleinman, Cannon et al. 1985; Liotta, Rao et al. 1986; Martin and Timpl 1987) along with proteoglycans and nidogen (Carlin, Jaffe et al. 1981; Timpl, Fujiwara et al. 1984; Leivo and Engvall 1988). BMs are connected to local cells via a network of integrins, who preferentially bind laminin and collagen IV in mass molecular self-assembly (Yurchenco, Tsilibary et al. 1986; Timpl and Brown 1996). Throughout this project, identification and analysis of laminin expression, is employed as a method of assessing EB development and mESC differentiation.

Laminin

Laminin, a family of extracellular matrix heterotrimeric glycoproteins, are the major non-collagenous constituent of BMs. In mammals they have been shown to be involved in diverse developmental processes including cell adhesion, differentiation, migration and metastasis, to name a few.

Laminins are composed of three non-identical chains (alpha, beta, gamma) as a laminin heterodimer in a cross-shaped structure. Three short arms are formed by a different chain and one long arm is composed of the three assembled coiled chains (Figure 1.4; Yurchenco and Mathus, 2000.). Of the three chains which make up the laminin heterodimer, beta 1 and gamma 1 are detected at the 2-cell stage, whilst alpha 1 is detected at the 8-16 cell stage (Cooper and MacQueen 1983; Dziadek and Timpl 1985).

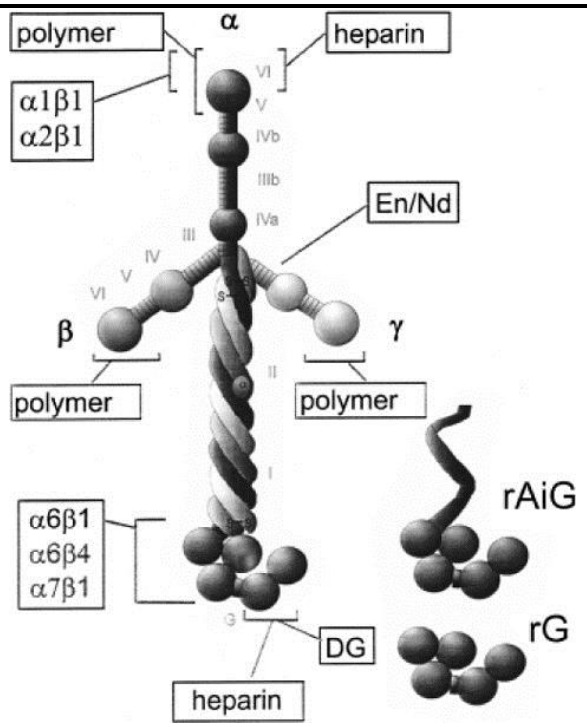

1.4. Laminin-1 Schematic diagram outlining the structure of laminin-1 as a model for other laminins, outlining the relationship of the 3 chains; α, β and γ joined together in a coiled-coil to form a crucifix shape. The heparin-binding domain (G) extends from the coil. Roman numberals indicate regions that vary between structures (Yurchenco and Mathus, 2000).

Mammals possess 15 different heterotrimers (compared to 2 or 3 in invertebrates) formed via combinations of 5 alpha, 4 beta and 3 gamma (Aumailley, Bruckner-Tuderman et al. 2005). Synthesis of the laminin heterodimer is thought to occur initially with dimerisation between beta and gamma chains intracellularly, followed by incorporation of the alpha subunits, to facilitate secretion. Ultimately, this model predicts that the alpha subunit dictates extracellular secretion (Morita, Sugimoto et al. 1985; Kumagai, Kadowaki et al. 1997; Goto, Aoki et al. 2001). Interestingly, research has shown that while the alpha subunit can be secreted alone as a monomer, secretion of beta and gamma chains requires simultaneous expression of all three chains and their heterotrimeric assembly (Yurchenco, Quan et al. 1997).

Upon secretion, laminins interact with each other via the small arms in order to undergo self assembly into a BM meshwork. During development, this process is more complicated and

requires the long arm to be tethered to receptors on cell surface (Urbano, Torgler et al. 2009). Laminins interact with many different receptors, including integrins, α dystroglycan and sulphated carbohydrates (sulphatides, heparin, heparan sulphates and HNK-1) (Miner and Yurchenco 2004). The importance of such interactions are not fully defined, but it appears that laminins employ integrins as a predominant method of mediating cellular response (Martin-Bermudo and Brown 1999; Urbano, Torgler et al. 2009).

The importance of laminin in development is well-documented and different laminin isoforms have proven crucial during different development stages. Laminin-111 (alpha 1, beta 1 and gamma 1) deficient mice lack BM formation and embryogenesis fails to persist beyond pre-implantation (Smyth, Vatansever et al. 1999; Scheele, Falk et al. 2005); moreover conditional laminin-111 knockout (to bypass embryonic lethality) displayed defects in cerebellum development in mice (Heng, Lefebvre et al. 2011). Laminin-511 (alpha 5, beta 1, gamma 1) deficient mice lack a normal developing intestine (Mahoney, Stappenbeck et al. 2008).

1.1.7.3 Signalling pathways important in lineage commitment

Bone Morphogenic Protein (BMP)

The bone morphogenic proteins (BMPs) as mentioned, were discovered over 40 years ago as orchestrators of bone formation (Urist 1965) and play a crucial role in ESC differentiation (as well as self renewal described previous). Since then, twenty BMPs have been identified, of which many have been discovered to be essential in early embryonic development, often linked to activation of Nodal signaling (Mishina 2003). BMP4 is highly expressed in extraembryonic ectoderm and primitive streak before gastrulation (Winnier, Blessing et al. 1995; Lawson, Dunn et al. 1999; Ying and Zhao 2001). Furthermore, BMP-4 has been shown to be necessary for mesoderm differentiation and interestingly, was also found to be

necessary for visceral endoderm differentiation (Sirard, de la Pompa et al. 1998; Yang, Li et al. 1998). BMP2 is also expressed in extraembryonic tissues and although BMP2-null mice can gastrulate, there is evidence of abnormal embryonic development (Zhang and Bradley 1996; Kishigami and Mishina 2005). Likewise, BMP6 and BMP7 null mice do not display restricted patterning during embryonic development (Dudley, Lyons et al. 1995; Luo, Hofmann et al. 1995).

Fibroblast growth factor (FGF) signaling pathway

There are 22 members of the fibroblast growth factors (FGFs) family and 4 identified FGF receptors (Ornitz and Itoh 2001; Reuss and von Bohlen und Halbach 2003), representing extracellular signalling proteins that act through receptor tyrosine kinase activity. Tyrosine phosphorylation occurs upon ligand stimulation and has been shown to activate MAPK pathways (Chen, Li et al. 2000; Li, Wang et al. 2007; Suwinska and Ciemerych 2011). The importance of FGF during development has long been highlighted, since mutations in different FGF species are shown to be embryo lethal after pre-implantation (Feldman, Poueymirou et al. 1995; Arman, Haffner-Krausz et al. 1998). Furthermore, an FGF docking adaptor protein, FRS2a, is shown to control intracellular response of mESCs to FGF (Hadari, Gotoh et al. 2001; Gotoh, Manova et al. 2005).

The role of FGFs in ESC behaviour however is inconsistent. Some studies suggest that FGFs have a role in ESC self-renewal (De Felici, Farini et al. 2009; Lanner and Rossant 2010; Hsieh, Intawicha et al. 2011). For instance, FGF4, specifically has been shown to be regulated by Oct4 and Sox2, markers of ESC pluripotency (Yuan, Corbi et al. 1995) and, basic FGF (FGF2) is shown to support hESC self-renewal via stabilisation of the signalling above a certain threshold (Levenstein, Ludwig et al. 2006; Eiselleova, Matulka et al. 2009) and are similarly important in mESCs (Diecke, Quiroga-Negreira et al. 2008). However, in

contrast, a more long-standing idea is that FGF influences differentiation. This is supported by recent data suggesting that the role of LIF in maintenance of mESC pluripotency is to block FGF signaling downstream of ERK (Silva and Smith 2008; Ying, Wray et al. 2008). Ornitz et al., identified that many FGFs are crucial in early development (Ornitz 2000; Wang, Ai et al. 2004); FGF2 has been shown to be crucial in brain development (Qiao, Meyer et al. 2003) and blood vessel formation (Sperinde and Nugent 2000), furthermore, FGF4-null mESCs were shown to fail to respond to differentiation inducers (Ids), suggesting a specific role for FGF4 in mESC differentiation (Wilder, Kelly et al. 1997; Kunath, Saba-El-Leil et al. 2007).

Overall, much is already known of the intrinsic factors that regulate ESC self-renewal and differentiation, but much less is known about the role of extracellular factors, such as growth factors and the extracellular matrix (ECM), in regulating ESC behaviour.

One master extrinsic regulator however, is heparan sulfate (HS), a polysaccharide synthesised by all mammalian cells shown to mediate many signalling pathways responsible for cell proliferation, migration, differentiation and apoptosis throughout early development (Delehedde, Deudon et al. 1996; Guimond and Turnbull 1999; Harmer 2006).

1.2 Heparan Sulfate

Heparan Sulfate (HS) is a linear polysaccharide and a class of glycosaminoglycan (GAG), made by virtually all mammalian cells. In biological terms, it is often referred to as heparan sulfate proteoglycan (HSPG), since this GAG is commonly found attached to a protein. Interest in HSPGs has grown massively of late with the realisation that this complex macromolecule plays fundamental roles in growth factor signalling and morphogenesis.

1.2.1 Glycosaminoglycans (GAGs)

Glycosaminoglycans (GAGs) are large linear polysaccharides, of which there are five classifications:

- Hyaluronan
- Chondroitin Sulfate (CS)
- Dermatan Sulfate (DS)
- Heparin/heparin sulphate (HS)
- Keratan Sulfate (KS)

Hyaluronan, a major carbohydrate component of the ECM and found in abundance in load-bearing joints, is unique since it is the only GAG which is unsulfated and not found attached to a protein (Laurent 1989; Chen and Abatangelo 1999). KS, fibrous filaments found in the cornea, does not contain a uronic acid disaccharide component, unlike the other GAGs. DS is the predominant GAG found in skin (Trowbridge and Gallo 2002; Trowbridge, Rudisill et al. 2002), and more recently has been linked to cardiovascular disease and tumourgenesis (Tollefsen). Chondroitin and heparin/HS are the most abundant GAGs. CS, commonly found as the proteoglycan aggregan, is a major component of cartilage, loss of which results in osteoarthritis (Miller and Clegg). Of all the GAGs, HS is the most deeply investigated, often described as a master extrinsic regulator of cellular behaviour.

The biological activity and significance of HS, like any GAG, is attributed to its structure and biochemical make-up; one classic example is that all GAGs function in part to maintain ECM hydration, attributed to their hydrophilicity and net negative charge (Prydz and Dalen 2000).

1.2.2 HS structure

HS is not a single molecule but instead a diverse family of related molecules, consisting of repeating uronic acid-glucosamine disaccharide subunits, arranged in sulfated (NS) and unsulfated (NA) regions with spacers between; Figure 1.5. Variability in substitution of the disaccharide subunits with N-sulfate, N-acetyl and O-sulfate groups means that theoretically 48 disaccharides could exist, although to date, only 24 have been identified. Generally, the same set of disaccharides exist in most tissues but their relative content varies quantitatively (Esko and Lindahl 2001); HS and heparin being an exemplar. HS and heparin display identical building blocks but the disaccharide subunits are present in different proportions; SO_4 content is lower in HS than heparin, therefore resulting in a fine structure that can encode for higher diversity of information (Rabenstein 2002).

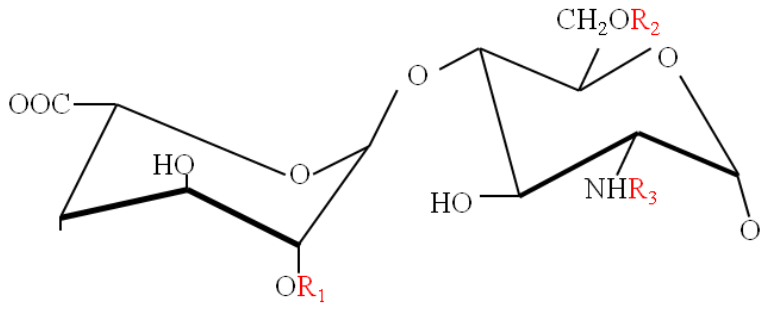

1.5. GAG repeating unit Schematic diagram outlining the molecular structure of the HS disaccharide building blocks. A disaccharide repeat of uronic acid and glucosamine, and corresponding potential sites of sulfation (red; R1, O-sulfation at C2 of uronic acid; R2, O-sulfation at C6 of glucosamine; R3, either SO_3 or acetate) indicate the potential diversity and heterogenous nature of HS.

1.2.3 HS Biosynthesis

Biosynthesis of HS occurs sequentially in the Golgi apparatus, where a Xyl-Gal-Gal-GlcA linker oligosaccharide is initially built up, attached to the serine residues of proteins (which become the core proteins). The HS chain is then produced via the activation of membrane-bound enzymes. These enzymes are present in multiple isoforms, where expression is spatially and temporarily regulated giving rise to different GAGs during different stages of development (Raman, Sasisekharan et al. 2005; Nairn, Kinoshita-Toyoda et al. 2007). Elongation of the HS chain occurs via alternating addition of N-acetyl-glucosamine (GlcNAc) residues followed by D-glucuronic acid (GlcA), mediated by two copolymerase enzymes (GlcNAc transferase II and GlcA transferase II) products of *EXT1* and *EXT2* genes. The HS chain is then transported across the Golgi apparatus and the nascent chain is modified by several enzymes (summarised in Table 1.1); firstly replace NDSTs which can replace N-acetyl with N-sulfate, then O-sulfates can be added at C2 by 2-O-glucuronic/iduronic sulfotransferase (2OST), and finally further O-sulfation of HS can occur at C6 and C3 positions of glucosamine residues if 6-O-sulfotransferase and 3-O- sulfotransferase are present, respectively (Whitelock and Iozzo 2005). Modifications are not template-driven though, and therefore these reactions do not modify the entire chain to completion, resulting in structural heterogeneity (Figure 1.6).

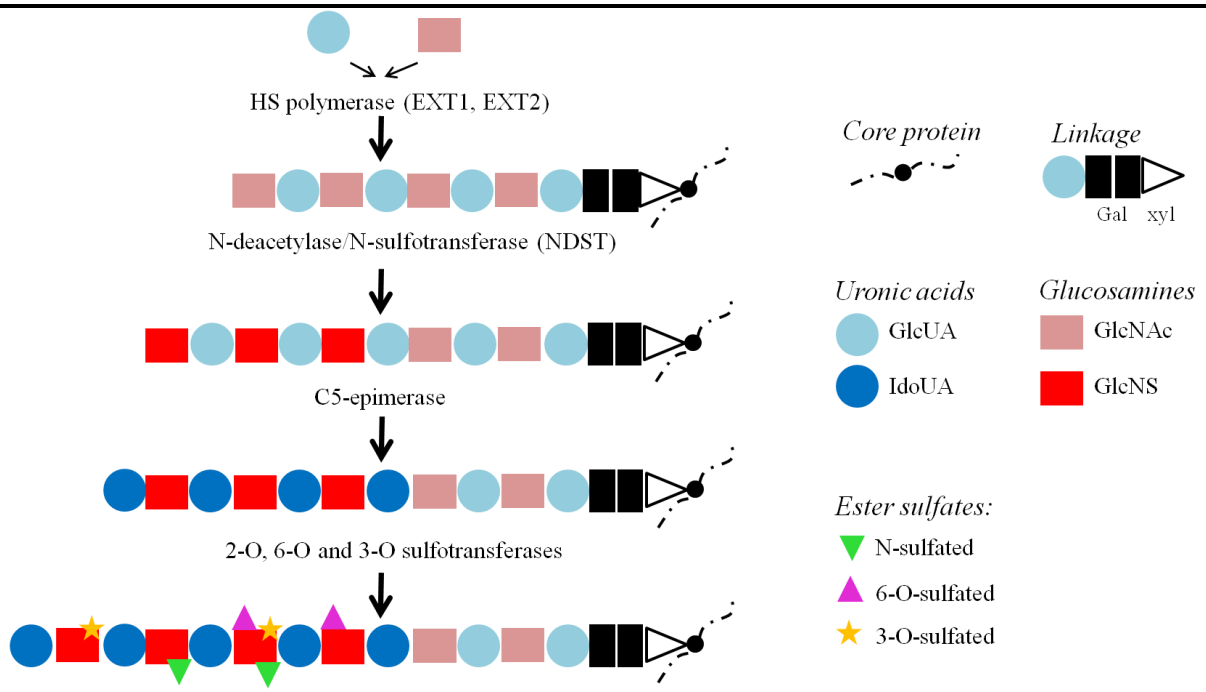

1.6. HS biosynthesis Schematic outline of HS biosynthesis. Chain polymerisation occurs by alternating addition of GlcNAc and GlcUA monosaccharides to the tetrasaccharide linker (GlcA-Gal-Gal-Xyl) which is attached to serine residues of the core protein, followed by sequential chain modification; deacetylation and sulfation according to the presence of NDSTs, C-5 epimerase and 2-O, 6-O and 3-O sulfotransferases.

Table 1.1 HS biosynthetic enzymes and their respective roles

Enzyme	Name	Function
EXT1	Exostosin1	First step of chain initiation; adds alternating units of glucuronic acid (GlcA) and GlcNAc to the non-reducing end of the chain (Busse, Feta et al. 2007; Presto, Thuveson et al. 2008)
EXT2	Exostosin 2	First step of chain initiation; adds alternating units of glucuronic acid (GlcA) and GlcNAc to the non-reducing end of the chain (Busse, Feta et al. 2007)
HS20ST	Heparan sulfate 2-O sulfotransferase	Transfers the sulfo group from 3'-phosphoadenosine 5'-phosphosulfate (PAPS) to the 2-OH position of the uronic acid adjacent to N-sulfated glucosamine (Xu, Song et al. 2007)
HS30ST1-6	Heparan sulfate 3-O sulfotransferases (6 isoforms)	Transfers the sulfo group from 3'-phosphoadenosine 5'-phosphosulfate (PAPS) to the 3-OH position of the glucosamine which are N-sulfated
HS60ST1-3	Heparan sulfate 6-O sulfotransferases (1-3)	Transfers the sulfo group from 3'-phosphoadenosine 5'-phosphosulfate (PAPS) to the 6-OH position of the glucosamine which is N-sulfated or N-acetylated (if adjacent to an N-sulfated glucosamine)
NDST1-3	N-deactylase/N sulfotransferases 1-3	Replaces acetyl groups with sulfate groups at the N-position of the glucosamine
Sulf1	6-O-endosulfatase	Removes 6-O sulfate groups (Dhoot, Gustafsson et al. 2001; Morimoto-Tomita, Uchimura et al. 2002)
Sulf2	6-O-endosulfatase	Removes 6-O sulfate groups (Morimoto-Tomita, Uchimura et al. 2002; Holst, Bou-Reslan et al. 2007)
C-5 epimerase	C-5 epimerase	Conversion of glucuronic (GlcA) acid to iduronic acid (IdoA) (Feyerabend, Li et al. 2006)

Ultimately, HS biosynthesis dictates the resultant HS molecule, which largely governs HS-protein interactions, according to sulfation pattern. A simple demonstration of this is how increased HS sulfation of HS is typically correlated with increased signalling activity (Baldwin, ten Dam et al. 2008). However, the core protein represents a method of classifying overall HSPGs as an alternative to degree of sulfation, and often underpins their functionality in development, since the core proteins carry the chains for display at specific locations.

1.2.4 Core proteins

Commonly, HS GAGs are attached to a core protein, of which there are three basic types, each representing a different mode of cell-interaction and therefore determines if that specific HSPG is expressed on the cell surface or in the ECM (Gandhi and Mancera 2008);

- Syndecans
- Glypicans
- Basement membrane proteins

Syndecans are classified into four subfamilies; syndecan1, 2, 3 and 4, based on distinct gene products which vary on the size of the extended extracellular domain onto which associated GAG is attached. They contain a conserved transmembrane domain and a characteristically small cytoplasmic domain (Lopes, Dietrich et al. 2006). Syndecans are detected on blastomere surfaces at the morula stage but restricted in the blasteol cavity (Jokimaa, Inki et al. 1998; San Martin, Soto-Suazo et al. 2004).

*Glypicans a*re categorised into three subfamilies; Gpc1 and 2, Gpc3 and 4 and Gpc5 and 6; all distinct gene products with 14 highly conserved cysteine residues which form an extended region (2 or 3 Ser-Gly sequences) near the plasma membrane; the glycosylphosphatidyl inositol anchor (GPI) (Bernfield, Gotte et al. 1999).

ECM proteins, as the name suggests, represent ECM constituents, given that these HSPGs, unlike syndecans and glypicans, are secreted from the cell into the ECM. They are thought to have a multi-domain structure (Lindblom, Carlstedt et al. 1989; Kallunki and Tryggvason 1992) and there are three predominant sub-types (Iozzo, Cohen et al. 1994; Murdoch, Liu et al. 1994);

- Agrin
- Perlecan
- Collagen XVIII

Agrin is responsible for the formation, maintenance and regeneration of the neuromuscular junction, widely expressed in the central nervous system (CNS) (Kroger and Schroder 2002) and accumulating evidence suggests it has a major role in Alzheimers disease (Cole and Halfter 1996; Bezakova and Ruegg 2003). Perlecan is more broadly expressed throughout early embryonic development, identified in underlying uterine epithelia and trophoblast. In the pre-implanted mouse embryo, expression is transient before the morula stage and by the blastocyst stage, perlecan expression is enhanced (Rohde, Janatpore et al. 1998; Abraham, Riggs et al. 2010). It is also expressed in interstitial matrix tissue of cartilage and bone (Schofield, Gallagher et al. 1999; Farach-Carson, Hecht et al. 2005). The C-terminal domain of Collagen XVIII, endostatin, is reported to have angiogenesis properties and promotes tumour growth via inducing apoptosis of endothelial tissues (Seppinen and Pihlajaniemi; Marneros and Olsen 2005). Proteoglycans are therefore diverse molecules, depending on the number of GAG chains, type of core protein and class of GAG side chain (Turnbull and Gallagher 1991; Lyon, Deakin et al. 1994; Maccarana, Sakura et al. 1996).

Unlike HS biosynthetic enzyme knockout studies, mutations in HSPG core proteins generally stimulate mild defects, suggesting that core proteins are more dispensable and/or can be

compensated for. Syndecan4 knockout mice display defective fetal blood vessel formation (Ishiguro, Kadomatsu et al. 2000) and are more susceptible to renal damage (Ishiguro, Kadomatsu et al. 2001). Syndecan-3 null mice demonstrate defects in muscular development (Cornelison, Wilcox-Adelman et al. 2004), development of the digestive system (Westphal, Murch et al. 2000) and display impaired nervous system development (Kaksonen, Pavlov et al. 2002). Syndecan-1 null mice display defects in respiratory system development; specifically hypo-responsiveness (Xu, Park et al. 2005) and impairment in immune system function (Park, Pier et al. 2001; Gotte, Joussen et al. 2002). Gpc3 null mice result in overgrowth (Cano-Gauci, Song et al. 1999; Chiao, Fisher et al. 2002) and display skeletal problems attributed to a lack of BMP interaction (Paine-Saunders, Viviano et al. 2000). Perlecan-null mice display defects in fetal tissue development (Costell, Gustafsson et al. 1999).

1.2.5 Heparin: a close relative of HS

Heparin is a close structural relative or subset of the HS family, and unlike HS, which is found synthesised by all mammalian cells, heparin is restricted to mast cells, where its primary function is to store histamine and proteases (Montgomery, Lidholt et al. 1992).

Heparin and HS share the same polysaccharide backbone, as described previous; a repeating uronic-glucosamine disaccharide. The two molecules differ only in the degree of sulfation, and although the same pathway is used during biosynthesis, heparin undergoes more extensive sulfation and uronic acid epimerization. More than 85 % of GlcNAc residues are N-deacetylated and N-sulfated and more than 70 % of the uronic acid is converted to IdoA. Consequently, heparin is a more sulphated, homogeneous molecule, typically represented by approximately 2.4-2.6 sulfates/disaccharide, compared to heterogenous HS sulfation represented by 0.8 - 1.8 sulfates/disaccharide. Taken together, heparin is well-studied and

understood, and is therefore a long standing model or proxy molecule for HS (Rabenstein 2002; Carlsson, Presto et al. 2008).

1.3 Heparan sulfate in development

1.3.1 Early embryonic development

The importance of HS in development is outlined neatly by Lin et al., who demonstrate that $EXT1^{-/-}$ mouse mutants, deficient in HS synthesis, do not survive beyond gastrulation, thought to be attributed to an inability to implant into the uterine wall (Lin, Wei et al. 2000). Similarly, EXT2 null mice display arrested growth by day 6 and fail to develop (Stickens, Zak et al. 2005). Defects in other HS biosynthetic enzymes further emphasize the importance of HS sulfation in development. NDST1-deficient mice, display immature lung development, eye defects and defects in vascular development (Pallerla, Pan et al. 2007; Ringvall and Kjellen 2010); similarly NDST2-deficient mice display defective embryonic development (Forsberg and Kjellen 2001) and disruption in 2-O sulfation (HS2OST), was shown to result in principally the lack of kidney organogenesis (Bullock, Fletcher et al. 1998; Turnbull, Powell et al. 2001). HS sulfation is vital in throughout development and is conserved across many species (Gorsi and Stringer 2007), elegantly demonstrated since the loss of sulfation has been shown to affect Wingless (Wg), FGF and Hedgehog (Hh) (Lin, Buff et al. 1999; Toyoda, Kinoshita-Toyoda et al. 2000; Luders, Segawa et al. 2003), discussed in greater detail later. Furthermore, a loss of 6-O sulfation (HS60ST) is correlated with a lack of FGF, Wnt and BMP signalling (Kamimura, Fujise et al. 2001; Irie, Habuchi et al. 2003; Sedita, Izvolsky et al. 2004).

Aside from facilitating differentiation during development, it is thought that HS is also crucial to maintaining an ESC niche (Nurcombe and Cool 2007; Grunert, Nurcombe et al. 2008), emphasised by studies suggesting that HS is necessary for ESCs to sustain

pluripotency (Sasaki, Okishio et al. 2008). Furthermore self renewal of mesenchymal stem cells from human adult bone marrow is shown to be enhanced via supplementation with embryonic form of HS (HS-2)(Helledie, Dombrowski et al. 2011).

1.3.2 HS-protein interactions

Heparan sulfate-interacting proteins include growth factors, morphogens, ECM components and many more, of which most have been identified as functionally significant throughout development.

1.3.2.1. Heparin: an important anticoagulant

As mentioned, HS and heparin are structurally, very closely related. Understanding and studying heparin as a model for HS, has led to the idea that specific HS motifs and sulfation patterns facilitate specific protein binding, in turn governing signalling pathways. The classic example is the discovery of the antithrombin (AT)-binding pentasaccharide sequence in heparin (Petitou, Casu et al. 2003). Heparin was discovered in 1916 and over 20 years later was shown to have anticoagulant properties, providing a plasma cofactor was present (Abildgaard 1968). It has since been proven that the AT-binding region specifically consists of three GlcN residues (two of which are required to be N-sulfated), one GlcA and one IdoA, furthermore binding is enhanced upon the presence of two O-sulfated groups, a 6-O sulfate and a 3-O sulfate (Petitou, Casu et al. 2003). Alongside the AT-binding site, the requirement for a specific 3-O sulfated HS structure in the binding of herpes simplex protein to cell surface HS during infection (Shukla, Liu et al. 1999) exemplifies the important of specific sulfation pattern. Likewise it appears that 6-O sulfates may contribute importantly to specific protein binding and selectivity of recognition (Ashikari-Hada, Habuchi et al. 2004; Powell, Yates et al. 2004; Mahalingam, Gallagher et al. 2007). The relationship between HS sulfation pattern, conformation and activity has been difficult to establish fueling a debate within the glycomics field as to whether the important of HS sulfation pattern is actually an artifact of

HS conformation. Support for this, amongst many examples, is that the activation of the serpin protease inhibitor AT, by binding to this pentasaccharide is a consequence of conformational change which increases the rate of inactivation of proteases involved in coagulation (Factors IIa and Xa for example). The glycosidic linkage geometry is more recently proving crucial, both influencing and being influenced by the degree and position of sulfation. Biophysical techniques have shown that conformation stability of the glucosamine varies according to varying degrees of sulfation (Molloy, 1993 and Yates, 1996). Likewise, in one study, eight systematically sulfated HS structures were shown to alter the uronic acid conformation and upon conversion to different cation forms (Na^+, K^+, $Mg2^+$, $Ca2^+$ and $Cu2^+$ for example) resulted in distinct conformations and varying degrees of flexibility. Additionally Cu2+ and K+ conversions of HS modififed activated a previously inactive FGF2-FGFR1c signal (Rudd and Yates, 2007) exemplifying the influence conformation has on functionality.

1.3.2.2. HS-growth factor interactions

Growth factors are a class of soluble proteins that stimulate a wide range of cellular responses, for many of which HS mediates the function. The HS-FGF interaction is the most extensively studied.

HS-FGF complex

FGF signalling, as outlined previously, is crucial in early embryonic development. The integrity of FGF signalling is dependent on tight regulation of FGF activity and receptor specificity, which has been shown to depend on HS and the existence of a HS-FGFR-FGF complex (Pye, Vives et al. 1998; Guimond and Turnbull 1999), supported by the identification of a heparin-binding domain within the FGF structure (Eriksson, Cousens et al. 1991; Kan, Wang et al. 1993) and evidence that HS is thought to stabilise FGFs against

degradation and act as a storage reservoir for ligands (Hacker, Nybakken et al. 2005; Beenken and Mohammadi 2009).

The proposed signalling complex is thought to consist of an FGF dimer, bound to two receptors with an HS oligosaccharide. However, the physical orientation of the ligands, receptors and HS chains remains controversial (Plotnikov, Schlessinger et al. 1999; Plotnikov, Eliseenkova et al. 2001). In the instance of FGF1, Wu et al., propose that HS interacts both with FGF and FGFR and furthermore, since molar ratio of HS, FGF1 and FGFR1 were shown to be independent of HS size, suggested the complex must take place on the cell surface (Wu, Zhang et al. 2003). Powell et al., showed that both FGFR1 and FGFR2 bind to HS, albeit with different binding affinities owing to their kinetic, dynamic interactions with FGF (Powell, Fernig et al. 2002). Another study suggests that FGF and FGFR act together to identify suitable, unique HS motifs once bound together (Mohammadi, Olsen et al. 2005). Interestingly regarding the importance of HS sulfation, 6-O desulfated heparin was shown to display reduced selectivity for several different FGF-FGFR complexes, supporting the idea of tissue-specific nature of HS-FGF interactions (Zhang, Zhang et al. 2009). HS is shown to increase the binding affinity of FGF-2 by 10-fold therefore high concentrations of FGF can signal in a HS-free environment although high affinity signalling is limited to full ligand-receptor-HS structure (Pellegrini 2001). HS interaction with FGF-2 is shown to control cell-proliferation in the adult brain (Mercier and Arikawa-Hirasawa 2011), and is similarly important in breast carcinoma development (Qiao, Meyer et al. 2003).

Despite controversy surrounding the dynamics of the formation and structure of HS-FGF-FGFR interaction complex, there is growing evidence to suggest that the sulfated regions of HS underpin HS-FGF interactions. Although ionic interactions will encourage and dictate a general affinity for FGF-HS binding (Pye, Vives et al. 1998), more evidence exists for specific HS-FGF binding depending on specific arrangements of NA and NS segments

(Faham, Hileman et al. 1996; Ford-Perriss, Guimond et al. 2002) and since none of the amino acid residues in the HS binding region of FGF are conserved (Faham, Linhardt et al. 1998), it is likely that different FGFs have different affinities for different HS structures.

In *Drosophila*, the sulfateless gene (*Sfl*) resulted in unmodified HS, which could not activate FGF (Lin, Buff et al. 1999) and additionally, 2-O sulfation is shown to be required for FGF/FGFR binding and additional 6-O-sulfation is required for mitogenic activity (Rapraeger 1995; Pye, Vives et al. 1998; Guimond and Turnbull 1999).

HS-VEGF complex

The vascular endothelial growth factors (VEGFs) are a family of endothelial cell mitogens with potent permeability properties, crucial in vascular system development and angiogensis (Folpe, Veikkola et al. 2000; Veikkola, Karkkainen et al. 2000). VEGFs have also been shown to play a role in early embryonic development and surrounding tissues, since high levels of VEGF are detected in the early egg sac and hemangioblasts within the yolk sac by E8-11, as well as in multiple fetal tissues including lung, kidney and heart (Jakeman, Armanini et al. 1993; Cheung 1997).

Alternative splicing of VEGF gives rise to at least six isoforms, categorised by heparin-binding ability; $VEGF_{121}$ does not bind heparin, $VEGF_{165}$ binds with moderate affinity and $VEGF_{189}$ binds heparin strongly (Robinson and Stringer 2001). As in HS-FGF binding, there is evidence that HS binding is necessary to mediate VEGF function, for example many studies have demonstrated the importance of HS in the binding of $VEGF_{165}$ to VEGFR2 for mitogenic activity (Gitay-Goren, Soker et al. 1992; Gengrinovitch, Berman et al. 1999), and furthermore, a lack of HS-VEGF binding has been shown to disrupt VEGF concentration gradients in the ECM and display uncharacteristic extracellular localisation of VEGF, strongly implicating that HS plays an important role for HS in controlling VEGF diffusion.

Other HS-growth factor interactions (reviewed by Ori (Ori, Wilkinson et al. 2008), Zhang (Zhang 2010)) include hepatocyte growth factor (Lyon, Deakin et al. 1998; Rahmoune, Rudland et al. 1998), epidermal growth factor (EGF) (Dluz, Higashiyama et al. 1993), platelet-derived growth factor (PDGF) (Feyzi, Lustig et al. 1997; Feyzi, Trybala et al. 1997; Rolny, Spillmann et al. 2002) and transforming growth factor beta (TGFβ) (Lyon, Deakin et al. 1994; Mulloy and Rider 2006; Rider 2006).

HS-ECM components

HSPGs perlecan, agrin and collagen XVIII, as described previously, are major components of the ECM and owing to their residency in the ECM, interact with many other ECM components including fibronectin (Haugen, Letourneau et al. 1992), laminin (Dow and Riopelle 1990; Riopelle and Dow 1990; Battaglia, Mayer et al. 1992; Mayer, Kohfeldt et al. 1998), and collagens (LeBaron, Hook et al. 1989; Specks, Mayer et al. 1992) to contribute to ECM assembly and function. The importance of HS-ECM interactions was demonstrated since cells grown in sodium chlorate, a well known GAG-inhibitor, lacked the ability to produce a BM, attributed to a reduced capacity to bind laminin (Brauer, Keller et al. 1990). Furthermore, like many HS-protein interactions, HS-ECM interactions display a degree of specificity attributed to HS sulfation (Perrimon and Bernfield 2000).

HS-morphogen interactions

Morphogens are signalling molecules that re-locate from an original tissue to generate a gradient of morphogen concentration which functions to induce cellular responses via concentration-dependent activation of genes.

The distribution of morphogens during development determines cell fate and has often been shown to be regulated by HS, neatly demonstrated by *Drosophila* wing formation. Wingless

(Wg) (Wnt protein), Decapentaplegic (Dpp) a BMP protein and Hedgehog (Hh), three particularly important morphogens in wing patterning (Strigini and Cohen 1999) are shown to depend on adequate HS binding, since disruptions in HS biosynthetic enzymes was shown to affect Hh diffusion (Bellaiche, The et al. 1998), Wg and Hh functionality (bornemann 2004, takei 2004).

Interestingly, like HS-FGF, HS sulfate motifs have been demonstrated to be of great importance in HS-morphogen interactions; for example mutations in the sulfateless gene in Drosphillia (*Slf)* which competes with PAPs to prevent sulfation, is shown to disrupt Wg signalling (Binari, Staveley et al. 1997; Hacker, Lin et al. 1997). Furthermore, FGFs acting as morphogens, for example during mesoderm patterning from the cardiac tissue to foregut and endoderm in liver and lung development (Serls, Doherty et al. 2005), are dependent on HS sulfation, exemplified by the requirement for FGF8 gradient in the embryo stimulating downstream phosphorylation with consequential embryo development (Dubrulle and Pourquie 2004).

1.3.2.3 HS Tissue specificity

HS purified from different tissues/cell types has led to identification of structural differences depending on tissue of origin (Naimy, Leymarie et al.; Warda, Toida et al. 2006). HS has been isolated and purified from a wide variety of animals from *C.elegans* to humans (Gomes and Dietrich 1982; Dietrich, Nader et al. 1983; Warda, Toida et al. 2006) and substantial differences in HS structure have been identified (Linhardt, Turnbull et al. 1990; Medeiros, Mendes et al. 2000; Toyoda, Kinoshita-Toyoda et al. 2000; Warda, Mao et al. 2003; Vongchan, Warda et al. 2005).

Allen et al., neatly demonstrated that HS is tissue-specific using the HS-FGF complex as a model tool. Mice embryos responded to different FGFs depending on developmental stage;

for example FGF4 was not shown to recognise HS in the heart and major blood vessels but was apparent in all other tissues (Allen, Filla et al. 2001). Furthermore, FGF10-FGFR-HS complex is detected in varying stages of development for the activation of specific pathways at specific times (Avivi, Yayon et al. 1993; Yan, Fukabori et al. 1993; Igarashi, Finch et al. 1998; Patel, Knox et al. 2007). Tissue-specific differences in HS is likely to exist because of affinity and binding ability attributed to specific HS structures (Faham, Linhardt et al. 1998). This is supported by work which highlights the specificity of different FGFs for different FGFRs; FGF4 affinity for FGFR1 and FGFR2 depends on HS concentration (Aviezer, Safran et al. 1999). Furthermore, specific patterns of HS N-sulfation and O-sulfation have been shown to activate different FGFs; 1, 2 and 4 for instance (Guimond and Turnbull 1999; Kreuger, Jemth et al. 2005; Harmer 2006).

Moreover, HSPGs have been shown to undergo structural changes during progressive pathological events (Lindahl and Lindahl 1997; Rykova and Grigorieva 1998). Collectively, these results support the idea that structure and function of HS is hugely diverse of HS across organs, species, developmental stages and disease status.

1.4 Biomaterials

Considering the complex nature of the ECM *in vivo,* as demonstrated extensively in previous sections, it is unsurprising that bioengineers are struggling to meet the demands for an artificial ECM. As mentioned, any ESC-based clinical application requires a standardised system of generating high ESC numbers. Therefore a biomaterial demonstrating biocompatibility, mechanically stability, cost efficacy and ease of surface modification is required for cell expansion. Materials with all these properties are currently elusive.

1.4.1 Overview of biomaterials

Biomaterials represent synthetic materials with excellent biocompatibility defined as 'the ability of a material to perform with an appropriate host response in a specific application' (Williams 2003). Biomaterials were in some capacity exploited in the early 1900's, when bone plates were successfully implemented to stabilise bone fractures and to accelerate their healing. By the 1950's, blood vessel replacement using polymers was in clinical trials (Chlupac, Filova et al. 2009) and artificial heart valves and hip joints were in development from the 1970s.

Biomaterials are generally classified into three groups and subcategorised according to application, whereby they display different mechanical properties, outlined in Table 1.2. Several classes of biomaterials can be used in any one application such is the demand of biomaterials to function seamlessly and dynamically, as natural materials would.

Orthopaedic applications

Metallic materials are typically employed as load bearing members of a joint replacement for example (pins, plates and femoral stems for instance) in conjunction with a ceramic wear-resistant surface; alumina or zirconia for example (Heimke, Leyen et al. 2002; Campbell, Shen et al. 2004). Hydroxyapatite is often used

Table 1.2 Classifications of biomaterials; metals, ceramics and polymers and their applications according to physical properties

Class	*Sub-class*	*Properties*		*Common application*
		+	-	
Metals	Titanium Cobalt-chromium Alloys 316L stainless steel	Strong, load bearing	Expensive, corrosive	▪ Joint replacements ▪ Orthopaedic fixation ▪ Stents
Ceramics	Alumina Zirconia Carbon Hydroxyapeptite	Wear resistance, hardness	Brittle; fail under tension	▪ Dental implants ▪ Joint parts
Polymers	Polystyrene Poylethylene Gortex Polyurathane	Cheap to manufacture and easily chemically modified	Poor mechanically; lack rigidity and strength	▪ Joint sockets ▪ Sutures ▪ Blood vessels

for bone-bonding applications to assist implant integration (Chen, Wong et al. 2004; Porter, Buckland et al. 2006) and polymers such as ultra high molecular weight polyethylene (UHMWPE) are used as articulating surfaces against ceramic components in joint replacements (Davidson and Schwartz 1987; Davidson 1993).

Dental applications

Metallic biomaterials have long been successfully employed as pins for anchoring tooth implants, mimicking the root of a tooth as well as in parts of orthodontic devices, whilst ceramics have found uses as tooth implants including alumina, zirconia and dental porcelains (Ozkurt and Kazazoglu), owing to their wear-resistant nature. Hydroxyapatite has been used for coatings on metallic pins and to fill large bone voids caused by disease or trauma. Likewise, polymers are also in used as orthodontic devices such as plates and dentures.

Cardiovascular

Many different biomaterials are used in cardiovascular applications depending on the specific application and design. For instance, carbon in heart valves and polyurethanes for pace maker leads (Stokes and Cobian 1982). Vascular grafts are typically made of polytetrafluoroeythlene (PTFE) (Peck, Gebhart et al.) and vascular stents can be made from titanium or polymers or both (Steinemann 1998; Stone, Ellis et al. 2004) depending on its function and longevity requirements.

Cosmetic

Silicones have been used in cosmetic surgery for applications such as breast augmentation (Duffy 1990; Duffy 2005) and chin and nasal replacement during maxillofacial surgery (Hinderer 1991). Polymers represent the optimal material for contact lens applications, owing to their sophisticated transparency, flexibility, hydrophilicity and oxygen-permeability properties (Wheeler, Woods et al. 1996; Nicolson and Vogt 2001; Goda and Ishihara 2006).

This project is underpinned by the long-term goal of synthesizing and optimising a synthetic substrate to act as an artificial ECM for routine, long-term ESC expansion, thus replacing current animal-derived materials, which limit ESCs from reaching clinical phase.

Polymers represent a class of biomaterials which suit ESC scale-up applications; in terms of cost effective, simple manufacture and ease of chemical manipulation. The lack of mechanical strength does not influence their applicability here, since *in vitro* culture of ESCs does not involve the exertion of much force.

Polymers, or 'plastics', represent chemical compounds consisting of repeating structural units created via polymerisation, which gives rise to a macromolecule of high relative molecular mass, consistent with natural, biological polymers, such as polyamides (proteins), polynucleotides (nucleic acids) and polysaccharides. A polymer of the same repeating monomer is termed a *homopolymer*, whilst variations in monomer backbone structures define a *copolymer*.

Polymer properties and attributes are governed by the monomers which make up the polymer, the bonding between monomers, the physical arrangement of this monomer backbone and polymer chain length, which collectively gives rise to a specific microstructure and architecture, as a consequence of polymerisation.

Polystyrene

Discovered in 1839, polystyrene (PS) is a homopolymer comprised of styrene monomers, represented by a hydrocarbon backbone. PS properties are generally determined by relatively weak attractions between polymer chains, known as van der Waals attractions, which confer flexibility and elasticity. During manufacture, upon heating, PS chains slide past each other, underpinning the ability of PS to be easily softened and moulded to suit any shape or application (Figure 1.8).

Tissue culture polystyrene (TCPS), commonly known as 'tissue culture plastic', has been used for the expansion of cells *in vitro* since the 1960s (Curtis, Forrester et al. 1983), largely

because it is cost effective to manufacture, clear and solid at room temperature and importantly, can withstand sterilisation involving high pressures and temperatures (Jayabalan 1995; Sladowski, Grabska-Liberek et al. 2008). TCPS differs from PS only in surface treatment, since PS is modified to optimise electrostatic and hydrophobic cell-biomaterial interactions, necessary due to the non-adhesive nature of polystyrene (Maroudas 1977; Ward, Knox et al. 1977; Grinnell 1978). However, TCPS is often further modified, depending on application, using animal-derived materials to serve as an ECM, examples of which include collagen (He, Ma et al. 2005; Wojtowicz, Shekaran et al. 2010), fibronectin (Barrias, Martins et al. 2009; Maciel, Oliveira et al. 2012), laminin (Huber, Heiduschka et al. 1998; Huang, Huang et al. 2007), and gelatine (Goetz, Scheffler et al. 2006; Hosseinkhani, Hosseinkhani et al. 2008; Rao and Winter 2009; Sun, Huang et al. 2012). It is therefore clear that TCPS never truly interacts with any cells (cells sit on the cell-derived coating not the TCPS), but instead acts merely as a platform on which to build an animal-derived substrate. Thus, there such is an on-going effort to identify an entirely synthetic material to support ESC scale-up and eradicate the usage of animal products.

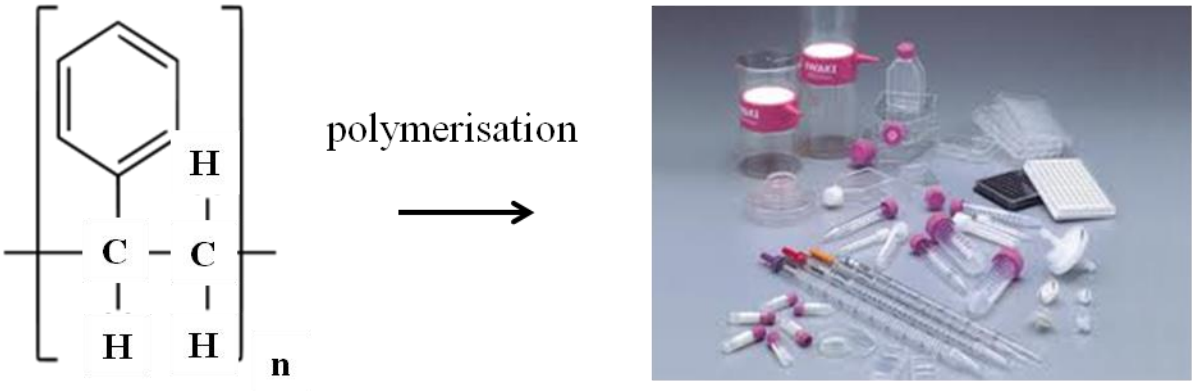

Figure 1.8. Polystyrene application in cell culture. Styrene monomers represent the hydrocarbon polystyrene backbone, which can be easily softened and moulded to suit the application or shape. PS is often treated to enhance surface properties for cell-based applications and typical laboratory plasticware includes tissue culture dishes, culture plates, disposable pipettes and culture media bottles (from www.agc.com).

Since TCPS, what's new?

Since the discovery and common employment of TCPS for cell culture, many different polymers have been identified as biocompatible and now successfully function in an array of medical applications, outlined in Table 1.3. These polymers therefore represent great promise in the area of ESC scale-up too, and many are currently being explored as TCPS alternatives, as well as in tissue-engineering applications.

Table 1.3 Uses of common polymers in medical applications and corresponding monomers

Polymer	Name	Application
PE	(poly) ethylene	▪ Catheters ▪ Hip prostheses
PET	(poly) ethylene terephalate	▪ Vascular grafts (Struszczyk, Bednarek et al. 2002) ▪ Vertebrae disc prostheses (Ambrosio, De Santis et al. 1998)
PMMA	(poly) methyl methacrylate	▪ Bone cement (Reichenberger, Stoff et al. 2007) ▪ Dental materials (Kaufmann, Jensen et al. 2002)
PTFE *(GORE-TEX)*	(poly) tertrafluoroethylene	▪ Synthetic blood vessels (Sanchez, Wain et al. 1997) ▪ Patches for tissue regeneration (Koschwanez and Broadbent) ▪ Surgical sutures
PEG	(poly) ethylene glycol	▪ Laxative ▪ HMW PEG used as dietary preventative for colon cancer (Corpet, Parnaud et al. 2000) ▪ Suppressor of carcinogens(Borgens and Bohnert 2001)

PDMS	(poly) dimethylsiloxane	▪ Heart valve ▪ Drug-delivery devices ▪ Intravitreo implants
HEMA	(poly) 2- hydroxethyl methacrylate	▪ Contact lens ▪ Catheters

1.4.2. Optimising polymer surfaces to enhance polymer-cell interaction

Polymer properties and functionality in medical devices are not normally determined by bulk properties but instead related more to the micro and nano structures on the surface. Surface properties are usually underpinned by wettability, hydrophilicity, roughness and ionic charge, reviewed (Wang, Robertson et al. 2004; Ma, Mao et al. 2007) and manipulation of these features chemically, can provide the potential to tailor any polymer surface to suit a specific application.

The importance of polymer surface properties is outlined by studies which demonstrate that the control of cellular behaviour can be attained using various polymer surface patterning techniques; for example neuron behaviour can be controlled by nano-patterned polymer surfaces (Murugan, Molnar et al. 2009) and similarly, nano-patterning has been shown to direct differentiation of hMSCs (Curran, Chen et al.). Furthermore, the performance of PDMS in microfluidic devices has been successfully enhanced via altering surface wettability (Zhou, Khodakov et al.) and osteoblast expansion for bone regeneration and engineering, has been enhanced via chemical manipulation of polymer surface properties (Saranya, Saravanan et al.).

1.5 Work leading to current studies

Preliminary work from our group suggested that HS is required for the differentiation of extraembryonic endoderm (EEE) in mESC-derived EBs and that ESCs synthesise low levels of sulfated HS. Furthermore it was suggested that the loss of differentiation to EEE from mESCs, attributed to a lack of serum and feeders, cannot be rescued when cells were re-plated onto heparitinase-treated feeders. Taken together, and considering the requirement of FGF in EEE differentiation, it is likely that EEE facilitates FGF signalling and vice versa, in an HS-dependent manner.

This raised a number of questions to be addressed in the current study including; (i) is HS required for differentiation of mESCs to other lineages, (ii) is HS present in feeders and/or serum and if so (iii) what HS structures are present and finally, (iv) could this information be exploited to synthesize artificial substrates with stem cell regulatory properties?

1.6 Project Aims

1. Identify differences in mESC behaviour according to variations in culture conditions, and thus determine if feeder cells, or serum, or both are required for differentiation.
2. Identify the requirement for HS in specific lineage commitment; primarily to endoderm differentiation.
3. Identify differences in structure of HS from ESCs, according to culture condition.
4. Determine if exogenous HS can rescue defects in EB development due to variant culture conditions.
5. Evaluate novel polymers and polymer-HS conjugates for supporting the growth and differentiation of mESCs.

2. Materials and Methods

2.1 Materials

2.1.1 Solutions

0.1 % w/v gelatine: 1 g porcine gelatine was added to 1 L distilled water and autoclaved.

4 % (w/v) paraformaldehyde (PFA): 4 g PFA was added to 100 mL PBS in conical flask, heated to 60°C and agitated with magnetic flea in fume cupboard until PFA had dissolved and solution was clear. It was stored at 4 °C for 1 week.

15 % sucrose: For 1 L, 150 g sucrose was added to 1 L 1 X PBS.

7.5 % gelatine: For 100 mL: 7.5 g porcine gelatine and 15 g sucrose was added to 100 mL 1 X PBS.

Toluidine blue solutions

Stock; 1 % toludine blue: For 50 ml: 0.5 g tolluidine blue in 50 ml 70 % EtOH.

Working; 0.1 % toluidine blue: For 50 ml: 5 ml tolludine blue stock solution in 45 ml 1 % sodium chloride in water.

Subbing solution: 500 mL distilled water was heated to 60°C and 2.5 g gelatine type A (bloom 300, Sigma) was added (0.5 % solution). The solution was mixed vigorously with magnetic flea (temperature not allowed to exceed 60°C), until completely dissolved and then allowed to cool to 40°C. Once sufficiently cooled, 0.25 g chromium potassium sulphate (CrKSO4.12H20) was added (0.05 % solution).

BODIPY solution: 5 mg of BODIPY was freeze-dried and solid content was transferred to eppendorph tube. 1 ml of pre-chilled methanol was added to original viale.

2.1.2 Buffers

10 X phosphate buffered saline (PBS): For 1 L, 80 g NaCl, 2.0 g KCl, 11.5 g Na_2HPO_4 and 2.0 g KH_2PO_4 were added to 1 L distilled water and autoclaved (For 1X PBS 100 mL of 10 X solution was added to 900 mL dH_20).

5 X lyase buffer: 500 mM sodium acetate, 0.5 mM calcium acetate: For 10 ml, 0.4102 g sodium acetate, 1 ml of 500 mM stock, added to HPLC-grade water

SAX – HPLC buffers

A: 150 mM NaOH: For 1 L, 15 ml NaOH added to 1 L HPLC-grade water.

B: 2 M NaCl 150 mM NaOH: For 1 L, 15 ml NaOH, 116.88 g NaCl added to 1 L HPLC-grade water.

D: 2 M NaCl 300 mM NaOH: For 500 mL, 15 ml NaOH, 58.44 g NaCl added to 500 mL HPLC-grade water.

2.1.3 Cell lines

STO cells, a mouse embryonic fibroblast cell line, were a gift from Dr Neil Smith, Cardiff University, Wales.

E14 mESCs, a mouse embryonic stem cell line were a gift from Professor Mark Boyd, University of Liverpool, UK.

$EXT1^{-/-}$ mESCs, a HS deficient mouse embryonic stem cell line, were a gift from Dr Cathy Merry, University of Manchester, UK.

KSCs-GFP, a kidney-derived stem cell GFP-expressing line, were derived by Dr Ranghini, University of Liverpool.

2.1.4 Biomaterials

Polymers were synthesised in-house at SpheriTech (The Heath, Science Park, Runcorn), our CASE partner. Hydrogels and poly-Ɛ-lysine (PƐL) macroporous polymers were synthesised as outlined below in Table 2.1 and 2.2, respectively.

Table 2.1 Synthetic SpheriTech hydrogels and corresponding compositional ratios. Sixteen different hydrogels were employed as potential biomaterials for ESC maintenance and support; their compositional ratios are outlined.

copolymer	*Methacrylic*	*Acrylic*	*PEG 360 methacrylate*	*PEG 526 methacrylate*	*2-hydroxethyl methacrylate*	*M-N dimethyl acrylamide*
1	1		1			
3	1			1		
5	1				1	
6	1				15	
7		1	1			
9		1		1		
11		1			1	
12		1			15	
13		1				1
14		1				15
15	1					1
16	1					15

Table 2.2 Poly-Ɛ-lysine (PƐL) macroporous polymers composition

Component
Poly-Lys
Dicarboxylic acid
N-hydroxysuccinimide (NHS)
Water soluble carbodiimide (WSC)

2.2 Methods

2.2.1 Cell Culture

2.2.1.1 Preparation of gelatineised culture dishes

0.1 % (w/v) gelatine solution was added to tissue culture dish and incubated at RT for approximately 15 min. The gelatine solution was aspirated and replaced with media when necessary.

2.2.1.2 Medium

STO/EB medium High glucose DMEM (Gibco, Invitrogen, UK) was supplemented with 10 % fetal bovine serum (PAA), 2 mM L-glutamine (Gibco Invitrogen, UK), 1 % NEAA (Gibco, Invitrogen, UK), 1 mM 2-βmercaptoethanol (Gibco Invitrogen, UK).

ESC medium Advanced^{TM} high glucose DMEM (Gibco, Invitrogen, UK) was supplemented with 1 mM β-mercaptoethanol (Gibco, Invitrogen, UK), 2 mM L-glutamine (Gibco, Invitrogen, UK), 1000 U / mL leukaemia inhibitory factor (LIF) (Millipore, UK) and 2% fetal bovine serum (PAA).

Serum free medium Advanced^{TM} high glucose DMEM (Gibco, Invitrogen, UK) was supplemented with 1 mM β-mercaptoethanol (Gibco, Invitrogen, UK), 2 mM L-glutamine (Gibco, Invitrogen, UK) and 1000 U / mL leukaemia inhibitory factor (LIF) (Millipore, UK)

2.1 Routine culture of E14 mESC

E14 mESCs were cultured on 3.5 cm tissue culture dishes (Nunc, Thermo Scientific, Denmark) coated with 0.1 % gelatine in mESC medium. mESC medium was removed from confluent dish of E14 mESCs and cells were washed once with PBS. 1 x trypsin/EDTA (PAA, UK) was added for 3-5 min, and subsequently neutralised with STO medium, before centrifugation at 64g for 2.5 min. STO medium was removed and E14 mESCs resuspended in mESC medium depending on culture condition, outlined in Figure 2.1. Typically, E14

mESCs were sub-cultured every second day at a ratio of 1:3 and incubated at 37°C and 5 % CO_2, unless otherwise stated.

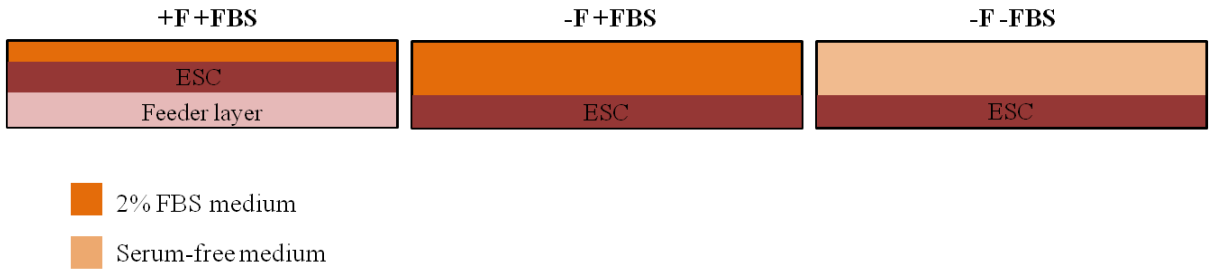

Figure 2.1 Schematic outlining the three distinct 2D culture conditions employed during E14 mESC expansion, throughout this study. mESCs were maintained in the presence of 2% FBS and on a feeder layer (+F +FBS); a culture condition commonly employed for expansion and maintenance of mESCs. A second condition was feeder-free, whilst medium is supplemented with 2% FBS as before (-F +FBS). Thirdly, mESCs were maintained in a serum-free, feeder-free culture system (-F –FBS). All three culture conditions were supplemented with LIF.

2.2.1.4 Serum-free E14 mESCs culture

mESCs were cultured in mESC medium, except that FBS was not added to medium. Under these conditions sub-culture technique is exactly as described previously, except mESCs were passaged every 3.5 days.

2.2.1.5 Serum-free E14 mESCs culture supplemented with heparin

mESCs were cultured exactly as described in 2.2.1.4, however dishes were supplemented with 1 µg/mL porcine mucosal heparin (Celsus, #HO-3105; www.heaprin.com) immediately prior to incubation.

2.2.1.6 Routine culture of STO feeders

STO cells were cultured in 10 cm tissue culture dishes (Corning) and coated with 0.1 % gelatine in STO medium. STO medium was removed from a confluent dish of STO cells and cells were washed once with PBS. 1 x trypsin/EDTA was added for 3-5 min, and

subsequently neutralised with STO medium, before centrifugation at 64g for 2.5 min. STO medium was removed and cells re-suspended in fresh STO medium. STO cells were sub-cultured every second day at a ratio of 1:4 and incubated at 37°C and 5 % CO_2.

2.2.1.7 Preparation of STO feeders

One confluent 10 cm dish of STO cells were inactivated with mitomycin-C (Gibco, Invitrogen, UK). 5 mL of total 10 mL of STO medium was removed from a confluent dish and 100 µL of 1 mg / mL stock of mitomycin-C (final concentration = 20 µg/mL) added. The cells were incubated for 2 h in 37 ° C and 5 % CO_2. The medium was removed and cells washed thoroughly three times with PBS, then 5 mL 1x trypsin/EDTA was added for 3-5 min. The trypsin was neutralised by transferring to 5 mL STO medium before centrifugation at 64g for 2.5 min. STO medium was removed and cells re-suspended in 9 mL STO medium. 0.5 mL of cell suspension was added to 12 x 3.5 cm gelatineised tissue culture dishes. The volume was made up to 1.5 mL with STO medium and incubated at 37°C and 5 % CO_2.

2.2.1.8 Routine culture of mKSCs-GFP

mKSCs-GFP were cultured in 10 cm tissue culture dishes (Corning) and coated with 0.1 % gelatine in medium supplemented with 10% FBS. Medium was removed from a confluent dish of KSCs-GFP and cells were washed once with PBS. 1 x trypsin/EDTA was added for 3-5 min, and subsequently neutralised with medium, before centrifugation at 64g for 2.5 min. Medium was removed and cells re-suspended in fresh medium. KSCs-GFP were sub-cultured every second day at a ratio of 1:4 and incubated at 37°C and 5 % CO_2.

2.2.1.9 Freezing cells

Medium was removed from the culture dish and cells were washed once with PBS, followed by trypsinisation with 1 X trypsin/EDTA for 3-5 min, which was neutralised with equal volumes of STO medium, before centrifuging at 64g for 2.5 min. Medium was again

removed and cells were re-suspended in cell culture freezing medium (Gibco, UK), typically in 0.5 mL volume in a cryovial. The cryovial was placed in a freezing chamber containing isopropanol overnight at - 80°C. The cells were transferred to liquid nitrogen if long term storage was necessary.

2.2.1.10 Thawing of cells

The cryovial containing the desired cells was removed from liquid nitrogen and thawed rapidly in a water bath at 37°C. The cells were then transferred to STO medium and centrifuged at 64g for 2.5 min. Medium was removed and replaced with appropriate medium (depending on cells i.e. STO medium for STO cells), and cells were finally transferred to culture dish and incubated at 37°C 5 % CO_2.

2.2.1.11 EB formation

Medium was removed from 3.5 cm dish of E14 mESCs and cells were washed once with PBS. 1 mL 1xtrypsin/EDTA was added for 3-5 min, and neutralised with 1 mL mESC medium, before centrifugation at 64g for 2.5 min. The medium was removed and cells were re-suspended in STO/EB medium (volume depends on number of dishes of EBs is required). If mESCs were previously cultured on plain tissue culture dishes, cells were counted using haemocytometer (cells/mL) and an appropriate density of mESCs were plated onto bacteriological dishes (Sarstedt) containing appropriate volume of STO/EB media (typically used 200 x 10^3 cells/mL, total volume 1.5 mL). If mESCs were previously cultured on feeders, following re-suspension in STO/EB media after centrifuge, cells were transferred to gelatineised 6 cm dish and incubated for approximately 1 h to reduce the number of feeder cells. After incubation, cells remaining in suspension were counted and an appropriate density was seeded onto bacteriological dishes, as previously described. The medium was changed every 2 days by swirling the culture dish in circular motion until EBs gathered in

centre of dish, old medium was aspirated from edge and replaced with fresh STO/EB medium.

2.2.1.12 Maintenance and expansion of KSCs-GFP on macroporous poly-Ɛ-lysine based polymers

Kidney-derived stem cells (KSCs) derived from mice expressing green fluorescent protein (KSC-GFP) were seeded at a density of 2 x 10^5/mL onto PƐL-based polymers using a trans-well insert, as outlined in Figure 2.2. KSCs-GFP were allowed to proliferate and medium was changed every second day, via aspiration from upper and lower chambers.

2.2.1.13 Cell viability (Trypan blue)

Cell suspension (1 x 10^5 cells/mL) was diluted 1:1 with 4 % trypan blue solution and allowed to incubate at room temperature for 1 – 2 min. Cells were counted using a haemocytometer, whereby stained blue cells were counted as unviable and unstained cells were counted as viable cells. This was repeated in triplicate for each condition and time-point from more than three biologically distinct populations.

2.2.1.14 Quantification of cell proliferation

STO and KSC-GFP proliferation were analysed with regard to interaction with different PƐL macroporous polymers over time, using an MTS assay (Promega, CellTiter96 #G5421, UK). At appropriate time-points (dependent upon time-point of interest), the MTS compound was added to the upper chamber of the trans-well (1:5 MTS/PMS:medium, with final concentrations 333 μg/mL , 25 μM) and incubated for 4 hours at 37°C and 5 % CO_2. Subsequently, 100 μL of MTS/PMH-medium solution was added to 96-well plate and absorption was measured at 490nm using nanodrop spectrometer (Nanodrop 2000, ThermoScientific, UK). Absorption readings were measured in triplicate for each condition and each time-point, from three biologically distinct culture dishes.

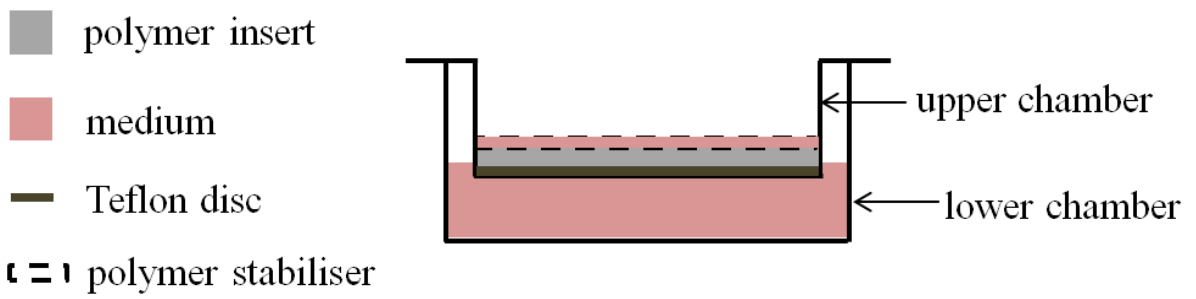

Figure 2.2 Schematic diagram depicting the trans-well set-up used to culture KSCs-GFP on PƐL-based macro porous polymers. KSCs-GFP were seeded onto PƐL discs which had been cut appropriately to fit the trans-well insert in a 6 well dish, where a Teflon disc and a polymer stabiliser were used to secure the polymer in position throughout culture. 3 ml KSC medium was added to the lower chamber and 0.5 ml added to upper chamber each time medium was added/replaced.

2.2.1.15 Poly-Ɛ-lysine-based polymer synthesis

PƐL macroporous polymers were synthesised via solubilisation of poly-Lys in distilled water, heat-induced linkage with NHS to form polymer backbone, and activation of polymerisation via carboxylic bonding with dicarboxylic (components of which were outlined in Table 2.3), generating a stable polymer with 100 % neutralisation (105% cross-linkage). However, in the case of PƐL polymer cross-linked with RGD, compositional ratios varied accordingly. Moreover in the case of PƐL polymers which were modififed with HS compounds via ionic interactions, cross-linking was reduced via reduction of NHS component.

2.2.1.16 Sterilisation and preparation of polymers

Polymers were washed three times in 100 % EtOH, followed by three washes with 1 X PBS and exposure to UV light for 1 hour prior to contact with KSCs-GFP. Similarly with Teflon discs and the polymer stabiliser rings used in the trans-well set up; both were soaked in 100 % ethanol overnight and washed three times in 1 X PBS, followed by UV exposure for 1 hour prior to usage in culture system.

2.2.1.17 Surface modification of poly-Ɛ-lysine based polymers

Six different HS-mimetic compounds, four of which are synthetic and made in-house* (University of Liverpool, UK), outlined in Table 2.4, were passively adsorbed onto surface of polymers via ionic interactions. 50 µg/mL of each HS compound was added to the surface of poly-Ɛ-lysine based polymer discs, once the polymers had been secured into trans-well set up, and incubated for 1 h, followed by three washes with 1 X PBS. Gelatine and FBS were adsorbed in exactly the same manner, as positive controls.

Table 2.4 HS compounds adsorbed to surface of poly-Ɛ-lysine macroporous. Six different HS mimetic heparin compounds were adsorbed to surface of PƐL via ionic interactions, as a method of discrete polymer surface modification.

HS compound	*Sulfation*
PMH	Heparin control – homogenous sulfation pattern
PMHS	HS control – heterogenous sulfation pattern
NAc	Unsulfated HS structure
2OS	Low sulfation at 2-O position only
6OS	Low sulfation, at 6-O position only
Per	Over-sulfated HS structure

2.2.2 Immunochemistry and histology

2.2.2.1 Fixation of cells (mESCs, STO, EXT1$^{-/-}$ or KSC-GFP)

The medium was removed and 4% PFA was added to the cells. The cells were incubated at RT for 5 min, before removing PFA and washing cells thoroughly three times in PBS. Cells were stored for up to 7 days in 4°C until needed.

2.2.2.2 Fixation of EBs

EBs were transferred from 3.5 cm dish to 15 mL conical flask and allowed to settle to bottom. For relatively young EBs (i.e. 2/3 days) EBs were centrifuged at 64g for 1 - 2 min.

The medium was removed and replaced with 4% PFA, and cells were incubated with PFA at RT for appropriate length of time (1-3 d EBs -10 min; 4-7 d EBs – 20 min; 7d – 30 min). After incubation, PFA was removed and EBs were washed three times in PBS. Samples were stored at 4°C in PBS until needed.

2.2.2.3 Gelatine embedding

PBS was aspirated from EBs, and 10 mL 15 % sucrose was added. Cells were left to soak in sucrose solution overnight at 4°C. The sucrose solution was removed and replaced with 4 mL 7.5 % gelatine solution (molten). Cells were incubated in a water bath at 37°C for 30-60 min (sometimes more) until EBs had dropped. During incubation, several mLs of molten gelatine was added to weighing boat and allowed to set. After water bath incubation, gelatine solution was removed from EBs, leaving 100 – 500 µL. Carefully, droplets of EB (within the gelatine) were plated onto the set gelatine in the weighing boat. Once gelatine droplets had set, EBs were cut from the weighing boat and mounted onto cork disc using cryoprotectant (OCT). EBs within the gelatine were covered in cryomount and, using forceps, they were transferred to a beaker of chilled isopentane. Once samples had turned white, they were transferred to liquid nitrogen (LN). Samples were retrieved from LN, wrapped in aluminium foil and stored at – 20 ° C until sectioning.

2.2.2.4 Sectioning EBs

Samples were cut using cryostat set at – 20°C and 10µm thickness. Once cut, sections were transferred to subbed slide.

2.2.2.5 Preparation of subbed slides

Slides were loaded into slide holder, soaked in 100 % EtOH for 10 – 15 min and washed five times in PBS. Slides were left soaking in distilled water whilst subbing solution was made up. Each slide was dipped in the subbing solution for 25 seconds and allowed to dry overnight.

2.2.2.6 Toludine blue stain

Frozen EB sections were placed into a coplin jar containing 1 X PBS and incubated in a water bath at 37°C for 30 min to ensure EB sections were adequately thawed and that the gelatine had melted off. Slides were placed in a slide rack and submerged in dish containing toluidine blue working solution. The slide rack was removed and submerged in water for several seconds and repeated three times, immediately followed by submerging in 95 % EtOH for 2 min, followed by submerging in 100 % EtOH for a further 2 min. The slides were then transferred to xylene for 3 min before mounting with histomount, and applying a coverslip.

2.2.2.7 Immunostaining of cells

PBS was aspirated after fixation and washing step and blocking solution was applied (10 % fetal bovine serum, 0.1 % Triton X-100 in PBS). Cells were incubated with blocking solution at RT for 40-60 min. After incubation, the blocking solution was removed and the primary antibody solution was added, cells were incubated at 4°C overnight. After incubation with primary solution, cells were washed three times in PBS, the first two washes for 5 seconds and final third wash was left during preparation of secondary antibody. Secondary antibody solution was added to cells and cells were incubated at RT for 1 – 2 h. After incubation with secondary antibody solution, cells were washed thoroughly three times in PBS. When counterstaining with DAPI, DAPI solution was applied instead of third wash (1 mL DAPI: 1 µL (1/100** working stock + 1 mL PBS) and cells were incubated at RT in dark for 5 min. Cells were washed three times in PBS and mounted on a slide with a coverslip and fluorescent mountant. Staining was visualised using an inverted microscope (Leica microsystems, 291185).

All solutions were centrifuged for 5 min at 13,000 rpm.

2.2.2.8 Immunostaining of EBs

Slides were placed in a coplin jar filled with PBS in water bath at 37°C for approximately 20 min to ensure that the gelatine had melted off. A hydrophobic pen was used to highlight EBs location on slide. Staining procedure is as in the case of immunostaining of mESCs, except permeabilisation with Triton-X is unnecessary.

Antibodies used were against pan-laminin (1:100, #L9393, Sigma-Aldrich, USA) laminin alpha 1 (1:200, #ab78287, abcam, Cambridge, UK) Oct4 (1:500 Santa Cruz Biotechnology Inc.), Nanog (1:400, #ab80892, abcam, Cambridge, UK), Gata6 (1:400, #AF1700 R&D Systems Inc.), 10E4 (1:100, Seikagaku Biobusiness Corporation, #370255), 3G10 (1:200, Seikagaku Biobusiness Corporation, #370260). Secondary antibodies were Alexa-488 chicken-anti goat IgG (H+L), Alexa-594 chicken-anti goat IgG (H+L), Alexa 488 goat-anti rabbit IgG (H+L), Alexa-594 goat-anti rabbit IgG (H+L) (A11012, Invitrogen), Alexa-594 goat-anti mouse IgG2b (γ2b). The negative controls for all antibodies can be found in Appendix I.

2.2.2.9 Immunostaining of polymer sections

After appropriate time of incubation with cells polymers were embedded in gelatine and sectioned, exactly as outlined in 2.2.2.3 and 2.2.2.4, respectively. Immunostaining was conducted as in the case of EB sections, again outlined previous, 2.2.2.7.

2.2.2.10 Quantification of immunostaining

Quantification of immunostaining was achieved by counting cells displaying positive immunoreactivity, typically conducted for four discrete regions on any one dish, repeated over three biologically distinct dishes. In the case of Nanog, whereby expression is typically represented by a gradient of immunoreactive intensities in any one population, only highly intensely positive cells, were counted as positive, exemplified in Figure 2.3. For

quantification of existence of basement membrane (laminin and LamA1 expression), a scaling system was used whereby EBs were counted as positive if a continuous BM was present in > 50 % of the EB circumference, outlined in Figure 2.4.

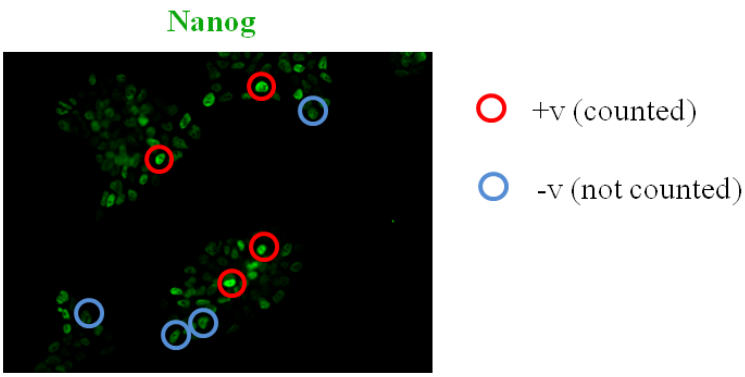

Figure 2.3 Diagram outlining the quantification of a Nanog immunostain. Typically, Nanog immunoreactivity is represented over a range of intensities in any one cell population, therefore a system was used whereby only highly intensely positive cells were counted as positive (red circles) and counted in any quantification, whilst low intensely positive cells were not counted (blue circles).

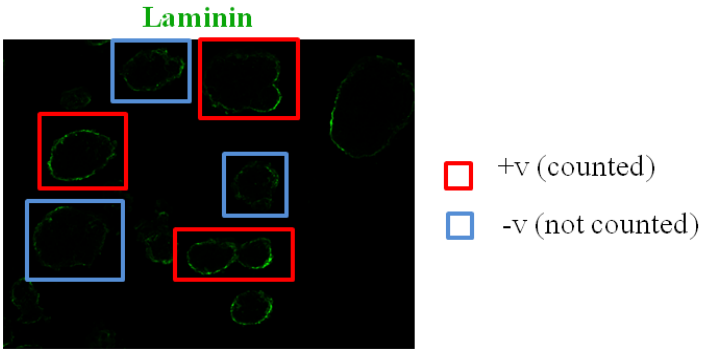

Figure 2.4 Diagram outlining the quantification of differentiating EBs with regard to Laminin expression. Quantification of adequately differentiating EBs was achieved in part by counting EBs with > 50 % circumference displaying positive Laminin expression, as shown with red boxes. EBs with < 50 % circumference Laminin expression were not counted blue boxes).

2.2.3 Real Time Polymerase Chain Reaction

2.2.3.1 RNA extraction

EBs were isolated from bacteriological dish to 1.5 mL microfuge tube and centrifuged at 64g for 3 min. The medium was removed and replaced with 0.5 mL TRIzol, cells were homogenised and a further 0.5 mL TRIzol was added. 200 µL chloroform was then added to

the microfuge tube, which was shook for 20 seconds followed by centrifugation at 4°C at 12,000 rpm for 15 min, during which time 1 µL glycogen was added to new 1.5 mL microfuge tube. After centrifugation, the upper aqueous phase was transferred to prepared 1.5 mL microfuge tube (typically 500 µL) and an equal volume of isopropanol was added (typically 500 µL). The microfuge tube was inverted 4-5 times, to ensure gentle mixing, and EBs were incubated at RT for 10 min followed by centrifugation at 4°C at 12,000 rpm for 10 min. The supernatant was discarded after centrifugation and remaining pellet was washed in 1 mL 75 % ethanol, followed by centrifugation at 7.5,000 rpm for 5 min. Ethanol was removed and the pellet was allowed to dry (approximately 2 min). The pellet was dissolved in 10-50 µL nuclease free water (usually 20µL as pellets are typically small). If RNA was to be stored, rather than used for cDNA synthesis immediately, the pellet was stored at – 20°C, in 1 mL 75% ethanol.

2.2.3.2 DNase treatment

8 µL of the RNA solution was transferred into a 0.2 mL microfuge tube, and 1 µL DNase buffer and 1 µL DNase were added. Sample was incubated at 37 °C for 30 min. The reaction was stopped by adding 1 µL STOP buffer and the sample was incubated at 60°C for 15 min. Samples were placed on ice in preparation of reverse transcriptase reaction.

2.2.3.3 cDNA synthesis

cDNA was synthesised with SuperScript III First-Strand Synthesis System for RT-polymerase chain reaction (PCR) (Invitrogen, UK) according to instructions. 6 µL DNase treated RNA was transferred to 0.2 mL microfuge tube and 5 µL nuclease-free water and 2 µL 100 ng/µL stock of random hexamers were added and incubated at 65°C for 5 min. The sample was chilled on ice for 1 min, pulse centrifuged and 4 µL X 1^{st} strand buffer, 1 µL DTT (0.1M), 1 µL dNTP mix (10 mM stock) and 1 µL superscript III reverse transcriptase (200 U/µL) were added. The solution was mixed gently by pipetting and incubated at RT for

5 min. A further incubation at 50°C for 60 min and inactivation was achieved by heating at 70°C for 15 min.

PCR was performed using KAPA Sybr Fast (Labtech, UK) and light cycler (Rotor-gene RG-3000) was used. Values were normalised to GAPDH levels and the delta-delta ct method was used to calculate relative change in expression between different EB growth conditions, assuming primer efficiency.

Relative change in expression compared to normal conditions = $2^{-\Delta\Delta Ct}$

Normal conditions were considered to be EBs derived from E14 mESCs grown in presence of serum and feeders (+F +FBS). Treated samples were any conditions other than this; EBs grown in absence of feeders (-F +FBS), EBs grown in absence of serum and feeders (-F –FBS), EBs grown in serum-free feeder-free conditions but supplemented with endogenous heparin (-F –FBS +1ug/ml heparin).

Primer sequences are shown in Appendix II.

2.2.4 Compositional disaccharide analysis of HS

2.2.4.1 DEAE purification of HSPGs

Medium samples were rotated with 0.1 ml DEAE-Sephacel beads (GE healthcare, UK) / 10 mL sample overnight at 4°C. Samples were centrifuged at 2800g and the supernatant was removed. The beads were washed with 10 x volume PBS, followed by a 0.25 M NaCl wash; supernatant was removed after each wash. The sample was finally eluted with 10 x volume 2 M NaCl.

2.2.4.2 Desalting of eluted fractions

Samples were desalted using HiPrep desalting columns on an AKTA purifier: 26/10 G-25 superfine column pre-packed with Sephadex (GE Healthcare, UK) or DT G-25 superfine

column pre-packed with Sephadex (GE Healthcare, UK) , depending on sample volume. The fractions were injected into a 1 mL loop, using a Hamilton syringe, ensuring no air bubbles were injected into the circuit, and the flow rate was gradually increased to 1mL/min. Desalted fractions were freeze dried.

2.2.4.2 Digestion of medium sample with heparitinase enzymes

Recombinant Heparitinase I, II and III (Ibex; Ibex Technologies, Montreal, Quebec – Cat no. 50-010, 50-011, 50-012 respectively) were employed to enzymatically digest HS from each medium sample, in accordance with previous data that showed usage of these enzymes in conjunction, is a most efficient for disaccharide analysis (Linhardt, Turnbull et al. 1990).

Enzymes are generated from *Flavobacterium heparinum* (Galliher, Cooney et al. 1981) and each act on a different substrate, outlined in Table 2.5 to comprehensively digest the HS.

Freeze dried samples were re-suspended in MilliQ H_2O (typically 100 μL), 5 x lyase buffer and digested by addition of heparitinase enzymes: 2.5 mU of heparitinase I, heparitinase II, and heparitinase III enzymes per reaction. The samples were incubated at 37°C for 4 h and a further 2.5 mU of each enzyme was added and incubated overnight at 37°C.

Unit definition; 1 international unit (IU) represents the amount the enzyme will liberate 1 μmol of unsaturated oligosaccharides from HS per minute at 30 ° C and pH 7.5.

Table 2.5 Heparitinase enzymes for HS digestion to aid disaccharide analysis

Enzyme	Substrate
Heparitinase I	Broad specificity; cleaves linkages that have reduced density of sulfation and that contain beta-D-glucopyranosyluronic acid residues, typically N-acetylated or N-sulfated glucosaminido-glucuronic acid linkage.
Heparitinase II	Broad specificity; acts upon heparan sulfate producing disulfated, N-sulfated and N-acetylated-6-O-sulfated disaccharides, and small amounts of N-acetylated disaccharide, preferentially upon N, 6-O sulfated glucosaminido-glucuronic acid linkage.
Heparitinase III	Highly specific; cleaves highly sulfated polysaccharide chains containing linkages to 2-O-sulfated alpha-L-idopyranosyluronic acid residues.

2.2.4.3 Purification of sample with C18 column

High resolution separation and purification of samples was achieved using derivatised silica-based C18 columns with cetyltrimethylammonium (CTA) hydroxide to provide the basic group for anion exchange (Mourier and Viskov 2004). Samples were freeze dried and re-suspended in milliQ H_2O (typically 500 µL).

2.2.4.4 Fluorescent labelling of HS disaccharides

5 µL BODIPY was added to freeze dried samples, followed by centrifugation at 64g and samples were speed vacuumed. DMSO:acetic acid (17:3 vol:vol) was added to each sample and incubated in dark adapted chamber for 4 h at room temperature. 5 µL 1M sodium borohydride was added to each sample, followed by centrifugation at 64g and incubation for 30 min at room temperature. Samples were snap frozen in liquid N_2, freeze dried and re-suspended in 10 µL DMSO:milliQ H_2O.

2.2.4.5 Thin film liquid chromatography

Butanol and filter paper were added to a beaker (butanol approximately 1-2 cm deep and filter paper standing in beaker) sealed with cling film, so to create a butanol atmosphere. In

the meantime, samples that had previously been suspended in DMSO:milliQ H_2O were spotted onto TLC plates (Sigma Aldrich, cat # Z193275). TLC plates containing samples were then stood in the butanol-containing beaker (ensure that samples are spotted high enough on TLC plate so that when they stand in the beaker the sample spots are not submerged in butanol). Samples were incubated in the dark until butanol had carried unwanted components of the sample to top of TLC paper. TLC plates were hair-dryed and the process was repeated three times.

Using a clean blade, spotted sample and immediately surrounding area on the TLC plate was scraped from surface of plate. Samples were added to an eppendorph, diluted with milli-Q H_2O (approximately 200 μL) and vortexed. The supernatant (sample) was removed and diluted again in milli-Q H_2O and further votexed (repeated three times).

2.2.4.6 Strong anion exchange (SAX) purification

Strong anion exchange (SAX) chromatography is a technique used to separate anionic molecules based on net charge – employed here to separate purified HS disaccharide structures based on their relative negative net charge via interaction with a positive column.

A Propac column PA1 (Dionex, UK) was employed and represents a high resolution column specifically used for separation of HS/heparin, providing reliable elution times necessary for separation and disaccharide analysis. Positive charges on the matrix are due to a strong base derivatised onto a support medium which remains positively charged across pH 1-14. Upon introduction of a sample into the mobile phase, ionic binding to the column occurs and content of sulphate groups, carboxyl groups and strength of buffer underpins the strength of binding. Elution of the sample followed using a gradient salt wash between 0-100 % over 55 min in B (Hold in A (150 mM NaOH in HPLC water) for 10 min to allow free BODIPY tag

to elute, 0-45 % B (2M NaCl 150 mM NaOH) for 40 min, 45-100 % B for 15 min for elution of sample, finally hold in D (2M NaCl 300 mM NaOH) for 10 min to wash the column).

Elution of material from the column was achieved using a gradient salt wash over time and accordingly, disaccharides elute in a specific order as outlined in Table 2.6.

Table 2.6 Order of disaccharide standards elution during HPLC-SAX analysis with time

HS disaccharide standard	*Structure*	Elution time (min)
1	UA-GlcNAc	15.75
2	UA-GlcNS	21.0
3	UA-GlcNAc6S	23.0
4	UA2S-GlcNAc	24.75
5	UA-GlcNS6S	29.5
6	UA2S-GlcNS	31.25
7	UA2S-GlcNAc6S	37.0
8	UA2S-GlcNS6S	44.75

2.2.5 Sample (polymer) preparation for SEM analysis

2.2.5.1 Fixation

All polymer samples were removed from the culture systems and incubated with 2.5 % EM-grade gluteraldehyde for 30 min at room temperature, followed by three washes with distilled water.

2.2.5.2 Dehydration

After fixation, samples were dehydrated via incubation in 70 % EtOH for 30 min, followed by incubation in 90 % EtOH for 30 min and final incubation for 30 min in 100 % EtOH.

2.2.5.3 Critical Point Drying (CPD)

Dehyrdrated samples were loaded into CPD boat containing 100 % EtOH, ensuring that they were submerged fully in 100 %. EtOH. The CPD chamber was filled with liquid CO_2 and the

chamber was allowed to cycle and displace EtOH for approximately 5 min, while vents were open. Once chamber was filled with CO_2, all vents were closed and samples were left for 1 hour. The CPD chamber was emptied of CO_2 to a degree (level now just below the boat containing samples), and pressure within the chamber was increased via heating to 35°C, to ensure prevention of recondensing; critical point is 31°C 1500psi. Samples were removed once chamber was emptied and pressure reduced. CPD set-up is outlined schematically in Figure 2.6.

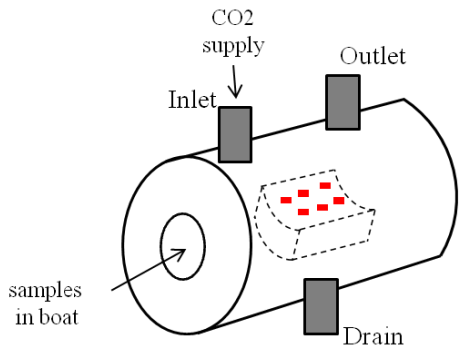

Figure 2.6 Schematic of CPD set-up. Samples (represented by red squares) are contained within a closed system, under controlled pressure and temperature, during filling and emptying with CO_2.

2.2.5.4 Chromium sputter coating

The inability of polymers to conduct electrons means that under SEM analysis without a metal sputter coating, polymers tend to 'charge'. Charging is underpinned by the inability of the polymer sample to dissipate secondary electrons; electrons build up, induce a static electric field and therefore result in the deflection of electons thus generating unrepresentative, inconsistent contrasting image. Chromium (Cr) sputter coating was therefore employed. Samples were placed in vacuum whereby Ar gas was introduced, a potential was applied across target sample and therefore the Ar gas is ionized. Ar ions sputter off Cr atoms, producing a 'cloud' of Cr atoms, which subsequently coat the surface of the polymer.

2.2.6 Statistical Analysis

Each experiment consisted of three replicates, statistical significance determined using Student *t* test, significance set to $p < 0.05$, unless otherwise stated. Error bars represent SEM, unless otherwise stated.

3. Variations in mESC culture condition influences behavior

3.1 General Introduction

ESCs are pluripotent cells with the ability to replicate indefinitely in an undifferentiated state whilst maintaining the ability to give rise to derivatives of all three embryonic germ layers. mESCs are routinely cultured in the presence of serum and on feeder cell layers (Evans and Kaufman 1981; Thomson, Itskovitz-Eldor et al. 1998). Under these conditions, the majority of cells within the population display the typical morphological characteristics of mESCs, including high nuclear:cytoplasmic ratio and prominent nucleoli, as well as a tendency to form compact, multilayered colonies (Matise 2000), and express mESC pluripotency markers, Oct4 and Nanog (Medvedev, Shevchenko et al. 2008; Orkin, Wang et al. 2008). However, little is known about the effect that the absence of serum and/or feeders has on mESC expansion, important given that the eventual implementation of ESCs in medicine will rely on xeno-free scale-up. Similarly, there is limited knowledge surrounding the affect culture condition (+/- feeders +/- serum) has on ESC differentiation capacity.

A well established model of early development is the embryoid body (EB) model (Robertson 1987), employed in this project to investigate differentiation according to 2D culture condition. Once grown in a suspension culture, mESCs clump together to form aggregates known as embryoid bodies (EBs). EBs were generated using several discrete 2D culture conditions and major hallmarks of EB development were monitored to assess differentiation capacity as a function of culture condition. Key stages of successful EB development include compact clustering by day 2, differentiation of primitive endoderm at the periphery of the EB by day 3 (Murray and Edgar 2000), visceral and parietal endoderm differentiation by day 4, and formation of the basement membrane (BM), which initially appears thin until parietal endoderm cells deposit a thick BM similar to Reichert's membrane (Smith and Strickland 1981; Gersdorff, Muller et al. 2005). Some inner mESCs, rather than differentiating to

columnar epiblast epithelium (CEE), undergo programmed cell death (Coucouvanis and Martin 1995), represented by the formation of a cavity, typically seen by day 7 (see Figure 1.3 in chapter 1).

As outlined in detail previously, BM is a highly organised structure composed of ECM molecules, which form an interface between many different cell types, provides mechanical stability and regulates cellular activity (Engvall 1995; LeBleu, Macdonald et al. 2007; Tzu and Marinkovich 2008). A key component of the BM is the non-collagenous trimeric glycoprotein laminin, which is essential for embryogenesis (Beck, Hunter et al. 1990; Huang, Hall et al. 2003; Miner, Li et al. 2004; Miner and Yurchenco 2004) and the molecule of choice when identifying BM synthesis in the EB throughout this project. Laminin is composed of three non-identical chains (alpha, beta, gamma) arranged in a cross-shaped structure, in which three short arms each form by a different chain, and one long arm is composed of the three assembled coiled chains, detailed previously. To date, it is suggested that only laminin trimers, not individual chains, are secreted extracelluarly, as identified in the case of laminin-111 and laminin-511 (Matsui, Wang et al. 1995; Yurchenco, Quan et al. 1997); thus functional BM is only formed once all three chains are present and successfully configured.

This chapter demonstrates:

- That mESCs can be maintained in 2D culture with/without feeders and/or serum for > 10 passages under all three conditions; mESCs retain typical morphological features, and the proportion of cells expressing Oct4 and Nanog is similar.
- That mESCs maintained in serum-free feeder-free culture systems display significantly slower proliferation rates when compared to mESCs maintained in conditions containing serum +/- feeders.

3.2 mESCs maintained in the absence of feeders and/or serum, remain undifferentiated and display typical behaviour during 2D culture

Before investigating the effect of feeder cells and serum on EB development, it was first necessary to confirm that mESCs cultured for > 10 passages in the absence of feeder cells and/or serum, remained undifferentiated and behaved typically with regard to morphology and proliferation.

mESCs were maintained in three distinctly different 2D growth conditions; on feeders and in the presence of serum, without feeders but in the presence of serum and without feeders and in the absence of serum, demonstrated in Figure 2.1. mESCs maintained in all three culture conditions displayed typical mESC behaviour, irrespective of culture condition. Whether serum and/or feeders were present during ESC expansion for > 10 passages (> 24 days), mESCs maintained typical morphology, namely, high nuclear: cytoplasmic ratio and prominent nuclei. Furthermore there was evidence of multilayered colonies in all three conditions (Figure 3.1). To further confirm that the mESCs had not differentiated following > 10 passages under the different culture conditions, co-immunostaining was performed for Oct4 and Nanog. mESCs remained positive for Oct4 and Nanog throughout expansion in all three conditions (Figure 3.2); moreover, quantification confirmed that proportions of Oct4 and Nanog positive mESCs were not different between the three groups (Figure 3.3).

The proliferation rate of mESCs during 2D expansion, however, was affected by culture condition. mESCs maintained in serum-free feeder-free culture conditions displayed a significantly lower proliferation rate detected by day 3, when compared to mESCs cultured in standard conditions, (in the presence of serum and feeders). The trend was consistent with time. mESCs expanded in the absence of feeders but in the presence of serum, displayed similar proliferation rates to mESCs expanded in normal conditions up to 2.5 days, however,

by 3 days the proliferation rate was significantly lower than mESCs cultured in the presence of serum and feeders (Figure 3.4).

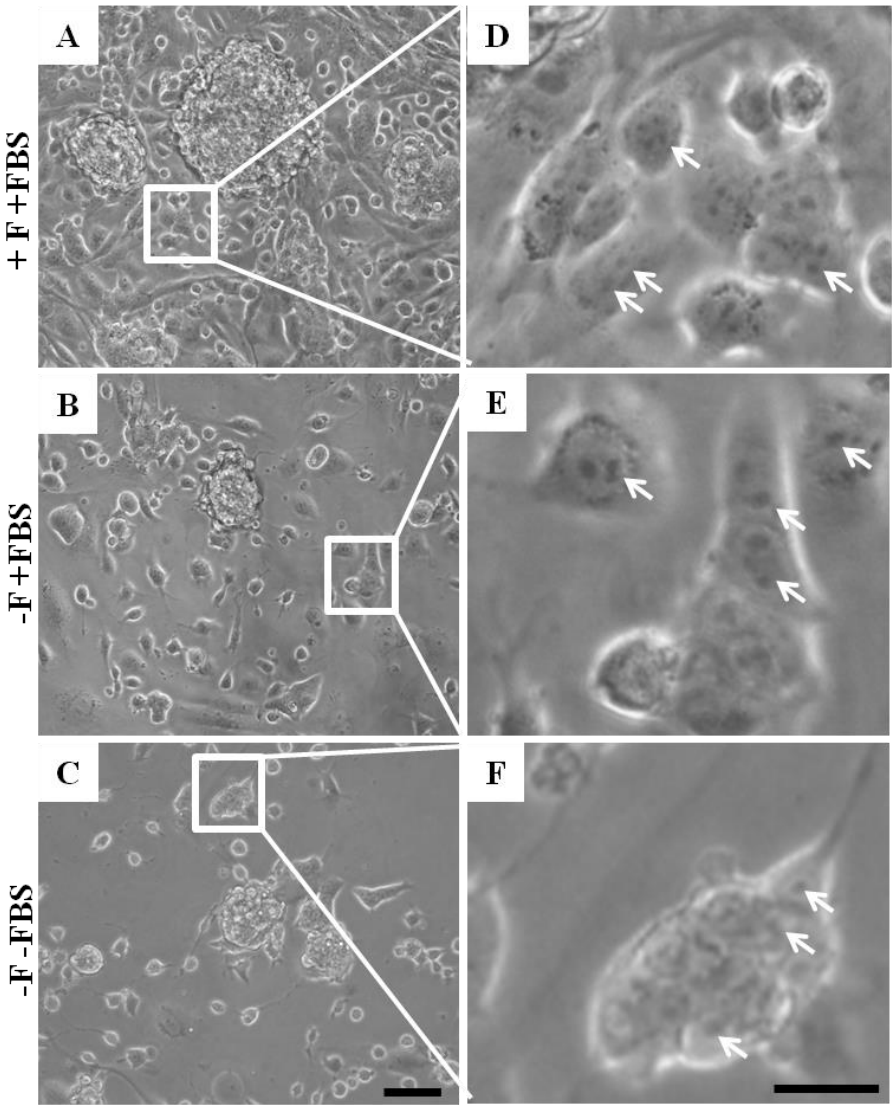

Figure 3.1. E14 mESC display typical morphology in the absence of feeders and/or FBS. E14 mESCs were maintained *in vitro* for > 10 passages (P16) in three different culture conditions using different combinations of with/without feeders (+/-F) and in the presence/absence of serum (+/-FBS): A) +F + FBS, B) –F + FBS, C) –F –FBS. mESC morphology was similar under all three conditions; i.e., ESCs showed high nuclear:cytoplasmic ratio and prominent nucleoli (arrows) and could form multilayered colonies. In all three conditions, some cells without typical mESC morphology were present, suggesting that there was a degree of spontaneous differentiation. The experiment was repeated > 6 times and images are representative of for each condition. Scale bar represents 50 μm.

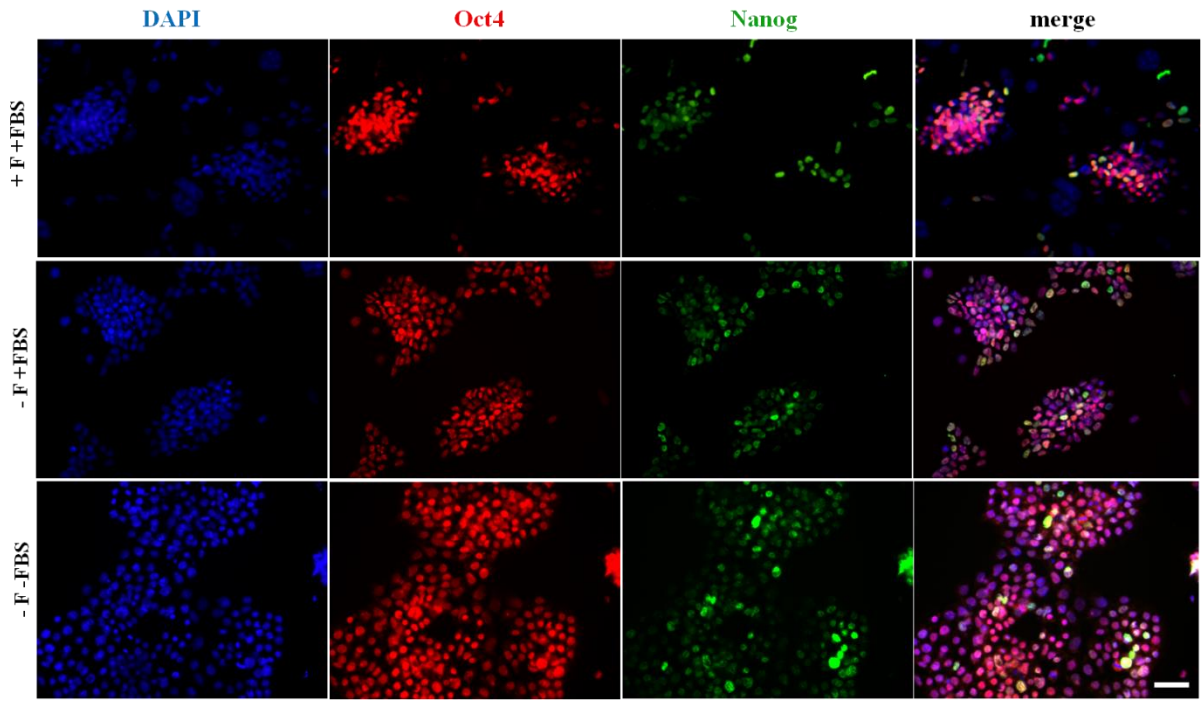

Figure 3.2 E14 mESCs express Oct4 and Nanog in the absence of feeders and/or FBS. E14 mESCs were maintained *in vitro* for > 10 passages in 3 different culture conditions; with serum and feeders (+F + FBS), without feeders but in the presence of serum (–F + FBS) or serum-free feeder-free (–F –FBS). mESCs maintained in all 3 conditions express the pluripotency markers Oct4 and Nanog. The experiment was repeated > 6 times and all images are representative of entire cell populations. The scale bar represents 100 µm.

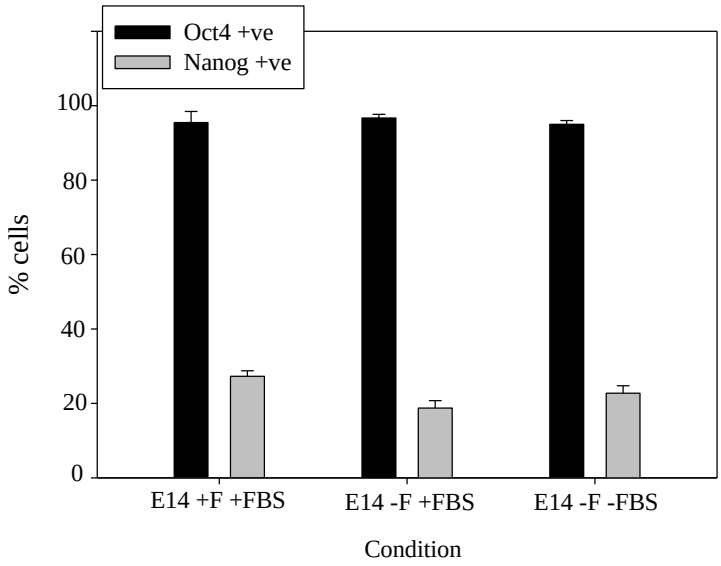

Figure 3.3 The proportion of Oct4 and Nanog positive E14 mESCs was comparable in all three culture conditions. mESCs were maintained in 3 different culture conditions > 10 passages; with feeders and serum (+F +FBS), without feeders but in the presence of serum (-F +FBS) or serum-free feeder-free (-F –FBS). The percentage of cells that stained positively for Oct4 and Nanog was not statistically different between the three different culture conditions, n = 6; error bars represent SEM.

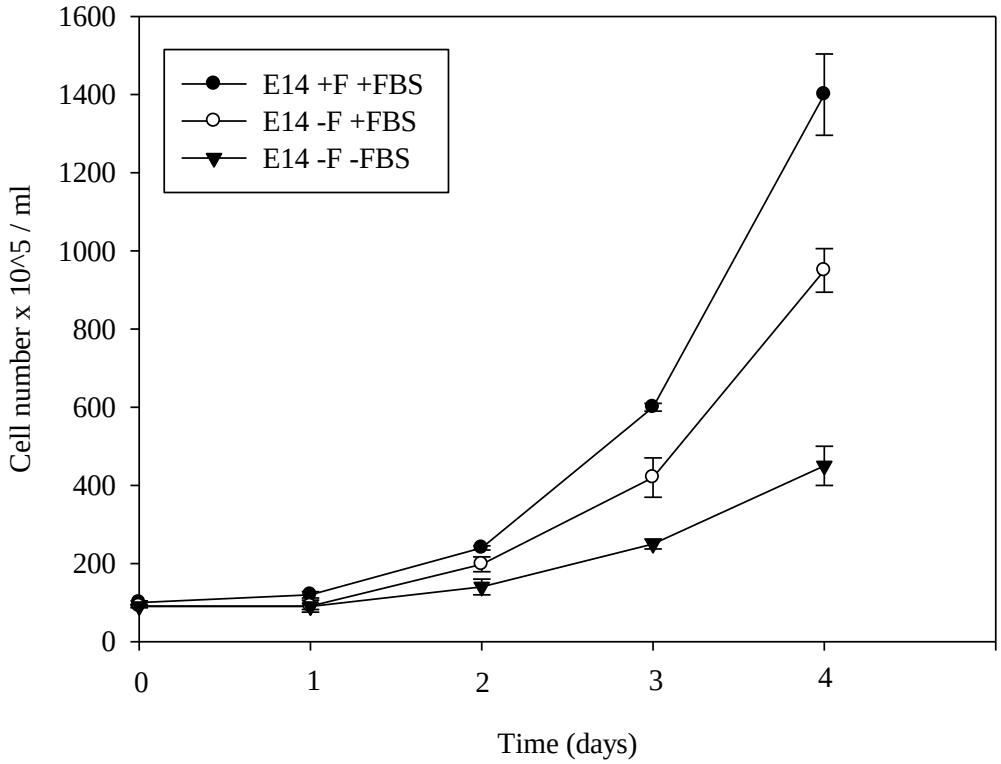

Figure 3.4 E14 mESC proliferation rate is dependent on culture condition. E14 mESCs were maintained in three different culture conditions; +F +FBS, -F +FBS and -F –FBS. Cell numbers were counted daily for 4 days to determine respective proliferation rates. mESCs maintained in serum-free feeder-free culture conditions had a significantly slower proliferation rate compared to that of mESCs maintained with feeders and/or serum. mESCs maintained in the presence of serum and feeders had a doubling time of approximately 18 h, feeder-free mESCs had a doubling time of 20 h and serum-free feeder-free mESCs displayed a doubling time of approximately 36 h. n = 12; error bar; SEM.

3.3 mESC development in the EB model is dependent upon 2D culture conditions prior to EB formation

E14 mESCs were expanded *in vitro* in three different growth conditions (+F +FBS, -F +FBS, -F –FBS; Figure 2.1) for > 10 passages, essentially a 2D model, followed by growth in suspension, to induce EB formation. EB formation occurred via the removal of LIF, aggregation culture and in 10% FBS. The EB differentiation pattern was investigated, comparing the effect that the different growth conditions had on formation, development and differentiation of mESCs over time. Specifically, mESC differentiation to endoderm and BM formation was investigated, followed by evaluation of mesoderm and ectoderm differentiation.

Quantification of differentiating EBs was achieved, as outlined previously (Materials and Methods, 2.2.2.10) using a scaling system, whereby EBs were counted as positive if a continuous BM was present in over > 50% of the EB circumference, an exmaple of which is shown in Figure 2.4.

3.3.1 EB characterisitcs including morphology, size and cavitation all differ depending on 2D mESC culture conditions

An initial observation was that –F –FBS conditioned EBs were significantly smaller in diameter when compared to EBs generated from mESCs cultured in the alternative two remaining conditions (+F +FBS, -F +FBS) as shown in Figure 3.5 and 3.6, respectively. Moreover, -F –FBS conditioned EBs appeared less compact, and generally disorganised when compared to EBs pre-conditioned in the presence of serum. There appeared to be no initial difference in the size or gross structure of EBs when comparing the presence or lack of a feeder layer.

EB morphology was further assessed using toluidine blue staining. At day 7, EBs conditioned in the presence of feeders and serum displayed signs of typical EB development, whereas serum-free conditioned EBs displayed obvious defects. In +F +FBS conditioned EBs there were tall cells on the periphery, probably representative of visceral endodermal cells, along with multilayers of round cells, which were likely to be parietal endoderm. -F +FBS conditioned EBs displayed fewer of the tall visceral endoderm-like cells on the periphery, and instead, almost all outer cells were round, like parietal endoderm cells, or squamous, like primitive endoderm cells. Nonetheless, EBs conditioned in the presence of serum (+/- feeders) displayed endoderm-like cell morphology, and in both cases displayed evidence of a BM represented by a space separating outer and inner cells. In contrast, there was little evidence of BM deposition in –F –FBS conditioned EBs. Cavitation was detected and obvious in EBs conditioned in the presence of serum and feeders, although less apparent in EBs conditioned in the absence of feeders (+/- serum), as shown in Figure. 3.7.

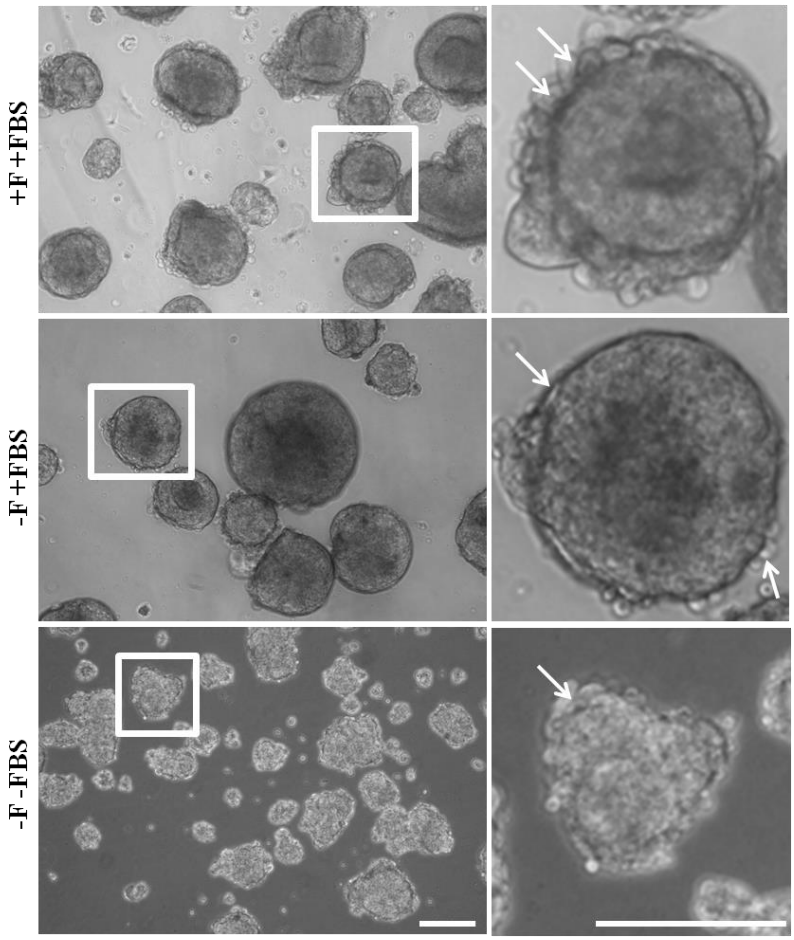

Figure 3.5 Serum-free feeder-free EBs are significantly smaller than EBs derived from mESCs cultured with serum +/- feeders. EB populations of day 7 EBs from serum-free feeder-free 2D pre-condition were represented by a relatively heterogeneous population compared to EB population from culture conditions containing serum and/or feeders. Moreover, serum-free feeder-free conditioned EBs were smaller in size, were less compact and appeared to lack outer endodermal cells (arrows) when compared to culture conditions where serum was present. Images are representative of entire EB populations for each condition. Scale bar represents 200 μm.

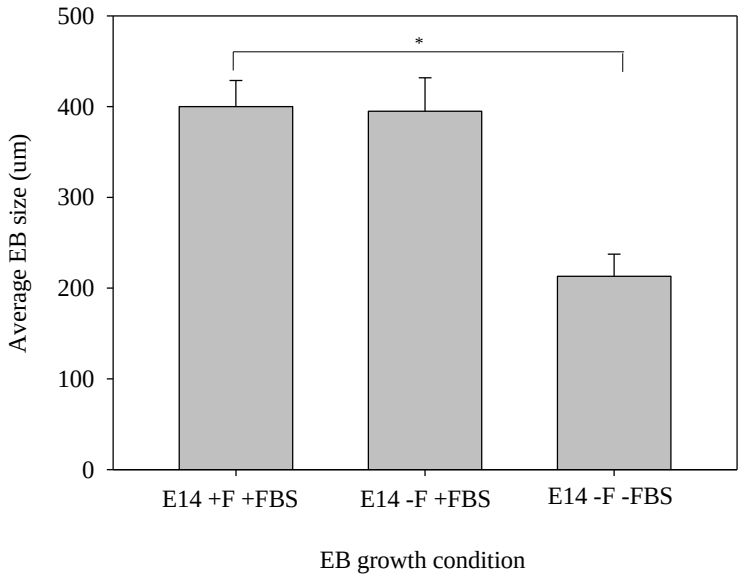

Figure 3.6 Serum-free EBs are smaller than EBs conditioned with serum. Quantification of EB diameter showed that serum-free feeder-free EBs were significantly smaller than EBs conditioned with serum (+/- F); 200 μm in diameter, compared to 350 μm and 400 μm. n = 6, * $p < 0.05$; error bars are representative of SEM.

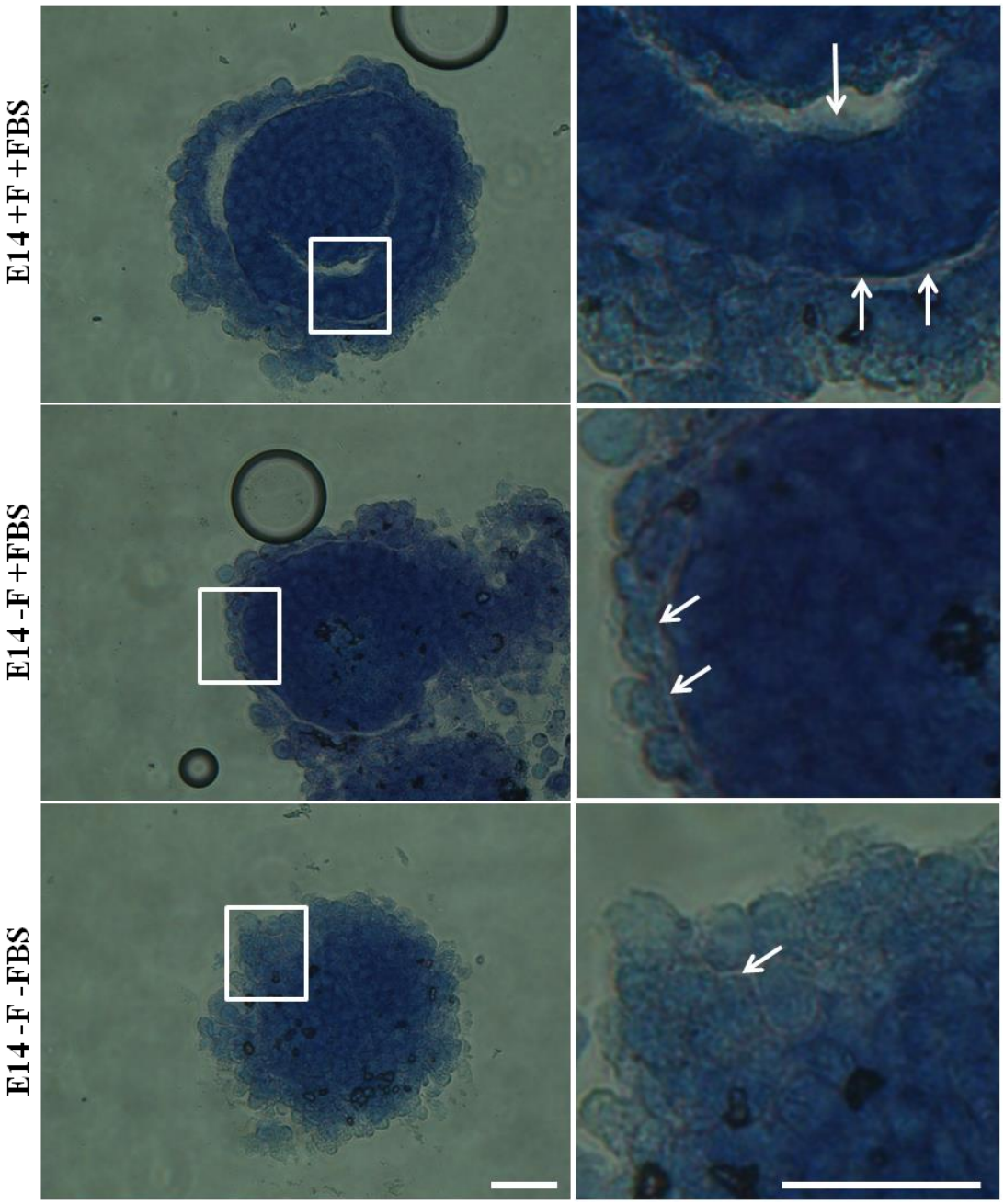

Figure 3.7 E14 mESCs EB development and morphology is different and dependent on 2D growth conditions prior to EB formation. E14 mESCs were maintained in three distinct culture conditions; +/- serum, +/- feeders for 7 days and stained with toluidine blue. –F –FBS conditioned EBs lack compaction, any signs of cavitation, show few signs of peripheral endoderm cells and display little evidence of BM. EBs conditioned in the presence of serum (+/- feeders) show complete BM although feeder-free EBs lack cavitation, as shown with arrows. EBs shown are representative of the entire EB population for each growth condition. The experiment was repeated > 6 times. Scale bar represents 100 μm.

To further confirm morphological observations and identify and quantify any initial differences in the number of differentiating EBs between the three different conditions, EBs were co-immunostained with the PE marker, Gata6, and BM marker, LamA1. Quantification of the number of differentiating EBs, at least initially, suggested that EBs generated from –F –FBS conditions displayed delayed/atypical EB development. Such EBs had significantly lower proportions of EBs with > 50% LamA1 expression when compared to EBs generated from +F +FBS conditions (Figure 3.8 B). Similarly, proportions of Gata6 positive cells on the outer surface of –F –FBS conditioned EBs was significantly lower than those conditioned in +F +FBS conditions (Figure 3.8 A). The intermediate condition, -F +FBS conditioned EBs, displayed comparable results to +F +FBS conditioned EBs; proportions of Gata6 positive cells and LamA1 immunoreactivity were no different. Cavitation however, was detected in significantly fewer EBs (Figure 3.8 C).

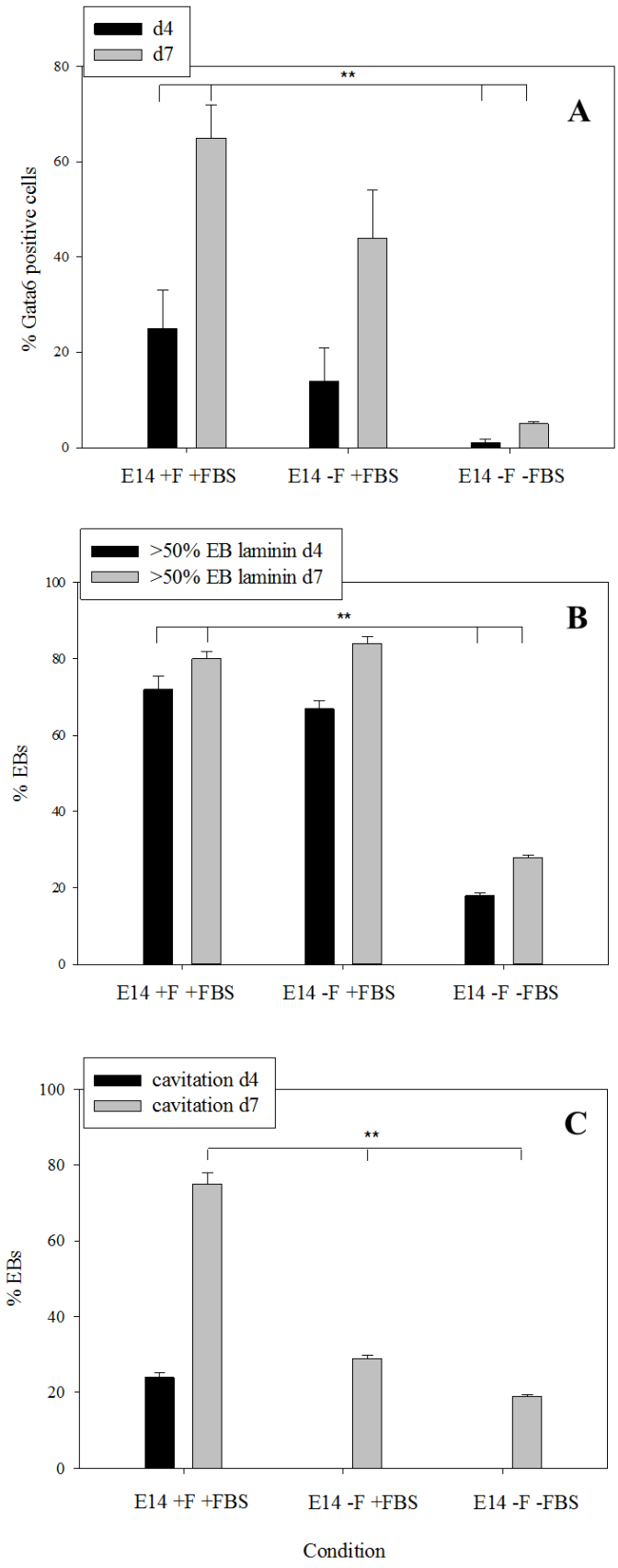

Figure 3.8 EB development is influenced by 2D growth conditions prior to EB formation. E14 mESCs were maintained in three distinct culture conditions; with serum and on a feeder layer (+F+FBS), without feeders but in presence of serum (-F +FBS) and serum-free feeder-free (-F –FBS). Serum-free feeder-free conditioned EBs display a delayed/restricted development pattern when compared to EBs conditioned in the presence of serum (+/- F). Specifically, serum-free EBs lacked extensive BM deposition by day 4 or day 7, characterised by > 50% of EB circumvented by LamA1+ BM (B). Furthermore, serum-free EBs showed fewer Gata6-positive cells on the EB periphery, again compared to EBs conditioned in presence of serum (+/- F), evident at both day 4 and day 7 (A). Evidence of cavitation is detected at day 4 only in EBs conditioned in presence of serum and feeders. By day 7, evidence of cavitation exists in all conditions, however the proportion of EBs displaying cavitation is significantly higher in EBs conditioned on feeders and in presence of serum (C). n = 20; error bar represents SEM, students T-test, ** $p < 0.01$

3.3.2 mESC differentiation capacity is impaired in EBs generated from serum-free feeder-free conditions

It is well known that the environmental cues dictate mESC behaviour however identifying the exact role of serum and/or feeders during *in vitro* differentiation is unclear. Oct4 and Nanog, common markers of pluripotency, were used to investigate the presence of undifferentiated mESCs within EBs comparing the three different growth conditions employed throughout. Typically, it is expected that the number of Oct4 and Nanog positive cells should reduce with time, as the EB differentiates (Pesce and Scholer 2001).

EBs conditioned in the presence of serum (+/- feeders), displayed distinct loss of Oct4 expression over time; specifically, by day 7, the percentage of Oct4 positive cells was represented by approximately 15% and 20% of the population of +F +FBS and –F +FBS conditioned EBs, respectively, compared with approximately 40% for that of serum-free feeder-free conditioned EBs (Figure 3.9). This was supported by *Oct4* expression analysed by qRT-PCR (Figure 3.11). Localisation of Oct4 expression was limited mostly to a few inner cells in EBs conditioned in the presence of serum (+/- feeders), whereas Oct4 localisation of EBs derived from serum-free feeder-free conditions, was identified in outer cells as well as inner cells (Figure. 3.10). Nanog expression and distribution displayed a similar trend to that of Oct4 when comparing the three conditions. In serum-free feeder free conditioned EBs, Nanog positive cells represented approximately 30% of entire EB cell population, compared to approximately 15% for the other two conditions. Moreover, localisation of Nanog expression was detected across the entire EB for serum-free feeder-free, including outer cells. EBs conditioned in the presence of serum (+/- feeders), however, displayed Nanog positive cells localised centrally as well as in more outer cells (Figure 3.12).

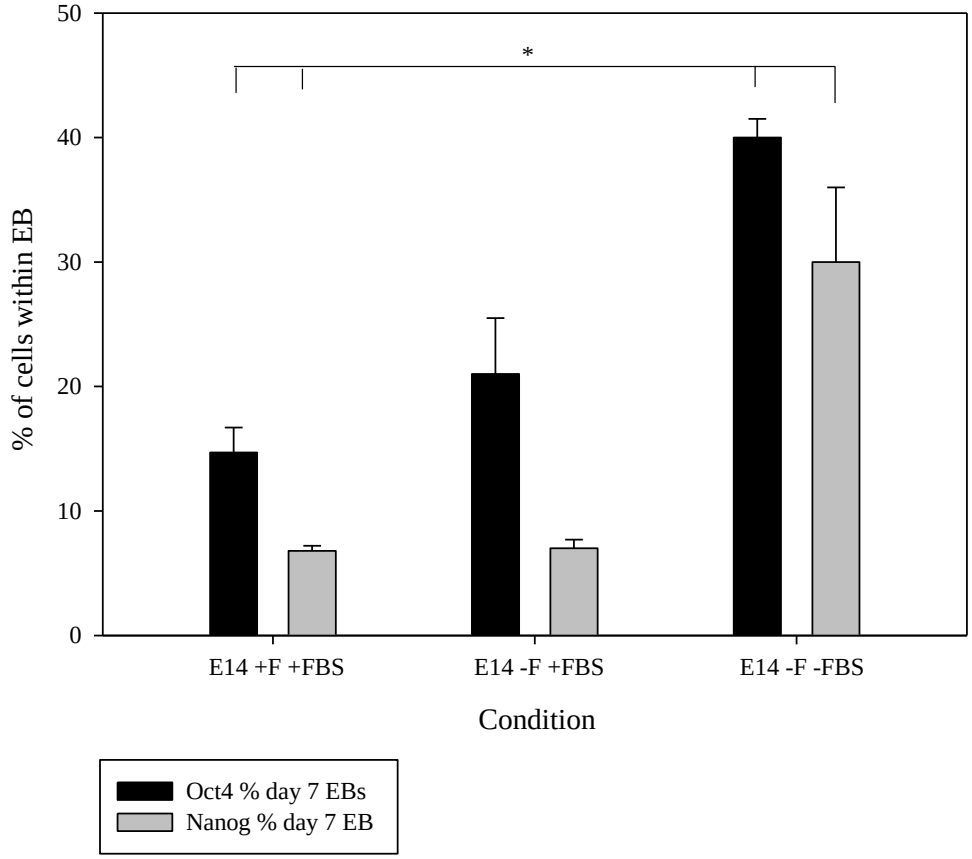

Figure 3.9 Percentage of Oct4+ and Nanog+ cells within 7d EBs depends on prior 2D culture conditions. Serum-free feeder-free conditioned EBs displayed a significantly higher proportion of Oct4 and Nanog positive ESCs in 7d EBs compared to EBs conditioned in the presence of serum. Oct4 positive cells comprised approximately 15% and 20% of the population in +F +FBS and –F +FBS conditioned EBs, respectively. In comparison, approximately 40% of ESCs were Oct4 positive in serum-free feeder-free EBs. Similarly, Nanog positive cells were infrequent (approximately 8%) in EBs conditioned in the presence of serum with or without feeders, but comprises 30% of the population in serum-free feeder-free EBs. $n = 6$, * $p < 0.05$ student's T-test, error bar, SEM.

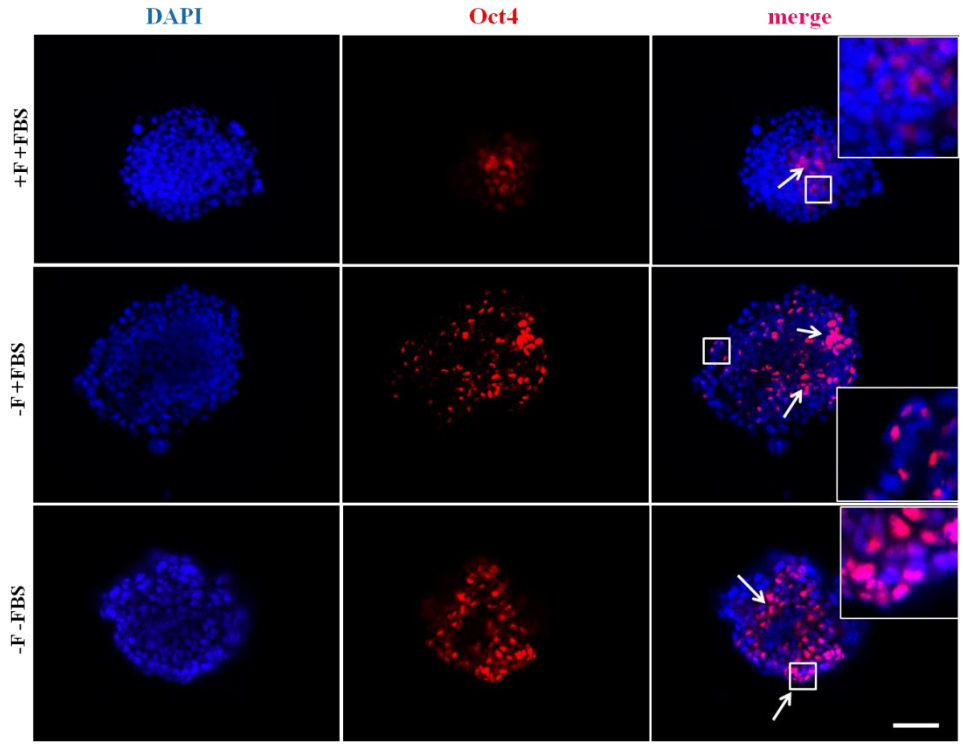

Figure 3.10 Localisation of Oct4 positive mESCs EBs changes with different mESC culture conditions. Serum-free feeder-free conditioned day 7 EBs displayed Oct4 positive cells distributed across entire EB, with many Oct4 positive ESCs localised to outer edge of EB, as shown in magnified region. EBs conditioned in presence of serum displayed lower proportions of Oct4 positive cells moreover localisation was rarely identified in outer cells. –F +FBS conditioned EBs did display few Oct4 positive cells on outer edge of EB (magnified region) but generally were located more centrally. +F +FBS conditioned EBs Oct4 localisation was typical, whereby no outer ESCs were identified as Oct4 positive. Arrows indicate regions of Oct4 positive cells. EBs are representative of entire EB population, experiment was repeated 3 times. Scale bar represents 200 µm.

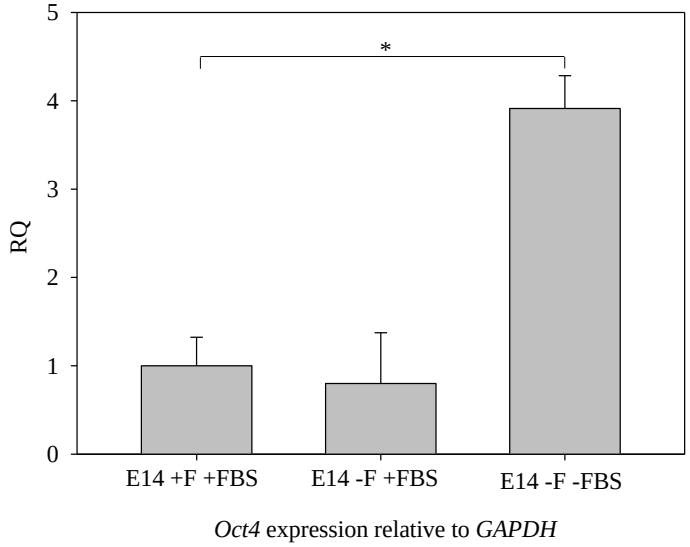

Figure 3.11 *Oct4* mRNA levels are significantly higher for serum-free feeder-free conditioned day 7 EBs. qRT-PCR showed that *Oct4* mRNA levels are significantly higher in serum-free conditioned EBs, whereas +/- feeders had no effect on *Oct4* mRNA levels. n = 6, * $p < 0.05$, student's T-test, error bar, SEM.

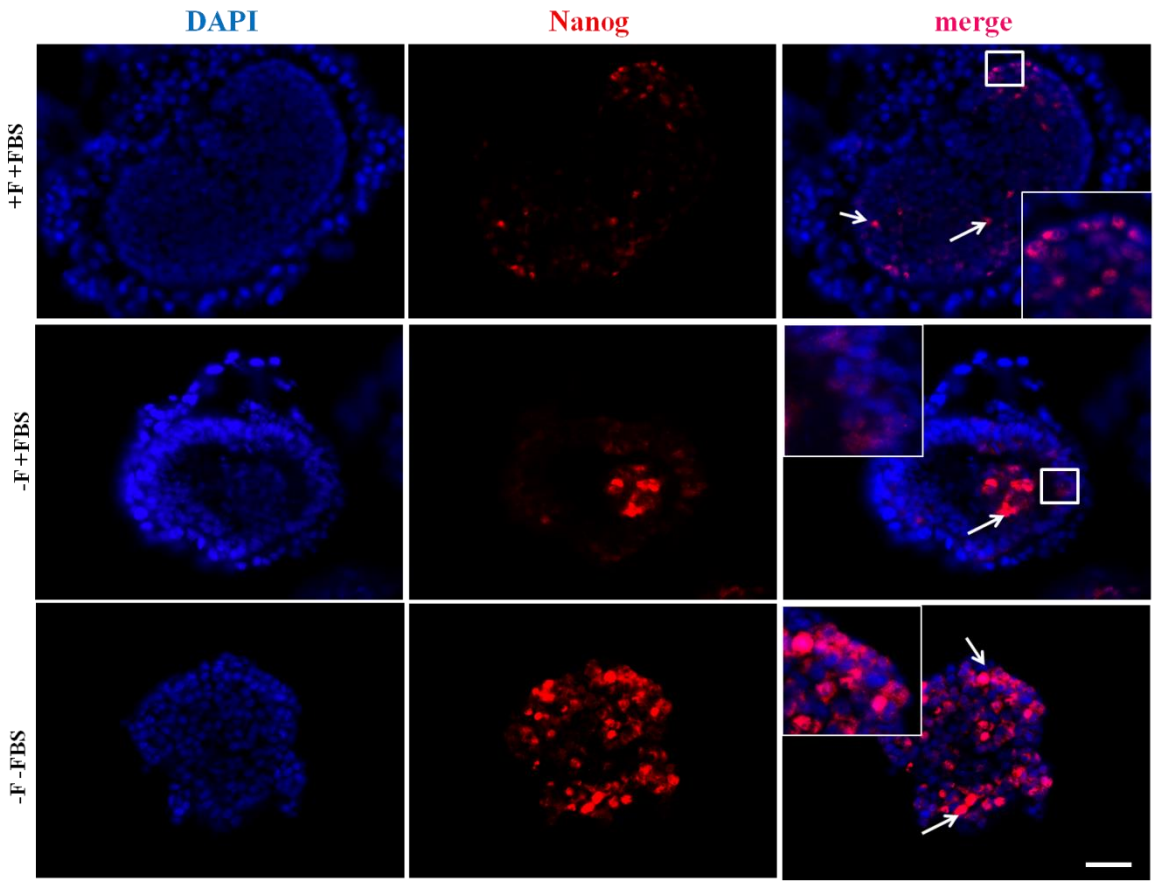

Figure 3.12 Localisation of Nanog differs depending on culture condition. Serum-free feeder-free conditioned day 7 EBs displayed Nanog positive cells localised to outer cells (magnified image) as well as inner cells, whereas EBs conditioned in presence of serum largely displayed Nanog positive cells localised relatively centrally in EB; magnified images show outer-most Nanog positive cells. Arrows indicate Nanog-positive cells. EBs are representative of entire EB populations and the experiment was repeated 3 times. Scale bar represents 200 μm.

3.3.3 Differentiation of extraembryonic endoderm and BM formation within EBs is influenced by mESC pre-culture conditions

As mentioned previously, upon the removal of LIF, mESCs cultured in suspension form EBs and differentiate, giving rise to derivatives of the three germ layers. Extraembryonic primitive endoderm cells first start to differentiate at the EB periphery on day 2. They deposit a BM between themselves and the inner EB cells. By day 4, some primitive endoderm cells undergo further differentiation to generate visceral and parietal endoderm cells. Parietal endoderm cells secrete copious amounts of ECM proteins, resulting in the deposition of a thick Reichert's-like BM (Smith and Strickland 1981). Visceral endodermal cells secrete alpha fetoprotein (AFP), the most abundant serum protein in the developing embryo in vivo (Tomasi 1977). Expression of Gata6 and AFP were therefore investigated, to determine the effect of different growth conditions (+/- F, +/- FBS) on extraembryonic endoderm (EEE) differentiation. Previous results showed that EBs generated from mESCs cultured in the absence of feeders (i.e., -F +FBS and –F -FBS) were less likely to cavitate than those generated from mESCs cultured on feeders. To investigate if reduced cavitation was due to a defect in primitive endoderm differentiation (and/or BM, investigated later) EB sections were stained for the EEE marker, Gata6. AFP immunostaining was also performed to detect differentiation to visceral endoderm. In addition to EEE, investigation into BM synthesis pursued, since EEE and BM synthesis are complimentary events, therefore EB sections were stained for laminin, using a pan laminin-111 antibody and an antibody specific for the LamA1 chain.

Gata6 was expressed in the nucleus of cells located at the periphery of day 7 EBs conditioned in the presence of serum and feeders. These Gata6 positive cells were frequently present in a multilayer, suggesting that they were parietal endoderm cells, because of the three types of extraembryonic endoderm, only parietal endoderm cells are non-epithelial; both primitive and

visceral endoderm cells form a mono-layered epithelium at the EB periphery. In contrast to +F +FBS EBs, Gata6 positive cells in -F +FBS EBs were present in a single layer at the EB periphery, suggesting a lack of parietal endoderm differentiation in these EBs. In –F –FBS EBs, very few Gata6 positive cells were present at the EB periphery, suggesting that extraembryonic endoderm differentiation was inhibited in these EBs (Figure. 3.13). Quantification of *Gata6* mRNA levels supported this result, since feeder-free conditioned EBs (+/- serum) displayed significantly lower *Gata6* mRNA levels when compared to EBs conditioned in the presence of serum and feeders (Figure 3.14). AFP immunostaining in day 7 EBs conditioned in the presence of serum and feeders showed that some, but not all peripheral cells expressed AFP, indicating that visceral endoderm cells had differentiated; the cells at the periphery of these EBs that lack AFP expression are likely to be parietal endoderm cells. In -F +FBS conditioned EBs, AFP positive cells were mainly observed in a monolayer at the EB periphery, suggesting that only visceral endoderm and not parietal endodermal cells had differentiated in these EBs. In –F –FBS EBs, immunostaining showed that most AFP was present on the apical surface of peripheral cell, and weak expression was also observed within inner EB cells (Figure 3.15) mRNA levels of *AFP* between all 3 conditions did not differ (Figure 3.16).

Immunostaining for laminin-111 showed that a BM was present between the outer extra-embryonic endoderm cells and inner EB cells in the +F +FBS and –F +FBS conditioned EBs, although a BM was barely detectable in –F –FBS conditioned EBs (Figure 3.17). On closer inspection, it appeared that laminin was only localised to the BM (not in any inner cells) in EBs conditioned with serum (+/- F) but in the case of –F –FBS conditioned EBs, there was little evidence of BM deposition, and instead, laminin was detected in central EB cells, and tended to be localised near the apical surface of cells at the periphery of the EB. Discrete laminin deposits were sometimes observed near the periphery of these EBs, but they were not

organised into a BM. (Figure 3.18). LamA1 immunostaining gave similar results, except that no staining was detected in central EB cells. As with laminin-111 staining, discrete LamA1 deposits were sometimes observed near the periphery of –F -FBS EB cells but a continuous BM was rarely detected (Figure 3.19).

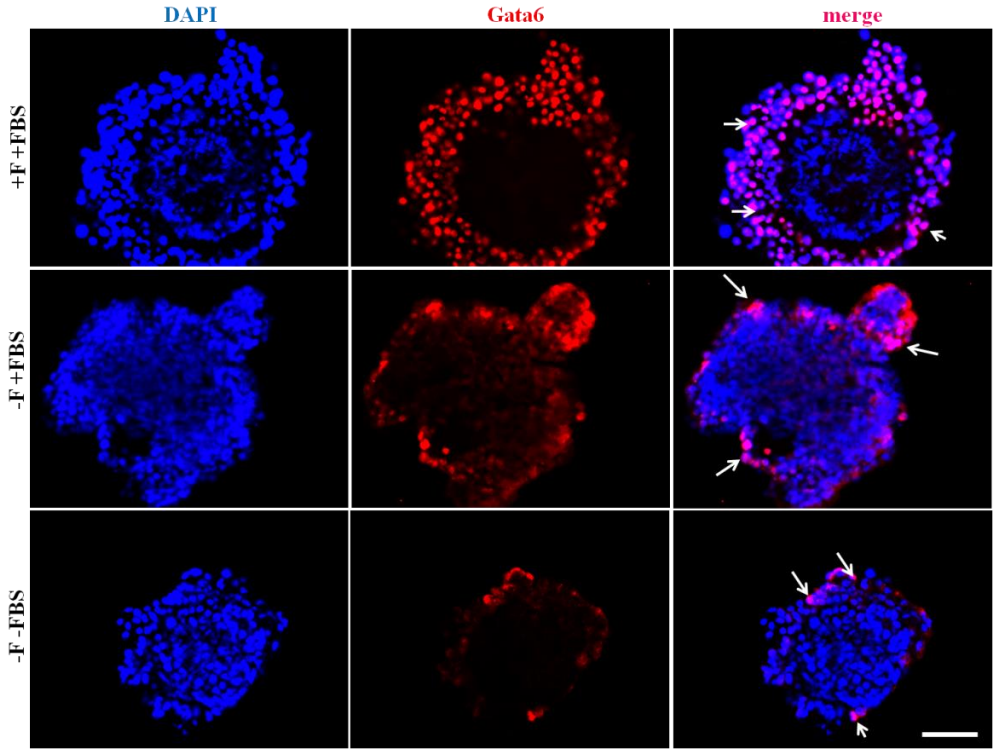

Figure 3.13 Gata6 positive cell numbers vary depending on culture condition. Gata6-positive cells, as indicated with arrows, represent a higher proportion in day 7 EBs conditioned in the presence of serum and feeders (+F +FBS), compared to EBs conditioned in the absence of feeders (-F +FBS) and/or without serum (-F –FBS). EBs are representative of entire EB population for each growth condition. The experiment was repeated 3 times. Scale bar represents 200 µm.

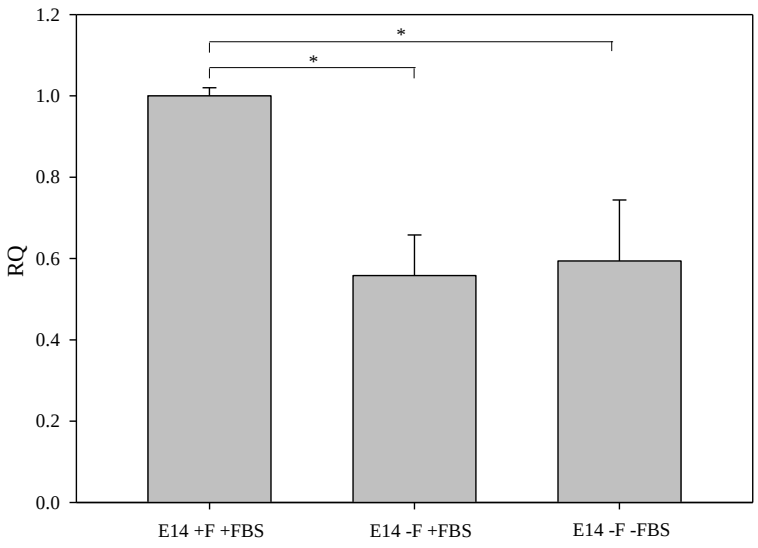

Day 7 EBs: *Gata6* expression relative to *GAPDH*

Figure 3.14 *Gata6* mRNA levels differ depending on culture condition. *Gata6* mRNA levels relative to *GAPDH* indicate that feeder-free and serum-free conditioned EBs display significantly lower *Gata6* positive endoderm cells when compared to EBs conditioned in the presence of feeders and serum, n = 4, * $p < 0.05$; error bar; SEM

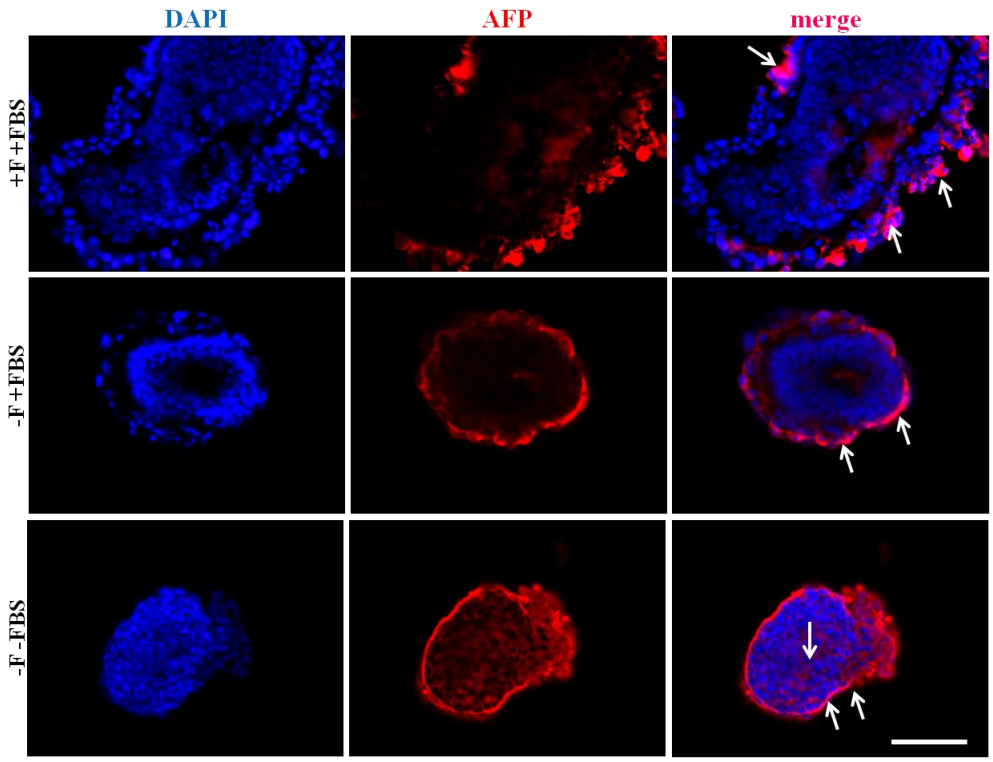

Figure 3.15 Primitive endoderm marker, AFP levels vary depending on culture condition. AFP-positive cells, highlighted with arrows, appear to represent a higher proportion of total day 7 EBs, from conditions where serum and feeders are present (+F +FBS) compared to EBs conditioned in the absence of feeders (+/- FBS). Serum-free feeder-free EBs displayed expression of AFP localised centrally in EB also, rather than solely to outer cells. EBs are representative of entire EB population and the experiment was repeated 3 times. Scale bar represents 200 µm.

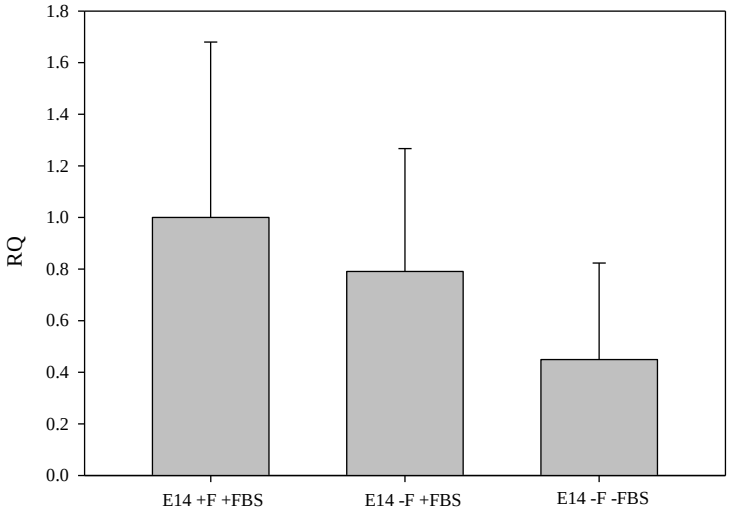

E14 7day EBs: *AFP* expression relative to *GAPDH*

Figure 3.16 *AFP* mRNA levels do not change between conditions. *AFP* mRNA levels relative to *GAPDH* indicate that there is no significant difference between growth conditions at day 7, n = 6, $p > 0.05$, error bar; SEM

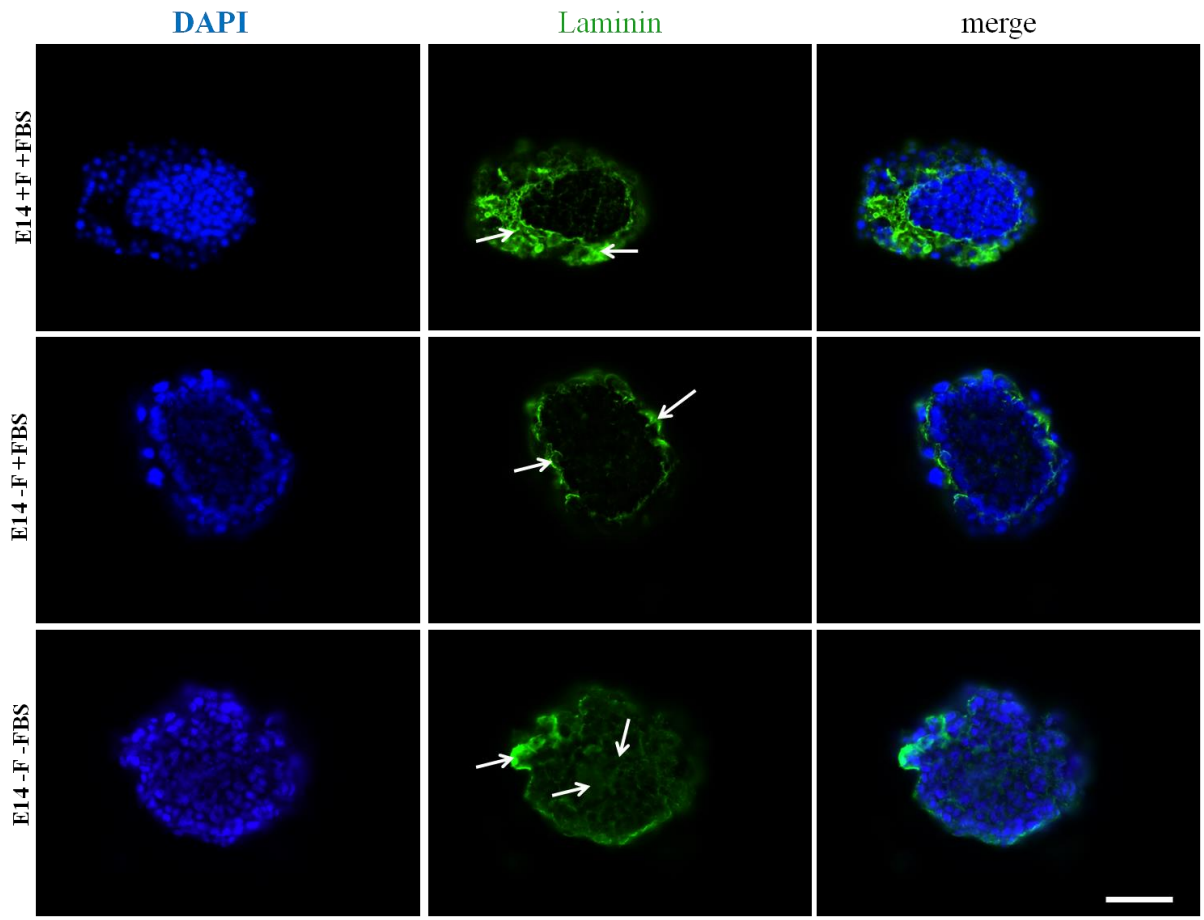

Figure 3.17 2D mESC culture conditions affect laminin distribution in EBs. The pattern of laminin111 expression was consistent with localisation within the BM underlying extraembryonic endoderm cells of 7 day EBs conditioned in the presence of serum (+/- feeders), and little immunoreactivity was detected elsewhere in the EB, as highlighted with arrows. Serum-free feeder-free EBs (-F –FBS) displayed laminin immunoreactivity throughout the EB, rather than localised only to the BM, indicated with arrows. EBs are representative of entire EB population and the experiment was repeated 3 times. Scale bar represents 200 μm.

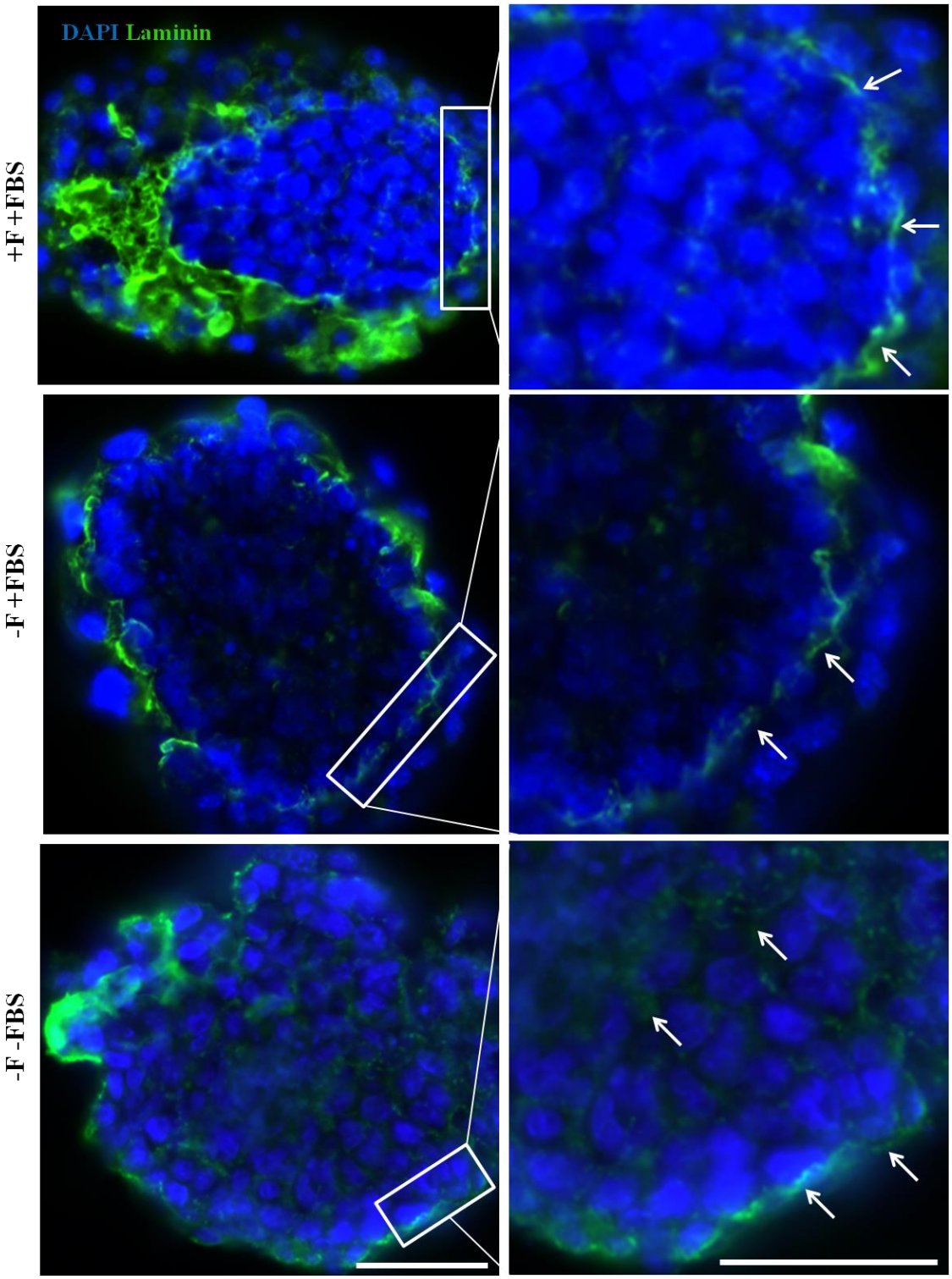

Figure 3.18 2D ESC culture conditions affect laminin distribution in EBs. Laminin-111 expression was mainly localised to the BM of 7 day EBs conditioned in the presence of serum (+/- feeders). Serum-free conditioned EBs displayed laminin immunoreactivity throughout the EB, as indicated with arrows. Images represent population, experiment was repeated > 3 times and scale bar represents 100 µm.

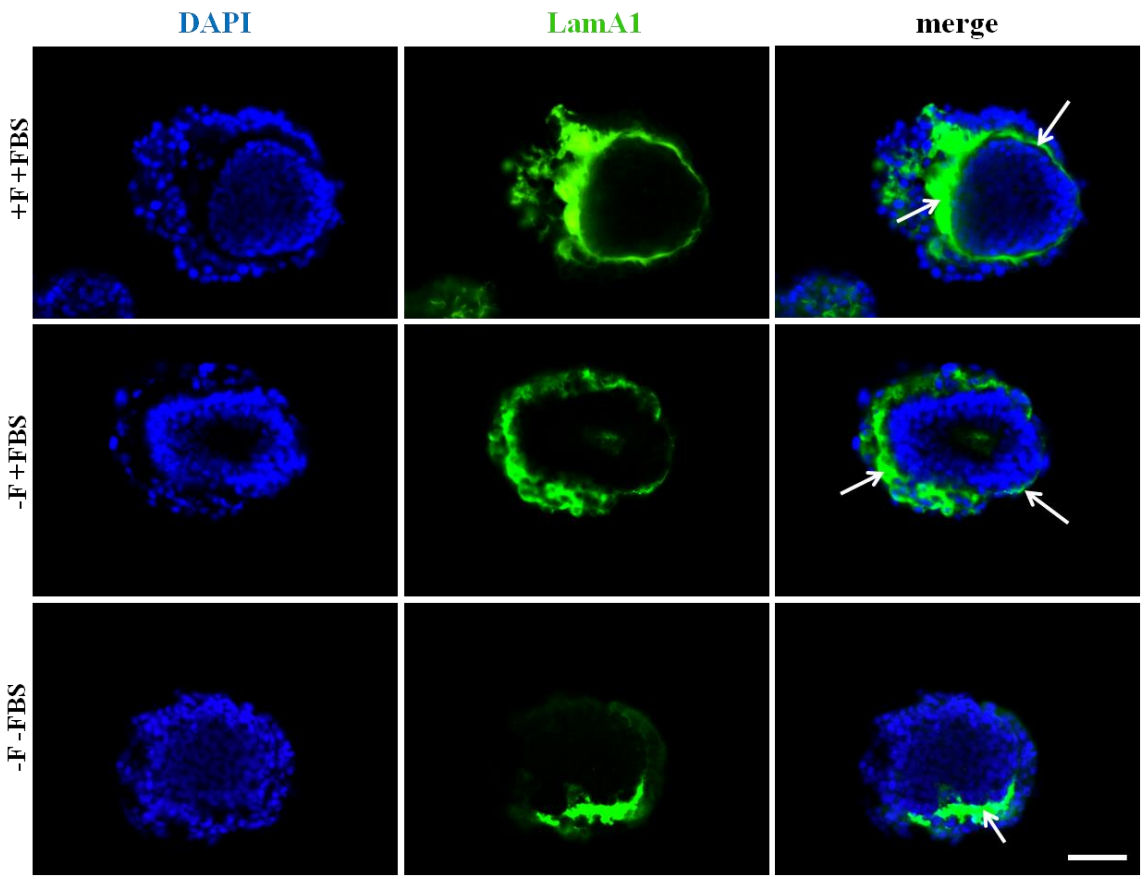

Figure 3.19 2D mESC culture conditions affect LamA1 distribution in EBs. The pattern of LamA1 immunostaining was comparable in day 7 EBs conditioned in the presence of serum (+/- feeders), and appeared to be localised to the BM between outer differentiated cells and inner EB cells. –F –FBS conditioned EBs displayed LamA1 localised in discrete regions only, as highlighted by arrows. Scale bar represents 200 µm. EBs are representative of entire EB population for each growth condition. The experiment was repeated 3 times.

Since, it has been shown that laminin trimer secretion is dependent on expression of the laminin A chain (Yurchenco, Quan et al. 1997). qRT-PCR was performed to investigate if the defect in BM deposition in –F –FBS conditioned EBs was due to reduced expression levels of *Lama1*. Indeed *LamA1* mRNA levels were significantly lower in serum-free feeder-free conditioned EBs compared with EBs conditioned in the presence of serum (+/- F), whilst expression levels of *LamB1* were similar in all three conditions (Figure 3.20). Furthermore, -F +FBS conditioned EBs displayed reduced *LamA1* mRNA levels compared to +F +FBS conditioned EBs, supported by a thicker BM identified in +F +FBS conditioned EBs compared to –F +FBS, described previous.

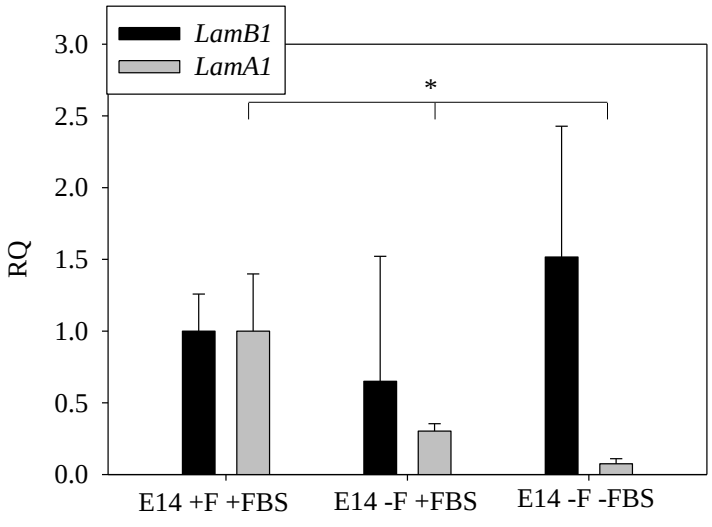

Figure 3.20 *LamA1* expression levels differ depending on culture conditions. *LamA1* mRNA levels were significantly lower in 7 day serum-free feeder-free EBs (-F –FBS) compared to EBs conditioned in the presence of serum (+F +FBS, -F +FBS). *LamB1* mRNA levels were no different when comparing the 3 conditions. n = 3; * $p < 0.05$, student's T-test; error bars, SEM.

3.4 Differentiation of mesendoderm and ectoderm within EBs is influenced by mESC pre-culture conditions

Brachyury (*Bry*) is expressed in mesendodermal cells that give rise to both definitive endoderm and mesoderm (Herrmann and Kispert 1994; Kispert and Herrmann 1994; Kubo, Shinozaki et al. 2004) . In the mouse embryo, following migration through the primitive streak, *Bry* is down-regulated and nascent mesoderm differentiates to form three subtypes: paraxial, intermediate and lateral plate mesoderm. Paraxial mesoderm is the first to form due to elongation of the primitive streak, and is marked by expression of *Tbx6* and *Foxc1* genes (Chapman, Agulnik et al. 1996; Fehling, Lacaud et al. 2003; Wilm, James et al. 2004). Given that expression of *Bry* is indistinguishable between definitive endoderm and mesoderm, expression of *Tbx6* and *Foxc1* can be explored. Intermediate mesoderm follows and finally, lateral plate mesoderm formation occurs.

Differentiation to the third germ layer ectoderm is often classified into three subsections; external ectoderm, neural crest and neuroectoderm (neural tube). Pax6 is one of the earliest markers of ectoderm differentiation, know to be of great importance in development of the eye and neural epithelial of the forebrain (Li, Yang et al. 1994). The interaction of mesoderm and ectoderm differentiation is crucial for successful development therefore expression of Pax6 was also investigated (Ang, Conlon et al. 1994; Lawrence, Johnston et al. 1994; San Martin and Bate 2001).

mRNA levels of the nascent mesoderm marker, *Bry* were shown to be significantly higher (approximately 100-fold higher) in serum-free conditioned EBs, when compared with EBs conditioned in typical ESC culture conditions in the presence of feeders and serum. A lack of feeders during mESC culture also affected *Bry* expression levels, which were 10-fold higher when compared to EBs conditioned in the presence of feeders (Figure 3.21). Investigation into paraxial mesoderm markers further supported the *Bry* expression data, since *Tbx6* and

Foxc1 mRNA expression levels were also shown to be affected by ESC culture condition. Serum appeared to be most crucial; -F –FBS conditioned EBs displayed significantly higher levels of both *Foxc1* (4-fold higher) and *Tbx6* (10-fold) when compared to EBs conditioned in the presence of serum. –F +FBS conditioned EBs however, displayed similar levels of *Foxc1*, although *Tbx6* was 2-fold higher than EBs conditioned in the presence of serum and feeders (Figure 3.22).

Furthermore, levels of ectoderm marker *Pax6* were significantly higher in serum-free EBs compared to EBs derived in the presence of serum and feeders. Interestingly the presence of feeders did not affect *Pax6* expression providing serum was present, since *Pax6* expression levels in +F+FBS and –F +FBS culture conditions were similar (Figure 3.23).

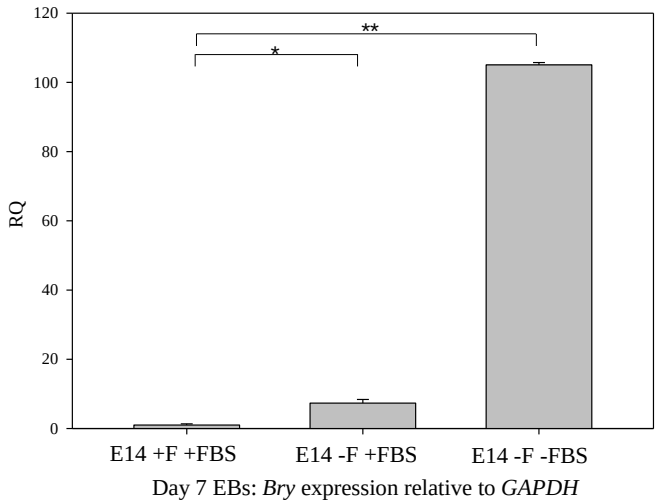

Figure 3.21 Levels of nascent mesoderm marker, *Bry* are significantly different for day 7 EBs depending on 2D culture conditions. Feeder-free EBs (-F +FBS) had significantly higher *Bry* levels, and a similar but more drastic trend for serum-free feeder-free conditioned EBs (-F –FCS) when compared to EBs conditioned in presence of serum (+F +FCS, -F +FBS). n = 6, * p < 0.05, ** p< 0.001, student T-test, error bars; SEM

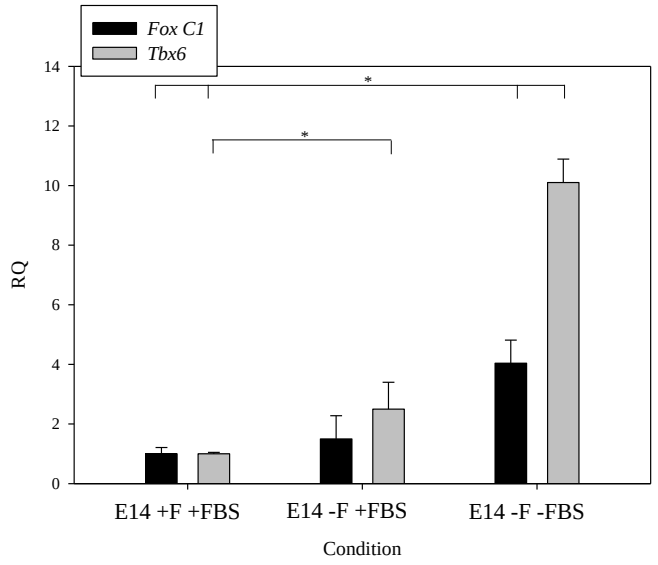

Figure 3.22 Levels of paraxial mesoderm makers *Foxc1* and *Tbx6* in day 7 EBs significantly differ depending on 2D culture pre-condition. *Foxc1* and *Tbx6* mRNA levels relative to *GAPDH* were significantly higher for serum-free feeder-free conditioned EBs when compared to EBs conditioned in presence of serum (+F +FBS). n = 3, * p < 0.05, student T-test, error bars; SEM

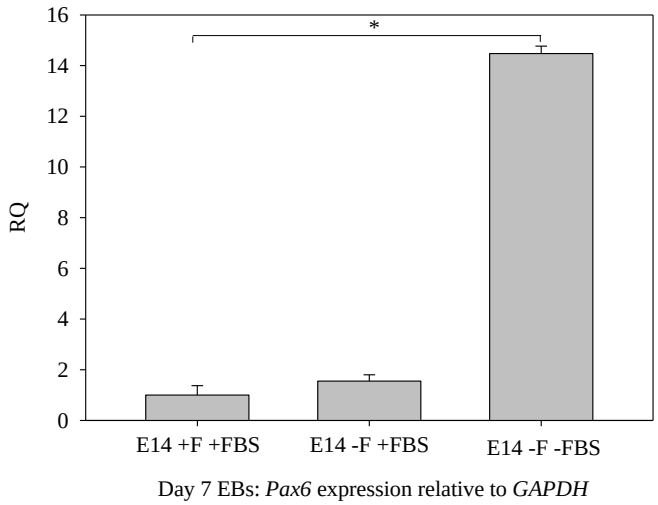

Figure 3.23 Levels of early ectoderm marker, *Pax6* are significantly different between culture conditions. *Pax6* mRNA levels relative to *GAPDH* indicate that serum-free feeder-free conditioned EBs (-F –FBS) display significantly higher Pax6 levels at day 7 when compared to EBs conditioned in presence of serum (+F +FCS, -F +FBS). n = 6, * p < 0.05, student T-test, error bars; SEM

3.5 Discussion

mESCs and hESCs have long been propagated using feeder cells and serum (Heath and Smith 1988; Smith, Heath et al. 1988; Brook and Gardner 1997), although the exact mechanisms of their supportive roles are undetermined and undefined. STO feeder cells used in this study, like any fibroblast, secrete an array of cytokines, chemokines and proteins; their role in ESC maintenance is thought to be largely mediated by these secreted factors, but the mechanisms are unknown. Some years ago it was discovered that feeder cells secreted LIF (Resnick, Bixler et al. 1992), which promotes mESC self-renewal (Smith, Heath et al. 1988), but more recently, other factors have been found to influence mESC self-renewal. Feeder cell secretion of BMP-4 was reported to be required for the maintenance of mESC pluripotency due to interactions with LIF and subsequent inhibition of the MAPK pathway (Qi, Li et al. 2004; Li and Chen 2012). Similarly, the importance of a feeder layer in the maintenance of hESCs has been linked to secretion of ActivinA (Jozefczuk, Drews et al. 2012), potentially underpinned by feeders displaying TGF-beta thus governing ActivinA, as demonstrated in one study (Chen, Lee et al. 2012). Characterisation of STO feeder cell conditioned media has shown that a variety of factors are present, including ActivinA and some FGFs whilst LIF is low or undetected (Van Hoof, Heck et al. 2008; Talbot, Sparks et al. 2012). The employment of serum during mESC culture is also very common (Cormier, zur Nieden et al. 2006), although again, the exact role is unknown. It is more than likely however, that the activity of serum is linked to the multitude of different proteins and growth factors present. Interestingly, one study has shown that serum-free ESC growth conditions however, can sustain pluripotent ESCs providing inhibitor of differentiation (Id1), a direct target of BMP-4, is over-expressed (Galvin, Travis et al. 2010; Romero-Lanman, Pavlovic et al. 2012). Likewise, another study demonstrated that the maintenance of mESCs in serum-free feeder-free conditions, can be sustained via over-expressing Blc-2, an antiapoptotic factor (Opferman and Korsmeyer 2003;

Yamane, Dylla et al. 2005). Results in this chapter have demonstrated that whilst a lack of feeder cells results in discrete alterations in ESC behaviour (a lack of cavitation and multilayered extraembryonic endoderm) they largely appeared dispensable during mESC expansion. Serum, however, was shown to be vitally important for normal ESC behaviour, both during 2D monolayer culture and in the 3D EB model *in vitro*, without which, ESC behaviour was drastically and significantly altered, outlined in Table 3.

The absence of feeder cells or serum had no affect on Oct4 or Nanog expression during 2D culture. Despite variations in culture conditions, Oct4 and Nanog expression was consistent across all conditions (Figure 3.2, 3.3), suggesting that LIF supplementation is sufficient to maintain ESC pluripotency. Yasuda et al., showed that feeder cells do not influence hESC pluripotency, therefore mechanisms which underpin this could be consistent with mESCs (Yasuda, Tsuneyoshi et al. 2006). However, the proliferation rate of mESCs was affected by culture condition; –F –FBS ESCs doubling time was 36 h, compared to 18 h for +F +FBS ESCs, and the absence of feeders was not shown to affect proliferation rate providing serum was present (Figure 3.4). Taken together, these results suggest not only that proliferation and pluripotency are independently regulated but also that serum, or a component of serum, affects proliferation. Interestingly, Faherty et al., investigated the interplay between FBS and LIF on mESC self-renewal and proliferation, and showed that variations in combinations of FBS and LIF resulted in correlation of low proliferation with increased self-renewal (Faherty, Kane et al. 2005), as seen in –F-FBS conditions. Over-expression of BMP-4 in STO feeder cells was shown to repress mESC proliferation (Kim, Lee et al. 2012); therefore, given the known interaction between BMP-4 and LIF, it was unsurprising that LIF was identified as the main factor for proliferation.

Table 3 Summary of 2D culture conditions prior to EB formation and the effects they have on subsequent EB development.

	E14 +F +FBS	**E14 –F +FBS**	**E14 –F –FBS**
2D monolayer culture	Typical morphology: High nuclear: cytoplasmic ratio and prominent nucleoli. Proliferation :doubling time,~18 h	Typical morphology, as in E14 +F +FBS. Proliferation: doubling time ~20 h	Typical morphology as in +F +FBS. Proliferation: doubling time, ~36 h
EB morphology and cavitation	Obvious cavitation by day 7	Occasionally, but not always signs of cavitation by day 7.	Few signs of cavitation by day 7
mESC self renewal in EB model	Few Oct4+ Nanog+ ESCs centrally located in EB by day 7	Oct4+ Nanog+ ESCs low and mostly centrally located in EB by day 7	Oct4+ Nanog+ ESCs represent significant proportion of cells in EBs and are located to outer surface of EBs at day 7 also
EEE differentiation	Gata6+ cells represented by multilayer on outer surface of EBs. AFP expression thick on outer surface of EB	Gata6+ cells represented by a single layer on outer surface of EBs. AFP expression present, although less apparent compared to +F +FBS EBs	Few Gata6+ cells on outer surface of EBs. AFP expression detectable, although levels lower than in +F +FBS conditioned EBs
BM deposition	Complete BM by day 4/5 : correct localisation of Laminin and LamA1 between outer Gata6+ cells and inner cells	BM present, as in +F +FBS conditioned EBs, although complete BM detected only from day 7	Disorganised, incomplete BM. Laminin expression atypical, detected in inner regions of EBs, as well as few discrete outer regions.
Differentiation to mesoderm and ectoderm	*Bry, Foxc1, Tbx6 and Pax6* expressed	Enhanced differentiation to mesoderm; increased *Bry* and *Tbx6* compared to +F +FBS. No change in *Pax6* expression	Increased expression of mesoderm and ectoderm markers at day 7; 100-fold increase in *Bry* and increased *Foxc1, Tbx6, Pax6* levels

One study suggested that insulin and LIF positively affect mESC proliferation, whilst zinc and L-cystine reduce cell growth (Knospel, Schindler et al. 2010). It is therefore possible that a lack of serum is correlated with a lack of insulin, resulting in reduced proliferation, which is feasible since insulin-like factors are known to be present in serum (Hey, Browne et al. 1987). Wnt has been shown to control stem cell proliferation in epidermal and hematopoietic systems (Reya, Duncan et al. 2003), and therefore, could also represent a major controlling factor here should Wnt signalling be down-regulated as a consequence of a lack of serum. Furthermore, Lianguova et al. showed that proliferation of mESCs is maintained by two separate mechanisms, one being a serum-dependent mechanism and the other a PI3K-based mechanism (Lianguzova, Chuykin et al. 2007). Interestingly, a long standing debate persists as to whether the tumour suppressor p53, restricts differentiation via repression of proliferation (Jain, Allton et al. 2012), which would also fit here. ZO-1, a tight-junction transmembrane protein known to affect cell proliferation, has also been shown to affect differentiation, since a lack of ZO-1 was shown to result in differentiation despite the presence of LIF (Xu, Lim et al. 2012).

Perhaps a consequence of the slow proliferation rate detected in –F- FBS conditions, was the initial observation from corresponding EBs, which demonstrated that EBs conditioned in the absence of serum were smaller in diameter (Figure 3.5, 3.6) and lacked certain differentiation capabilities. EB size has been demonstrated to affect self-renewal and differentiation; specifically, smaller EBs have been shown to display more chondrogenic potential whilst lacking endoderm potential compared to larger EBs (Messana, Hwang et al. 2008). A second observation of EBs from morphological assessment was related to cavitation; a lack of feeder cells, irrespective of serum presence, was shown to affect the ability of EBs to cavitate (Figure 3.7, 3.8C). One study demonstrated that BM is required for cavitation since BM-deficient EBs synthesise visceral endoderm but do not cavitate (Murray and Edgar 2000),

however one study demonstrated the dependency of visceral endoderm differentiation and subsequent cavitation on FGF-1 signalling (Esner, Pachernik et al. 2002). Perhaps a lack of STO feeder cells is correlated with a lack of FGF-1 signalling, although a lack of FGF-1 signalling would be expected to cause more severe disruptions in differentiation than is actually identified in –F +FBS conditioned EBs. Cavitation represents the first wave of programmed cell death in the developing embryo and its importance has long been known (Bellairs 1961; Saunders 1966). Cavitation in embryoid bodies, is largely thought to parallel development of the pro-amniotic cavity in the developing embryo *in vivo*, moreover is thought to require apoptosis inducing factor (AIF) (Joza, Susin et al. 2001; Feraud, Debili et al. 2007). ESCs that over-produce catalase, an enzyme which degrades hydrogen peroxide, do not cavitate (Hernandez-Garcia, Castro-Obregon et al. 2008), therefore perhaps in the absence of feeders, ESCs lack AIF and/or are stimulated to over-produce catalase and although this trend is exaggerated in the absence of serum, serum alone cannot compensate for a lack of feeders with regard to cavitation.

Variations in culture conditions were also shown to also affect ESC differentiation. Serum-free conditions did not appear to support ESC differentiation but instead favoured self-renewal, since –F –FBS conditioned EBs displayed significantly higher proportions of Oct4 and Nanog positive ESCs (compared to +/-F +FBS) (Figures 3.9 – 3.12), and simultaneously lacked differentiation to primitive endoderm, identified via reduced Gata6 levels (Figure 3.13, 3.14). This result, again suggests that serum, not feeders, is crucial for typical ESC behaviour, moreover in this instance, it appears that a component of serum regulates Oct4, Nanog or Gata6, or indeed all three. The interaction of Oct4, Nanog and Gata6 has long been studied. Interestingly, the loss of Nanog was shown to be a requirement for successful primitive endoderm differentiation (Hamazaki, Oka et al. 2004), although another study

suggested that initiation of primitive endoderm differentiation is independent of Nanog (Frankenberg, Gerbe et al. 2011; Filliers, Goossens et al. 2012). Oct4 and Gata6 interaction is more well studied although intracellular modulation of pluripotent and primitive endoderm factors is less defined. Knockdown of Oct-4 has been shown to result in the up-regulation of Gata6 (Hay, Sutherland et al. 2004), but there are many proposed regulatory factors. Myc, a proto-oncogene known to promote cell proliferation (Ifandi and Al-Rubeai 2003; Tamura, Hua et al. 2005) has been shown to control pluripotency (Oct4 expression included) via suppression of Gata6 (Smith and Dalton 2010; Smith, Singh et al. 2010). Another study showed that a target gene of Oct4, serine/threonine kinase40 (Stk40) links pluripotency and extraembryonic endoderm via activation of Erk/MAPK (Li, Sun et al. 2010). With this in mind, a lack of serum could stimulate a reduction in Myc, leading to slower proliferation and lack of Gata6 expression (as indentified in –F –FBS conditioned EBs), or indeed a lack of serum could affect the interaction between Oct4 and Stk40. Likewise, platelet derived growth factor alpha (PDGFα) has been shown to be essential for PE differentiation (Artus, Panthier et al. 2010), moreover it was shown that in serum-free conditions, only supplementation with PDGFα alongside other cytokines, can stimulate mesenchymal stem cells to differentiate to neuronal lineages (Tao, Rao et al. 2005). This suggests that that serum-free conditions lack an array of cytokines, of which PDFGα could be important. The feeder parameter however (+/-F) did not alter levels of Oct4 and Nanog positive cells in EBs, although it did affect differentiation to primitive endoderm. This is in contrast to work by Hamazaki et al., who showed that differentiation to primitive endoderm is achieved in mESCs without the presence of feeder cells (Hamazaki, Oka et al. 2004).

Visceral and parietal differentiation was also lacking in -F- FBS conditioned EBs, detected by reduced AFP levels (Figure 3.15, 3.16) and identified with morphology studies. Visceral and

parietal endoderm are derivatives of primitive endoderm (Lehtonen, Lehto et al. 1983; Artus, Piliszek et al. 2010), moreover Gata6 null embryos fail to form visceral and parietal endoderm (Morrisey, Tang et al. 1998; Cai, Capo-Chichi et al. 2008), outlining the importance of primitive endoderm differentiation for parietal and visceral differentiation. Cell lineage is not the only influential factor though, since it has been shown that parietal endoderm differentiation is only successfully achieved in the mouse once adequate cell-interactions with ectoderm cells occur (Hogan and Tilly 1981). A lack of serum, shown to affect differentiation to endoderm, could therefore be attributed to a lack of cytokine(s), or to a disruption in ectoderm differentiation, leading to insufficient cell-cell interactions and cross-talk. Nonetheless, results have shown that a lack of serum causes major disruptions in endoderm differentiation. Conley et al. showed that in serum-free media, hESCs do not differentiate to visceral endoderm (Conley, Ellis et al. 2007) and it is only upon the supplementation with BMP-4 that the visceral endoderm derivatives are reconstituted. Interestingly, it has been shown that the heterogeneous Nanog expression pattern, identified and true for all three culture conditions during monolayer culture, can dictate PE differentiation, furthermore Nanog is shown to directly repress Gata6 expression through binding to the proximal promoter region of Gata6 (Singh, Hamazaki et al. 2007). There is also growing evidence to suggest that differentiation to endoderm and primitive streak is governed largely by Wnt. Nakanishi et al. showed that in serum-free media, Wnt supplementation was necessary to stimulate primitive streak (PS) differentiation in hESCS and furthermore Wnt canonical pathway is essential for mESCs to differentiate into PS cells (Nakanishi, Kurisaki et al. 2009). It could be that –F –FBS conditions do not support the Wnt pathway.

BM formation was uncharacteristic in –F –FBS conditioned EBs also, attributed to atypical laminin expression and localization (Figure 3.17). BMs, as described previously, represent the earliest extracellular matrices produced during embryogenesis, of which laminin is a major component. Of the three chains which make up the laminin heterodimer, beta1 and gamma1 are detected at the 2 cell stage, whilst alpha1 is detected at the 8-16 cell stage (Cooper and MacQueen 1983; Dziadek and Timpl 1985). Disrupted BM synthesis, detected in –F –FBS conditioned EBs, is relatively unsurprising given the importance of endoderm cells, which are lacking in –F –FBS conditioned EBs, in the deposition of BM. BMs have been shown to play a role in endoderm differentiation and vice versa (Murray and Edgar 2000) and one recent study demonstrated the importance of laminin in regulating ESC polarity (Li, Edgar et al. 2003), important in the organisation of differentiation. Although LamA1 is known to be expressed between endoderm and mesenchyme, in the early stage of BM formation, as in the early stages of EB development, LamA1 is found exclusively expressed by endoderm cells (Simo, Bouziges et al. 1992). LamA1 chains are thought to drive secretion of laminin trimer regulated via beta1 integrins (Aumailley, Pesch et al. 2000). Studies have also shown that mESCs deficient in beta1 integrin, result in a lack of LamA1 secretion to extracellular space (Aumailley, Pesch et al. 2000), moreover a deficiency in beta1 integrin is shown to interfere with BM self-assembly specifically Laminin-111 (Sasaki, Forsberg et al. 1998), similarly identified in –F –FBS conditioned EBs. It is possible perhaps, that this condition lacks beta1 integrin, so crucial in BM self-assembly.

Expression of LamA1, commonly associated with BM secretion and functionality (Yurchenco, Quan et al. 1997; Miner, Li et al. 2004), was significantly lower in –F -FBS than +F +FBS conditioned EBs (Figure 3.20), and localisation was unusually central in EB rather than in an outer BM position (Figure 3.19). This would imply that LamA1 synthesis,

transportation and distribution is defective due to a lack of serum, suggesting that serum (or a component of serum) has a role in facilitating LamA1 transport. LamA1 domains have been shown to be essential for visceral endoderm differentiation (Akerlund, Carmignac et al. 2009), lacking in –F –FBS conditioned EBs, suggesting a lack of serum influences this interaction. LamA1 has been shown to be dependent on Sonic hedgehog in muscle progenitor cells (Anderson, Thorsteinsdottir et al. 2009) furthermore TGF-beta, was shown to induce LamA1 (Nguyen, Bai et al. 2002). Either mechanisms of LamA1 control could be lacking in –F –FBS conditions, resulting in significantly lower LamA1 expression and inadequate BM. In comparison, EBs conditioned in the presence of serum (+/- feeders) displayed correct localisation of laminin, found in the BM position, and moreover the BM was typically thick, Reichert's-like membrane. Research has shown that only once laminin is secreted (a consequence of LamA1 expression) can the different laminin trimers interact with each other and assemble into a functional meshwork (i.e. BM) (Urbano, Torgler et al. 2009). A lack of serum could potentially disrupt this process, whilst the presence of a feeder layer appears dispensable when considering BM synthesis and deposition.

As outlined previously, ESC differentiation to mesoderm and ectoderm was also different depending on culture condition. –F –FBS conditioned EBs were stimulated to mesoderm and ectoderm, detected by a 100-fold increase in *Bry* and 15-fold increase in *Pax6*. Brachyury expressing-cells represent a transient population, therefore although Bry expression in day 7 –F –FBS conditioned EBs was detected at significantly higher levels than +F +FBS conditioned EBs, it is known that under normal culture conditions, Bry is downregulated in EBs after day 4. Therefore, it is possible that the mesoderm markers had already peaked before day 7 in +F +FBS conditioned EBs, and therefore high *Bry* expression as detected in –F –FBS conditioned EBs, could represent delayed mesoderm differentiation. Bettiol et al.

suggested that media supplemented with serum (fetal bovine serum) increases expression, markers of endoderm (AFP) and mesoderm (Bry) in hESCs (Bettiol, Sartiani et al. 2007). Unpublished observations (personal communication, Dr Patricia Murray, University of Liverpool) suggest that in hESCs, high levels of *Bry* are directly correlated with *Oct4*, since hESCs co-express *Bry* and *Oct4*. However, since *Foxc1* and *Tbx6*, markers of paraxial mesoderm were also shown to significantly increase in –F –FBS conditioned EBs it would appear that differentiation to mesoderm is a true representation, since *Foxc1*, unlike *Bry*, is maintained in EB cultures following induction (unpublished observations of our Stem Cell group), therefore higher levels of this gene, are likely to truly represent enhanced differentiation to mesoderm in -F -FBS EBs. A lack of feeders was shown to affect mesoderm differentiation also (despite the present of serum); *Bry* expression increased 10-fold, compared to +F +FBS conditioned EBs, however differentiation to ectoderm, specifically *Pax6* expression, was unchanged when comparing +/-F +FBS, implying that serum, not feeders, is more important for Pax6 expression. It has been shown that differentiation of hESCs to paraximal mesoderm in serum-free media is only achieved providing TGF-beta signaling is inhibited (Mahmood, Harkness et al. 2010) and in one study, disrupted polarisation within the EB, as demonstrated in –F –FBS conditioned EBs, results in differentiation predominantly along mesechymal lineage and spontaneously produces hematoendothelial precursors (Krtolica, Genbacev et al. 2007).

Similarly, early ectoderm differentiation (detected by expression of *Pax6*) was significantly increased in serum-free conditioned EBs (-F –FCS) when compared to EBs conditioned in the presence of feeders and serum (+F +FCS) at day 7. Until a range of time points are investigated, it is unclear whether this result represents delayed ectoderm differentiation, or alternatively a definitive increase in ectoderm differentiation, as a result of different

environmental cues initiated by a lack of feeders cells or serum, compared to EBs grown in normal conditions, in presence of feeders and serum.

Overall and in conclusion, these results suggest that EB differentiation patterns become disorganised if growth conditions prior to EB formation, lack serum and/or feeders. In – F – FBS conditioned EBs, there is a lack of extraembryonic endoderm, BM deposition and cavitation, explained largely by a corresponding lack of Gata6 which has been shown to be required for LamA1 expression (Li, Arman et al. 2004). LamA1 is required for laminin trimer formation and secretion which in turn is required for BM deposition, known to be required for ectoderm polarisation and cavitation. Lonai et al., show that Gata6 induction is dependent on FGF signalling, therefore –F –FBS conditions could affect FGF signalling in the EBs, ultimately underpinning this disorganisation.

The -F +FBS conditioned EB phenotype however, is less explicable. Primitive endoderm and BM deposition appeared normal, however these EBs lacked a multi-layering of cells and thick Reichert's-like BM. This result suggests that there is an issue with parietal endoderm differentiation, attributed purely to a lack of feeders. This could be due to a lack of either a feeer cell-specific surface factor, or a soluble factor synthesised and secreted into the media, or both. A proteome study of STO feeder cell conditioned medium (CM) identified 136 unique proteins, of these many were known to play a role in ESC differentiation and ECM remodelling (Lim and Bodnar 2002; Shi, Xie et al. 2005; Buhr, Carapito et al. 2007). Furthermore one study showed that CM from visceral-endoderm-like cell line was sufficient to induce parietal endoderm differentiation (Mummery, van Achterberg et al. 1991). Taken together these data suggest that a soluble factor that is missing when feeders are removed, is crucial for parietal endoderm differentiation. However, a role for substrate contact has also been suggested to be important for parietal endoderm differentiation in EBs from teratocarcinoma cells (Grabel and Watts 1987). This could represent a role for feeder-cell

specific surface molecules necessary for the stimulation of parietal endoderm differentiation. Differentiation to parietal endoderm is often thought to require over-expressing Gata6 cells (Kim and Ong 2012), which are lacking in –F +FBS conditioned EBs, and this is often attributed to the effect on the upstream transcription factor Sox7 (Futaki, Hayashi et al. 2004; Niimi, Hayashi et al. 2004). Nodal signalling has also been identified as crucial for extraembryonic endoderm differentiation, therefore a lack of feeders could result in a disruption in this signalling pathway (Kruithof-de Julio, Alvarez et al. 2011). Metalloproteinases have been highlighted as regulators of parietal endoderm differentiation also (Behrendtsen and Werb 1997) and studies have suggested that differentiation to parietal endoderm is a plastic event, varying in response to BMP (Paca, Seguin et al. 2012). A lack of feeder cells could be correlated with on or indeed all of these factors, although the exact mechanisms are difficult to isolate since the precise roles of the feeder cells in ESC culture have yet to be characterized in any great depth.

4. Heparan Sulfate is crucial for normal mESC behaviour

4.1 General Introduction

A master controller of regulatory proteins involved in mESC differentiation is heparan sulfate (HS) and as discussed previously, there is accumulating evidence for the importance of HS in an array of physiological processes governing embryogenesis via its interactions with a plethora of protein ligands (Klagsbrun 1990; McKeehan, Wang et al. 1998; Ornitz 2000; Fuerer, Habib et al. 2010; Mundy, Yasuda et al. 2011; Shimokawa, Kimura-Yoshida et al. 2011). For example, mice lacking the HS biosynthetic enzyme, EXT-1, fail to gastrulate due to a major deficiency in HS synthesis (Lin, Wei et al. 2000).

Expression levels and activity of a number of HS biosynthetic enzymes dictates the final sulfation pattern of a mature HS chain, therefore dictates function. HS synthesis is an enzyme-driven process whereby HS chain polymerisation is followed by step-by-step chain modification (Sasisekharan and Venkataraman 2000). However, each step in the process does not reach completion, giving rise to heterogeneity in HS chains and a variety of structures depending on cell type, environment and stimuli (Prydz and Dalen 2000). Little is known of what regulates the process; however, studies have shown that upon differentiation, HS biosynthetic enzyme expression does alter in mESCs (Nairn, Kinoshita-Toyoda et al. 2007). The proteins EXT1, EXT2, NDST1, Sulf1 and Sulf2 are some of the key enzymes involved in the biosynthesis and modification of HS chains, their precise roles have been outlined previously. The exostosin genes, *EXT1* and *EXT2*, encode glycosyltransferases responsible for HS chain initiation and elongation (McCormick, Duncan et al. 2000; Busse, Feta et al. 2007). N-deacetylase/N-sulfotransferase (*NDST1*) is involved in HS N-sulfation (Kjellen 2003) and shown to be crucial in lung development, specifically for facilitation of BMP signalling (Hu, Wang et al. 2009; Ringvall and Kjellen 2010). *NDST1* levels have been

shown to alter in mESCs depending on differentiation state (Dagalv, Holmborn et al. 2011), and varying levels of *NDST1* and/or *NDST2* collectively effects the HS species that is synthesised in mESCs (Pikas, Eriksson et al. 2000; Holmborn, Ledin et al. 2004), Interestingly, levels of *EXT1* and *EXT2* have been shown to affect the levels and activity of *NDST1* (Presto, Thuveson et al. 2008). 6-O-endosulfatases 1 and 2 (Sulf1 and Sulf2) are extracellular enzymes which fine tune HS structure by removing 6-O-sulfate groups from HSPGs in the extracellular environment (Pempe, Burch et al. 2012). Loss of the sulf enzymes has been shown to feedback and alter the expression of other biosynthetic enzyme expression, thereby indirectly affecting HS sulfation pattern (Lamanna, Frese et al. 2008). During embryogenesis, the exact roles of *Sulf1* and *Sulf2* are unclear, with some suggesting that they exist mutually exclusively (Lum, Tan et al. 2007), whilst others suggest that their roles overlap (Holst, Bou-Reslan et al. 2007). Nonetheless they are important enzymes controlling HS structure and, therefore, function.

HS chains synthesised by different cell and tissue types differ both structurally and functionally (Thomas, Clayton et al. 2003; Holmborn, Ledin et al. 2004; Nairn, Kinoshita-Toyoda et al. 2007); every cell synthesises an array of structurally distinct HS chains. The structure of HS is also dynamic and directed by the extracellular environment. For example changes in HS chain length, sulfation pattern and domain organisation occur throughout lung development and brain development (Brickman, Nurcombe et al. 1998; Thompson, Connell et al. 2011). Furthermore, it has been shown that changes in HS species are a consequence of differentiation state and vice versa for mESCs as well as other cell types (Salmivirta, Safaiyan et al. 1998; Jackson, Murali et al. 2007; Smith, Meade et al. 2011). Conversely, HS sulfation pattern has been shown to affect differentiation of mESCs (Forsberg, Holmborn et al. 2012), for instance, to a neuronal lineage (Johnson, Crawford et al. 2007; Pickford, Holley et al. 2011).

Like all cell types, mESCs synthesise HS and present it as a HSPG either at the cell surface (Williams and Fuki 1997; Tumova, Woods et al. 2000) or secrete it into the ECM, regardless, either at the cell surface or in the ECM, HS is well positioned to control cell-cell interactions or cell-protein interactactions thereby facilitating numerous cellular processes, including the differentiation of mESCs (Johnson, Crawford et al. 2007; Lanner, Lee et al. 2010). Cell surface HSPGs can also be shed into the ECM via proteolytic cleavage of the protein core and/or endoglycosidic cleavage of the HS chains by extracellular heparanase (Bame 1993; Vlodavsky, Goldshmidt et al. 2002; Patel, Knox et al. 2007; Vlodavsky, Ilan et al. 2007) and it has been shown that these secreted proteoglycans govern proliferation of hESCs (Levenstein, Berggren et al. 2008). Interestingly, HS purified from a cell surface extract can be structurally distinct from HS in the cell conditioned medium, as identified in osteoblast cultures (Murali, Manton et al. 2009).

In the previous results chapter variations in mESC culture conditions were shown to cause defects in EB development. In the absence of feeders (but presence of serum), although EBs can form thin BMs, there is an effect on extraembryonic endoderm (EEE) development, since there is a tendency for these EBs to develop a single layer of flat Gata6 positive EEE on the surface. This result implies that further differenitation of primitive endoderm to parietal and visceral endoderm might be effected. A reduced level of cavitation than in controls was also identified, although the reasons for this are unclear. In –F –FBS conditioned EBs, the phenotype is more severe. Primitive endoderm differentiation is inhibited, as evinced by few Gata6 positive cells, there is limited deposition of BM, and little evidence of parietal/visceral endoderm differentiation. These EBs also show little cavitation and increased expression of mesoderm and ectoderm markers. An $EXT1^{-/-}$ mESC line was exploited in this chapter, in order to investigate the specific role and source of HS in typical mESC behaviour, since it is known that HS specifically influences FGF and BMP-4 signalling (Ornitz 2000; Shimokawa,

Kimura-Yoshida et al. 2011), required for primitive endoderm differentiation and visceral endoderm differentiation, respectively, both lacking in the defective –F –FBS conditioned EBs. Furthermore, supplementation with exogenous PMH was investigated as a possible method of rescuing atypical mESC behaviour, as seen with –F –FBS conditions.

$EXT1^{-/-}$ mESCs have a genetic mutation in the *EXT1* gene, which encodes a glycosyltransferase enzyme that catalyses HS chain polymerisation once the Xyl-linkage region is attached to the core protein. $EXT1^{-/-}$ mESCs are, therefore, defective in the ability to generate endogenous HS (Lin, Wei et al. 2000), and as a result, are HS deficient (Lind, Tufaro et al. 1998; McCormick, Leduc et al. 1998).

Should the role of serum/feeders be to supply a source of HS to the ESC culture, then HS-deficient $EXT1^{-/-}$ mESCs would be expected to develop normal EBs, comparable to wild-type EBs, providing serum and feeders are present. Alternatively, if the main effect of serum/feeders is to stimulate endogenous HS synthesis, then HS-deficient $EXT1^{-/-}$ mESCs would be expected to develop EBs similar to wild-type EBs cultured in the absence of serum/feeders. Taking these together, it is hypothesised here that FBS and/or feeders might provide a source of HS that is required for the normal development of EBs. Accordingly, biosynthetic enzyme expression was investigated for each culture condition, together with a structural analysis of cell-surface HS and soluble HS shed into media.

Results in this chapter demonstrate that:

- Following heparin supplementation, –F –FBS conditioned EBs:
    - deposit a BM
    - display Gata6+ EEE observed in regions of the EB periphery
    - expression of mesendoderm, paraxial mesoderm and ectoderm markers and are not significantly different from controls

- $EXT1^{-/-}$ mESCs cannot be maintained in the absence of serum
- HS structure and abundance differs depending on the origin/source

4.2. Defective EB development attributed to a lack of serum, can be rescued with exogenous porcine mucosal heparin (PMH)

The common marker of pluripotency, Oct4 was used to determine localisation and levels of self-renewing cells within EBs, exploring the effect of porcine mucosal heparin (PMH) after supplementation of serum-free conditioned EBs with PMH. Upon the addition of exogenous PMH Oct4 expression was mainly localised to central cells of the –F –FBS conditioned EBs and further, Oct4 levels significantly reduced (Figure 4.1, 4.3). This was further supported by qRT-PCR data, which showed that *Oct4* levels were no different from controls (EBs conditioned from +F +FBS) (Figure 4.6 A).

Differentiation to primitive endoderm, was investigated using an antibody specific to Gata6 to assess the potential of exogenous soluble heparin to rescue the lack of primitive endoderm differentiation previously identified in –F –FBS conditioned. Indeed, EBs derived from -F –FBS conditions, supplemented with PMH, displayed increased percentage of Gata6 positive cells (Figure 4.4) and expression was more typically localization to outer cells compared to –F –FBS conditioned EBs (Figure 4.2). Quantification of mRNA levels using RT-qPCR supported these findings (Figure 4.6 B); *Gata6* levels were no different to controls. Additionally, supplementation of serum-free ESC cultures with PMH was also shown to rescue localisation of LamA1, which had previously been shown to be lacking and atypically localised in –F -FBS conditioned EBs (Figure 4.5). In addition, qRT-PCR showed that mRNA levels of *Bry* and *Pax6*, markers of nascent mesendoderm and early ectoderm markers respectively, were rescued in –F –FBS following supplementation with exogenous PMH (4.6 C, 4.6 D).

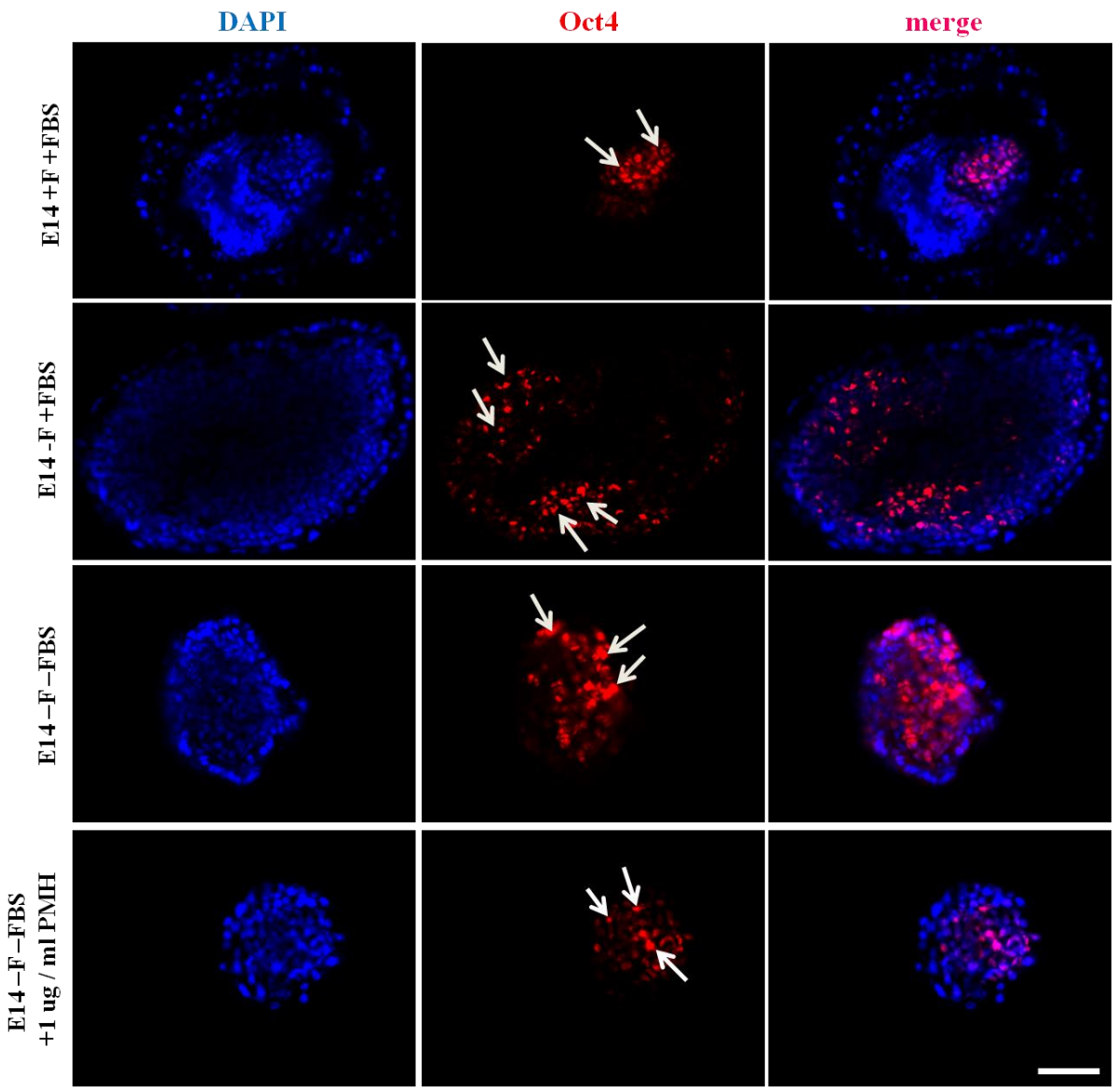

Figure 4.1 Exogenous PMH affects the distribution of Oct4 positive cells within EBs. Serum-free conditioned day 7 EBs displayed Oct4 positive cells localised across the entire EB rather than in discrete central areas, as is the case for EBs conditioned in the presence of serum (+/- feeders). Serum-free conditioned EBs when supplemented with heparin, displayed Oct4 positive cells localised predominantly in central regions, as indicated with arrows. Images are representative of the EB population; the experiment was repeated > 3 times and scale bar represent 200 μm.

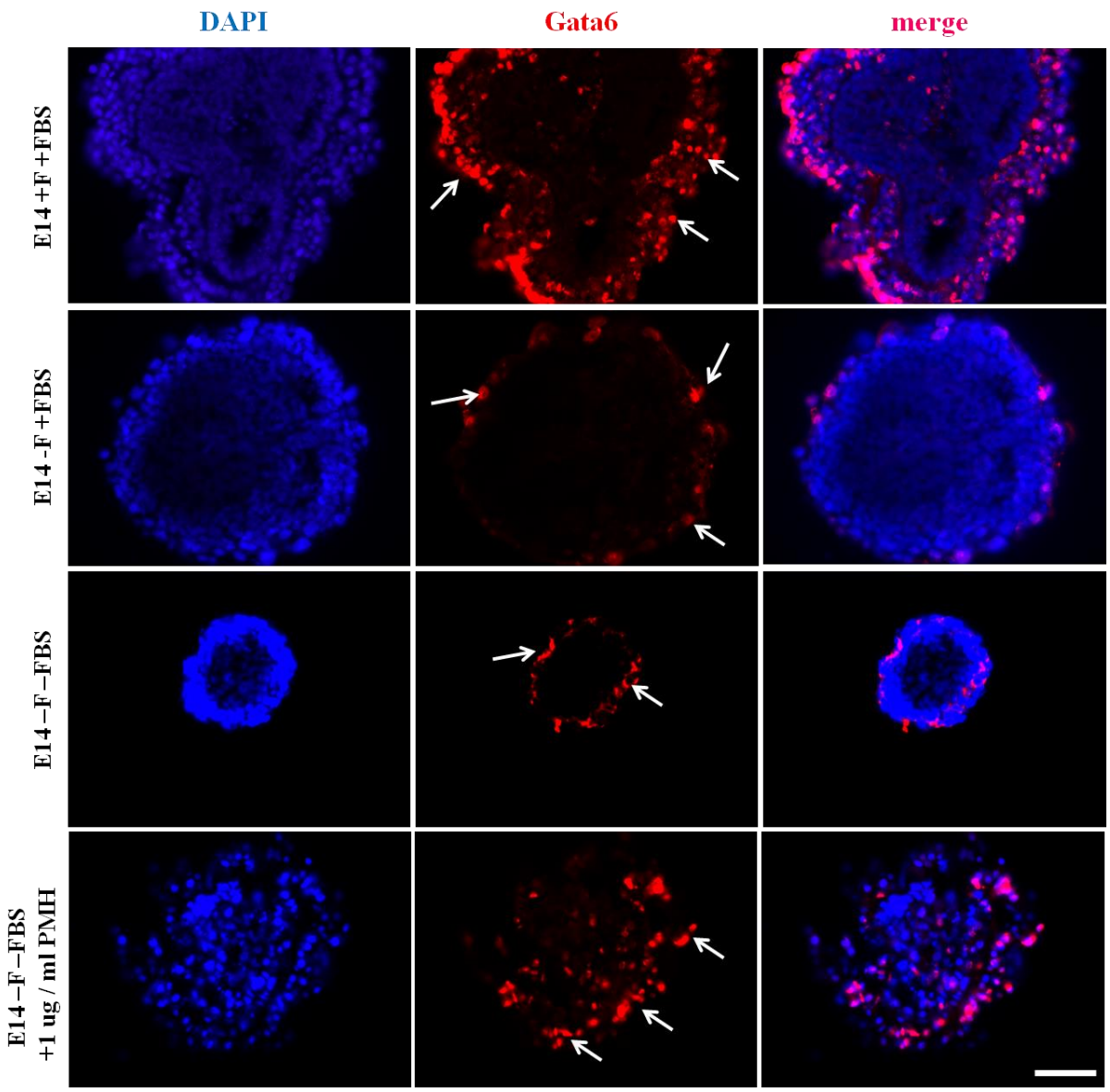

Figure 4.2 Exogenous PMH induces Gata6 expression in peripheral EB cells. Feeder-free and serum-free conditioned day 7 EBs contained fewer Gata6 positive cells than controls. Upon the addition of PMH for 3 passages prior to EB formation, Gata6 positive cells were observed at the EB periphery, comparable to +F +FBS conditioned EBs. Images are representative of the EB population; the experiment was repeated > 3 times and scale bar represent 200 µm.

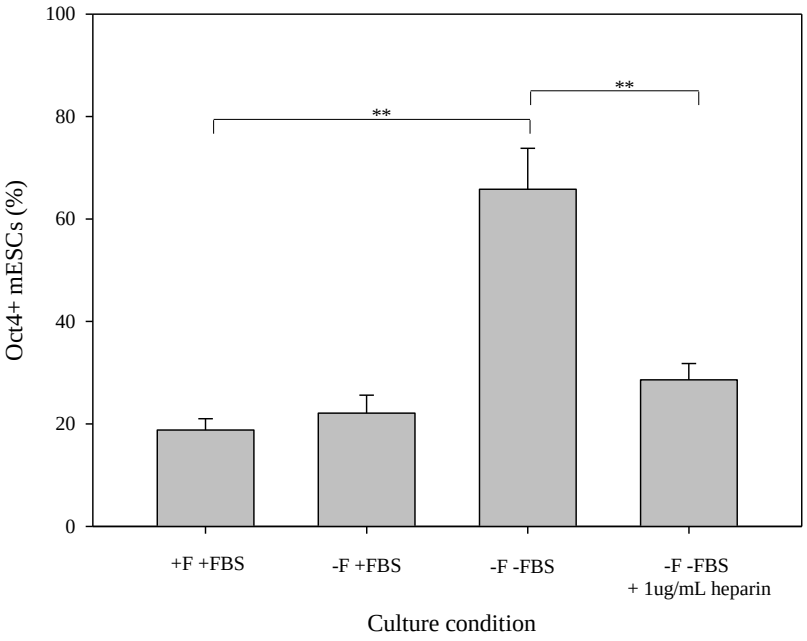

Figure 4.3 Exogenous PMH rescues the percentage of Oct4+ mESCs in feeder-free serum-free conditions, now comparable to +F+FBS conditions. mESCs maintained in –F –FBS supplemented with PMH displayed significantly reduced percentage of Oct4 positive cells, comparable with +F+FBS. n=4, **p<0.01 student's T-test and error bar represents SEM.

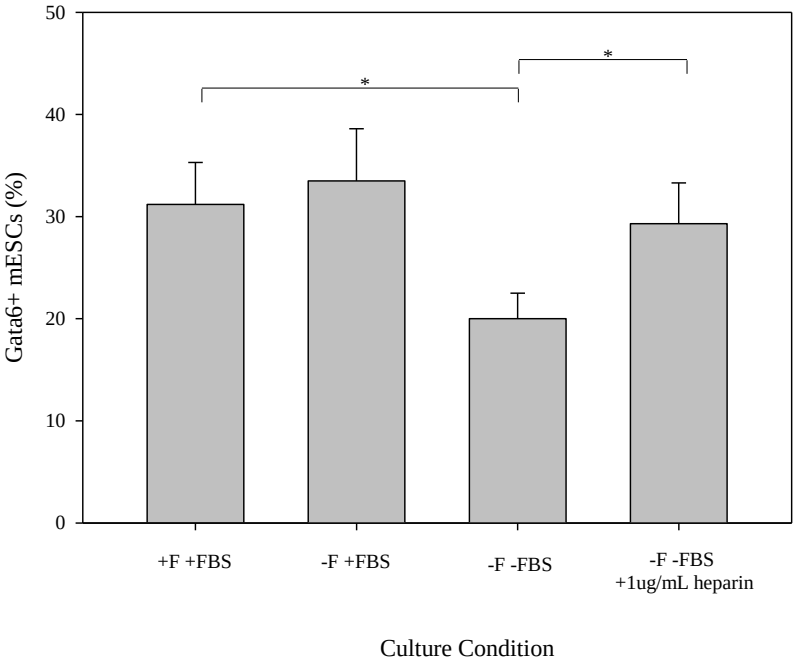

Figure 4.4 Exogenous PMH rescues the percentage of Gata6+ mESCs in feeder-free serum-free conditions, now comparable to +F+FBS conditions. mESCs maintained in –F –FBS supplemented with PMH conditions displayed significantly increased percentage Gata6 positive cells, comparable with +F+FBS conditions. n=4, *p <0.05 student's T-test and error bar represents SEM.

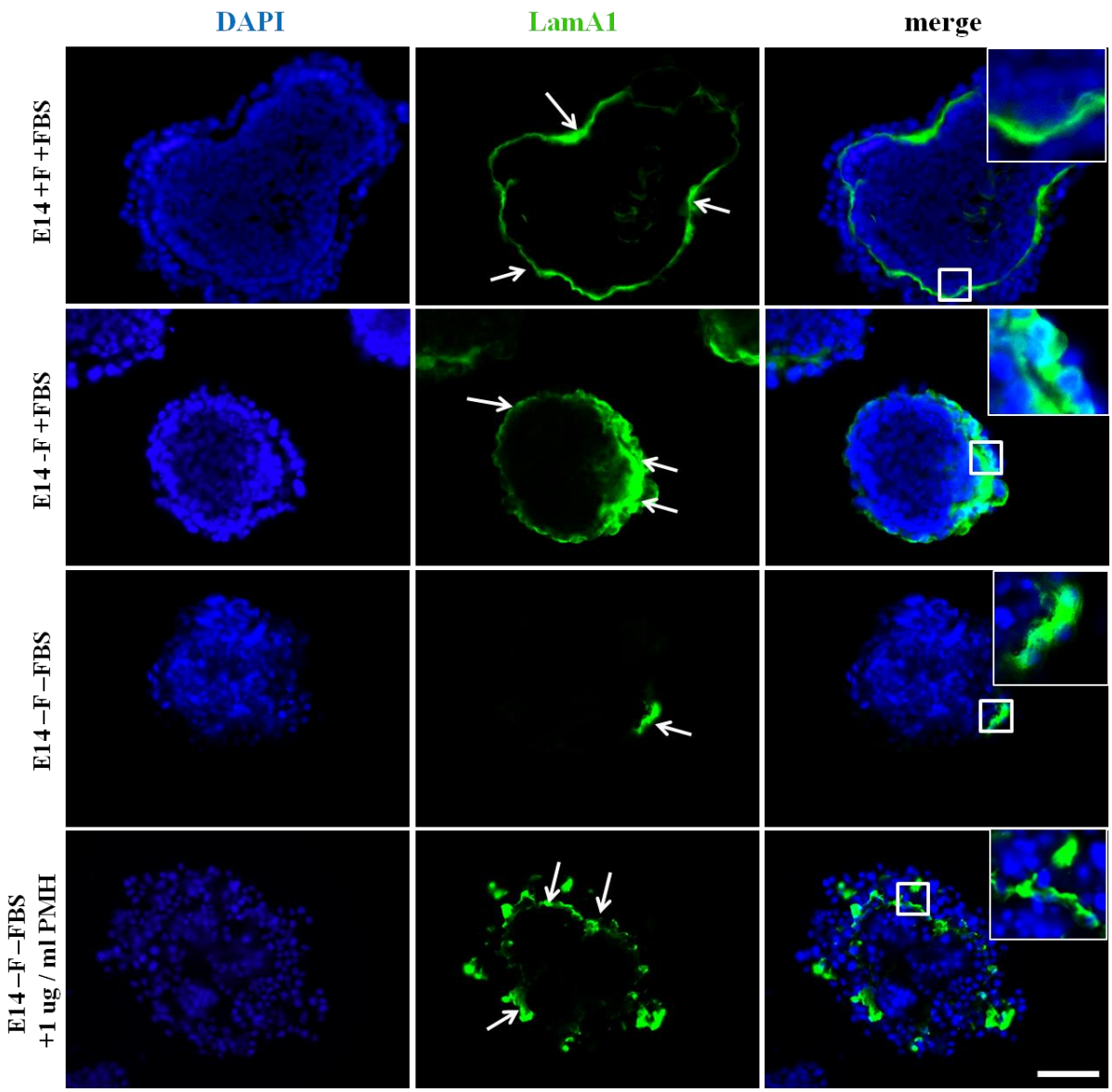

Figure 4.5 Effect of exogenous PMH on laminin expression. Serum-free conditioned day 7 EBs displayed LamA1 expression in discrete regions of EB on outer surface of the peripheral cells rather than in BM position, as indicated with arrows. Upon the addition of PMH for 3 passages prior to EB formation, LamA1 localised more typically to the BM position, again highlighted with arrows. Images are representative of the EB population; the experiment was repeated > 3 times and the scale bar represents 200 μm.

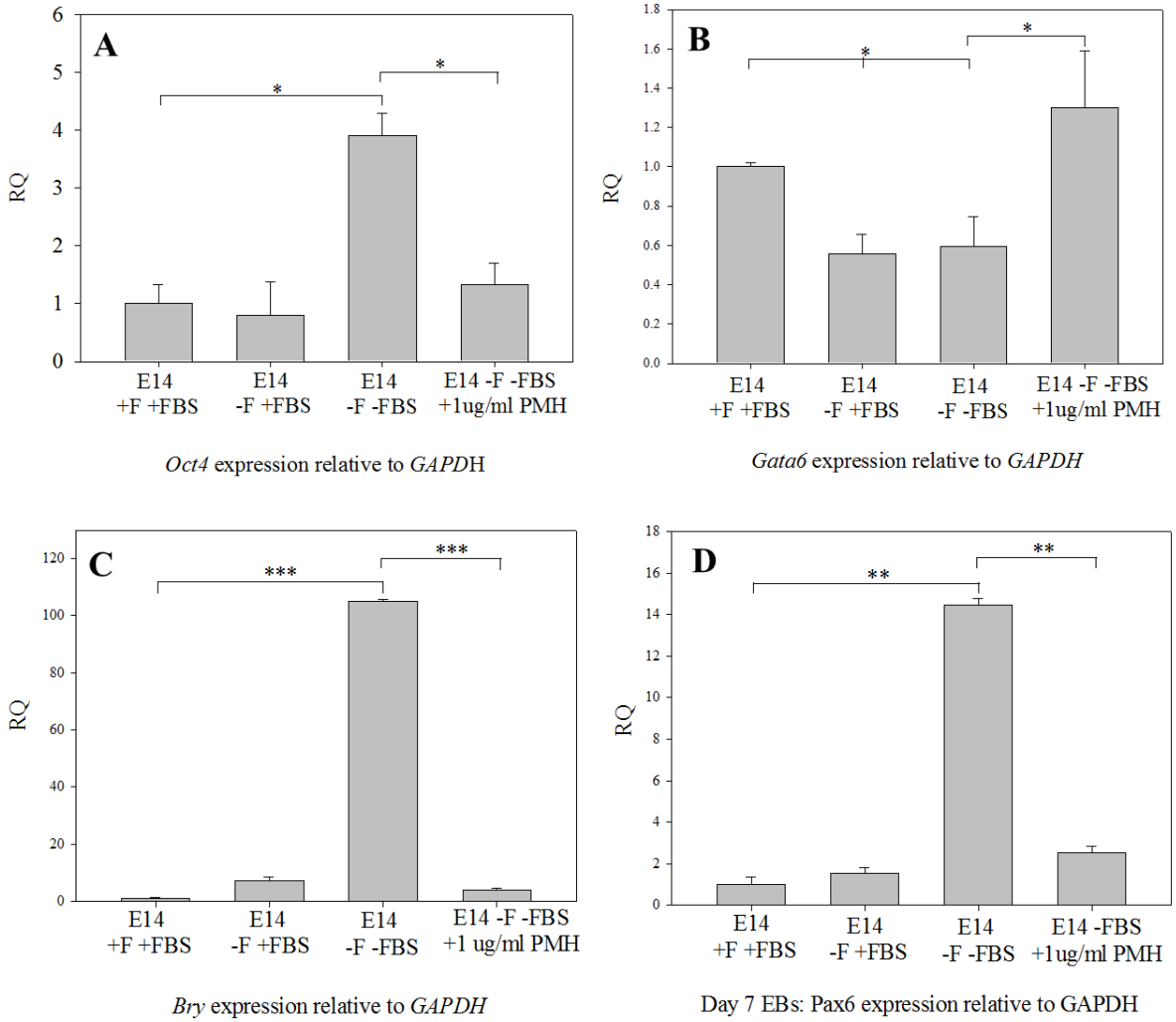

Figure 4.6 Exogenous PMH was shown to rescue a typical EB differentiation marker pattern expression in 7 day serum-free conditioned EBs. [Data for +F +FBS, -F +FBS and –F –FBS was reproduced from Figures 3.11, 3.14, 3.21 and 3.23, for corresponding *Oct*, *Gata6, Bry* and *Pax6,* for comparative purposes]. Serum-free conditioned EBs were shown to have significantly different early differentiation development profiles when compared to EBs conditioned in the presence of serum (+/- F). Specifically, serum-free EBs had significantly higher levels of *Oct4* (A), *Bry* (C) and *Pax6* (D) and significantly lower levels of primitive endoderm marker *Gata6*, when compared to EBs conditioned in the presence of serum +/- F. Addition of soluble heparin (1 ug / ml) to the –F –FBS cultures for 2 passages prior to EB formation, typical development was rescued; *Oct4, Bry and Pax6* were all significantly reduced to levels now comparable to EBs conditioned in presence of feeders and serum (+F +FCS). * $p < 0.05$, ** $p < 0.001$ ***$p < 0.0001$, n = 4, error bars, SEM.

4.3 HS-deficient EXT1$^{-/-}$ mESCs require serum and feeders for normal behaviour

Previously it was shown that supplementation with PMH rescued defects in E14 EB development attributed to a lack of feeders and more significantly, a lack of serum. This result suggested a deficiency in levels and/or species of HS, however, what remained unclear was the origin of HS; is it HS from feeders or serum, or both that is crucial in mESC behaviour?

4.3.1 HS-deficient mESCs cannot be maintained in the absence of serum during 2D expansion

HS-deficient EXT1$^{-/-}$ mESCs were maintained in three distinctly different 2D culture conditions. Of these, only two conditions were able to support EXT1$^{-/-}$ mESC expansion and viability long-term (> 10 passages). Serum-free conditions, although shown to previously support E14 mESCs during 2D culture, proved detrimental to EXT1$^{-/-}$ mESCs; mESCs displayed a rounded cell morphology, and became detatched from the culture dish (Figure 4.7 C). Quantification of viability confirmed this, since over 80 % of EXT1$^{-/-}$ mESCs grown in serum-free cultures were no longer viable by 48 h (Figure 4.8). In contrast, providing that serum was present (+/- feeder layer), EXT1$^{-/-}$ mESCs were maintained for more than 10 passages and displayed typical morphology, proliferation and colony formation (Figure 4.7 A and 4.7 B).

To further confirm that the EXT1$^{-/-}$ mESCs had not differentiated after 10 passages under the different culture conditions, co-immunostaining of Oct4 and Nanog was performed, common markers of ESC pluripotency. EXT1$^{-/-}$ mESCs remained positive for Oct4 and Nanog expression throughout expansion in both conditions (Figure 4.9). Quantification of Oct4 positive EXT1$^{-/-}$ mESCs confirmed that Oct4 expression was comparable to E14 mESCs, and additionally, there was no difference between culture conditions (+/- feeder layer). There was no difference in proportion of Nanog positive cells when comparing E14 mESCs and EXT1$^{-/-}$

mESCs cultured in the presence of serum and feeders (+F +FBS), however, in feeder-free conditions, HS-deficient EXT1$^{-/-}$ mESCs displayed higher proportions of Nanog positive cells compared to E14 ESCs cultured in the same condition. In addition, comparing the effects of culture condition on EXT1$^{-/-}$ mESCs pluripotency, Oct4 expression was unchanged, the proportion of Nanog-positive cells was however, significantly higher in EXT1$^{-/-}$ mESCs cultured in the absence of feeders, compared to EXT1$^{-/-}$ mESCs cultured with feeders (Figure 4.10).

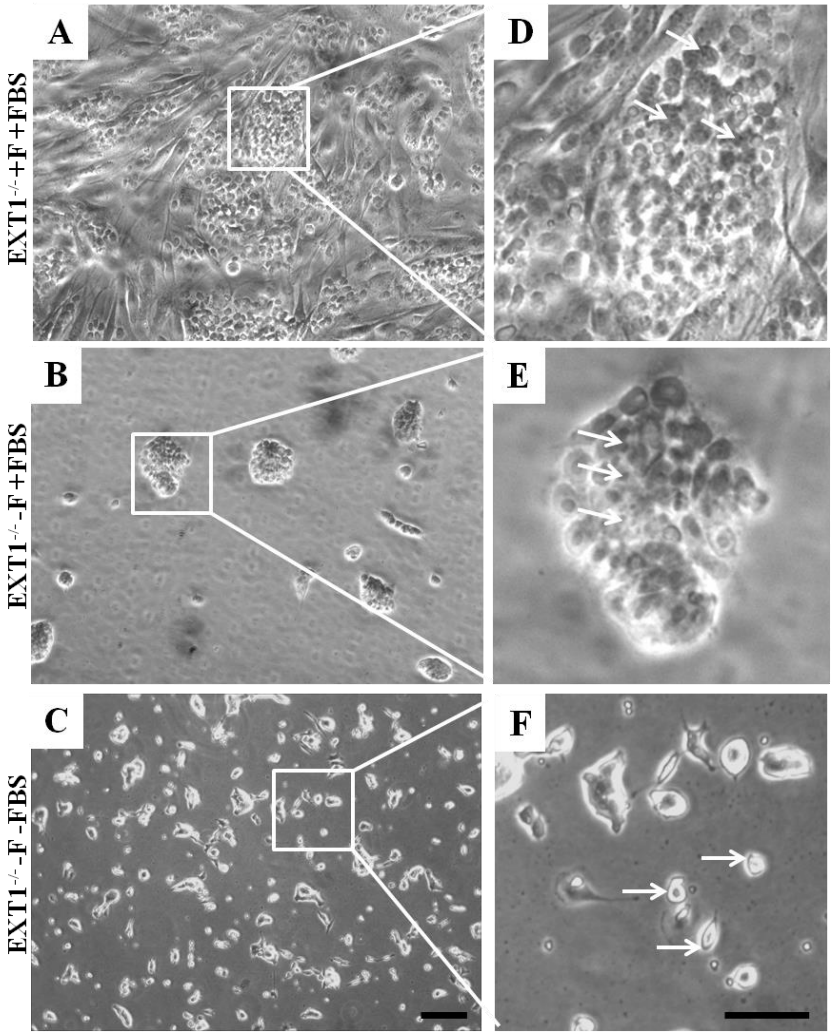

Figure 4.7 HS-deficient EXT1$^{-/-}$ mESC expansion was not supported in serum-free and feeder-free 2D culture conditions. EXT1$^{-/-}$ mESCs were maintained *in vitro* for more than 10 passages in three distinctly different culture conditions in parallel; with feeders and serum (+F + FBS), without feeders but with serum (–F + FBS) and without feeders or serum (–F –FBS), as explained previous. EXT1$^{-/-}$ mESC behaviour and morphology during monolayer culture varied depending on growth conditions. At 48 h EXT1$^{-/-}$ mESCs cultured in the presence of serum (A, B, D and E) (+F + FBS, –F + FBS) displayed typical behaviour; cells adhered to surface of dish and formed colonies. In contrast, EXT1$^{-/-}$ mESCs cultured in serum-free conditions (C and F) (-F –FBS) displayed abnormal behaviour; cells adopted a rounded morphology and became detatched from the dish surface, highlighted with arrows. Long term, the cells were unable to survive in serum-free, feeder-free conditions. Images are representative of the entire population for each condition and the experiment was repeated over 6 times. Scale bar represents 50 μm.

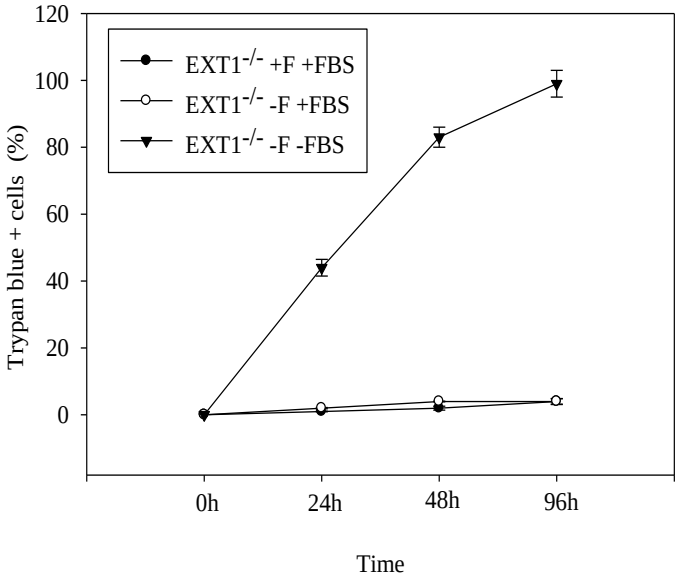

Figure 4.8 HS-deficient EXT1$^{-/-}$ mESC maintained in serum-free 2D conditions are not viable by 48 h. EXT1$^{-/-}$ mESCs were maintained in parallel in 3 different culture conditions; with feeders and serum (+F + FBS), without feeders but with serum (–F + FBS) and without feeders or serum (–F – FBS). The number of trypan blue-positive-cells were counted daily. After 96 h, EXT1$^{-/-}$ mESCs cultured in serum-free, feeder-free conditions were almost completely non-viable (99 %), demonstrating that this condition cannot support long term EXT1$^{-/-}$ mESC expansion. The experiment was repeated three times; error bars, SEM.

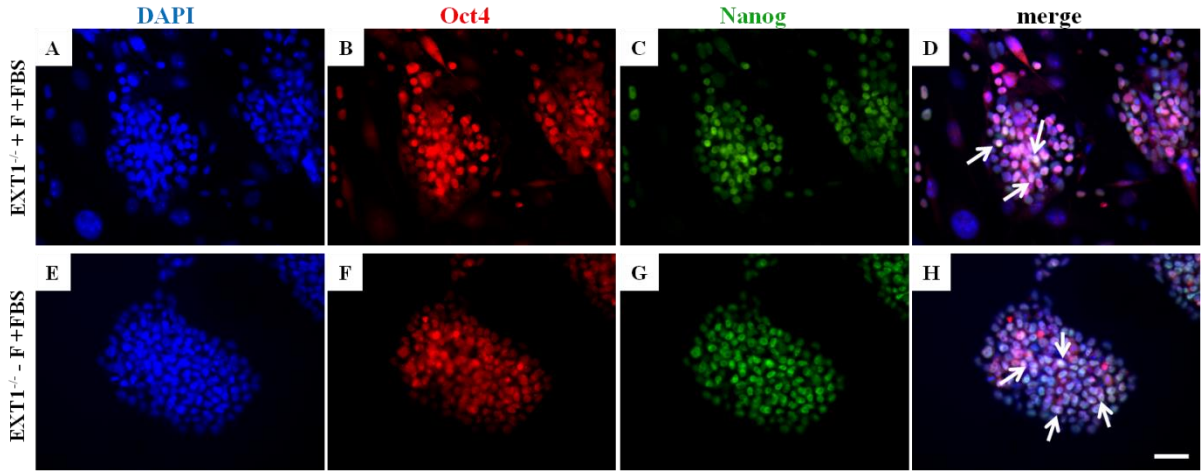

Figure 4.9 Oct4 and Nanog expression in HS-deficient EXT1$^{-/-}$ mESCs cultured in the presence or absence of feeder cells. EXT1$^{-/-}$ mESCs were maintained in two different culture conditions *in vitro* for more than 10 passages, with and without a feeder layer. After 48 h post sub culture, the expression of Oct4 was comparable between the two culture conditions (B and F). However, Nanog positive cells appeared to be more abundant in feeder-free cultures (G) compared to cells cultured in the presence of feeders (C). Furthermore Oct4 and Nanog co-expressing cells (yellow cells labelled with arrows in C and G) appeared more abundant in EXT1$^{-/-}$ mESCs cultured in the absence of feeders (-F +FBS) (H) compared to cells cultured in the presence of feeders. Images are representative of the entire cell population and the experiment was repeated over 3 times. Scale bar represents 100 µm.

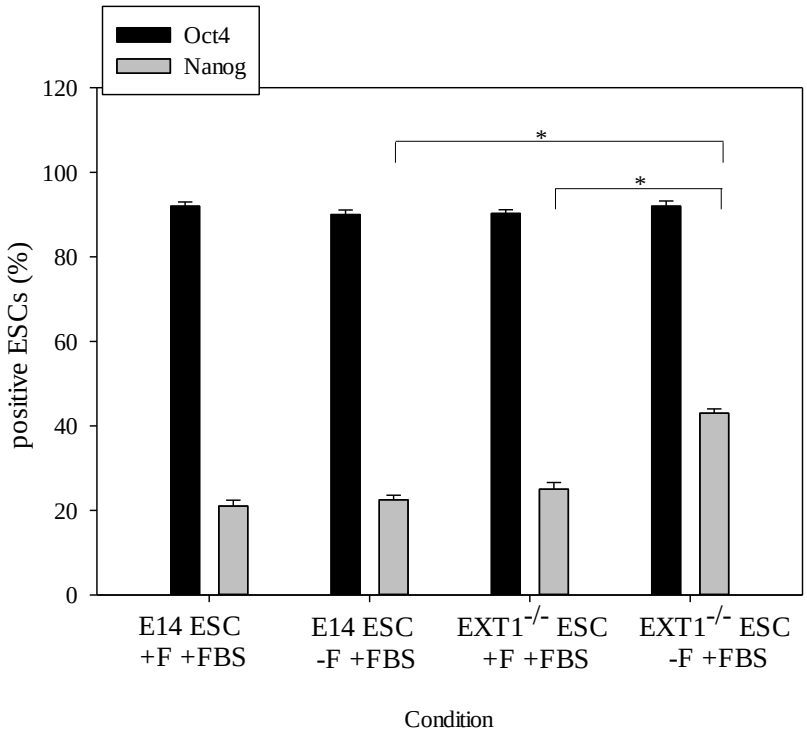

Figure 4.10 The percentage of Nanog positive mESCs is higher in HS-deficient EXT1$^{-/-}$ mESCs compared to E14 mESCs but only in the absence of feeders. EXT1$^{-/-}$ mESCs and E14 mESCs were maintained in parallel for more than 10 passages with or without feeders but in the presence of serum. The proportion of Oct4 and Nanog positive EXT1$^{-/-}$ mESCs and E14 mESCs were comprable in +F +FBS conditions. However when cultured in the absence of feeders, EXT1$^{-/-}$ mESCs displayed significantly higher proportions of Nanog positive mESCs than E14 mESCs cultured in the same condition. EXT1$^{-/-}$ mESCs cultured in the absence of feeders displayed significantly higher proportions of Nanog positive cells when compared to EXT1$^{-/-}$ mESCs cultured with feeders. The proportion of Oct4 positive cells was not significantly different when comparing cell type and conditions. n = 4, * $p < 0.05$, student T-test, error bars represent SEM.

4.3.2 HS-deficient EBs do not display characteristic morphological development

Following expansion of HS-deficient EXT1$^{-/-}$ mESCs in two different culture conditions for more than 10 passages, cells underwent growth in suspension to induce EB formation and differentiation upon the removal of LIF, as shown with E14 mESCs previously. The pattern of differentiation was investigated and compared to E14 mESC EBs and the effect of different growth conditions (+/- feeders) was also evaluated. EXT1$^{-/-}$ mESCs differentiation to EEE and BM formation was central in the analysis, as was the case for E14 mESCs.

One intial observation of HS-deficient EXT1$^{-/-}$ EBs was that they were significantly smaller in diameter when compared to E14 EBs derived from the same culture condition. However, it appeared that culture condition (+/- feeders) had no impact on EB size, since there was no significant difference when comparing EBs with or without feeders (Figures 4.11).

EB morphology was further assessed using toluidine blue, a basic dye which stains nucleic acids and polysaccharides. At day 7, HS-deficient EXT1$^{-/-}$ EBs culture in the presence of feeders and serum displayed evidence for a number of outer cells becoming flattened in morphology, accompanied by a few signs of mutilayering parietal-like cells, indicative of differentiation to endoderm and thin spacing underneath these cells indicating some BM-like structure (Figure 4.12). EXT1$^{-/-}$ EBs conditioned in the absence of feeders however, displayed fewer signs of typical EB development; very few flattened outer cells or mutilayering and a BM that was difficult to identify (Figure 4.12). All EXT1$^{-/-}$ EBs, despite culture condition, lacked cavitation. Generally, one would expect day 7 EBs to display more advanced morphological developmental characteristics, shown previously for E14 EBs, whereby a thick Reichert's-like membrane is apparent, outer cells are morphologically analogous to visceral and parietal endoderm cells and cavitation is evident.

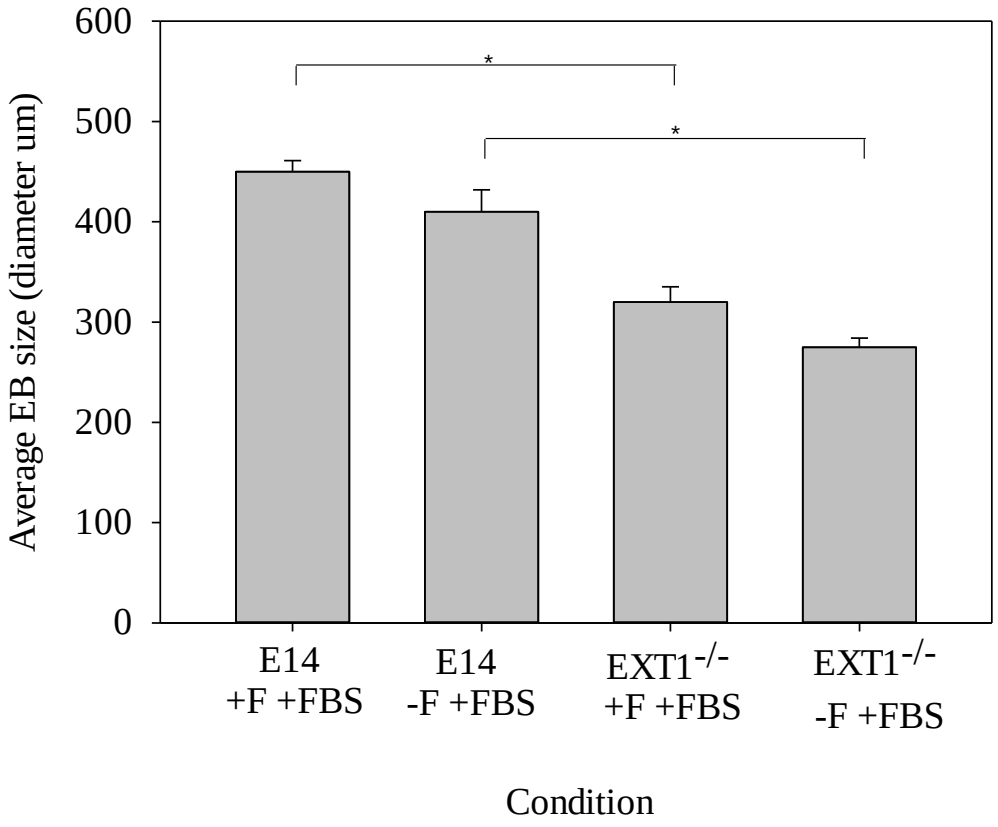

Figure 4.11 HS-deficient EBs are significantly smaller compared to E14 EBs. $EXT1^{-/-}$ EBs conditioned with feeders were significantly smaller than EBs derived from E14 ESCs cultured under identical conditions (+F +FBS). n = 6, * $p < 0.05$; error bars, SEM.

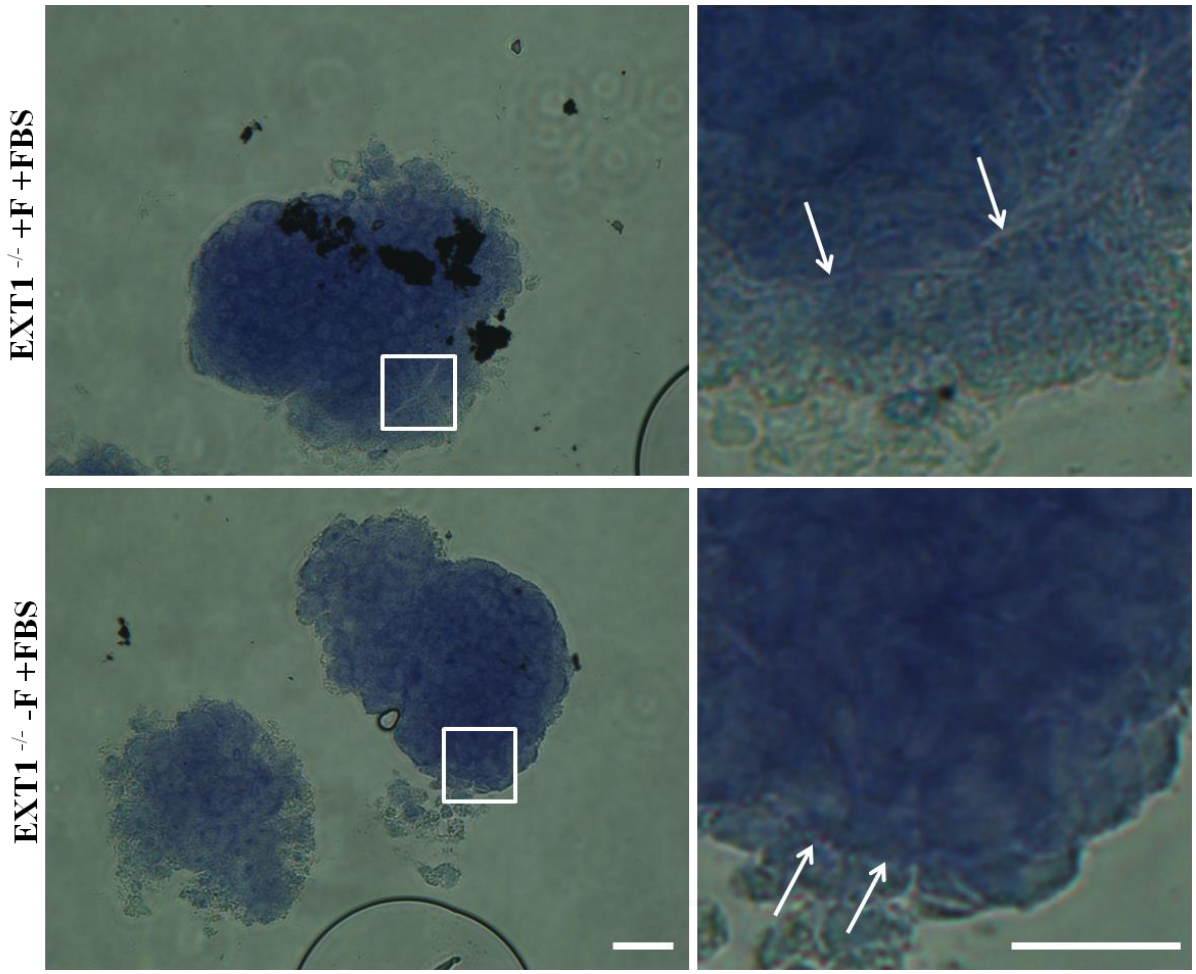

Figure 4.12 HS-deficient EXT1$^{-/-}$ EBs display some signs of normal development but lack cavitation, irrespective of culture condition. EXT1$^{-/-}$ mESCs were maintained in two distinct culture conditions (with or without feeders but in the presence of serum), for 7 days and stained with toluidine blue. In both conditions, EBs lacked cavitation, despite the fact there appeared to be evidence of some BM deposition (arrows) and visceral endoderm differentiation (cells in right panel positioned on EB periphery). EBs shown are representative of the entire EB population for each growth condition. The experiment was repeated over 6 times. Scale bar represents 50 µm.

To further confirm the morphological observations and quantify the differences in differentiation between EXT1$^{-/-}$ EBs and E14 EBs, EBs were co-immunostained for the BM marker LamA1 and cavitation was assessed. Quantification of differentiating EBs was achieved, as outlined previously (Materials and Methods, chapter 2) using a scaling system, whereby EBs were counted as positive if a continuous BM (identified by LamA1 staining) was present in over 50 % of the EB circumference. HS-deficient EXT1$^{-/-}$ EBs generated significantly fewer EBs with complete comprehensive EBs (> 50 % of EB circumference LamA1 +) compared to E14 EBs (Figure 4.13 A). In addition, there was little sign, if any, of cavitation compared to E14 EBs (Figure 4.13 B).

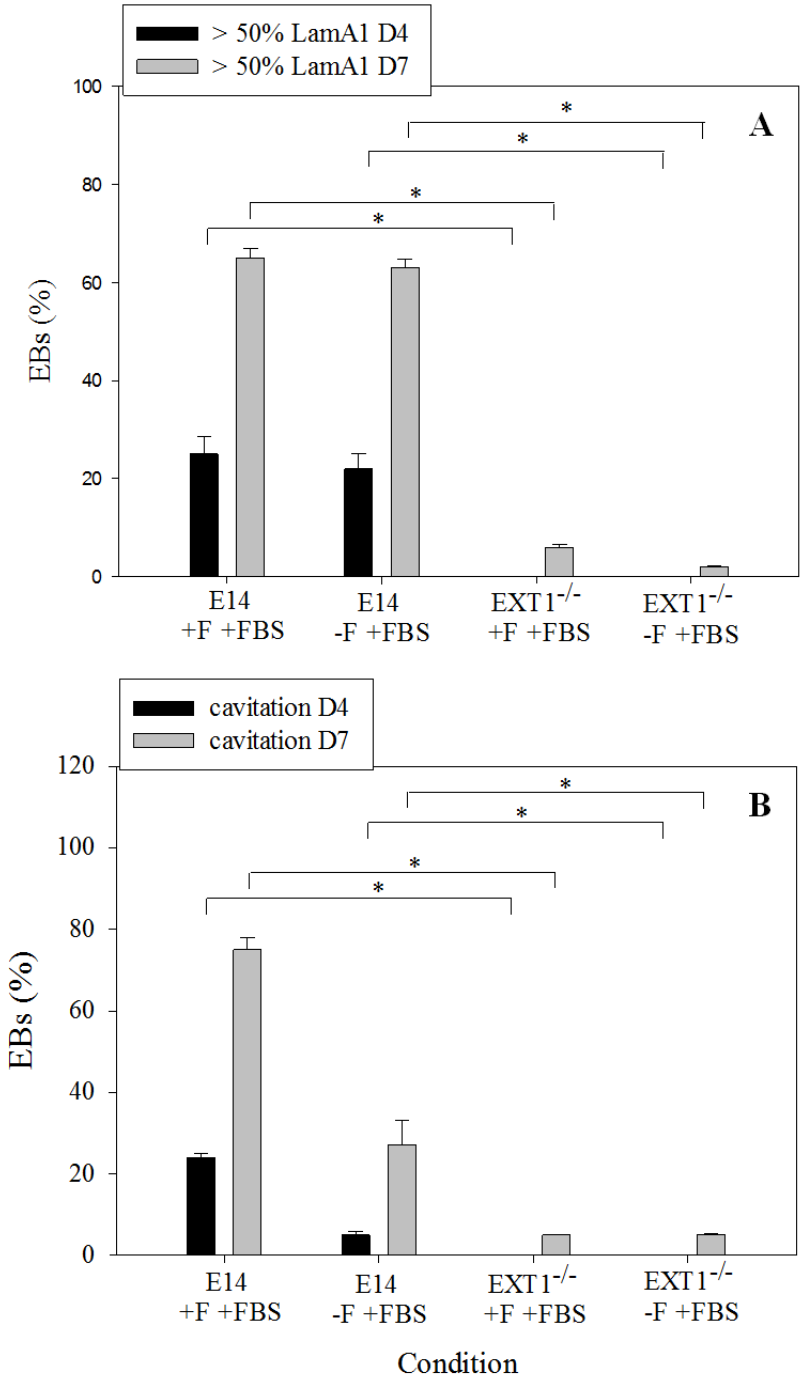

Figure 4.13 HS-deficient EBS lack cavitation and a complete BM. $EXT1^{-/-}$ mESCs were maintained with or without feeders and EB development was quantified to analyse the effect of different culture conditions, as well as make a direct comparison to E14 EBs at day 4 and day 7. The presence of LamA1 (A) was significantly lower in $EXT1^{-/-}$ EBs compared to E14 cells. Cavitation was also significantly lower in $EXT^{-/-}$ EBs (B). Results are consistent at day 4 and day 7. n = 6, error bar: SEM, students T-test, * $p < 0.05$.

4.3.3 HS-deficient EBs show restricted EEE differentiation

The role of HS in mESC pluripotency is misunderstood and inconsistently reported. Some studies have suggested that HS is required for mESCs to remain in a self-renewing state (Sasaki, Okishio et al. 2008; Lanner, Lee et al. 2010; Helledie, Dombrowski et al. 2011), whilst in contrast and more often, studies have demonstrated the requirement of HS for mESCs to exit self renewal (Kraushaar, Yamaguchi et al. 2010; Helledie, Dombrowski et al. 2011). The latter is supported by the studies in this chapter.

Self-renewal, BM synthesis and EEE differentiation have all been analysed for HS-deficient $EXT1^{-/-}$ EBs in order to demonstrate the differences when compared to E14 ESC EBs, which therefore highlights the need for HS in mESC differentiation.

Despite $EXT1^{-/-}$ mESCs being successfully maintained in 2D culture with or without feeders, it appeared from morphological studies that differentiation was impaired since $EXT1^{-/-}$ EBs lacked cavitation and only a few cells displayed characteristic parietal endoderm morphology, despite the fact that the removal of LIF was disruptive. This was, therefore, the subject of further investigation. Oct4, a common marker of pluripotency, was used to investigate the presence of undifferentiated mESCs within EBs grown under different culture conditions. Typically, Oct4 positive cells reduce with time as the EB differentiates (Pesce and Scholer 2001). The primitive endoderm marker Gata6 was also used to identify endoderm differentiation and the distribution of laminin was assessed in detail, using an pan laminin-111 antibody and antibody specific for LamA1, to analyse the ability of HS-deficient ESCs to synthesise functional BM.

$EXT1^{-/-}$ EBs (+/- feeders) displayed significantly higher proportions of Oct4 positive cells compared to EBs conditioned from E14 ESCs +F +FBS, moreover, Oct4 positive cells were distributed across the entire EB, rather than localised exclusively to the centre of the EB, as

observed in normal E14 EBs (Figures 4.14). Culture condition affected this further, since feeder-free conditioned EXT1$^{-/-}$ EBs displayed a significantly higher proportion of Oct4 positive cells, compared to EXT1$^{-/-}$ EBs derived from conditions containing feeders (Figure 4.15). This was further confirmed with RT-qPCR data, which showed that EXT1$^{-/-}$ EBs displayed significantly higher levels of *Oct4* compared to E14 EBs conditioned under the same culture conditions (Figure 4.16).

Investigation into the ability of EXT1$^{-/-}$ mESCs to differentiate to EEE and synthesise functional BM, further highlighted that HS-deficient mESCs do not behave typically. Differentiation of EXT1$^{-/-}$ mESCs to primitive endoderm, uncovered abnormal localisation of Gata6 and levels were significantly lower than those detected in E14 EBs derived from the same conditions (Figures 4.17, 4.18). This is in support of some recent studies which demonstrate the importance of HS for EEE differentiation, moreover propose the model is based on a lack of HS interactions with FGF (Lanner and Rossant 2010). In addition, day 7 EXT1$^{-/-}$ EBs displayed disrupted BM. Although *some* laminin expression was detected in EXT1$^{-/-}$ EBs (comparable +/- feeders), localisation appeared to be intracellular, as identified using an antibody specific to laminin-111. This is in contrast to E14 EBs which displayed laminin expression in the BM-position of EB separating multilayered parietal-endoderm-like outer cells from inner cells (Figure 4.19). Furthermore, LamA1 expression for EXT1$^{-/-}$ EBs, unlike E14 EBs, displayed LamA1 expression intracellularly, despite the identification of some outer primitive endoderm-like, flattened cells (Figure 4.20). Quantification of *LamA1* mRNA levels indicated that EXT1$^{-/-}$ mESCs expressed significantly lower levels of *LamA1* when compared to E14 EBs derived from the same culture condition, although *LamA1* levels did not change between EXT1$^{-/-}$ EBs cultured with or without a feeder layer (Figure 4.21). Generally, these results suggest that defects in EXT1$^{-/-}$ EBs, attributed to a lack of endogenous HS, is unable to be rescued by a feeder layer and/or the presence of serum.

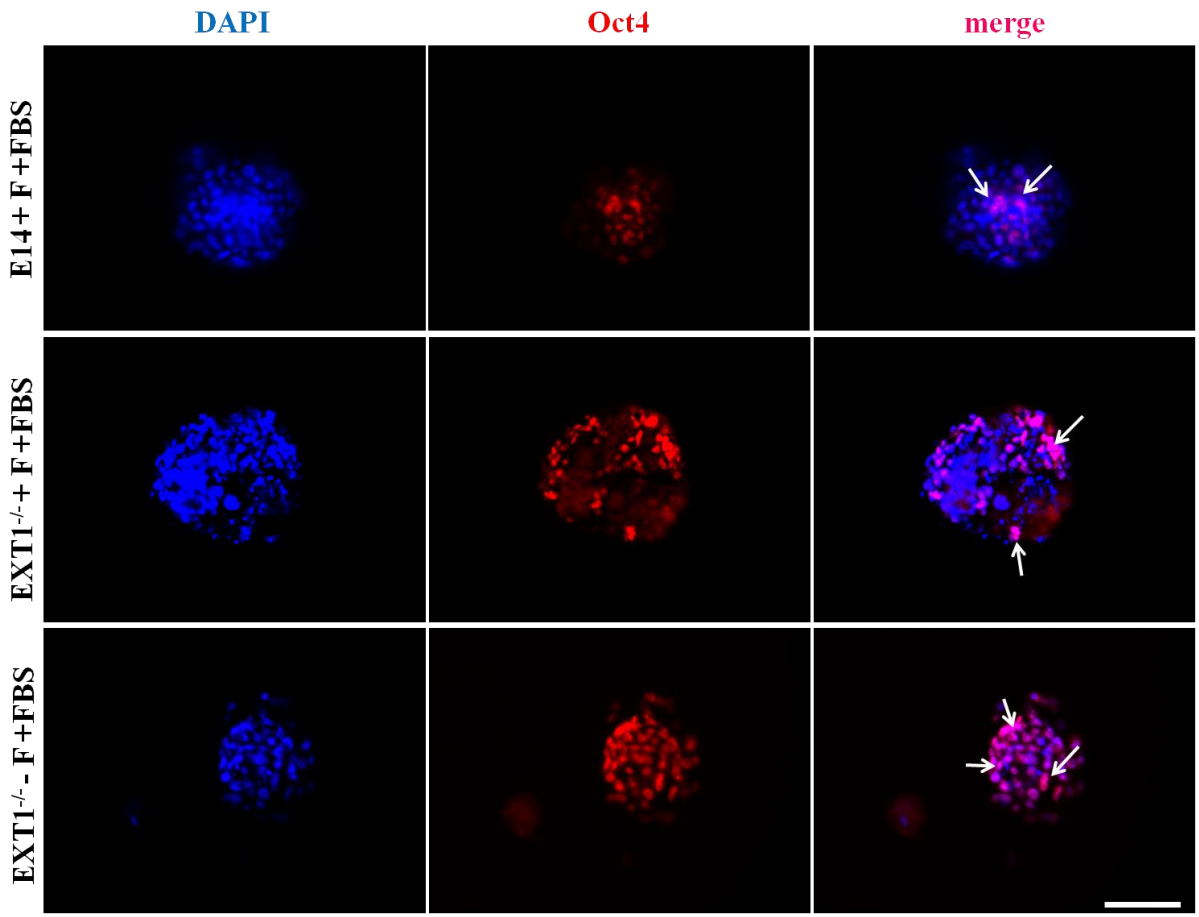

Figure 4.14 The distribution of Oct4 positive cells is more extensive throughout HS-deficient EBs compared to E14 EBs and a lack of feeders enhances this effect. EBs derived from EXT1$^{-/-}$ mESCs displayed Oct4 positive cells in both outer and inner cells of the EB for both conditions (+/- feeders) (arrows), which is in contrast to the E14 EBs, which displayed Oct4 positive cells in the centre of the EB only. The presence of feeders appeared to negatively influence Oct4 expression by EXT$^{-/-}$ EBs, since those conditioned with feeders and serum (+F +FBS) displayed fewer Oct4 positive cells than EXT1$^{-/-}$ EBs conditioned without feeders but with serum (-F +FBS), (arrows). Images represent the entire cell population and the experiment was repeated over 6 times. Scale bar represents 200 μm.

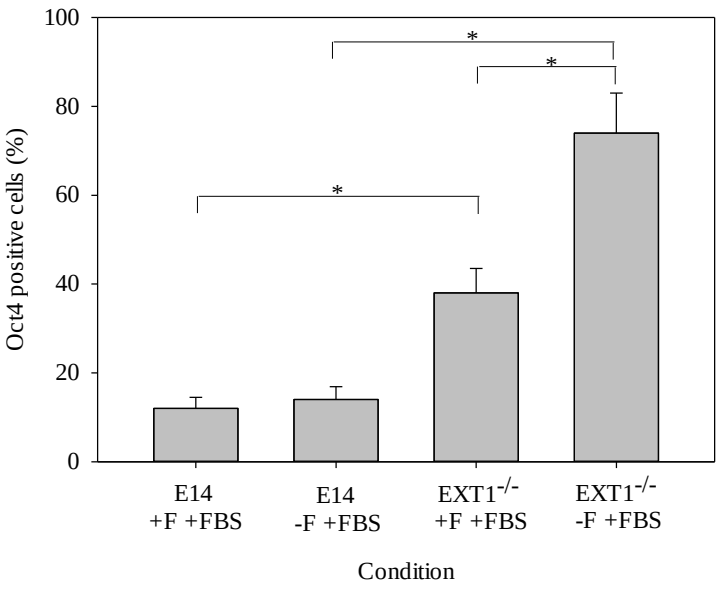

Figure 4.15 The percentage of Oct4 positive cells within HS-deficient EBs is higher than in E14 EBs. $EXT1^{-/-}$ EBs displayed a significantly higher proportion of Oct4 positive cells compared to E14 EBs cultured under the same conditions. $EXT1^{-/-}$ EBs conditioned in the absence of feeders displayed significantly higher proportions of Oct4 positive cells compared to $EXT1^{-/-}$ mESCs cultured without feeders. n = 3, * $p < 0.05$ student's T-test, error bars represent SEM.

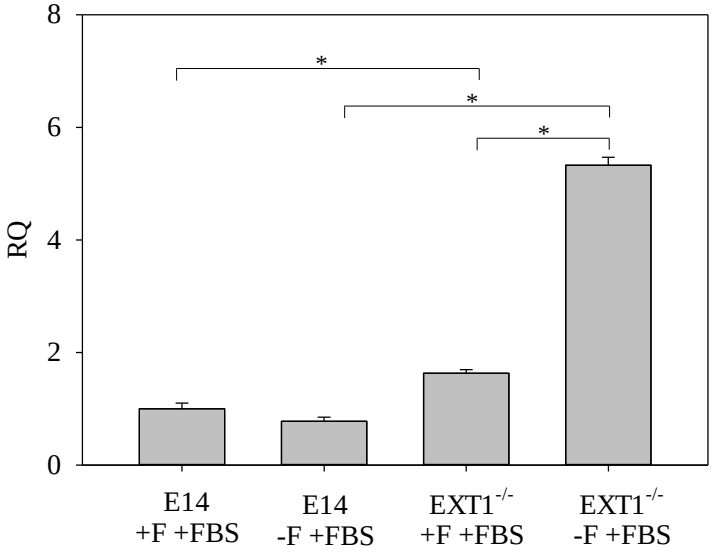

7 day EBs: *Oct4* expression relative to *GAPDH*

Figure 4.16 *Oct4* expression in day 7 EBs is significantly higher in HS-deficient $EXT1^{-/-}$ EBs compared to E14 EBs. EBs were derived from $EXT1^{-/-}$ ESCs and E14 ESCs after being maintained in parallel under different culture conditions (+/- feeders). HS-deficient $EXT1^{-/-}$ EBs displayed significantly higher *Oct4* levels compared to E14 EBs from the same culture conditions. $EXT1^{-/-}$ EBs conditioned in the absence of feeders displayed significantly higher *Oct4* levels compared to $EXT1^{-/-}$ EBs cultured in the presence of feeders. n = 3, * $p < 0.05$ student's T-test, error bars represent SEM.

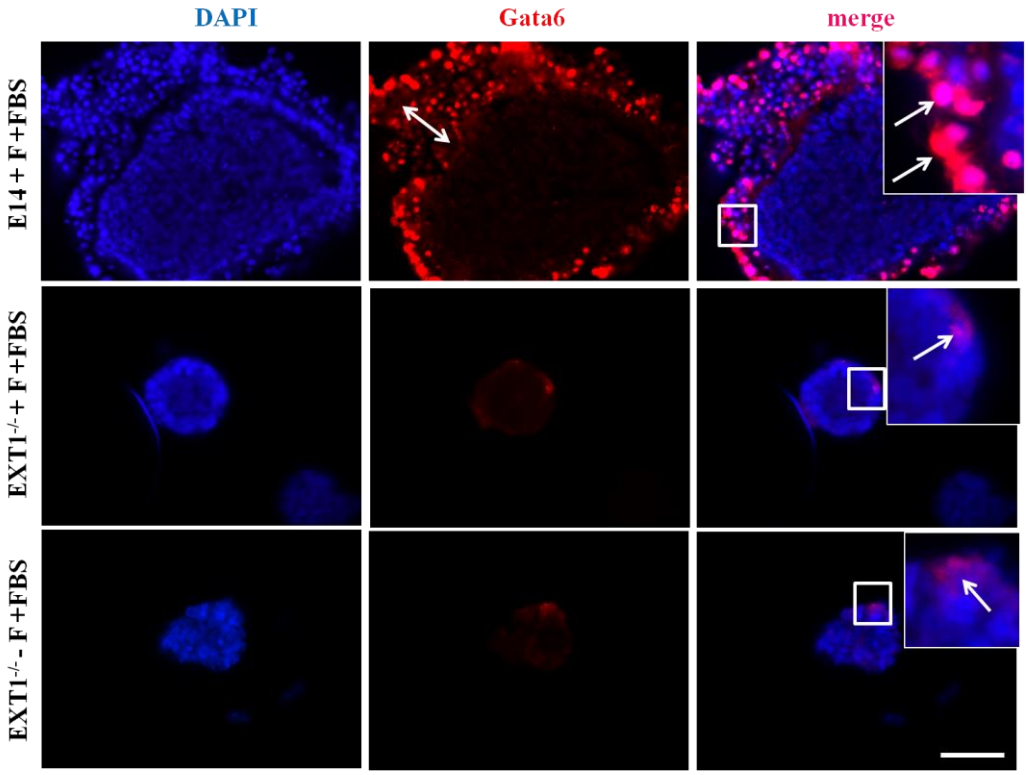

Figure 4.17 HS-deficient EBs display abnormal localisation of Gata6 positive cells. EXT1$^{-/-}$ mESCs were maintained in two different culture conditions, with or without feeders, for more than 10 passages prior to EB formation. EBs were then stained with a Gata6-specific antibody at day 7. In E14 EBs Gata6 expression was localised to outer cells of EBs in a multi-layered fashion. In contrast, Gata6-positive cells in EXT1$^{-/-}$ EBs (arrows) are poorly represented and incorrectly localised to some relatively inner cells in EXT1$^{-/-}$ EBs as well as few outer cells, similarly when derived in the absence of feeders. Images represent the entire EB population and the experiment was repeated more than 3 times. Scale bar represents 200 µm.

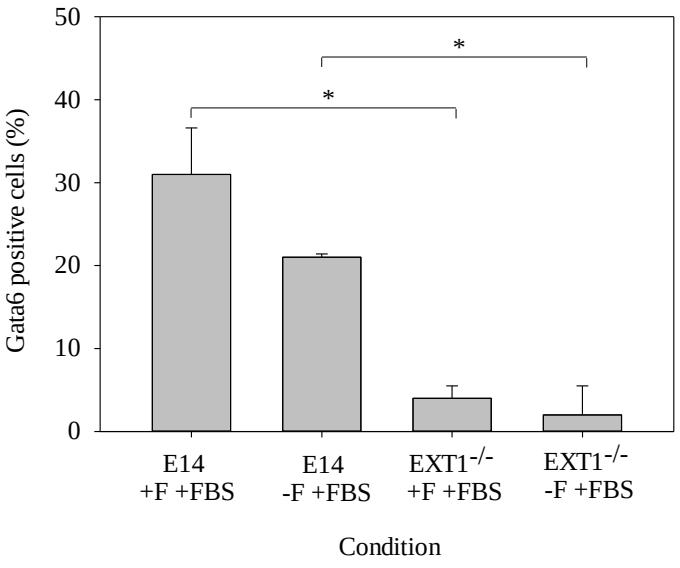

Figure 4.18 HS-deficient EBs display significantly lower Gata6+ cells in day 7 EBs compared to E14 EBs. EXT1$^{-/-}$ EBs displayed significantly lower proportions of Gata6+ cells compared to E14 EBs cultured under the same conditions. n = 3, * $p < 0.05$ student's T-test, error bars represent SEM.

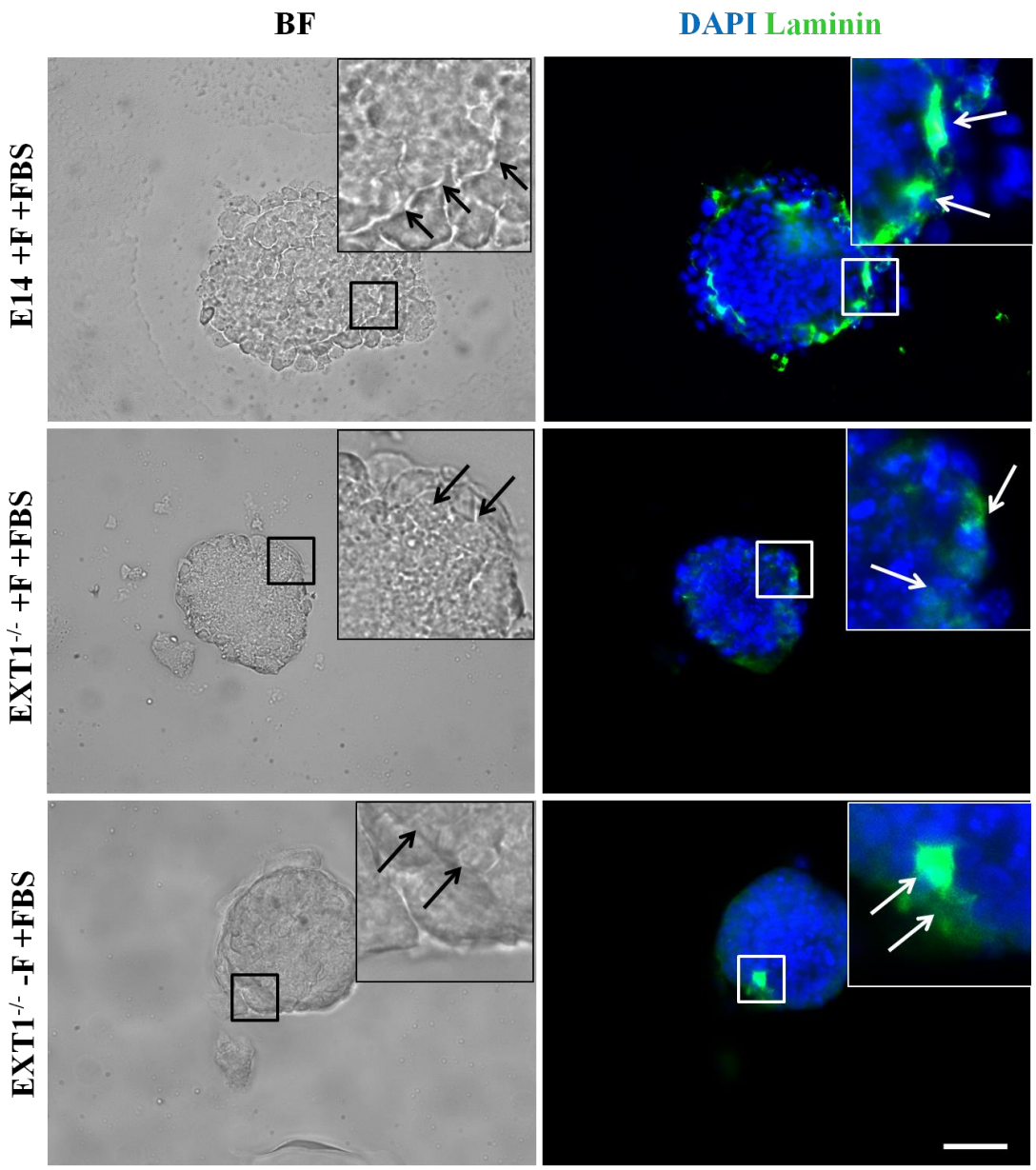

Figure 4.19 Laminin is abnormally localised in HS-deficient EBs. EXT1 $^{-/-}$ mESCs were maintained in two culture conditions (with or without feeders) for more than 10 passages in parallel with E14 mESCs, prior to EB formation. EBs were stained with an antibody specific to laminin-111 after 7 days. EXT1$^{-/-}$ EBs, despite the presence of a feeder layer, displayed predominantly intracellular laminin (arrows) despite the presence of some endoderm-like cells on the outer surface of the EB (arrows in corresponding brightfield (BF) images). E14 EBs from the same condition displayed substantial laminin expression localised between outer parietal endoderm-like multilayered cells and inner cells, as shown in the BF image (arrows). The experiment was repeated > 3 times, images represent the population and scale bar represents 100 µm.

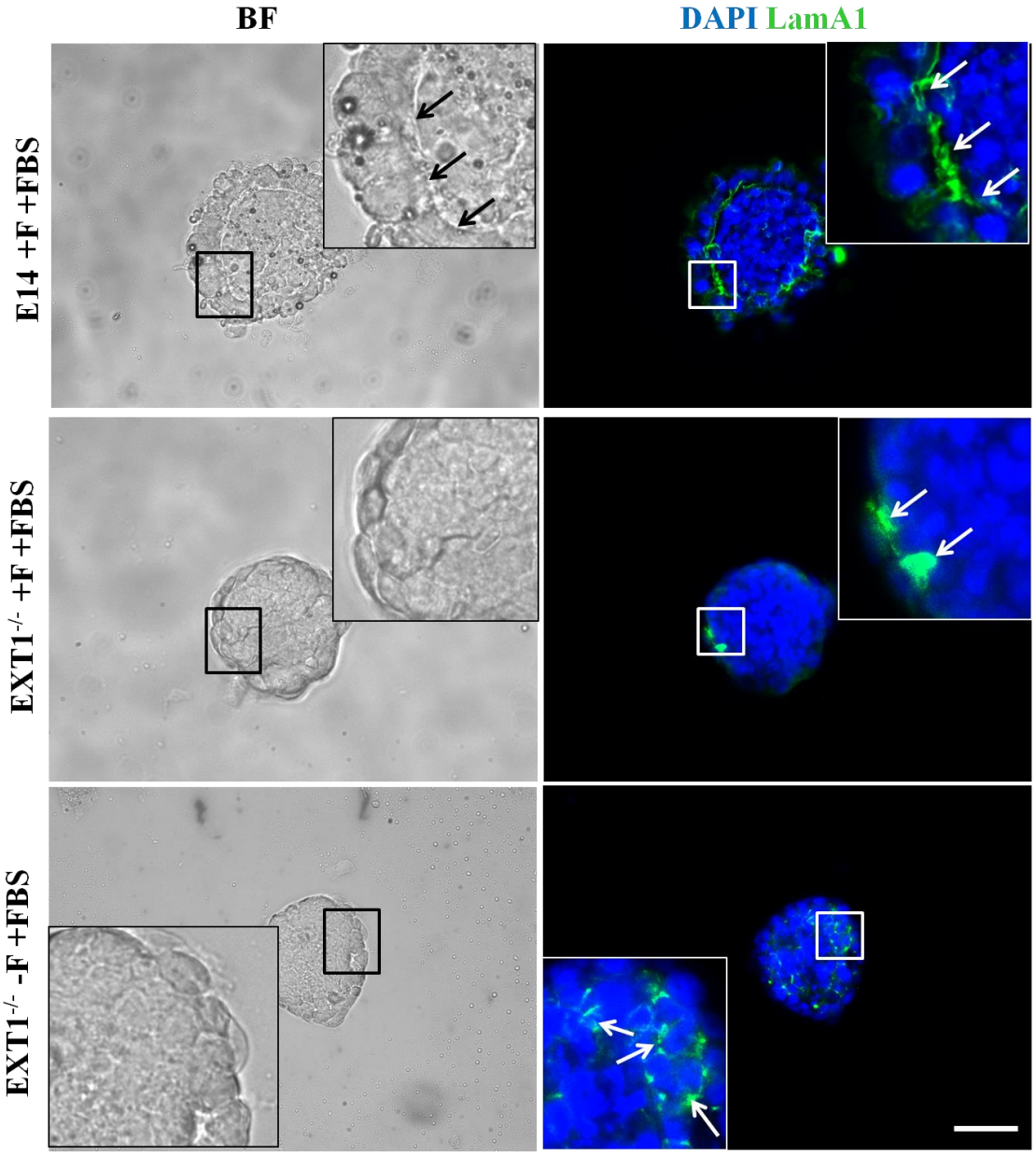

Figure 4.20 Abnormal intracellular LamA1 expression in HS-deficient EBs. EXT1 $^{-/-}$ mESCs were maintained in two culture conditions (with or without feeders) for more than 10 passages prior to EB formation in parallel with E14 mESCs, and stained with an antibody specific to LamA1 after 7 days. EXT1$^{-/-}$ EBs, despite culture condition (+/- F), LamA1 expression was abnormally localised intracellularly (arrows in 2nd and 3rd panels), despite the identification of some primitive endoderm-like flattened cells shown in the corresponding BF images. This is in contrast to E14 EBs, which displayed typical LamA1 expressed discretely located to BM-position (arrows) beneath outer tall parietal endoderm-like cells identified in the corresponding BF image (arrows). The experiment was repeated > 3 times, images represent the entire population and scale bar represents 100 µm.

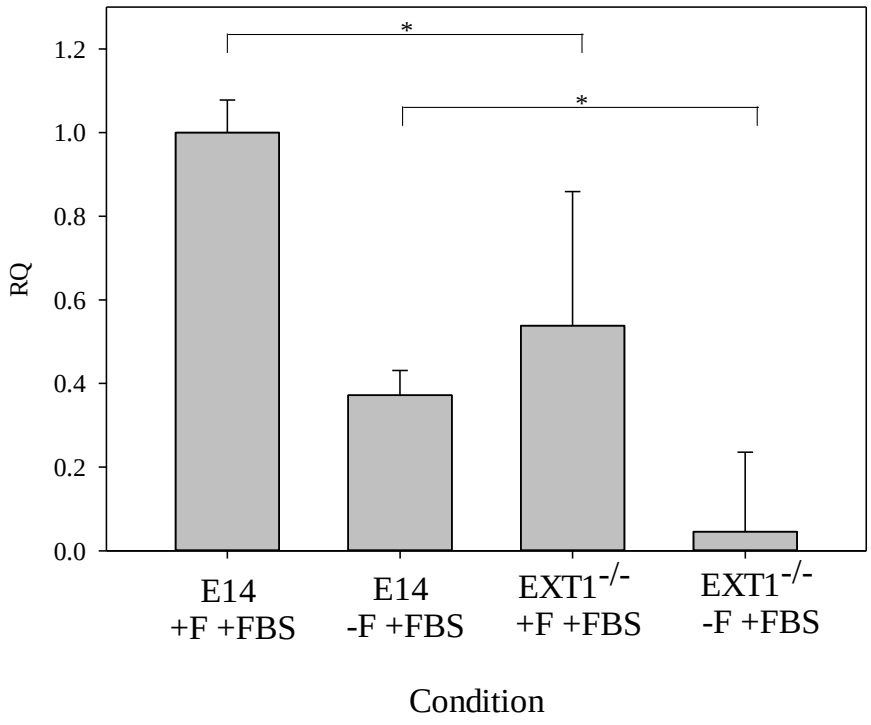

Figure 4.21 HS-deficient EBs display significantly lower LamA1 expression compared to day 7 E14 EBs derived from the same culture conditions. RT-qPCR quantification of *LamA1* expression showed that EXT1$^{-/-}$ mESCs display significantly lower *LamA1* levels compared to E14 mESC EBs derived from the same conditions. EXT1$^{-/-}$ EBs conditioned in the absence of feeders did not display any differences in LamA1 expression when compared to EXT1-/- ESCs cultured in the presence of feeders. n = 3, * $p < 0.05$ student's T-test and error bars represent SEM.

4.4 HS structure and abundance differs depending on mESC culture conditions

Results in previous chapters have demonstrated that discrete variations in 2D culture conditions significantly influence mESC behaviour, and this is possibly linked to a HS-dependent factor since exogenous PMH was shown to partially rescue these defects. Furthermore, HS-deficient mESCs do not differentiate to EEE and display uncharacteristic BM. Taken together, these results stress the importance of HS for normal mESC behaviour, therefore, a more in-depth characterisation and comparison of HS structures that are synthesised by cells under different culture conditions was investigated.

Considering that levels and structure of HS has been shown to often depend on culture conditions (Robinson and Gospodarowicz 1983; Gordon, Conn et al. 1985), characterisation of soluble HS from mESC conditioned media (CM) and cell-surface HS could, therefore, prove important in unravelling the link between mESC behaviour, culture condition and HS. Proteomic studies of mESC and hESC CM has highlighted the difference that discrete variations in culture conditions (+/- feeder layer) has on proteins important for the maintenance of mESCs (Prowse, McQuade et al. 2005; Buhr, Carapito et al. 2007; Prowse, McQuade et al. 2007).

HS structure and biosynthesis was characterised in mESCs cultured under different conditions (with or without feeders and with or without serum). HS shed by cells into their environment was analysed by purifying HS from mESC CM, digesting the HS to component disaccharides with heparinase enzymes, followed by separating the disaccharides using strong anion exchange (SAX) HPLC. Characterisation of cell surface HS was conducted using several different antibodies specific to structurally distinct HS-epitopes, and RT-qPCR was employed to quantify levels of HS biosynthetic enzymes, thus generating a comparative overview of HS levels and structures present within the different mESC culture systems.

4.4.1 mESC culture condition influences the structure of cell-surface HS

Two HS-specific antibodies, 10E4 and 3G10 were employed to detect cell-surface HS for mESCs. 10E4 is a monoclonal antibody that has been shown to identify N-sulfated HS structures (van den Born, Salmivirta et al. 2005) and 3G10 recognises neo-epitope or 'stub' generated after digestion of HS from HSPG core proteins with heparitinase (David, Bai et al. 1992).

Feeder cells appeared to predominantly express the 10E4 epitope rather than the mESCs (Figure 4.22) during mESC culture in the presence of serum and feeders, further confirmed at high magnification which demonstrated that mESCs nuclei were rarely found surrounded by 10E4 immunoreactivity (Figure 4.24 right panel). In contrast, in the absence of feeders (+/- serum) 10E4 HS epitope was expressed on the mESC surface in a relatively consistent, thin layer (Figure 4.22), further confirmed at higher magnification (Figure 4.24 right panel). Expression of the 3G10 HS epitope was identified localised to the surface of mESCs in all three culture conditions (Figure 4.23), however upon closer inspection, immunoreactivity appeared distinctly more intense on the surface of mESCs cultured in serum-free conditions, since expression was represented with by a thick layer, compared to relatively thin layers for mESCs cultured in the presence of serum (+/- feeders) (Figure 4.24 left panel). Both 3G10 and 10E4 immunoreactivity was absent from $EXT1^{-/-}$ +/-F mESC cultures, demonstrating the lack of cell surface HS synthesised by these cells.

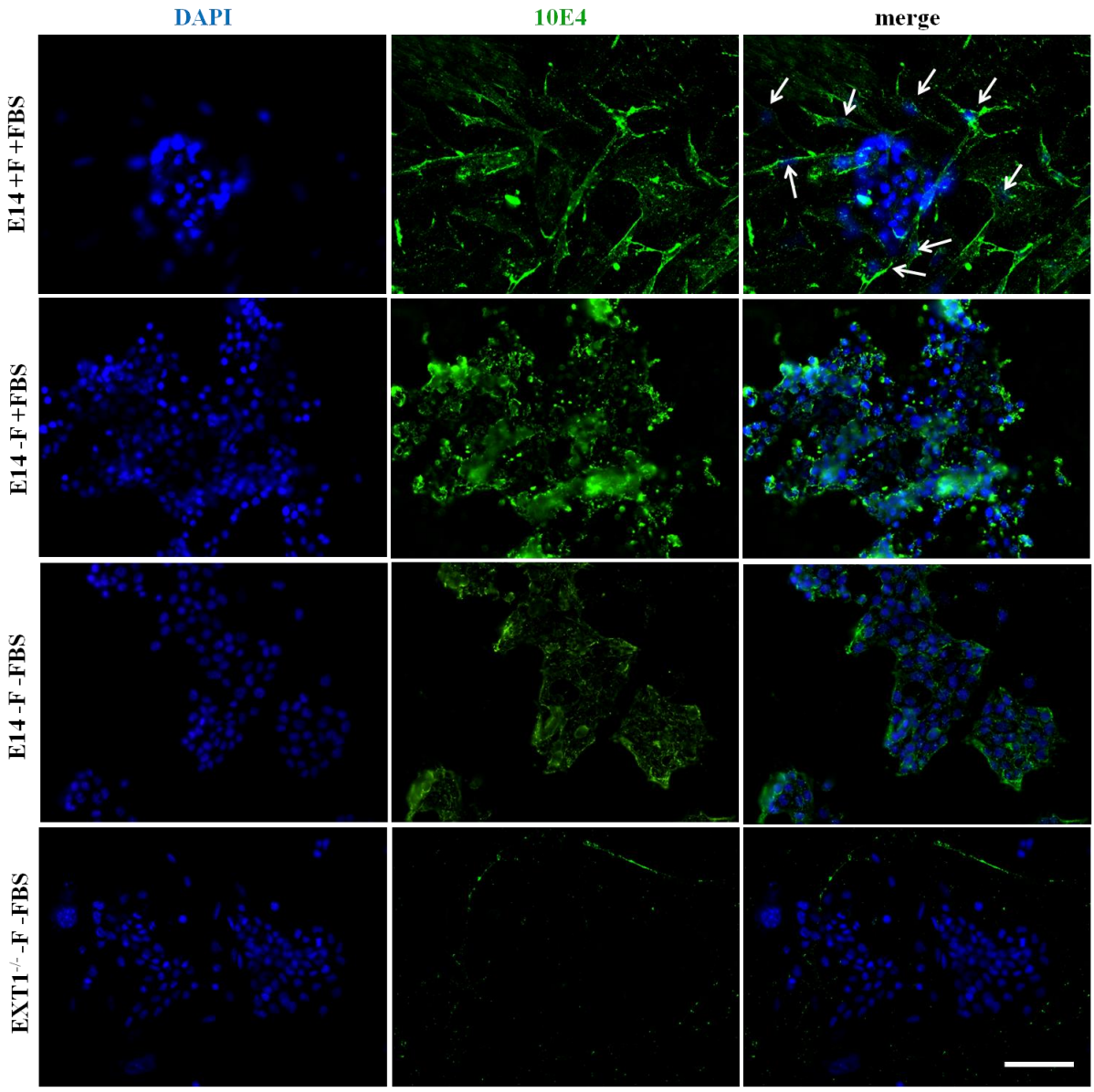

Figure 4.22 Expression of 10E4 HS epitope was detected in all three conditions but localisation differed and primary expression was by feeder cells. E14 mESCs were maintained in three different conditions for more than 10 passages and 10E4 antibody was used to stain cells 48 h post sub-culture to detect N-sulfated cell surface HS structures. In +F +FBS conditions, immunoreactivity of the 10E4 HS epitope was predominantly localised to the surface of the feeders cells, whose nulei are highlighted with arrows, whilst mESCs displayed very little of the HS epitope. In the two feeder-free conditions (+/- serum), 10E4 immuno-reactivity trend was comparable; expression was localised to the surface of mESCs. EXT1-/- ESCs displayed no specific immunoreactivity for 10E4, highlighting the lack HS on the surface of these mESCs. All images are representative of the entire cell population and the experiment was repeated 4 times. Scale bar represents 200 μm.

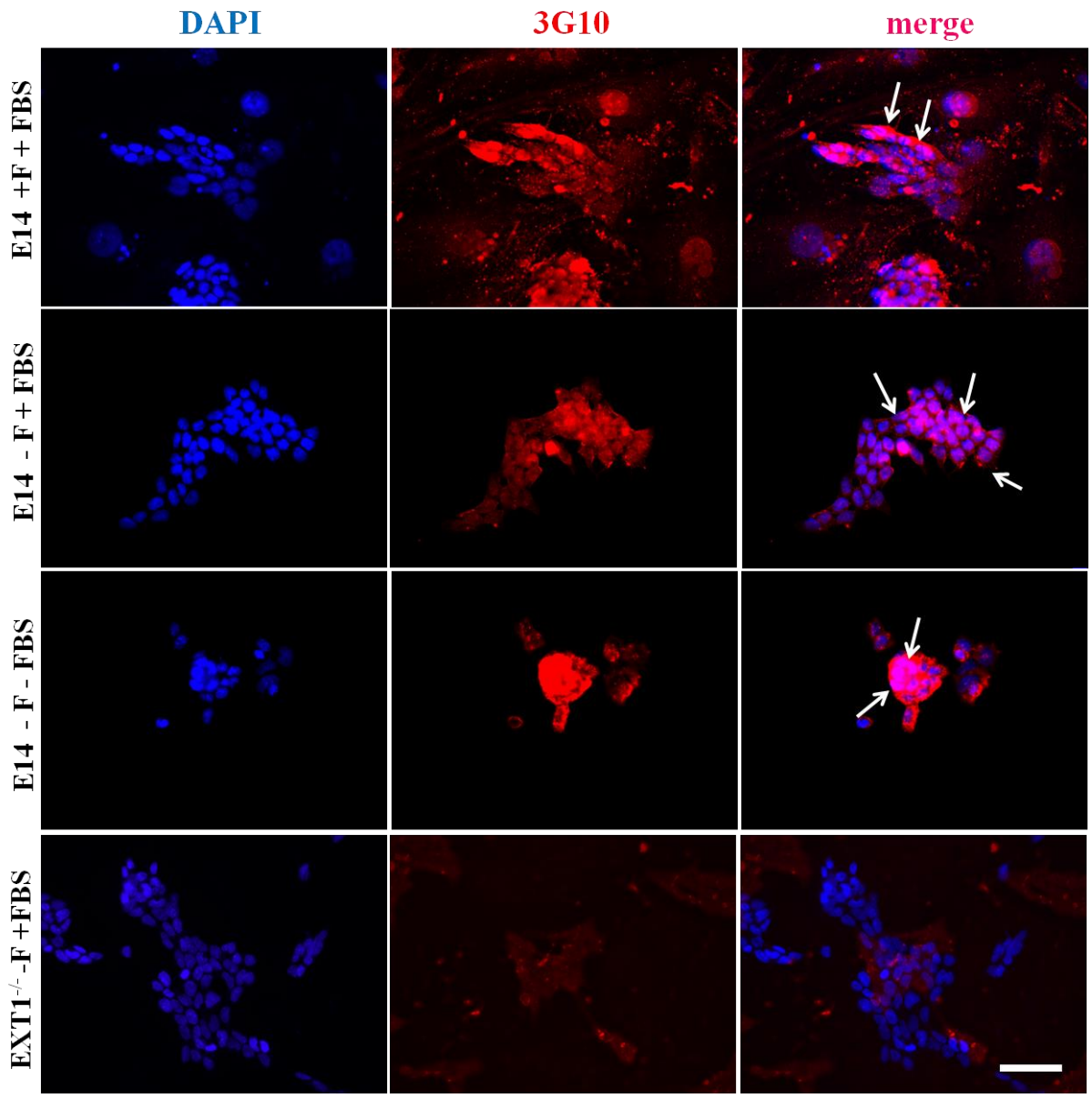

Figure 4.23 Levels of HSPGs on the surface of mESCs, identified by an antibody specific to the 3G10 HS-epitope, differed in three different culture conditions. E14 mESCs were maintained in three different conditions in parallel with EXT1$^{-/-}$ mESCs for more than 10 passages. 3G10, an antibody that identifies all HSPGs following removal of HS chains, was used to probe mESCs at 48 h post sub-culture. 3G10 immuno-reactivity was detected on the surface of mESCs in all three conditions, however, the levels differed between culture conditions. Highest HSPG expression was identified in –F -FBS conditions and expression appeared comparable between +/-F +FBS conditions. EXT1$^{-/-}$ mESCs alone lacked any specific iummunoreacitivity, emphasising the lack of HSPGs on the surface of these mESCs. Images are representative of the entire cell population and the experiment was repeated over 4 times. Scale bar represents 200 µm.

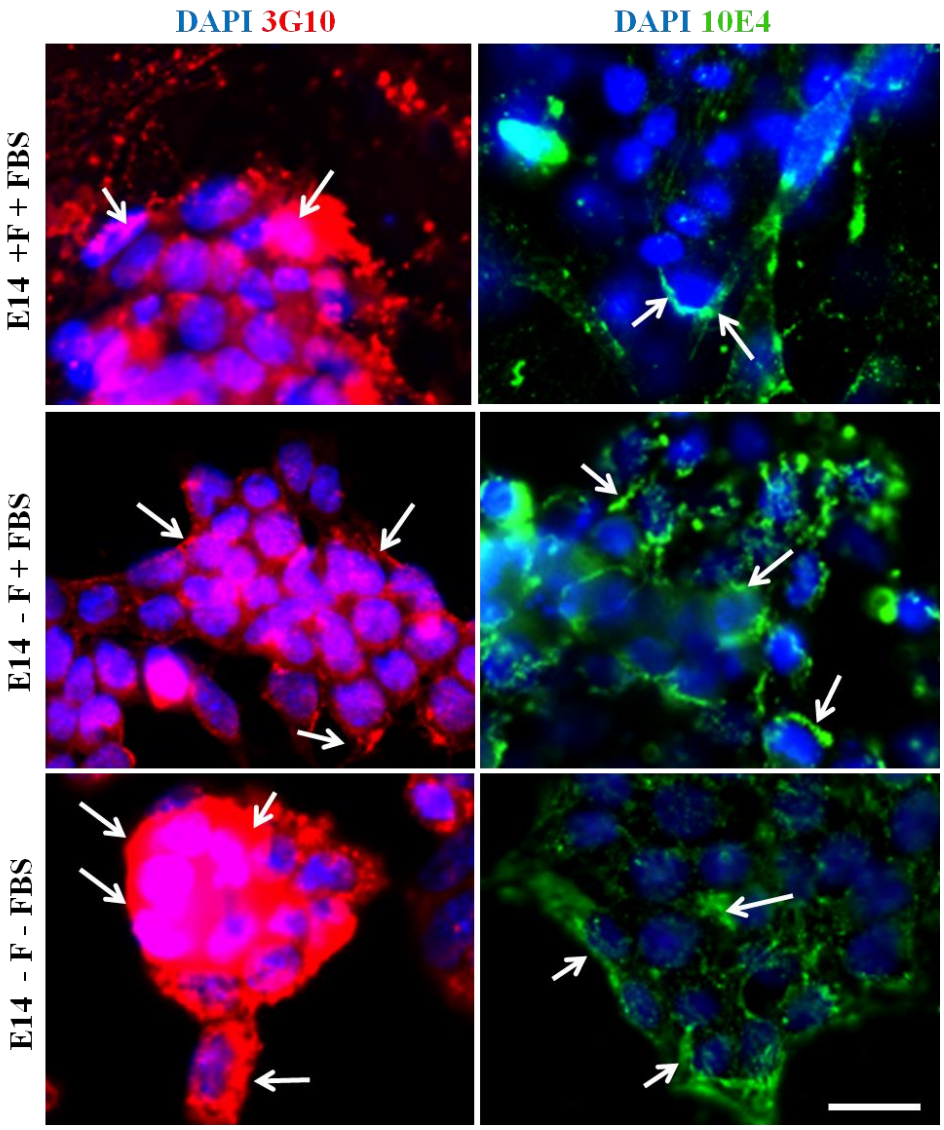

Figure 4.24 10E4 and 3G10 epitope expression levels and localisation differs depending on the mESC culture condition. E14 mESCs were maintained in three different conditions for more than 10 passages and HS-specific antibodies 3G10 and 10E4 were used to identify cell surface HSPGs and N-sulfated HS structures, respectively, 48 h post sub-culture. 3G10 epitope expression was localised to the outer surface of mESCs in all three culture conditions, although mESCs cultured in serum-free conditions display a thicker layer of 3G10 immuno-reactivity compared to mESCs cultured in the alternative conditions (left panel, arrows). 10E4 expression was localised predominantly to feeders; mESCs displayed very little cell-surface immunoreactivity in this culture condition, however mESCs cultured in the absence of feeders (+/- feeders) displayed similar immunoreactivity trends; expression of the 10E4 epitope was localised to the outer cell surface in a constant, relatively thin layer (right panel, arrows). The experiment was repeated more than 3 times and the images represent the entire cell population. Scale bar represents 50 μm.

4.4.2 Culture conditions influence the structure of HS synthesised by mESCs

Variations in culture conditions have been shown to affect mESC behaviour and also the localisation and abundance of cell surface HS, as detected using antibodies specific to N-sulfated HS structures (10E4) and the neo-epitope generated on all HSPGs after digestion of HS chains (3G10). Consequently, we asked the question, do soluble HS structure and abundance also vary depending on culture condition?

Preliminary SAX-HPLC analysis of HS purified from conditioned media (CM) and media components (Advanced DMEM and serum) demonstrated that HS levels and structures do vary depending on culture condition. Quantitation of HS was achieved by summing the peak areas for known disaccharides separated by SAX-HPLC and identified with respect to authentic standards. Firstly, total abundance of secreted HS purified from the different sources (CM and culture components) were different depending on the source (Figure 4.25). E14 –F –FBS CM contained the highest level of HS, 4-5-fold more than CM from E14 +F +FBS or E14 –F + FBS conditions. STO feeder cell CM displayed similar levels of HS to E14 + F +FBS. HS was also detected in Advanced DMEM, although levels were relatively low. HS-deficient $EXT1^{-/-}$ ESCs +F +FBS CM was negative for sulfated HS (although there was a peak correlated with standard 1 (UA-GlcNAc) the presence of contaminant signal not corresponding to any standards made accurate quantification difficult) (Figure 4.29).

A preliminary compositional analysis of the media components and CM suggested that HS species and sulfation patterns vary depending on source or conditions. HS purified from Advanced DMEM was largely composed of unsulfated UA–GlcNAc (approximately 81 %) with trace levels of sulfated structures including UA–GlcNAc6S, UA–GlcNS6S, and UA2S–GlcNS6S as well as a significant amount of UA2S-GlcNAc. UA–GlcNS and UA2S–GlcNS were undetected (Figure 4.27). HS purified from FBS displayed a more typical profile of

sulfated disaccharides for a highly sulfated HS with UA–GlcNS6S (30 %) and UA2S-GlcNS6S (16 %) major constituents of total HS (Figure 4.27). HS purified from STO feeder cell CM was a significant lower sulfated HS, with disaccharides; UA–GlcNAc (42 %) and UA–GlcNS HS (28 %) being predominant (Figure 4.28). Accordingly, HS purified from FBS presents 1.60 sulfates per disaccharide on average, compared to 0.60 and 0.93 sulfates per disaccharide, from HS purified from Adv DMEM only and STO feeder cell CM, respectively (Table 4.2).

HS species and levels varied between the three culture conditions that were shown previously to significantly affect ESC behaviour (chapter 3). Serum-free feeder-free CM displayed relatively high proportions of highly-sulfated HS structures; UA2S–GlcNS6S represented approximately 69 % of total HS abundance and UA2S–GlcNAc6S, undetected in the other E14 mESC growth conditions, represented approximately 5% of total HS abundance. HS purified from cultures containing serum (+/-F +FBS) displayed relatively low proportions of more highly-sulfated HS structures and generally, more low sulfated HS structures constituted a high proportion of total HS. Providing serum was present (+/-F +FBS) HS purified from +/- feeders CM was similar; the main difference was levels of standard 4 (UA2S-GlcNAc; 29 % and 3 % for +F +FBS and -F +FBS, respectively) (Figure 4.28). Consequently, HS purified from –F –FBS CM contains on average 2.44 sulfate groups per disaccharide, comparable to heparin, a homogenous highly sulfated type of HS, which has approximately 2.5 sulfates / disaccharide. In comparison, +F +FBS and –F +FBS CM have, on average, 1.19 and 1.13 sulfates per disaccharides, respectively (Table 4.2).

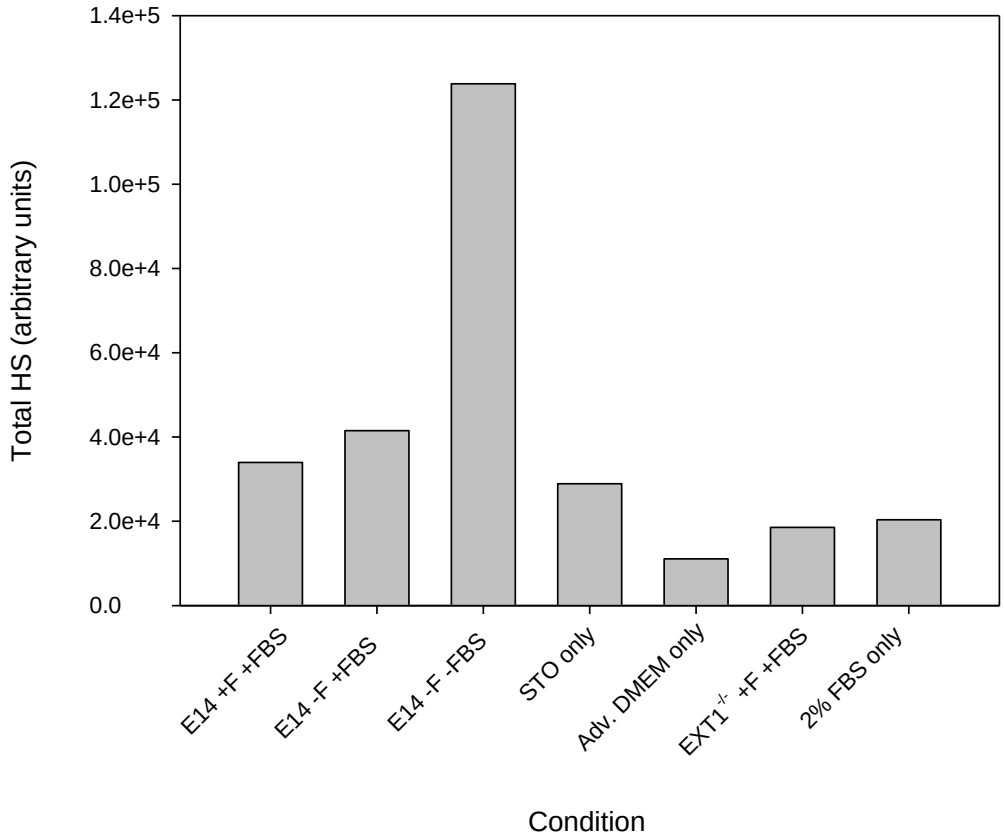

Figure 4.25 Quantitation of HS detected from equal volumes of starting material demonstrates differences in HS levels depending on source or culture condition. Conditioned medium was collected from the five different cell culture conditions as well as controls from Advanced DMEM alone and FBS alone and 40 ml of each was prepared with pooled media from multiple cell cultures. HS was purified, subjected to digestion with heparin lyases and separated by SAX-HPLC. Levels of HS were calculated based on total yield of disaccharides (sum of peak areas). E14 –F –FBS conditioned media appeared to synthesize the most HS, almost 10-fold more than E14 +/-F +FBS CM. STO feeder CM displayed similar levels of HS as E14 +/-F +FBS, whilst HS-deficient EXT1-/- ESCs +F +FBS CM generated approximately half that of normal E14 mESCs, comparable to levels detected in FBS alone. HS was detected in Advanced DMEM, although levels were relatively low. Sufficient material was only available for one experiment, although pooled media was collected from approximately 50 culture dishes.

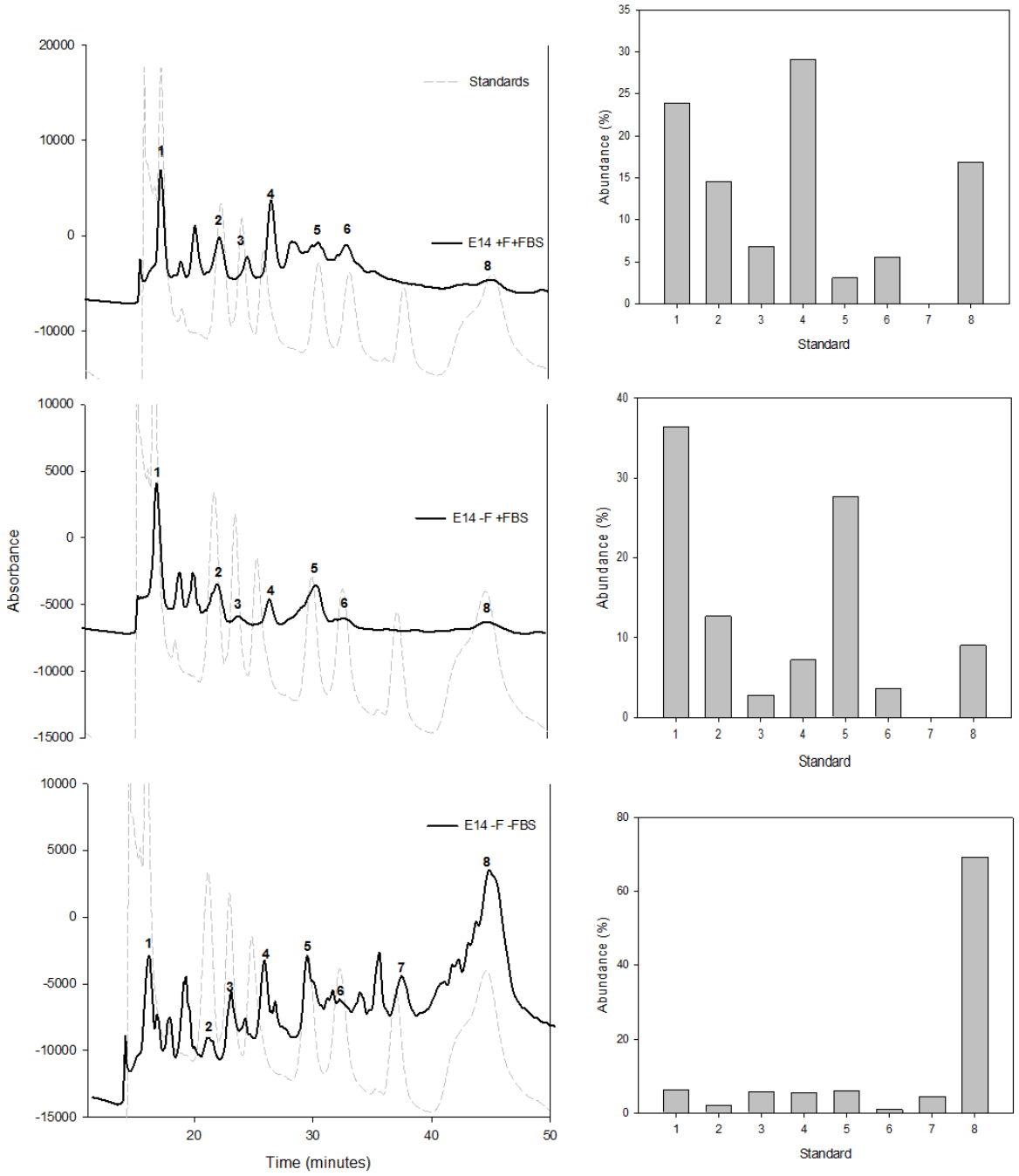

Figure 4.26 HPLC-SAX analysis of soluble HS purified from CM suggests that different conditions provide different HS structures. CM was collected from mESCs maintained in distinct culture conditions and prepared for SAX-HPLC analysis. More highly sulfated HS structures were found in higher abundance in –F –FBS CM compared to CM from mESCs maintained with serum (+/- F); HS purified from -F –FBS CM was predominantly composed of UA2S–GlcNS6S (approximately 70%). CM from mESCs maintained in the presence of serum (+/- feeders) displayed comparably lower levels of the more highly sulfated disaccharides; UA2S–GlcNAc6S was not detected and UA–GlcNS6S represented approximately 15 – 20% of total HS. Standards were defined in Table 2.6.

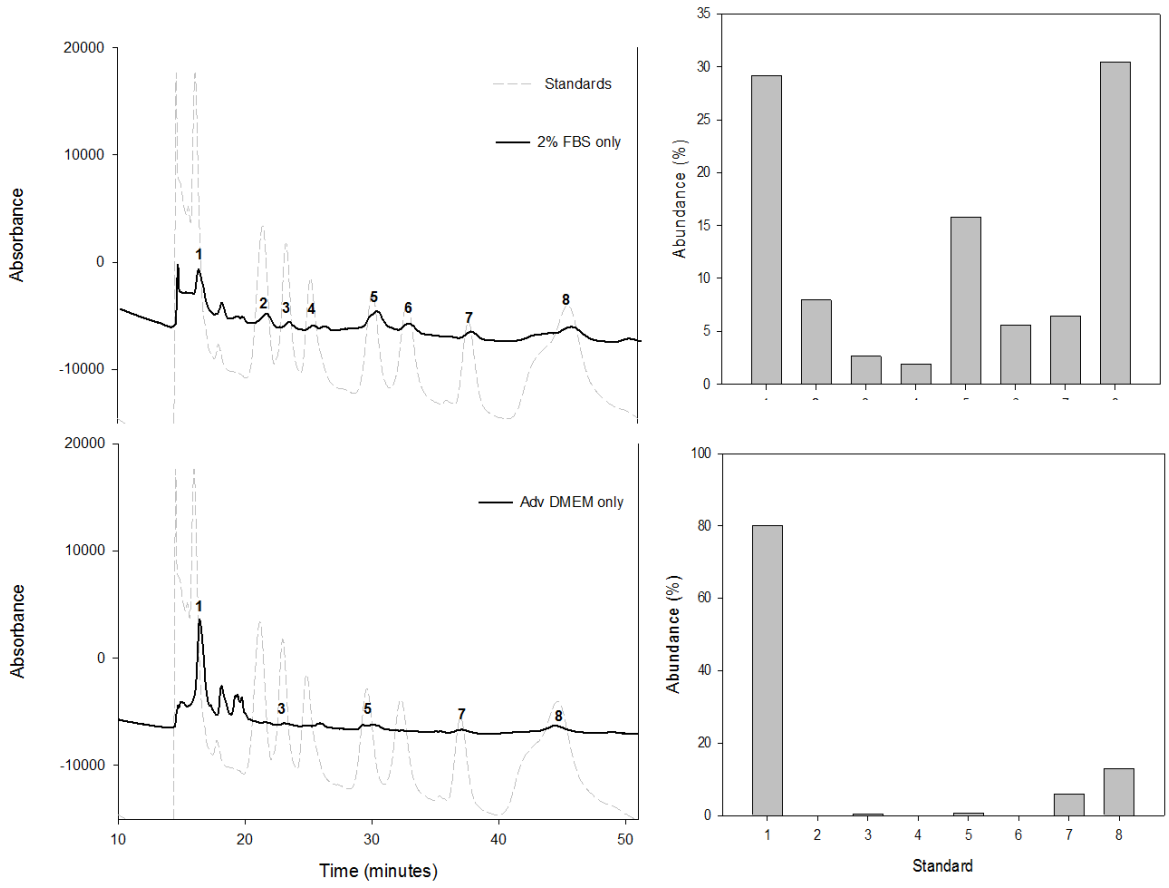

Figure 4.27 HPLC-SAX analysis of soluble HS purified from media components, Advanced DMEM and serum (FBS), demonstrates the abundance of HS and disaccharide compositional make-up. HS purified from 2% FBS displayed a range of HS structures; major components were UA–GlcNS6S HS (approximately 30 %), UA–GlcNAc (approximately 29 %) and UA–GlcNS6S HS (approximately 16 %). HS purified from Advanced DMEM alone contained predominantly UA-GlcNAc (approximately 81 %) with trace amounts of the other HS disaccharides.

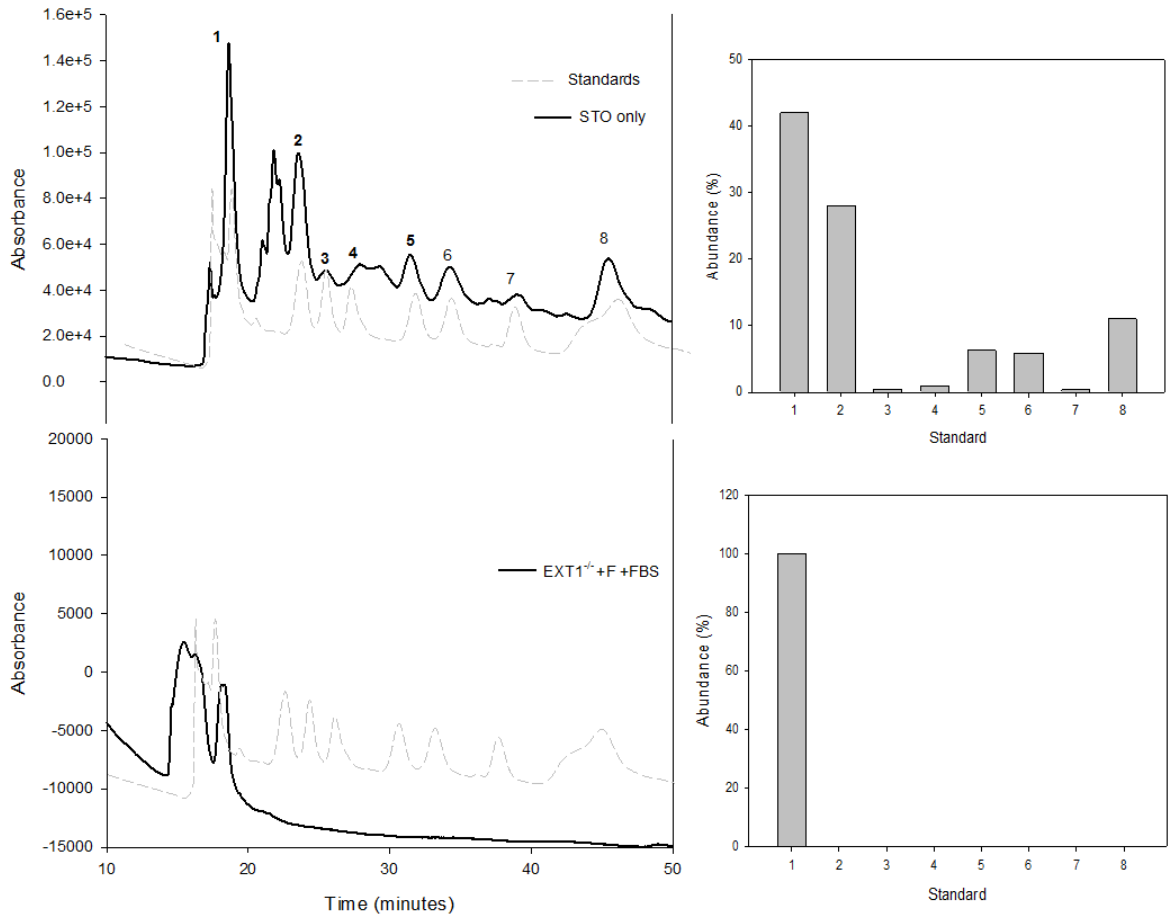

Figure 4.28 Compositional disaccharide analysis using SAX-HPLC highlights HS structures purified from STO feeder cell CM and the lack of soluble HS purified from EXT1$^{-/-}$ mESC CM. HS purified from EXT1-/- mESCs and STO feeder cells CM was collected, pooled and subjected to SAX-HPLC disaccharide analysis. STO feeder cell CM demonstrates the array of HS disaccharide structures, although is predominantly represented by low sulfated structures UA–GlcNAc (approximately 42 %), and UA-GlcNS (approximately 28 %). More highly sulfated structures were identified, although levels were low (< 10 %). HS purified from HS-deficient EXT1$^{-/-}$ ESCs CM correlated with only unsulfated UA–GlcNAc, however the poor resolution of the peak suggests it is a contaminant and therefore this CM is negative for HS.

Table 4.1 HPLC-SAX analysis demonstrated differences in soluble HS purified from conditioned media, from different culture conditions. This table summarises data from SAX-HPLC data in Figures 4.24, 4.25, 4.26 in terms of percentage abundance of each known disaccharide. STO feeder cell CM predominantly made up of UA–GlcNAc (68%) and UA–GlcNS HS (21%) whilst low abundance of UA–GlcNS6S (10%). 2 % FBS alone displayed low abundances of UA–GlcNS, UA–GlcNAc6S, UA2S–GlcNAc, UA–GlcNS6S, UA2S–GlcNS and UA2S–GlcNAc6S whilst UA–GlcNS6S (30%) and UA–GlcNAc (30 %) were major constituents of total HS. HS purified from Adv. DMEM displayed low levels of UA–GlcNAc6S, UA2S–GlcNAc, UA–GlcNS6S, UA2S–GlcNAc6S and UA–GlcNS6S.UA–GlcNS and UA2S–GlcNS were undetected whilst UA–GlcNAc was a major constituent (74%) of total HS. E14 mESCs disaccharide profiles varied depending on culture condition; for ESCs cultured in presence of serum (+/- F) UA2S–GlcNAc6S HS was undetected, however present in –F –FBS CM (5%). UA–GlcNS6S constituted 69% of total HS detected in –F –FBS E14 ESC CM, whereas levels were much lower in E14 ESCs cultured in the presence of serum (+/-F).

		Abundance of disaccharide standard relative to total HS (%)						
Standard number (in order of elution)	HS disaccharide structure	E14 +F +FBS	E14 –F + FBS	E14 –F -FBS	STO only	Adv. DMEM only	2% FBS only	$EXT1^{-/-}$ +F +FBS
1	UA – GlcNAc	23.93	36.39	6.30	43.9	73.78	29.19	100*
2	UA – GlcNS	14.58	12.66	1.94	20.63	0	7.95	0
3	UA – GlcNAc6S	6.83	2.75	5.69	3.45	1.47	2.65	0
4	UA2S – GlcNAc	29.10	7.91	5.46	1.11	2.48	1.89	0
5	UA – GlcNS6S	3.09	26.74	5.94	8.14	5.16	15.80	0
6	UA2S - GlcNS	5.60	3.61	0.97	7.65	0	5.59	0
7	UA2S – GlcNAc6S	0	0	4.49	5.2	5.32	6.48	0
8	U2S – GlcNS6S	16.87	9.03	69.21	9.92	11.79	30.46	0

*unclear if this peak correlates with standard 1 alone, since the peak is unresolved

Table 4.2 An approximation of the number of sulfates per disaccharides corresponding to HS purified from discrete culture conditions and culture components highlights differences in degrees of HS sulfation depending on source.

Culture condition/medium component	*Average number of sulfates/dp*	*%*		
		NS	*2S*	*6S*
E14 +F +FBS	1.18	40.14	51.57	26.80
E14 –F +FBS	1.12	52.95	20.56	39.42
E14 –F –FBS	2.43	78.06	80.14	85.33
Advanced DMEM	0.60	12.97	18.83	18.83
2% FBS only	1.60	59.80	44.42	55.38
STO feeder cells only	0.93			

4.4.3 Levels of HS biosynthetic enzyme expression in E14 mESCs differs depending on culture condition

Results thus far suggest that HS levels and structural composition varies depending on mESC culture condition, therefore an investigation into the expression of a number of HS biosynthetic enzymes (EXT1, EXT2, NDST1, Sulf1 and Sulf2) may further aid the understanding of why the final HS structures generated in the different conditions are distinct.

EBs produced from mESCs maintained in -F -FBS media displayed significantly higher levels of *EXT2* compared to EBs derived from mESCs maintained in the presence of serum (+/- feeders), whilst interestingly, *EXT1* levels did not change between conditions (Figure 4.29). *NDST1* levels from –F +/-FBS conditioned EBs were significantly higher than +F +FBS conditioned EBs, suggesting that not only serum, but feeders affect *NDST1* levels (Figure 4.30). *Sulf2* levels did not change between the three culture conditions, however *Sulf1* levels were shown to be significantly higher in EBs derived from mESCs maintained in –F +FBS conditions. In contrast, *Sulf1* levels were significantly lower in EBs derived from mESCs maintained in –F –FBS conditions (Figure 4.31).

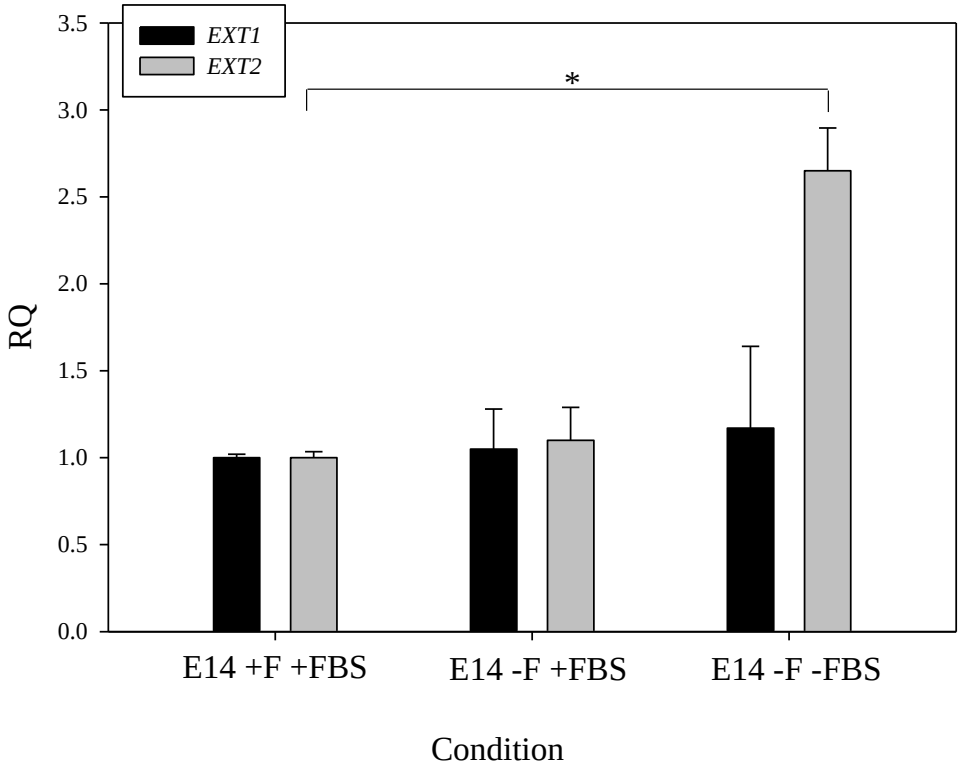

Figure 4.29 EBs generated from mESCs cultured in the absence of serum express higher levels of *EXT2* than EBs generated from mESCs cultured in the presence of serum. Analysis of mRNA levels of HS biosynthetic enzymes *EXT1* and *EXT2* relative to *GAPDH*, indicated that although *EXT1* levels remain unchanged when comparing the effect of EB pre-conditions, *EXT2* levels are significantly higher in EBs conditioned in serum-free feeder-free conditions (-F –FBS) compared to EBs conditioned in the presence of serum and feeders (+F +FBS). n = 3, * $p < 0.05$, student's T-test, error bars, SEM.

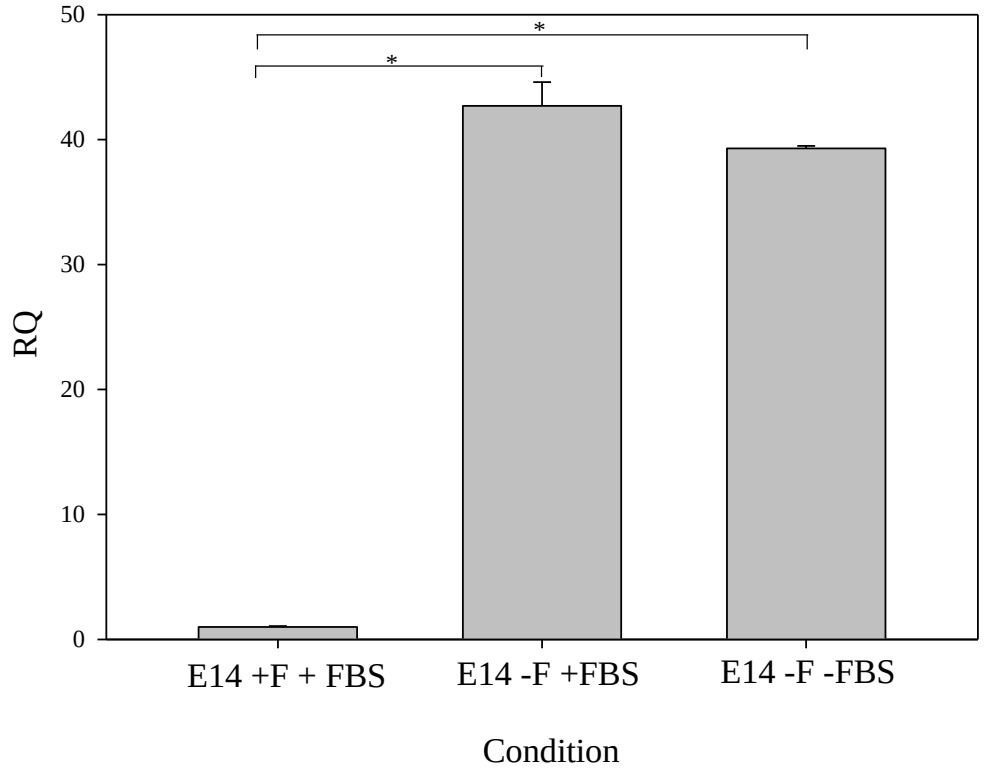

Figure 4.30 Levels of the HS biosynthetic enzyme *NDST1* are significantly different depending on mESC 2D culture condition. Levels of HS modification enzyme N-deacetylase/N-sulfotransferase (*NDST1*) relative to *GAPDH* was investigated using qRT-PCR for day 7 EBs. Levels of *NDST1* were significantly higher in –F +FBS and –F –FBS conditioned EBs compared to EBs conditioned in the presence of both serum and feeders (+F +FBS). n = 3, * $p < 0.05$, student's T-test, error bars, SEM.

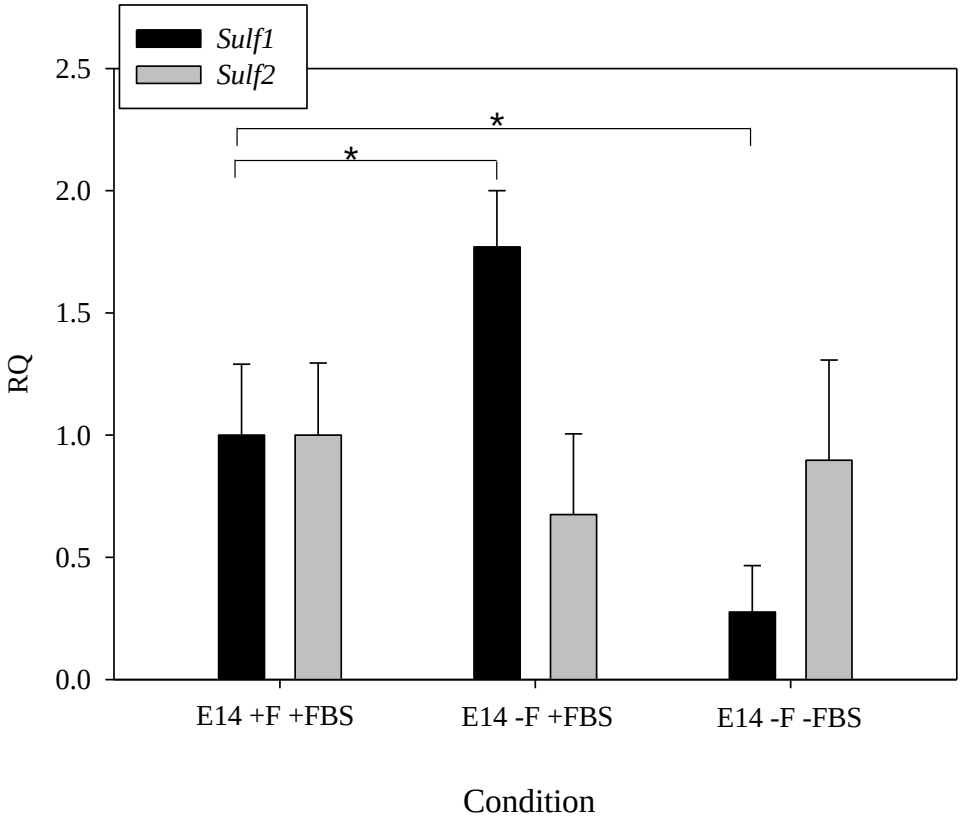

Figure 4.31 Levels of the HS modification sulfatase enzyme *Sulf1* are different depending on mESC culture condition but *Sulf2* levels are unchanged. Levels of HS modification sulftransferase enzymes *Sulf1* and *Sulf2* relative to *GAPDH* were investigated using qRT-PCR for day 7 EBs. Whilst *Sulf2* levels remained unchanged with varying culture condition, *Sulf1* levels differed. Specifically, -F +FBS conditioned EBs displayed significantly increased levels of *Sulf2*, whilst –F –FBS displayed significantly reduced levels of *Sulf2*, compared to +F +FBS conditioned EBs. n = 3, * $p < 0.05$, student's T-test; error bars, SEM.

4.5 Discussion

We found here that substantial defects in mESC behaviour, largely attributed to a lack of serum, were rescued with exogenous PMH. Serum-free conditions supplemented with 1μg/ml PMH, displayed more typical Gata6 levels and localisation of laminin, indicative of successful EEE differentiation. Simultaneously, these mESCs cultures supplemented with PMH gave rise to EBs displaying relatively low numbers of Oct4 positive cells, now comparable to mESCs cultured in the presence of serum and feeders. This provides evidence in support of the hypothesis that a lack of serum and/or feeders is linked with a lack of HS structure important in mESC behaviour. PMH, like HS, is a sulfated polysaccharide, but is more homogenously sulfated in structure than HS (Roden, Ananth et al. 1992; Faham, Hileman et al. 1996; Casu and Lindahl 2001) and more readily available, thus it is often utilised as a model for the protein interacting S-domains of HS in biochemical assays. Interestingly, it was reported that exogenous heparin can rescue BMP signalling and restore hematopoietic differentiation in $EXT1^{-/-}$ EB formation (Holley, Pickford et al. 2011) and furthermore in support of this, Conley et al. showed that in serum-free medium, BMP-4 supplementation was necessary to reconstitute differentiation of hESCs to visceral endoderm (Conley, Ellis et al. 2007). Taken together and considering the importance of HS in regulation of BMP signalling (Fisher, Li et al. 2006; Hu, Wang et al. 2009), a lack of serum could indirectly disrupt BMP signalling via the lack of HS. One study has shown how serum-free chemically defined media resulted in ESCs EBs displaying increased ectoderm differentiation, correlating with up-regulation of *Pax6*, commensurate with *Bry* expression (Wiles and Johansson 1999), this is similar to that seen in the present studies with –F –FBS conditioned EBs, the effects of which were rescued with exogenous PMH. Therefore, a highly sulfated, soluble HS-like structure could control/suppress this *Pax6* up-regulation.

HS-deficient mESCs ($EXT1^{-/-}$), unlike E14 mESCs, could not be maintained in serum-free culture conditions. This highlights the importance of HS and serum collectively in mESC cultures; which is unsuprising given the known importance of HS in embryogenesis. HS-deficient ESCs were successfully maintained in monolayer and displayed characterisitic morphology providing that serum was present (-/+ feeders). However, Nanog expression was higher compared to E14 ESC cultures in the same conditions, suggesting a specific role for HS in regulating Nanog expression. Unlike Oct4, Nanog is shown to promote mESC self-renewal independent of the LIF-STAT pathway (Chambers, Colby et al. 2003; Mitsui, Tokuzawa et al. 2003), and Kraushaar et al., have shown that HS inhibits Nanog expression via the FGF-signalling pathway (Kraushaar, Yamaguchi et al. 2010), therefore a disruption in FGF signalling via the lack of HS could result in up-regulation of Nanog. The involvement of Nanog specifically for FGF-4 regulation and vice versa has been highlighted, and N-sulfated HS structures are reported to be especially key (Kunath, Saba-El-Leil et al. 2007; Lanner, Lee et al. 2010; Shi, Gao et al. 2011), which is interesting since none of the N-sulfated HS structures (UA–GlcNS, UA–GlcNS6S, UA2S–GlcNS or UA–GlcNS6S) were identified either on the cell surface or from CM of $EXT1^{-/-}$ mESCs cultures (Figure 4.28). A putative "HS" species purified from $EXT1^{-/-}$ mESC cultures was also identified, consisting only of UA–GlcNAc, suggesting the possible existence of the unsulfated HS precusor molecule heparosan. It was originally thought that heparosan (and subsequently HS) synthesis can only sufficiently occur upon the formation of the hetero-oligomeric EXT1-EXT2 complex, after some studies showed that targeted deletion of either EXT1 or EXT2 leads to a complete lack of HS synthesis (Lind, Tufaro et al. 1998). However, results in this chapter suggest otherwise, in support of work from Okada et al., who showed that $EXT1^{-/-}$ mESCs do produce small amounts of HS (Okada, Nadanaka et al.), however since the peak (UA–GlcNAc) is poorly resolved from other early-eluting contaminating material, further work (for example mass

spectrometry) would be needed to confirm this assignment. Nonetheless, the putative non-sulfated HS structures synthesised by EXT1$^{-/-}$ mESCs are clearly not sufficient to facilitate normal mESC behaviour, since EXT1$^{-/-}$ EBs displayed restricted EEE differentiation and lacked a comprehensive BM. Nanog has been shown to block differentiation (Chambers, Colby et al. 2003; Niwa 2007), therefore it could be that sulfated HS structures, lacking in EXT1$^{-/-}$ mESC, promotes Nanog indirectly restricting differentiation, despite the removal of LIF. EXT1$^{-/-}$ mESCs displayed significantly higher levels of Oct4 and Nanog compared to E14 EBs from the same conditions. This result strongly suggests that a deficiency in HS is correlated with an increased capacity to self-renew. Inhibition of ECM-integrin interactions potentially via a lack of HS, have been shown to inhibit differentiation, thus promoting self-renewal in mESCs (Hayashi, Furue et al. 2007), which could possibly have occurred here. An array of growth factor and cytokine-dependent pathways crucial in differentiation rely on HS (Grunert, Nurcombe et al. 2008), for example IL-5 requires HS with numerous N-sulfated domains (Lipscombe, Nakhoul et al. 1998), TGF-betas are localized specifically with perlecan in the developing brain (Grave 2000), modulation of hematopoeisis via TGF-beta1 is partly due to GAG production (Luikart, Maniglia et al. 1990; Uhlman, Mooradian et al. 1990), HSPG interaction with BMP-2 dictates chondrogenesis (Fisher, Li et al. 2006), furthermore decreased HS sulfation is shown to increase BMP-2 bioactivity (Jiao, Billings et al. 2007). Therefore, it seems highly likely that EXT1$^{-/-}$ mESCs, despite the presence of serum and/or feeders, lack the network of growth factor and adhesion interactions required for typical behaviour. Interestingly, a lack of feeders during EXT1$^{-/-}$ mESC expansion was shown to further exaggerate the increased pluripotent capacity, since –F +FBS EXT1$^{-/-}$ mESCs displayed significantly higher levels of Nanog compared to +F +FBS conditioned EXT1$^{-/-}$ mESCs during 2D maintenance and in the 3D EB model. It would seem therefore, that feeders can compensate, to an extent, for HS-deficiency in EXT1$^{-/-}$ mESCs, perhaps via

synthesis of factors necessary for the loss of pluripotency. Differentiation of HS-deficient EXT1$^{-/-}$ mESCs to EEE was flawed and given the role of EEE in BM synthesis, it is unsurprising that EXT1$^{-/-}$ EBs also displayed disrupted BM synthesis; interestingly laminin and LamA1 expression appeared to be intracellular, rather than localised to BM-position, despite the identification of some primitive endoderm cells from bright field and morphological studies using toluidine blue. The importance of HSPGs specifically in BM synthesis and endoderm differentiation is often highlighted (Higuchi, Shiraki et al. 2010), frequently attributed to its interactions with laminin (Li, Chen et al. 2001; Li, Arman et al. 2004). Sulfation patterns of HS are further shown to affect BM synthesis, since inhibition of HS sulfation is proven to disrupt HS:laminin interactions and basement membrane assembly (Brauer, Keller et al. 1990). Furthermore, Yurchenco et al., showed how the binding of laminin to highly sulfated HS, drives laminin polymerisation and formation of BM (Yurchenco, Cheng et al. 1990). The data here, which showed that only unsulfated UA – GlcNAc HS structures are expressed on EXT1-/- mESC, both in CM and on the cell surface, support the view that sulfated HS is essential for normal assembly and function of laminin.

Importantly, variations in culture condition observed here to affect mESC behaviour were, as hypothesized, correlated with variations in HS structures (with the caveat that these data are preliminary, being based on a single analysis). Both cell surface HS and soluble HS purified from CM, differed in species and abundance depending on culture condition. The presence of feeders (+/-F), which was previously shown to have minimal effect on mESC behaviour (demonstrated in chapter 3), similarly had little effect on HS abundance and structure, suggesting that providing serum was present (+FBS) cells behave as normal. Analysis of expression levels of HS biosynthetic enzymes indicated that *EXT1*, *EXT2* and *Sulf2* levels were unchanged between +F +FBS and –F +FBS conditions and HS purified from CM were comparable (Table 4.1 and Figure 4.26). Consistent with the previous chapter however, –F –

FBS conditions resulted in substantial effects, this time with regard to HS species and abundance.

HS purified from -F –FBS ESC CM was in higher abundance compared to +/-F +FBS, and was quantified at levels almost 4-5-fold higher than HS purified from +/-F +FBS. This was supported by a significant increase in *EXT2* levels in –F –FBS conditioned EBs compared to +/-F +FBS conditioned EBs. Furthermore, cell surface HS, as detected with 10E4 and 3G10 antibodies, appeared more plentiful, suggesting that in the absence of serum, ESCs are stimulated to produce more HS than is typical. Detection of 3G10 immunoreactivity appeared to support quantification of HS abundance, since it was more prominently expressed on the mESC surface rather than on feeder cell surface. However, a lack of 3G10 staining on feeder cells could be attributed to incomplete digestion of HS chains, rather than a lack of HSPGs, and this is potentially caused by proteins bound to cell surface HS and a more extensive extracellular matrix preventing heparitinise enzymes from accessing the HS.

Unlike +/-F +FBS CM, the major constituent of -F –FBS CM was UA2S – GlcNS6S (approximately 70 % of total HS abundance), which was supported by significantly decreased levels of *Sulf1* compared to +/-F +FBS EBs. Accordingly, sulfation of –F –FBS ESCs HS can be estimated at 2.44 sulfates per disaccharide, which is a comparable level to that of heparin which has on average 2.6 sulfates per disaccharide. This indicates that HS purified from –F –FBS CM is a highly sulfated, heparin-like structure. In comparison, HS purified from +F +FBS and –F +FBS CM, can be represented by 1.19 and 1.13 sulfates per disaccharide, respectively, indicating low sulfated HS structures. This was supported by lower levels of the more highly sulfated HS structures detected in CM of +F +FBS and –F +FBS culture conditions and was further correlated with unchanged levels of *EXT1, EXT2,* and *Sulf2* (+/-F). However, lack of a feeder layer during culture resulted in significantly increased levels of *NDST1* and *Sulf1* compared to cultures with a feeder layer. Over-expression of Sulfs have

been shown to influence Wnt, FGF-2, FGF-4 and BMP signalling (Sanchez, Silos-Santiago et al. 1996; Ai, Do et al. 2003; Lai, Chien et al. 2004; Viviano, Paine-Saunders et al. 2004), therefore increased levels of *Sulf1*, attributed to a lack of feeders, could potentially disrupt these signalling pathways. Furthermore, TGF-beta1 has been proven to increase *Sulf1* expression accompanied by a decrease in 6-O sulfated disaccharides (Yue, Li et al. 2008), and Pax6, upregulated in –F –FBS conditioned EBs, is also shown to regulate Sulf1 (Genethliou, Panayiotou et al. 2009). This result suggests that feeder cells are not necessarily important for the synthesis of highly sulfated structures but in turn, maybe important in synthesising and secreting lower sulfated structures. One proteomic-based study suggested that the importance of feeders in hESC propagation is linked to the secretion of HSPGs, (Abraham, Riggs et al. 2010), although the exact HSPG species is unknown. Interestingly, HS purified from STO feeder cell conditioned medium was represented predominantly by unsulfated (UA–GlcNAc; 42 %) or low sulfated (UA-GlcNS; 28 %) structures; thus approximated sulfation represented by 0.93 sulfates per disaccharide. Therefore, although STO feeder cells synthesise more highly sulfated 6-O and 2-O sulfated HS structures in low abundances, unsulfated structures could underpin the role of feeders in regulating ESC behaviour.

Advanced DMEM and serum, the other media components, contained HS with approximately 0.60 sulfates per disaccharide and 1.60 sulfate groups per disaccharide, respectively. This implies that serum is associated with relatively highly sulfated HS structures, potentially underpinning its role as a culture component. HS purified from Advanced DMEM, was low in abundance and largely constituted by low sulfated HS structures, although this should be considered when employing this medium in ESC cultures where ‘well-defined’ conditions are paramount. HS purified from serum alone was represented by highly sulfated HS structures, for instance, UA2S–GlcNS6S HS constituted approximately 30 % of total HS abundance, and

other highly sulfated structures (UA–GlcNS6S, UA2S-GlcNS and UA2S–GlcNAc6S) were also well represented. It is possible that these structures are crucial for typical ESC behaviour, and if absent, as in –F –FBS conditions (these structures were largely under-represented in –F –FBS conditions), ESCs behaviour is consequently uncharacteristic. Taken together, a serum-free environment, as in –F –FBS conditions, perhaps presents an inadequate environment for the fine-tuning of HS, specifically for the removal of 6-O sulfate group by Sulfs. Decreased levels of *Sulf1* we noted would be expected to result in enhanced 6-O-sulfation, consistent with the changes in HS composition observed.Like *Sulf1*, *NDST1* was also significantly decreased in –F –FBS conditioned EBs. Interestingly, of the four N-sulfated structures (UA–GlcNS, UA–GlcNS6S, UA2S–GlcNS and UA–GlcNS6S) all except UA–GlcNS6S were extremely low in abundance for –F –FBS conditioned media compared to +/-F +FBS conditioned media. It is interesting to speculate that decreased *NDST1* might allow a greater influence of *NDST2* on HS sulphation, since NDST2 has been associated with biosynthesis of highly N-sulphated HS species like heparin (Dagalv et al 2011). Attempts at evaluation of *NDTS2* levels by RT-PCR failed (data not shown), but would be an interesting avenue for future work.The pattern of HS enzyme expression detected in cells from –F –FBS conditions appears unusual and overall will have some effect on the final HS structures present on the cell surface and in the CM. Increased *EXT2* and significantly reduced *Sulf2* and *NDST1* expression, suggests a possible relationship between these enzymes, as demonstrated by recent use of the term "GAGosome" discussed by Presto et al. (Presto, Thuveson et al. 2008), in which enzyme complexes clustered in specific Golgi compartments are proposed to result in production of divergent HS structures.

It appears that serum (or a component of serum) is required to facilitate N-sulfation and/or the release of the N-sulfated HS structures into the ECM. Interestingly, cell surface HS structures however, appeared to be well represented in mESCs from –F –FBS conditions

since cell-surface HS, as detected with 3G10 and 10E4 antibody, demonstrated increased immunoreactovoty on the surface of mESCs from –F –FBS conditions compared to +/-F +FBS. N-sulfated cell-surface HS, identified with the 10E4 antibody, was predominantly localised to feeder cells in +F +FBS and since N-sulfated HS species constituted a large proportion of total HS in STO feeder cell CM, the importance of feeders during mESC expansion, as previously proposed, may be linked to the synthesis of specifically N-sulfated HS. Nonetheless, upon the removal of feeders, mESCs appeared to compensate and N-sulfated cell-surface HS was also detected on the surface of mESCs. This result suggests that synthesis of N-sulfated HS in –F –FBS is supported, although shedding of these structures is lacking.

Mechanistically it is possible that FGF signalling is disrupted due to the lack of serum. 6-O-sulfation is required for FGF2 and FGF-4 signalling (Sugaya, Habuchi et al. 2008), therefore perhaps –F –FBS conditioned EBs lack adequate FGF-2 and/or FGF-4 signalling. Ablation of FGF-signalling is also correlated with a failure to assemble a BM and epiblast differentiation (Ekblom, Lonai et al. 2003). Therefore -F –FBS conditioned EBs, which fail to synthesise a functional BM, may lack the adequate FGF-signalling necessary, due to a lack of particular HS structures; for example UA–GlcNS6S, UA2S-GlcNS and/or UA2S–GlcNAc6S HS structures, identified in serum but lacking in –F –FBS CM.

In conclusion, it would seem that a lack of serum is correlated with a lack of HS, specifically UA2S–GlcNS6S, UA–GlcNS6S, UA2S-GlcNS and UA2S– GlcNAc6S disaccharides. Ultimately, a deficiency in these structures could prove key, without which, mESC behaviour is abberant.

5. Optimisation of polymers for the expansion of mESCs and KSCs *in vitro*

5.1 General Introduction

The methodology utilised to expand cells *in vitro* depends on the downstream application. 2D expansion has long been achieved (since the 1960s) via the employment of tissue culture polystyrene (TCPS) dishes (Curtis, Forrester et al. 1983), usually with an appropriate surface treatment to optimise electrostatic and hydrophobic cell-biomaterial interactions, necessary due to the non-adhesive nature of polystyrene (Maroudas 1977; Ward, Knox et al. 1977; Grinnell 1978). TCPS is modified either via controlling distinct surface chemistry, thus presenting charged groups, using UV for example (Saha, Mei et al. 2011), or via coating of TCPS with animal-derived materials to serve as an ECM.

Expansion of cells in a 3D environment using a synthetic scaffold is a more sophisticated process, owing to the dynamic nature of 3D bio-environments, and such expansion is often aimed at tissue-regeneration applications. Material choice, surface treatment and desirable bulk properties are carefully tailored to meet the specific application. For instance, a joint replacement will require material with good mechanical strength and wear properties, a muscular graft will primarily demand the material to support repetitive force exertion over time and potentially degrade over time upon the regeneration of healthy native tissue, any part of a kidney graft will require specific, well-controlled porosity to aid the diffusion of nutrients and waste (in and out, respectively) during filtration whilst being structurally sound. Exploiting any biomaterial for tissue regeneration purposes occurs *in vitro* firstly with endothelialisation and vascularisation, a consequence of maintaining healthy cells on the synthetic structure, followed by expanding cell numbers within the structure in 3D environment, culmilating with implantation *in vivo* to replace disease or damaged tissue. Such a demanding process has led to alternative avenues being investigated; one major one is

decellulisation of human tissue i.e. bone, so to generate a human-derived starting material as a way to overcome problems and issues with a synthetic structure.

Nonetheless, the common feature of 2D and 3D expansion is that often an ECM/animal-derived material is employed to improve performance, whether as a surface coating or incorporated during material synthesis. Common materials include, collagen (He, Ma et al. 2005; Wojtowicz, Shekaran et al. 2010), fibronectin (Barrias, Martins et al. 2009; Maciel, Oliveira et al. 2012), laminin (Huber, Heiduschka et al. 1998; Huang, Huang et al. 2007), and gelatine (Goetz, Scheffler et al. 2006; Hosseinkhani, Hosseinkhani et al. 2008; Rao and Winter 2009; Sun, Huang et al. 2012) to name a few, largely attributed to their hydrophilicity (Li, Cui et al. 2005; Li, Mills et al. 2005) and ECM-derived nature (Nakajima, Ishimuro et al. 2007; Flaim, Teng et al. 2008). Given that animal-derived products require elimination from *in vitro* expansion, bioengineers are focussed on generating synthetic alternatives, with specific attention focussed on exploiting physical and chemical attributes of potential alternatives, with regard to both surface and bulk properties.

One material property specifically exploited and investigated has been porosity (and thus indirectly surface area to volume ratio), through investigating hydrogels and macroporous polymers (classified as such due to their respective differing surface area to volume ratios). It is interesting that Gustafsson et al. demonstrated that providing a polymer (PET) scaffold displayed sufficiently high surface area to volume ratio, neither cell proliferation or cell density was improved by the addition of animal-derived protein coating (Gustafsson, Haag et al. 2012).

Through identification of HS as a factor in the need for serum in ESC maintenance and expansion (outlined in previous chapters), alongside the potential to couple compounds to

these hydrogels and macroporous polymers, suggest that there is much potential to generate a xeno-free culture system.

Hydrogels

Hydrogels present a promising field in regenerative tissue engineering, largely owing to their hydrophilic make-up, which underpin the highly absorbant properties and flexibility often compared to natural tissue. This, coupled with the proven ability to tune copolymer synthesis to optimise hydrogel-protein interaction (Palacio, Schricker et al. 2010; Schricker, Palacio et al. 2010) for improved interaction with cells (Orilall and Wiesner 2011), make them an attractive option . Controlling physical and chemical properties, such as swell, however, can be difficult and in turn, has been shown to affect ESC behaviour (Engler, Sen et al. 2006; Park, Guo et al. 2009). Methacrylate-based hydrogels have been shown to support ESC attachment and proliferation also (dos Santos, Coelho et al. 2006; Nichol, Koshy et al. 2010), as have hydroxyethyl methacrylates (Horak, Kroupova et al. 2004). Acrylic based materials have also shown great promise as drug delivery systems (Ciardelli, Cioni et al. 2004) and acrylamide-based hydrogels are often utilised to bridge particles via their polymer chains. Poly(lactic-co-glycolic acid) (PLGA) is an excellent example of a successful, biodegradeable hydrogel, approved by the FDA and currently used in an array of medical applications including vascular grafts and drug delivery (Gunatillake and Adhikari 2003; Uematsu, Hattori et al. 2005; Makadia and Siegel 2011). Even so, coating with ECM proteins is often necessary to improve performance (Lees, Lim et al. 2007). 2-hydroxethyl methacrylate (HEMA), one of the hydrogel components investigated in this project, is a hydrosoluble monomer with long standing biocompatible performance (Chappard, Laurent et al. 1982; Chappard, Alexandre et al. 1986). HEMA-based hydrogel tubes have been shown to act as nerve guide channels (Dalton, Flynn et al. 2002), furthermore, HEMA-PEG hydrogels displayed great promise as subcutaneous biosensors (Quinn, Pathak et al. 1995). PEG-based

block hydrogels copolymers, another material investigated in this project, have displayed potential as synthetic ECM, having been shown to support fibroblast and MSCs expansion (Zhang, Skardal et al. 2008). Likewise for many different methacrylate-based copolymers (Brafman, Chang et al. 2010; Mei, Hollister-Lock et al. 2010), attributed in one case to adsorption of fibrinogin and albumin (Long, Clarke et al. 2003). In some cases, it is thought that the hydrophilic component of hydrogels, acrylic acid for example, is responsible for performance, attributed to swell factor (Schricker, Palacio et al. 2010). Poly (***N,N***-dimethylacrylamide), used as a component in several of the SpheriTech hydrogels investigated, has been shown to be effective in the application and performance of amphillic copolymers in blood separation for example (Natori and Kurita 2007) and during modulation of fibrin clotting (Lai, Zou et al. 2010). Poly (***N,N***-dimethylacrylamide)-based hydrogels have also been shown to support chrondrogenesis, attributed to their low charge densities (Yang, Chen et al. 2010). Taken together, research suggests that combinations of these biocompatible monomers as hydrogels does, and therefore could, present novel materials as substrates for cell scale-up along with many drug-releasing applications, as outlined in Table 5.1.

Table 5.1 Outlining some common hydrogels successfully employed as biomaterials

Hydrogel	*Application*
HEMA-PEG	Injectable antibiotic- releasing hydrogels (Arica, Tuglu et al. 2008)
PEG-dimethylacrylamide	Drug-releasing hydrogels (Diramio, Kisaalita et al. 2005), quantum dot surface modification
PEG-Methacrylate	Drug releasing injectable hydrogels (Lutz and Zarafshani 2008; Wischerhoff, Uhlig et al. 2008)

Macroporous Poly-Ɛ-lysine

Aside from copolymer hydrogels, this project investigates the naturally occurring poly-Ɛ-lysine (PƐL), as bulk polymeric material. PƐL is a small homopolymer, naturally synthesised by bacterial fermentation and employed as a food preservative. It is naturally biodegradable by protease activity and its' protein-based structure impart biocompatibility (Hiraki, Ichikawa et al. 2003; Zhang, Feng et al. 2011; Kadlecova, Baldi et al. 2012). PƐL represents a polypeptide of 25 – 30 lysine residues, unique in the linkage of its residues. Unlike other polylysine analogues which have the alpha-carbon groups linked by a peptide bond, lysine residues in PƐL are linked molecularly via the amino and carboxyl groups (Yu, Huang et al. 2010), the chemical monomer is outlined in Figure 5.1. The compound is water soluble and has been shown to function in many ways including, antiphage and antimicrobial action (Ni, Takehara et al. 2010; Chang, McLandsborough et al. 2012), endotoxin-removal activity (Yamanaka, Kito et al. 2010) and antiobesity due to inhibition of pancreatic lipase (Hirayama, Sakata et al. 1999).

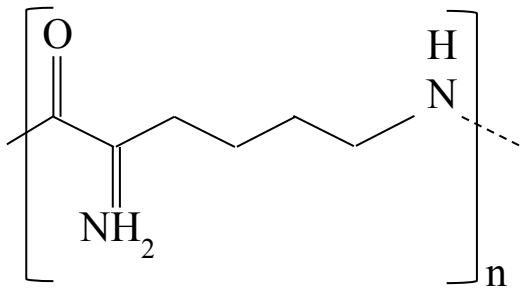

Figure 5.1 Poly-E-lysine polymer, showing the monomer subunit, n = 25 - 30.

Hydrogels incorporating PƐL have been shown to promote neural progenitor cell functions (Cai, Lu et al. 2012; Cai, Lu et al. 2012) and PƐL has demonstrated its ability to support functional vascular networks (Rauch, Michaud et al. 2008). Similarly, when employed as a hydrogel coating, PƐL has been shown to promote cell adhesion (Zhou, Li et al. 2011), likewise, Sprague et al., demonstrated that PƐL can support a dendritic cell response, comparable to Matrigel (Sprague, Muccioli et al. 2011), all suggesting that the charge-enhancing abilities of PƐL, underpins its potential in supporting cell expansion. In contrast, the specific architecture of PƐL has been shown to massively influence cell adhesion and application. Park et al., showed that surface topography of titanium coated with PƐL resulted in enhanced cell adhesion and numbers, attributed to micro-texture (Park, Olivares-Navarrete et al. 2012). PƐL nano-spheres have shown great promise in drug delivery (Eom, Kim et al. 2006; Eom, Park et al. 2007), again often attributed to shape rather than chemistry or ionic properties. Likewise, PƐL has been shown to influence and enhance biomimetics and porosity in silica materials (Gautier, Lopez et al. 2007), similarly in the case of hyaluranon-based hydrogels (Tian, Hou et al. 2005). Another study outlined that the high surface-area to volume ratio (achieved due to synthesis techniques of PƐL) rather than innate adhesion properties, is crucial in supporting proliferation and cell density of mesenchymal stem cells (Gustafsson, Haag et al. 2012), again suggesting that the architecture, as well as the specific components of an artificial microenvironment, is crucial.

Modification of PƐL with RGD and heparin

The importance of HS in kidney organogenesis and function has long been demonstrated, therefore support of KSC-GFP expansion via synthetic HS-mimetic coatings on PƐL substrates could facilitate this *in vitro*, via acting as an artificial ECM. In some renal disease models, mesangial sclerosis for example, whereby rapid glomerularsclerosis occurs, changes in ECM composition and decreased HSPGs in the glomerular basement membrane, is correlated with renal failure (Yang, Zhang et al. 2001), highlighting the importance of HSPGs in renal function via the ECM. Cell surface HSPGs from renal-fibroblasts have been shown to be essential in nephrogenesis (Clayton, Thomas et al. 2001), and Shah et al., showed that 2-O sulfated HS is of great importance for successful uteric bud branching (Shah, Sakurai et al. 2011) via presence of HS2OST (Shah, Tee et al. 2009; Shah, Sakurai et al. 2010). Furthermore, TGF-beta1, a target of HS, is shown to regulate ECM composition, outlined to be important specifically in the renal model (Douthwaite, Johnson et al. 1999).

Investigation into the affect of treating biocompatible polymers with heparin or HS analogues on performance as an artificial ECM is proving fruitful. Heparin-carrying polystyrene for example, was shown to direct and select cell expansion (Ishihara, Saito et al. 2000). Polysaccharide-surface coatings, specifically immobilized GAGs, have been shown positively influence proliferation and differentiation of mesenchymal stem cells (Uygun, Stojsih et al. 2009; Almodovar, Bacon et al. 2010), compared to untreated polymers, such is the availability of commercial culture dishes treated with immobilized GAGs currently. Heparin-functionalized PEG gels are shown to enhance hMSCs cell adhesion, proliferation and differentiation, compared to PEG gels alone (Benoit and Anseth 2005). Moreover, identification and optimisation of specific HS structures as coatings for different applications is on-going. Since HS sulfation pattern is dynamic depending on cell type and stage of development, the sulfated structure of any HS coating material will depend on application,

and should be tailored accordingly, outlined in one study that 2-O sulfated HS coating was optimal in enhancement of osteogenic potential (Ratanavaraporn and Tabata 2012).

Renal-applications for substrates

Early kidney development represents a major area of research within our group. Given the advances in stem cell research and simultaneously the need for therapeutic treatments for both acute and chronic renal failure, it represents a fitting niche and one which is explored in this project.

The kidney possesses an impressive regeneration capacity, often attributed to the contribution of native stem cells, found from stromal cells and bone marrow-derived stem cells within the adult kidney (Maeshima, Yamashita et al. 2003; Lin 2006). In ischemic injuries for example, it has been shown that bone-marrow-derived stem cells take part in renal regeneration via differentiation into resident renal cells (Kale, Karihaloo et al. 2003; Lin, Cordes et al. 2003), although this has since been disputed (Duffield, Park et al. 2005; Lin, Moran et al. 2005). The ability of the kidney to regenerate upon severe kidney damage though, during chronic kidney disease for example, which has now been recognised as a global health issue (Levey, Atkins et al. 2007), is elusive. Severe kidney damage leads to loss of kidney structure, in turn causing a complete loss of kidney function. The solution appears to require de novo development of the entire kidney, for which stem-cell based treatments display great promise. The employment of stem cells as a tool in the treatment of kidney failure has been investigated (Morigi, Imberti et al. 2004; Lazzeri, Crescioli et al. 2007; Guillot, Cook et al. 2008), however little is known about optimal substrates on which initial expansion of kidney-derived stem cells (KSCs) can be achieved before directed differentiation can be achieved or well controlled. Ultimately, *de novo* development of the kidney requires a synthetic substrate

to support initial KSC expansion so to achieve sufficiently high cell numbers, prior to directed differentiation.

As discussed, surface properties often govern cell-material interactions; wettability, charge and topography for example, can influence cell-polymer interactions; employing a protein coating such as fibronectin and laminin, is a common example (Ito, Kajihara et al. 1991; Altankov, Grinnell et al. 1996). However more recently, cell-recognised peptide motifs have shown greater promise. RGD (R; arginine, G; glycine, D; aspartic acid) is a cell-recognised peptide motif, specifically a sequence of fibronectin, identified many years ago as a minimal essential cell adhesion sequence (Pierschbacher and Ruoslahti 1984; Pierschbacher and Ruoslahti 1984). Since then however, it has been additionally identified in many other ECM proteins including laminin (Tashiro, Sephel et al. 1991), collagen (Taubenberger, Woodruff et al. 2010) and fibrinogen. Much work has been done in defining how RGD functions to increase cell adhesion; in the main it is thought that a subset of integrins, well established cell-surface proteins that act as receptors for cell adhesion, recognise the RGD (D'Souza, Ginsberg et al. 1991; Ruoslahti 1996).

Polymers coated or coupled with RGD have been shown to outperform uncoated polymers in an array of applications, demonstrates a reproducible affect that is consistent across many different cell types and conditions. PLGA 3D polymers coated with RGD resulted in enhanced osteoblast in-growth (Eid, Chen et al. 2001), effective for orthopaedic applications. Likewise, RGD-modified polyethylene sutures displayed enhanced adhesion and proliferation of tenocytes compared to untreated polymers (Kardestuncer, McCarthy et al. 2006; Mazzocca, Trainer et al. 2012), an important feature in wound healing. PTFE treated with RGD caused accelerated endothelialisation in both vascular grafts and heart valves (Tweden, Harasaki et al. 1995). PEG-based hydrogels displayed increased biocompatibility and support for MSC expansion once RGD was incorporated into synthesis (Grover, Lam et al. 2012).

One study outlined how RGD-functionalised polymers exhibited robustly enhanced cell adhesion, proliferation and often differentiation too, irrespective of the underlying polymer (Joy, Cohen et al. 2011), again highlighting the massive potential that RGD-treated polymers have as biomaterials. Similarly, research has shown that the bio-application of poly-Ɛ-lysine can be improved via covalent attachment of RGD. Polylysine coupled with RGD was shown to promote attachment and spread of human dermal fibroblasts (VandeVondele, Voros et al. 2003); similarly, titanium coated with polylysine that had been modified with RGD, resulted in expansion of osteoblasts, unlike RGD-free polylysine coatings, which displayed reduced cell attachment correlated with increased differentiation (Tosatti, Schwartz et al. 2004).

SpheriTech, an SME based in Runcorn, UK, and collaborator on this CASE studentship project, have developed unique techniques for the synthesis of different 3D scaffolds based upon cross-linked PƐL, a number of which were investigated here.

Results in this chapter cover:

- Acrylic/methacrylic based copolymers do not support the attachment or spread of fibroblasts.
- Poly-Ɛ-lysine polymers do support the attachment and self renewal of ESCs, or the proliferation and attachment of fibroblasts and kidney stem cells.
- Poly-Ɛ-lysine polymers can be modified with HS analogues to enhance performance as an artificial ECM for ESC scale-up.

5.2 Hydrogels for cell attachment or viability

Twelve different hydrogels, outlined in Table 5.2, were synthesised in accordance with SpheriTech Ltd protocols. Hydrogel performance and the ability to support fibroblast adherence and spread were assessed.

Table 5.2 Ratios of hydrogel components. Twelve different hydrogels were synthesised in-house by SpheriTech Ltd, constituents of which were based on different ratios of methacrylic, acrylic, PEG 360 methacrylate, PEG 526 methacrylate, 2-hydroxethyl methacrylate and M-N dimethyl acrylamide.

copolymer	*Methacrylic*	*Acrylic*	*PEG 360 Methacrylate*	*PEG 526 methacrylate*	*2-hydroxethyl methacrylate*	*M-N dimethyl acrylamide*
1	1		1			
3	1			1		
5	1				1	
6	1				15	
7		1	1			
9		1		1		
11		1			1	
12		1			15	
13		1				1
14		1				15
15	1					1
16	1					15

Givent the novelty of these polymers and preliminary status at least initially, STO fibroblast cells rather than mESCs were employed to determine foremost, the biocompatibility of the polymers and secondly the ability of the polymers to support cell adhesion, given that fibroblasts are robust, anchorage-dependent cells which are maintained without the expensive LIF supplement. STO fibroblasts were seeded onto the hydrogels and allowed to proliferate, initially for up to 48 h, after which time morphology and proliferation were assessed. Of the six different methacrylic-based hdyrogels, only methacrylic: PEG 526 methacrylate 1:1 (copolymer 3) displayed any signs of supporting fibroblast attachment and spreading, as detected by little evidence of fibrils and processes (Figure 5.2E). However, this elongation and spread was much less obvious when compared to fibroblasts seeded in optimum conditions on fibronectin-coated cover slips, which displayed extensive elongation and spreading (Figure 5.6C). Nonetheless, contact with this methacrylic: PEG 526 methacrylate 1:1 hydrogel, unlike the other methacrylic-based copolymers, stimulated minimal cell death; trypan-blue positive cells represented less than 10 % of cell population after 48 h (Figure

5.7A). In contrast, the five remaining methacrylic-based hydrogels did not support any fibroblast attachment; fibroblasts were identified floating in suspension and adopted rounded cell morphology (Figure 5.2D, F, Fig 5.3D, E, F). In addition, fibroblasts seeded onto these hydrogels (methacrylic:2-hydroxethyl methacrylate 1:1 (copolymer 5), methacrylic:2-hydroxethyl methacrylate 1:15 (copolymer 6), methacrylic:360 PEG 1:1 (copolymer 1), methacrylic:N,N-dimethylacrylamide 1:1 (copolymer 15) and methacrylic: N,N-dimethylacrylamide 1:15 (copolymer 16)) were not viable by 48 h, moreover the majority of cells were not viable, as early as 2 h (Figure 5.7), compared to the negative control (Figure 5.6 D).

Of the acrylic-based hydrogels, acrylic: PEG 526 methacrylate 1:1 (copolymer 9) and acrylic: N,N-dimethylacrylamide 1:15 (copolymer 14) supported cell attachment by 48 h and there was evidence of typical fibroblast elongated morphology. This was demonstrated by evidence of processes, suggesting cell spread, similar to that of the positive control represented by a fibronectin-coated cover slip (Figure 5.6C), albeit to a lesser extent.

In contrast, the remaining acrylic-based hydrogels; acrylic: 360 PEG 1:1 (copolymer 7), acrylic: 2-hydroxethyl methacrylate 1:1 (copolymer 11), acrylic: 2-hydroxethyl methacrylate 1:15 (copolymer 12) and acrylic: M-N-dimethylacrylamide 1:1 (copolymer 13), appeared to discourage fibroblasts from adhering to the surface. Fibroblasts were identified floating in suspension and assumed a rounded morphology as early as 2 h and 48 h post-seeding (Figures 5.4D and F, 5.5D and F, respectively). Furthermore, more than 97 % of fibroblasts seeded onto these hydrogels were non viable after 48 h (Figure 5.7). Hydrogels that were seen to support fibroblast adhesion (acrylic: PEG 526 methacrylate 1:1 (copolymer 9) and acrylic: M-Ndimethylacrylamide 1:15 (copolymer 14)) displayed a largely viable fibroblast population after 48 h.

Of the twelve hydrogels therefore, only methacrylic: PEG 526 methacrylate 1:1 (copolymer 3), acrylic: PEG 526 methacrylate 1:1 (copolymer 9) and acrylic: M-N-dimethylacrylamide 1:15 (copolymer 14) showed any promise, not least because more than 90 % of fibroblasts seeded onto these copolymers survived after 48 h, but also because there was evidence in all three cases, of fibroblast adhesion to the copolymer surface and spread, attributed to elongated, fibroblast-like morphology.

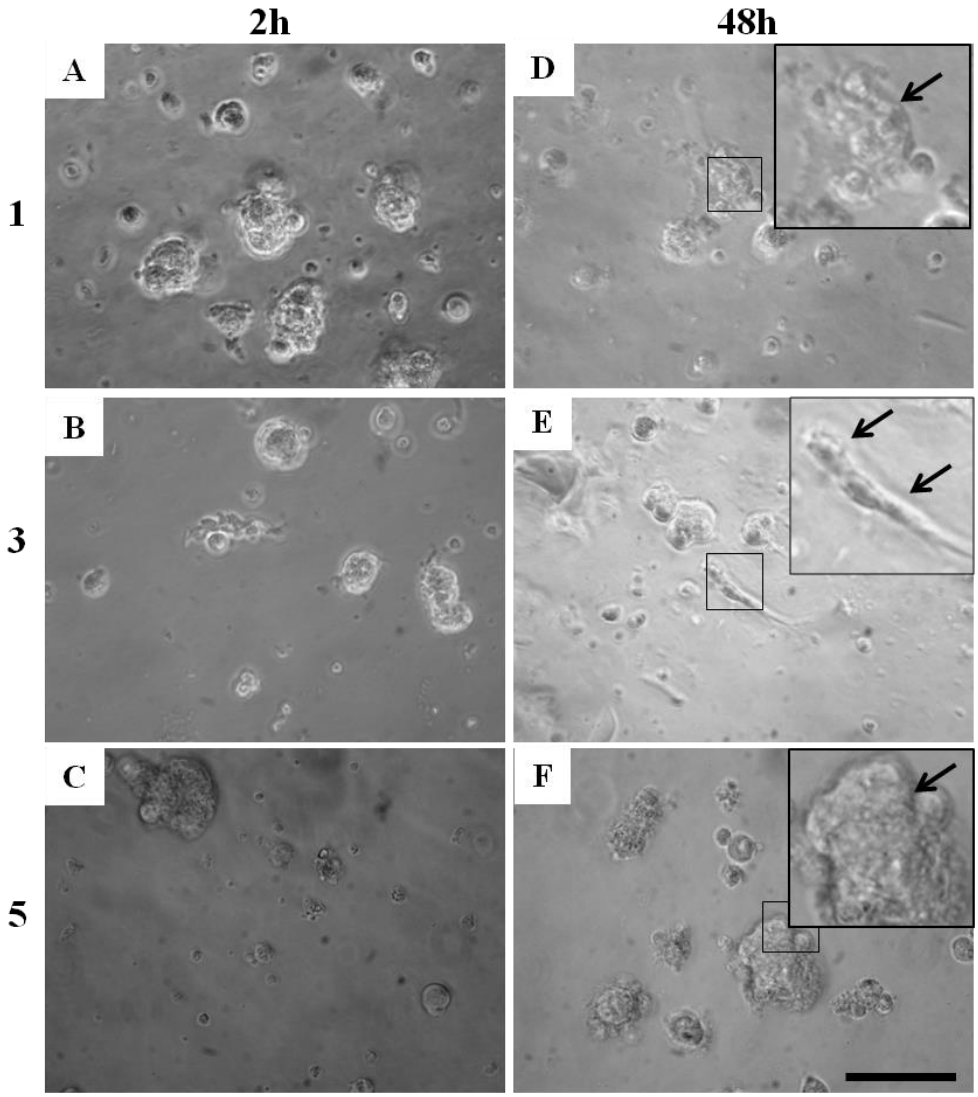

Figure 5.2 Methacrylic-based hydrogels 1, 3 and 5 do not support fibroblast attachment or proliferation. Fibroblast cells were seeded onto copolymers after usual sterilisation procedures and allowed to attach for up to 48 h. Methacrylic:360 PEG 1:1 did not support cell attachment neither at 2 h (A) or after 48 h (D); instead cells retained a rounded morphology and floated in suspension (arrows). Likewise, fibroblasts seeded onto methacrylic:2-hydroxethyl methacrylate 1:1displayed a rounded morphology at 2 hours (C) and after 48 h (F) (arrows). Methacrylic: PEG 526 methacrylate 1:1 appeared to support some fibroblast attachment and spreading after 48 h (E) (arrows), displaying signs of fibrils, but cells were unattached and rounded after 2 h (B). The experiment was repeated more than 3 times, images are representative for each population, scale, 50 μm.

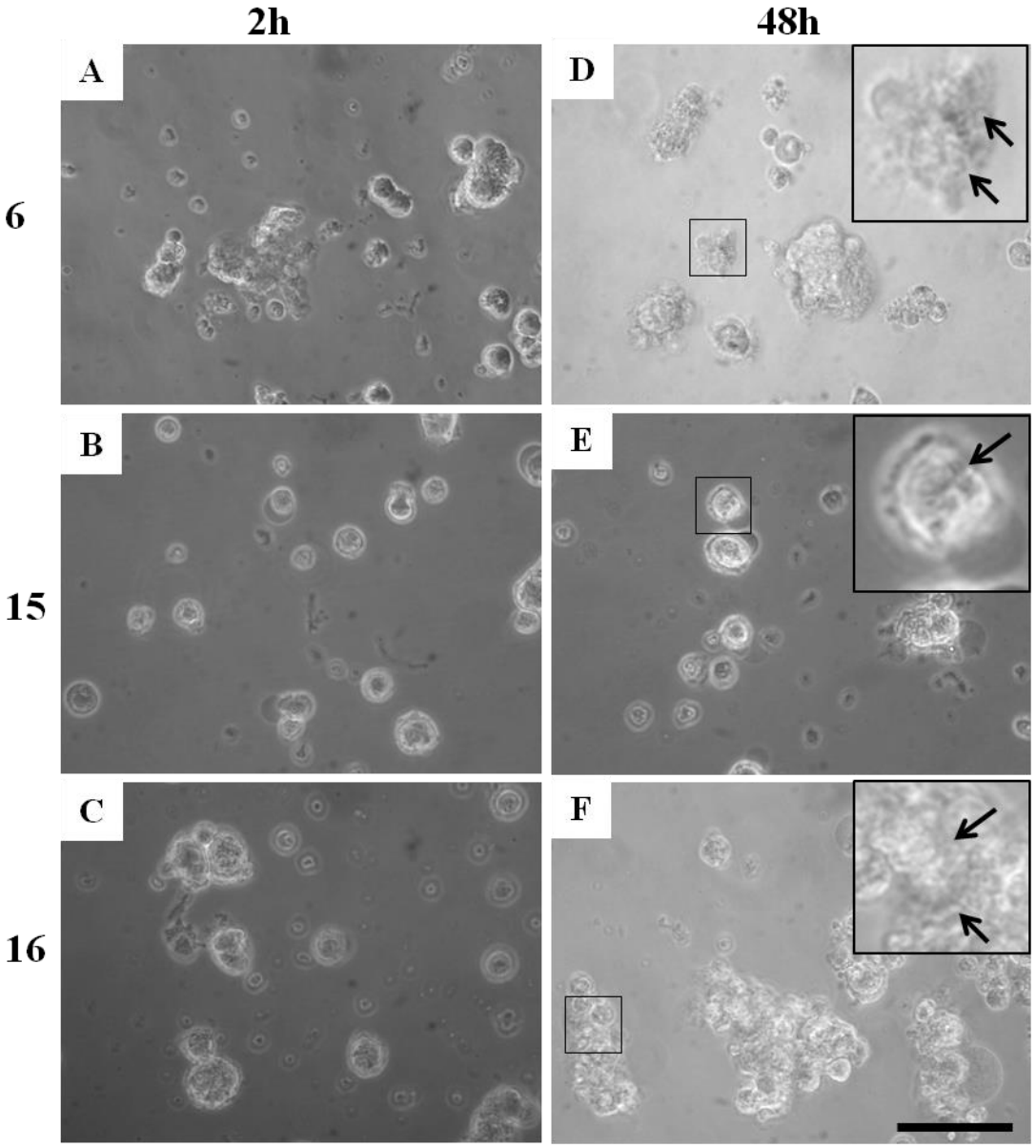

Figure 5.3 Methacrylic-based hydrogels 6, 15 and 16 do not support fibroblast attachment or proliferation. Fibroblast cells were seeded onto copolymers after usual sterilisation procedures and allowed to attach for up to 48 h. Methacrylic:2-hydroxethyl methacrylate 1:15 did not support cell attachment neither at 2 h (A) or after 48 h (D); fibroblasts displayed a rounded morphology (arrows). Methacrylic:M-Ndimethylacrylamide 1:1did not support fibroblast attachment neither after 2 h (B) nor after 48 h (E) as cells retained a rounded morphology. Likewise, methacrylic: M-Ndimethylacrylamide 1:15, did not support any fibroblast attachment, instead, fibroblasts were identified in clumps floating in the medium with a rounded morphology. The experiment was repeated more than 3 times, images are representative of each population, scale bar, 50 μm.

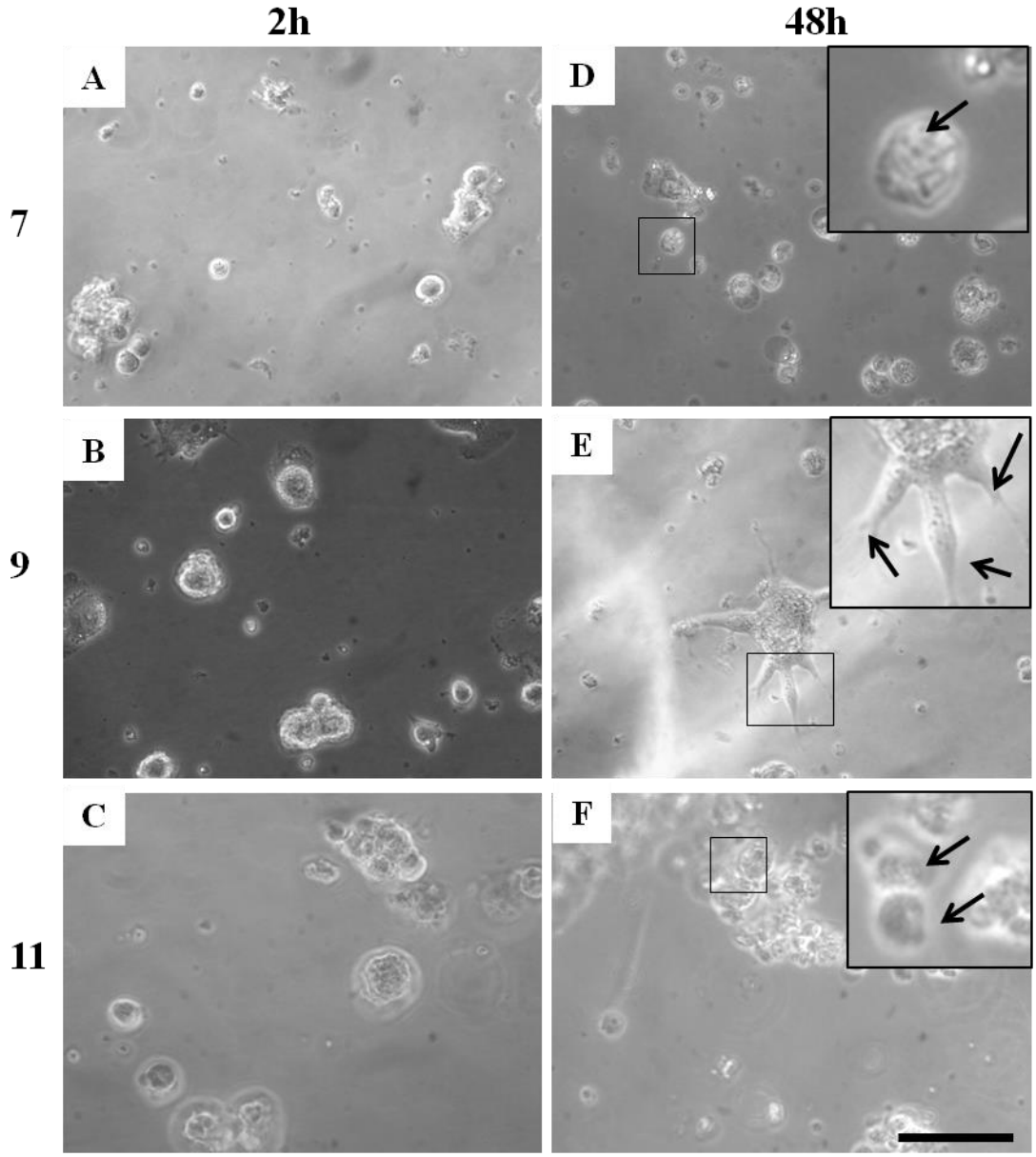

Figure 5.4 Acrylic-based hydrogels 7, 9 and 11 display little evidence of supporting fibroblast attachment and spread. Fibroblast cells were seeded onto copolymers after usual sterilisation procedures and allowed to attach for up to 48 h. Fibroblasts seeded onto acrylic: 360 PEG 1:1 retained a rounded morphology at 2 h post seeding (A) and 48 h post seeding (D) (arrows). Likewise, upon seeding fibroblast cells onto acrylic:2-hydroxethyl methacrylate 1:1, cells did not attach but instead remained floating in suspension after 2 h (C) and 48 h (F) (arrows). Fibroblasts seeded onto Acrylic:PEG 526 methacrylate 1:1 although rounded at 2 h (B), appeared to attach and display signs of spreading by 48 h (E) (arrows). The experiment was repeated more than 3 times, images are representative of each population, scale bar, 50 μm**.**

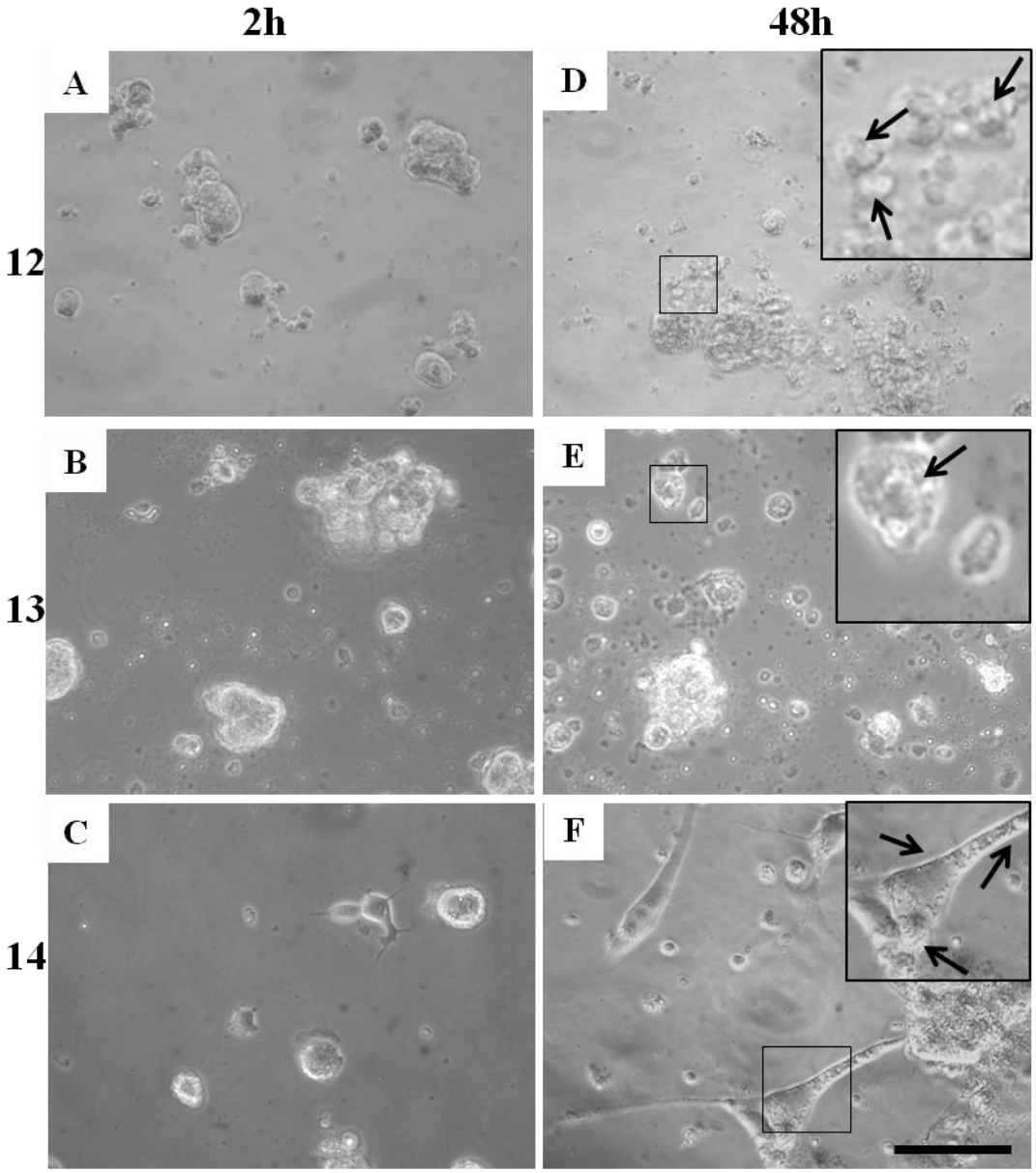

Figure 5.5 Acrylic-based hydrogels 12, 13 and 14 display little evidence of supporting fibroblast attachment and spread. Fibroblast cells were seeded onto copolymers after usual sterilisation procedures and allowed to attach for up to 48 h. Fibroblasts seeded ontoacrylic:2-hydroxethyl methacrylate 1:15 retained a rounded morphology at 2 h post seeding (A) and 48 h post seeding (D) (arrows). Likewise, upon seeding fibroblast cells onto acrylic: M-Ndimethylacrylamide 1:1, cells did not attach but instead remained floating in suspension with a rounded morphology after 2 h (B) and 48 h (E) (arrows). Fibroblasts seeded onto Acrylic: M-Ndimethylacrylamide 1:15 however, did support fibroblast attachment and spreading identified by 48 h (F), although the majority of cells remained rounded in morphology at 2 h (C). The experiment was repeated more than 3 times, images best represent each population and scale bar represents 50 μm.

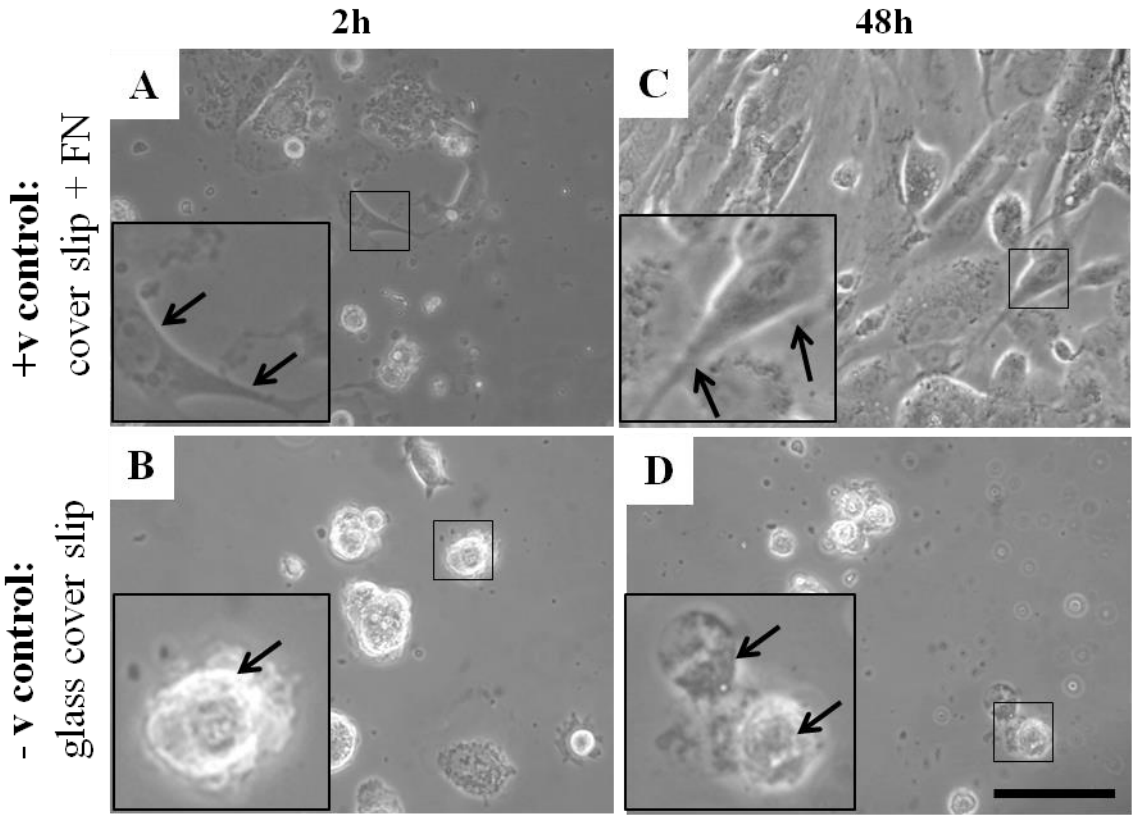

Figure 5.6 Fibroblast morphology varies according to ability to spread. STO fibroblasts were seeded onto two different control conditions, one to encourage cell attachment and spread (fibronectin-coated cover slip) and another to discourage cell attachment (uncoated glass cover slip). Cell morphology was assessed accordingly, 48 h post seeding. The positive control, represented by a cover slip coated with fibronectin, resulted in fibroblasts attaching to the surface after 2 h (A) displaying some signs of cell spread, identified by elongated morphology and processes (A, arrows). After 48 h, the majority of cells were attached to the surface of the cover slip and appeared to be spreading, identified by typical, elongated fibroblast morphology (C arrows). In contrast, the negative control; an uncoated glass cover slip, caused fibroblasts to remain floating in suspension after 2 h (B) displaying a rounded morphology (B arrows). This was consistent also after 48 h, as cells were detected in clumps floating in suspension (D), all displaying a rounded morphology (D arrows). The experiment was repeated more than four times and images are representative of cell populations. Scale bar, 100 μm.

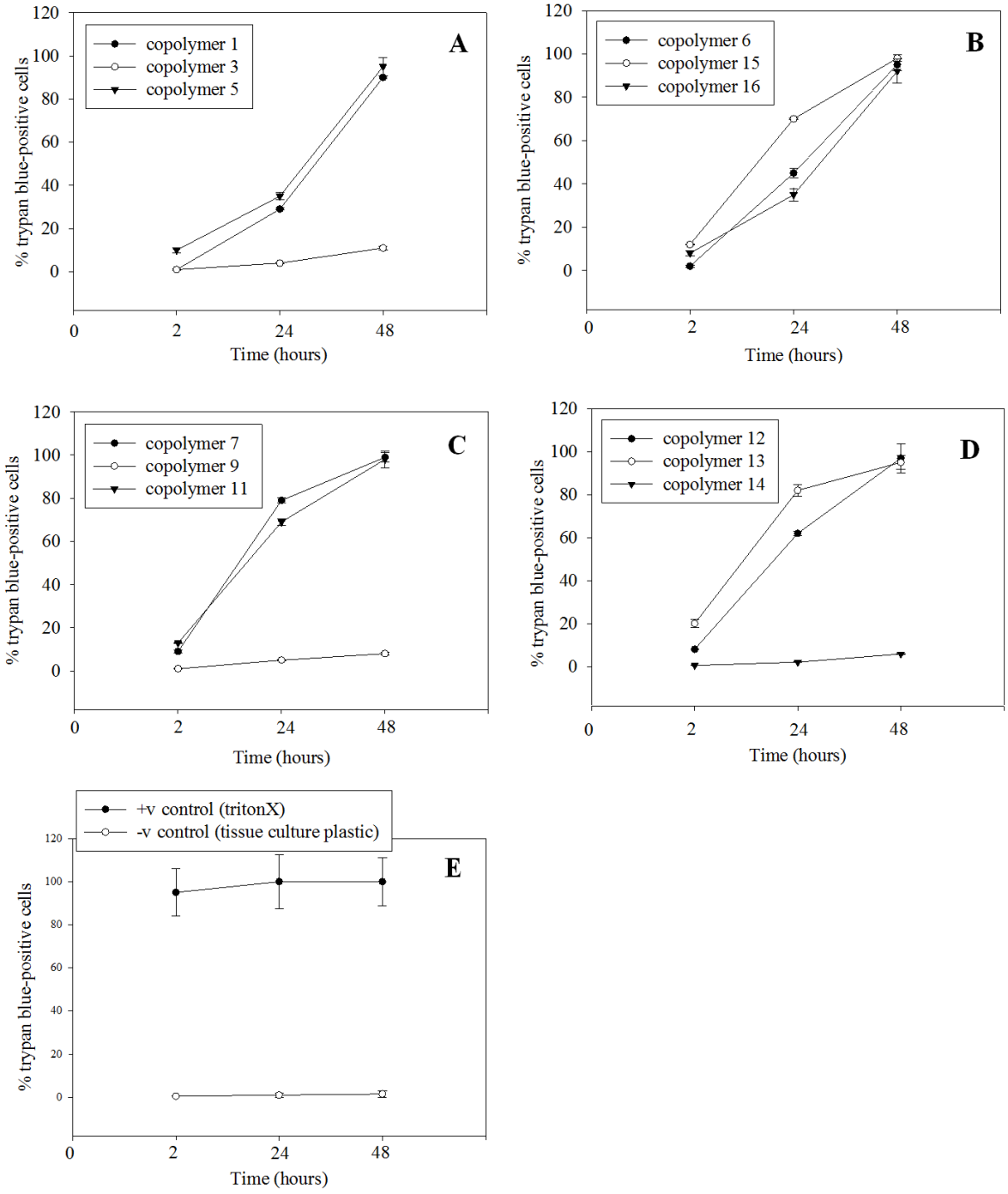

Figure 5.7 Fibroblast viability was completely lost in all but three hydrogels. Fibroblast cells were seeded onto twelve different hydrogels and incubated for 48 h, after which trypan blue was used to detect non-viable cells. Only copolymer 3, 9 and 14 supported fibroblast viability up to 48 h (A, C and D respectively). All other copolymers; 1, 5, 6, 7, 11, 12, 13, 15 and 16 resulted in loss of more than 95 % of cells, positive for trypan blue after 48 h. The experiment was repeated more than three times and error bars, SEM.

5.3 Poly-Ɛ-lysine based polymers support mESC viability and self renewal

A range of copolymers investigated in section 5.2., generally proved unsuccessful in supporting fibroblast expansion. Consequently, investigations were pursued into an alternative polymer, poly-Ɛ-lysine as a synthetic substrate for cell expansion. The employment of polylysine in biomaterials represents a new, yet promising field within biomaterials.

As mentioned previously, SpheriTech have developed a novel method to develop and synthesize 3D macroporous poly-Ɛ-lysine polymers with well controlled porosity and these were investigated here.

mESCs were seeded onto SpheriTech PƐL polymers using a transwell system as described in Materials and Methods to assess the potential of these novel 3D macroporous polymers in ESC expansion and maintenance. Polymers were removed from the culture system after 10 days and proliferation was assessed, as well as exploring the effect that contact with these polymers had on mESC self-renewal (via investigating alkaline phosphatase expression and Nanog expression, common markers of pluripotency).

mESCs were identified adhering to the poly-Ɛ-lysine polymers after 10 days, as detected with DAPI (Figure 5.8A) and assessment of proliferation using an MTS assay, showed that, whilst proliferation of mESCs on these synthetic polymers was significantly slower compared to standard gelatine-coated tissue culture plastic, mESCs were proliferating in contact with these PƐL polymers (Figure 5.8D). Furthermore, mESCs in contact with PƐL polymers remained alkaline phosphatase-positive (Figure 5.8B and C). Similarly, mESCs maintained Nanog expression up to 10 days post seeding onto the polymers (Figure 5.9E and 5.9F). Closer inspection of the localisation of mESCs on the polymer, revealed that mESCs appeared to congregate on the periphery of the pores; moreover, cells were identified with a rounded

morphology and as single cells; there was no evidence of cells clustering together in colonies, as is often typical (Figure 5.9C and D).

Scanning electron microscopy (SEM) was employed to investigate surface topography and corresponding mESC morphology. PƐL polymers displayed a distinctly spherical topography, attributed to the methodology of polymer synthesis (Figure 5.10). This topography therefore demonstrates high surface area: volume ratio, and well controlled porosity; both attributes ideal for cell scale-up *in vitro* and diffusion of nutrients through the polymer.

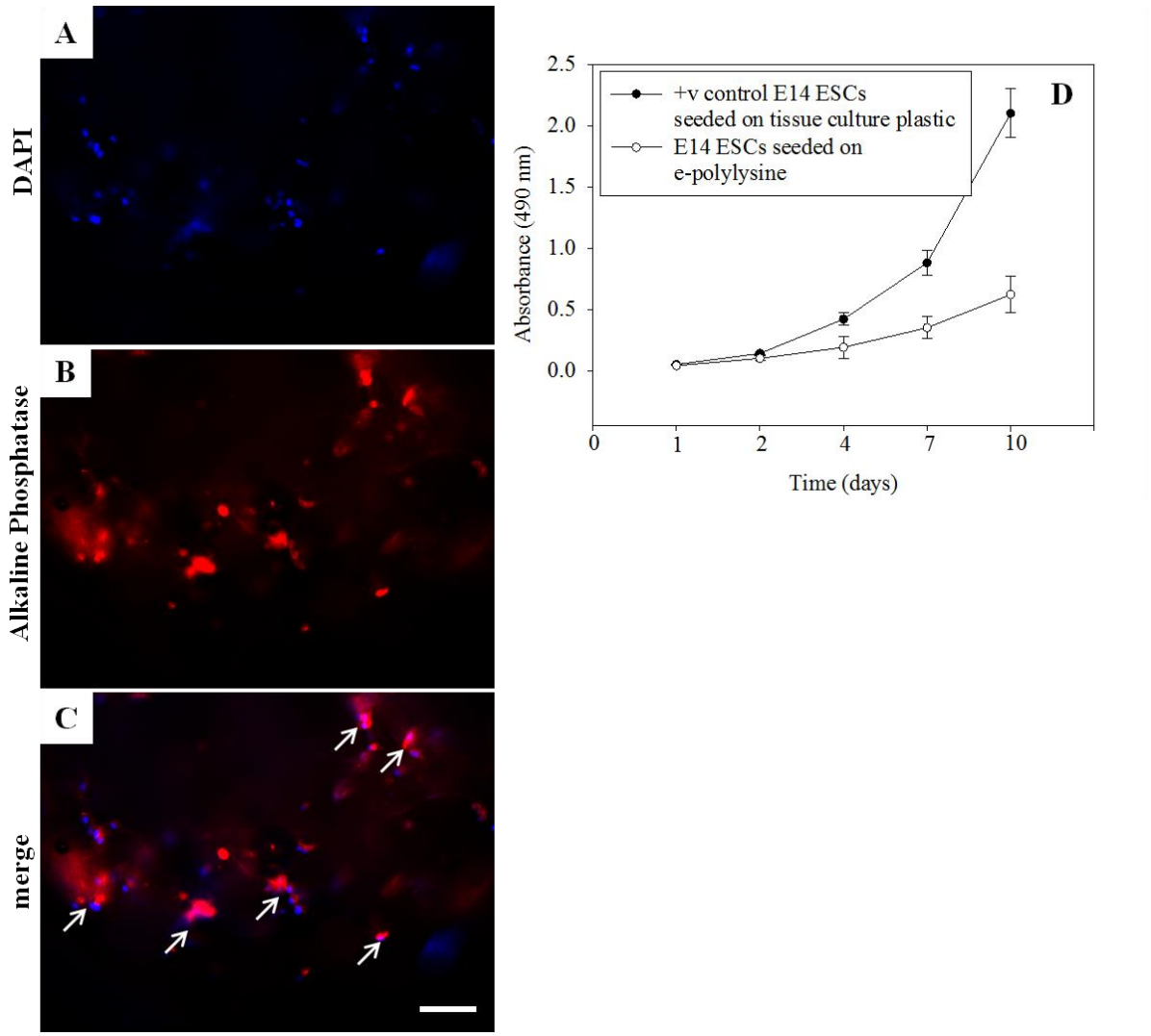

Figure 5.8 mESCs seeded onto poly-Ɛ-lysine polymers, attach, proliferate and retain alkaline phosphatase expression up to 10 days. E14 mESCs were seeded onto PƐL polymers and allowed to attach and proliferate for up to 10days, when polymers were stained for alkaline phosphatase. Cells were identified on polymers via DAPI stain (A), correlated with alkaline phosphatise stain (B) displaying alkaline phosphatise positive mESCs attached to polymer (C) (arrows). Cell proliferation quantification using an MTS assay showed that mESCs proliferate when in contact with PƐL polymer, albeit at a slower rate than compared to normal culture plastic, according to metabolic acitivity (D). All experiments were repeated more than three times, images are representative of the population and error bars, SEM. Scale bar represents 100 μm.

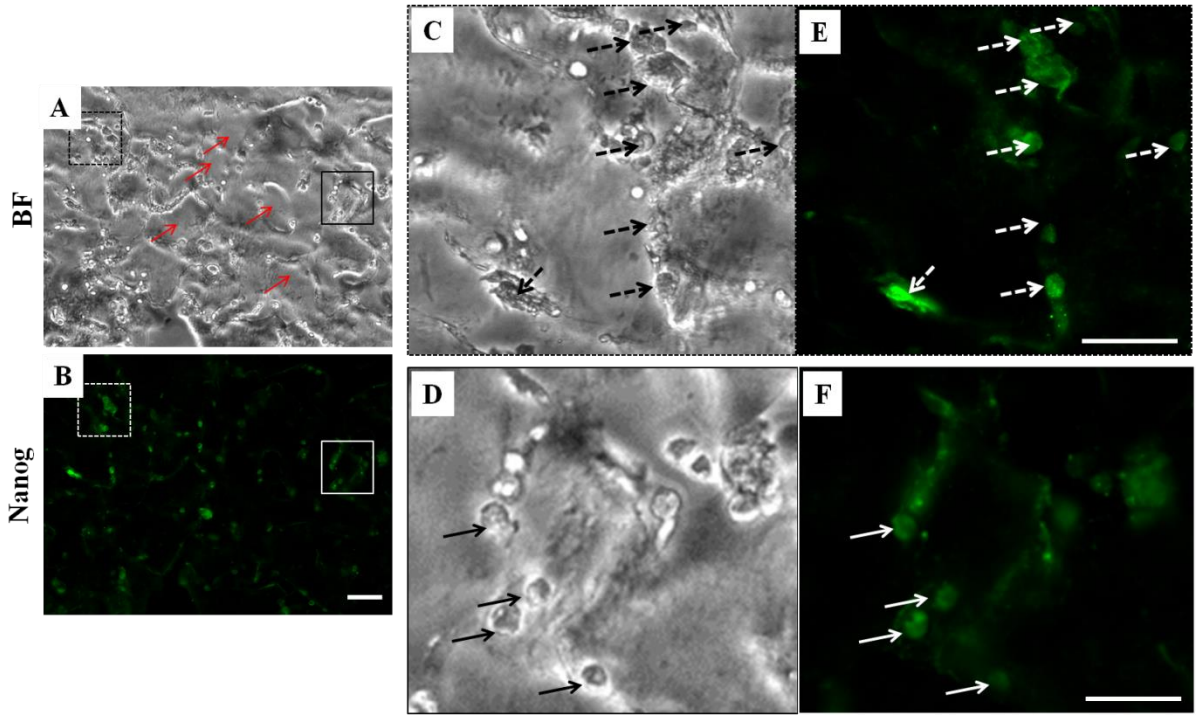

Figure 5.9 E14 mESCs maintain Nanog expression when seeded onto poly-Ɛ-lysine-based macroporous polymers and topography of polymer directs location of mESCs. E14 mESCs were seeded onto PƐL and allowed to proliferate during incubation for 10 days, after which polymers were frozen, sectioned and stained for pluripotency marker Nanog. Using bright-field (BF) microscopy, mESCs were identified on the periphery of pores within the polymer (highlighted by red arrows in A), as shown in magnified images from two different fields of view; dashed arrows in (C) and normal arrows in (D). mESCs were Nanog positive, as shown in B, highlighted at higher power (E and F). The experiment was repeated more than three times and images are representative of the cell population. Scale bars; 100 μm.

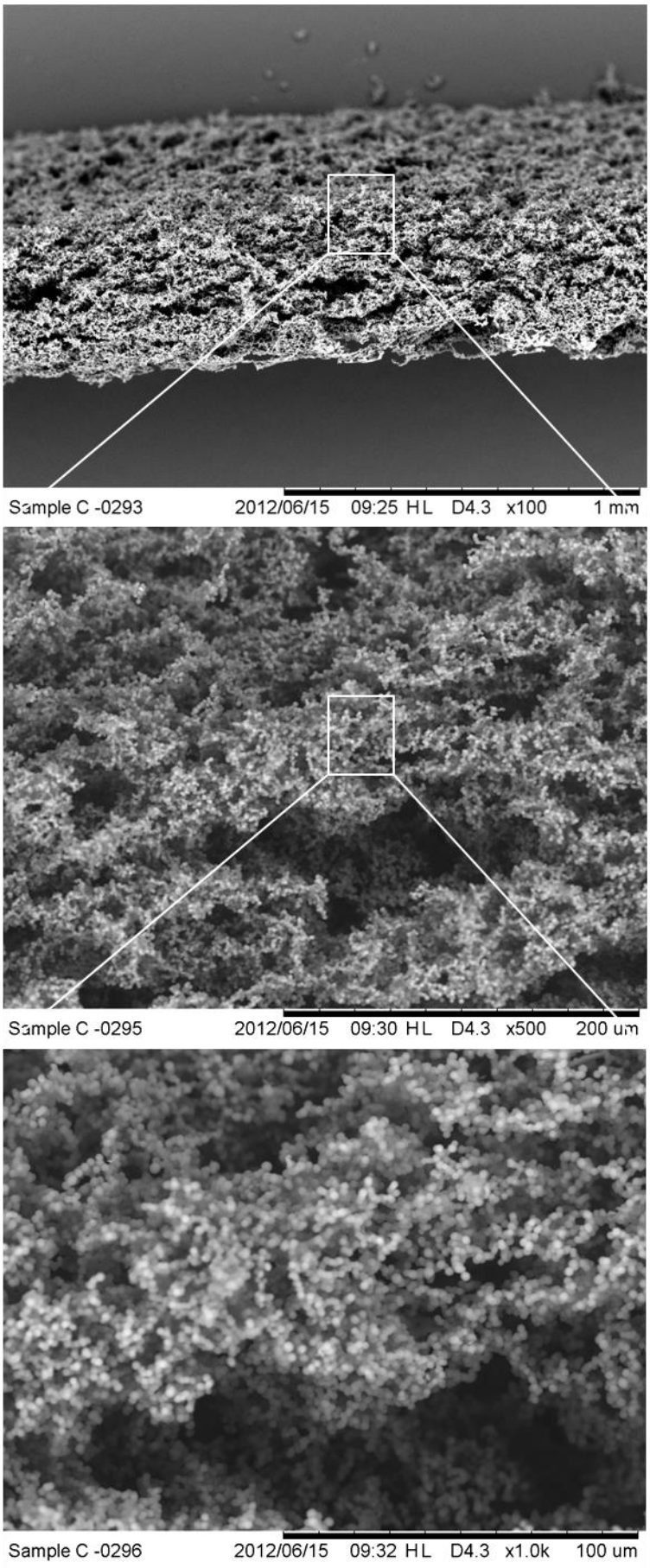

Figure 5.10 Poly-Ɛ-lysine topography and architecture. PƐL spherical topography demonstrates high surface area: volume ratio and well controlled porosity, ideal for expansion of cells and diffusion of nutrients. PƐL polymers were analysed under SEM after synthesis. Results show a high surface area: volume ratio and well defined pores. The experiment was repeated more than three times.

5.4. Growth of kidney stem cells on poly-Ɛ-lysine

3D PƐL macroporous polymers were shown to support mESC adherence, proliferation and self renewal, attributed to its cationic surface and well controlled porosity (section 5.3). Considering the requirement for a synthetic substrate to be applied and the success of the PƐL for ESC culture, this section explores the potential to exploit this polymer in renal-based applications. Additionally, given the methodology of polymer synthesis, derived and modified by SpheriTech, and the very nature of PƐL, coupling functional groups to these polymers represents an exciting approach to further enhance polymer performance.

The potential of PƐL and RGD-crosslinked analogues, to support KSC expansion was explored, for the eventual employment of these expanded KSCs as a kidney regeneration tool. The kidney-derived stem cell line was derived from mice expressing the green fluorescent protein (GFP), employed to increase the ease of tracking *in vitro* and to tailor the initial mESC-based investigation to suit a more renal, downstream application.

5.4.1. Poly-Ɛ-lysine-based polymers +/- RGD support KSCs-GFP

Kidney-derived stem cells derived from mice expressing green fluorescent protein (GFP) (KSCs-GFP) were seeded onto PƐL macroporous polymers, which had previously been shown to support mESC attachment, proliferation and self-renewal. KSC-GFP cells were identified adhering to the surface of the polymer using immunofluorescence detection of GFP in conjunction with DAPI at 4, 7 and 10 days (Figure 5.11 A, B, C, respectively). Similarly, PƐL coupled with RGD displayed KSCs on the polymer surface at 4, 7 and 10 days post seeding (Figure 5.11 D, E, F, respectively). Investigation of the proliferation of KSCs as a result of contact with these PƐL polymers (+/- RGD), demonstrated that PƐL coupled with RGD stimulated KSCs to proliferate significantly faster than that KSCs seeded on PƐL without RGD (Figure 5.12). However, both PƐL polymers (+/- RGD) displayed proliferation rates significantly slower than standard gelatine-coated tissue culture plastic (Figure 5.13).

Inspection of KSC-GFP morphology and interaction with PƐL polymers (+/- RGD) using SEM three days post seeding, revealed that KSCs appeared to be located within the pores of the polymer, although spreading appeared limited, due to lack of elongated fibroblast-like morphology detected both in the case of PƐL with and without RGD (Figure 5.13 A, B, C,D, respectively). In comparison, typical KSC-GFP morphology can be represented by elongated, fibroblast-like morphology, as shown by SEM images of KSCs-GFP cultured on gelatine-coated tissue culture plastic (Figure 5.13 E and F). Evidently, KSCs-GFP coated the surface of the polymers with ECM molecules, as detected by a coating like surface on the surface of the polymers after culture with KSCs-GFP, and highlighted by the less distinct spherical topography.

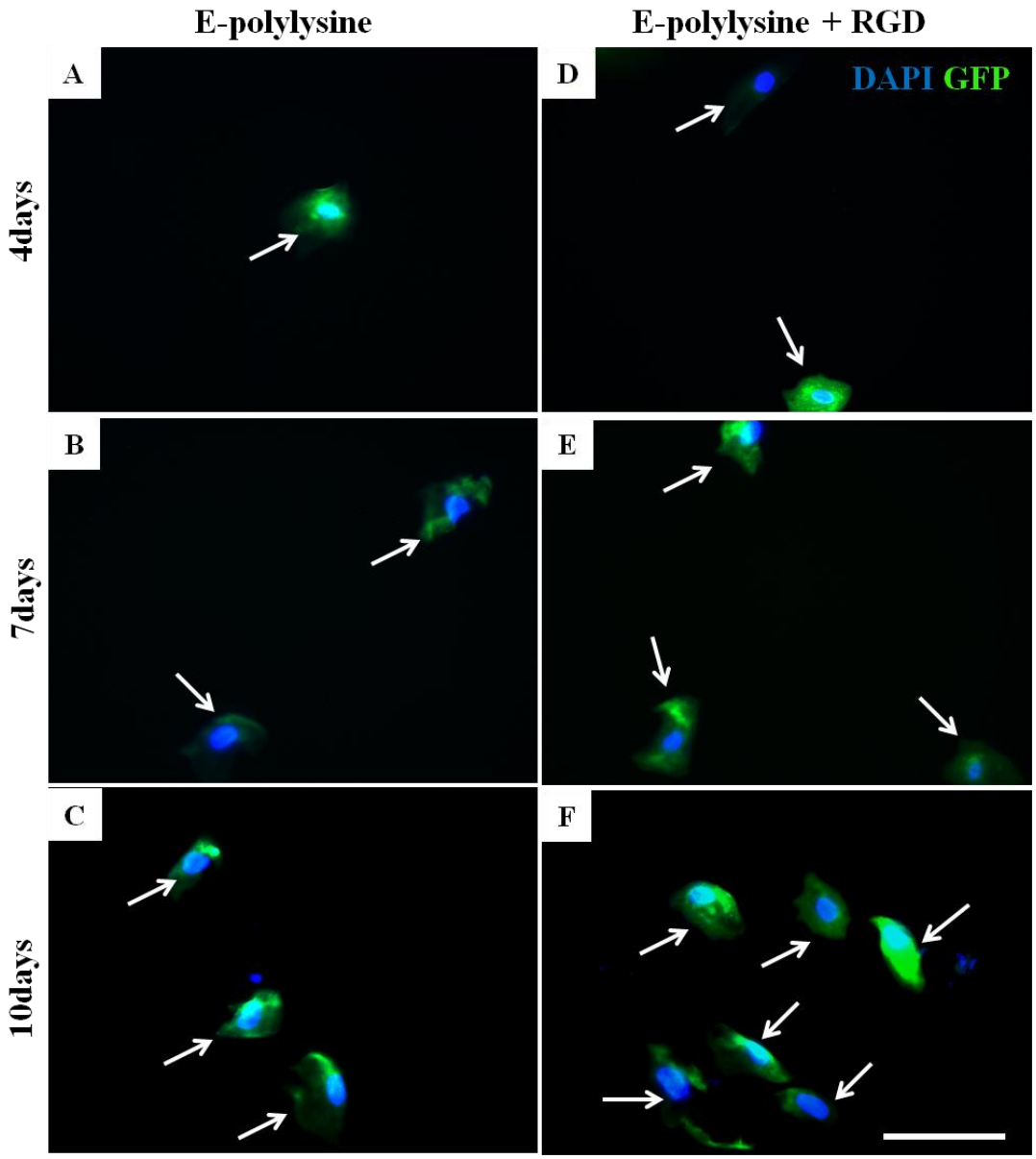

Figure 5.11 Poly-Ɛ-lysine macroporous polymers (+/- RGD) support KSCs-GFP attachment and proliferation up to 10 days. KSCs-GFP were seeded onto macroporous PƐL polymers with and without RGD cross-linked. Cells were allowed to proliferate and at 4, 7 and 10 days, polymers were frozen and prepared for sectioning, followed by DAPI stain. After 4 days, low numbers of single cells were identified in any one field of view +/- RGD (A and D, respectively). After 7 days in culture, PƐL cross-linked with RGD appeared to display KSCs-GFP at higher density (E) compared to cells identified on PƐL alone (B). This was consistent and more apparent at 10 days, whereby PƐL alone displayed regions of relatively populated (C), however poly-Ɛ-lysine cross-linked with RGD displayed more highly dense cell populations (F). The experiment was repeated three times and images are representative of the cell population. Scale bar; 100 μm.

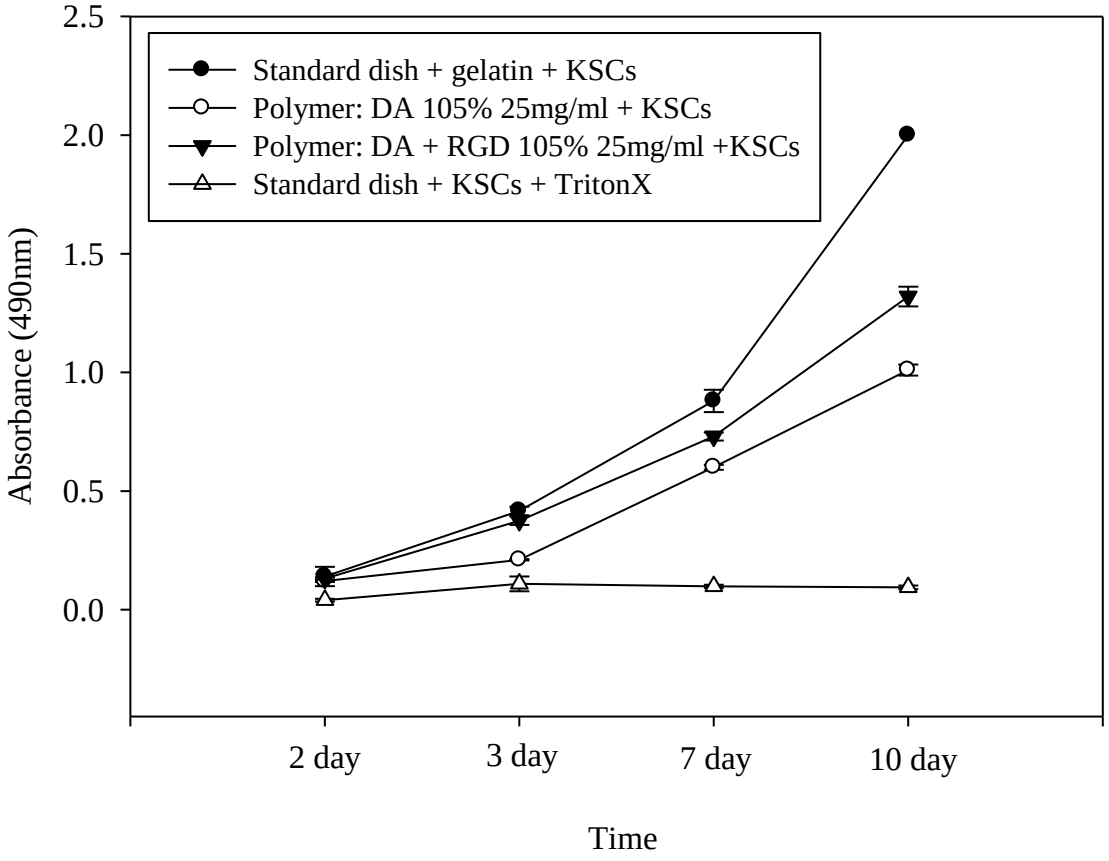

Figure 5.12 Synthetic poly-Ɛ-lysine coupled with RGD, supports KSCs-GFP proliferation at a higher rate than poly-Ɛ-lysine not coupled with RGD. KSCs-GFP were seeded onto PƐL polymers which were all 100% cross-linked (denoted 105%) with and without RGD (+/- RGD) and allowed to proliferate up to 10 days. At 2, 3, 7 and 10 days, MTS assay was used to determine cell proliferation with regard to metabolic activity and absorbance readings were taken at 490 nm. Metabolic activity increased over time for both polymers (+/- RGD) suggesting cell proliferation, however PƐL coupled with RGD, outperformed PƐL without RGD, displaying higher metabolic acitivty at every time-point. Both polymers (+/- RGD) displayed significantly lower absorbance values than standard culture conditions, however significantly higher than samples incubated with TritonX. The experiment was repeated more than three times and error bars, SEM.

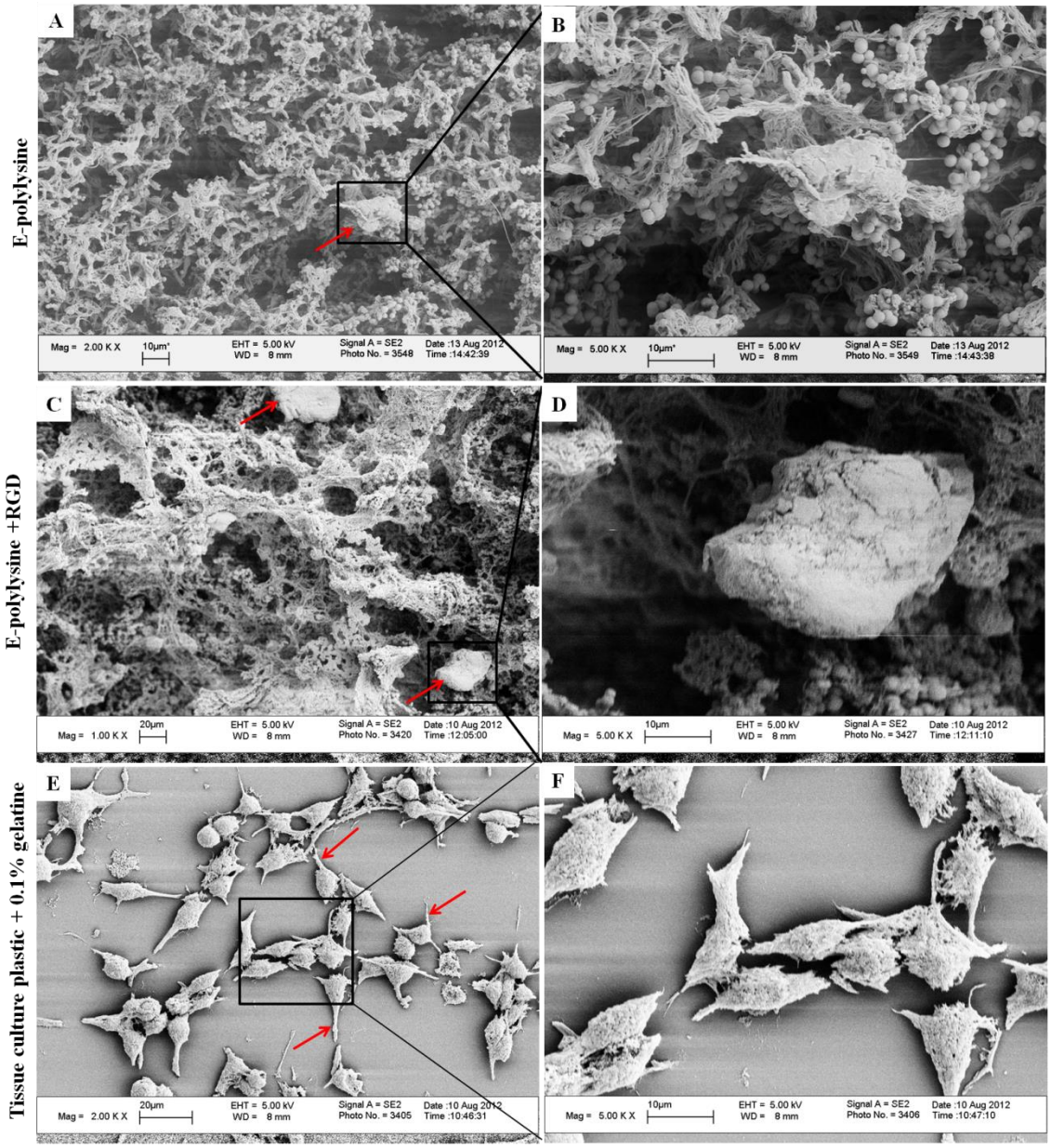

Figure 5.13 KSCs-GFP populate the pores of the poly-Ɛ-lysine or on the surface of the spheres, and fibroblast-like processes appear to be lost compared to standard tissue culture plastic. KSCs-GFP were seeded onto standard tissue culture plastic coated with 0.1 % gelatine and PƐL polymers +/- RGD, allowed to proliferate and samples were then prepared for SEM, 3 days post seeding. KSCs-GFP displayed typical fibroblast-like morphology identified with fibrils and processes spreading across the dish (red arrows in C) when seeded onto tissue culture plastic coated with gelatine, further outlined in (F). PƐL polymers appeared to support KSC-GFP attachment in both +/- RGD samples, although interaction with the polymer was inconsistent; often KSCs-GFP were seen contacting the spheres of the structure of the polymer (A and B), but also seen to settle in the pores of the polymer structure (B and E). The experiment was repeated four times and the images are representative of the cell population. Scale bars ; 10 µm and 20 µm, respectively.

5.5 Poly-Ɛ-lysine-based polymers modified with HS analogues

Results here have demonstrated that PƐL 3D macroporous polymers can support KSC-GFP attachment and proliferation, and moreover if coupled with RGD, polymer performance was shown to be enhanced (section 5.4). Additionally, results in chapter 2 outlined a role for soluble HS in maintaining typical mESC behaviour, potentially linked to the need for serum. Taken together, PƐL coated with synthetic HS structures could provide an artificial alternative to current *in vitro* cell expansion systems that typically involve animal-derived products, such as gelatine and serum for example.

Accordingly, PƐL synthesis was modified to accommodate the binding of HS-mimetic structures via ionic interactions with free alpha-amine groups (Figure 5.1). Synthetic HS mimetic structures, chemically modified heparins with selectively reduced sulfation, were synthesised in-house (Yates, Guimond et al. 2004).

Initially, the effect of these HS-mimetic heparin structures was tested by absorption onto the surface of standard tissue culture plastic simply via ionic adsorption. Investigation into the effect that different structures had on KSC-GFP adherence, proliferation and spread was pursued, with a view to employing the best-performing structures as alternatives to current, highly expensive synthetic plastics and/or animal-derived coatings.

Per-sulfated (over-sulfated) heparin coating and PMH coating were demonstrated to have similar effects on KSC-GFP attachment and morphology, 48 h post seeding. KSCs-GFP cultured on PMH-coated tissue culture plastic (Figure 5.14A) and per-sulfated heparin-coated tissue culture plastic (Figure 5.14B) resulted in KSCs-GFP attachment to the surface, moreover there was evidence of cell spreading due to identification of processes and spindle-like morphology, as in the control condition (gelatine-coated tissue culture plastic) (Figure 5.14F).

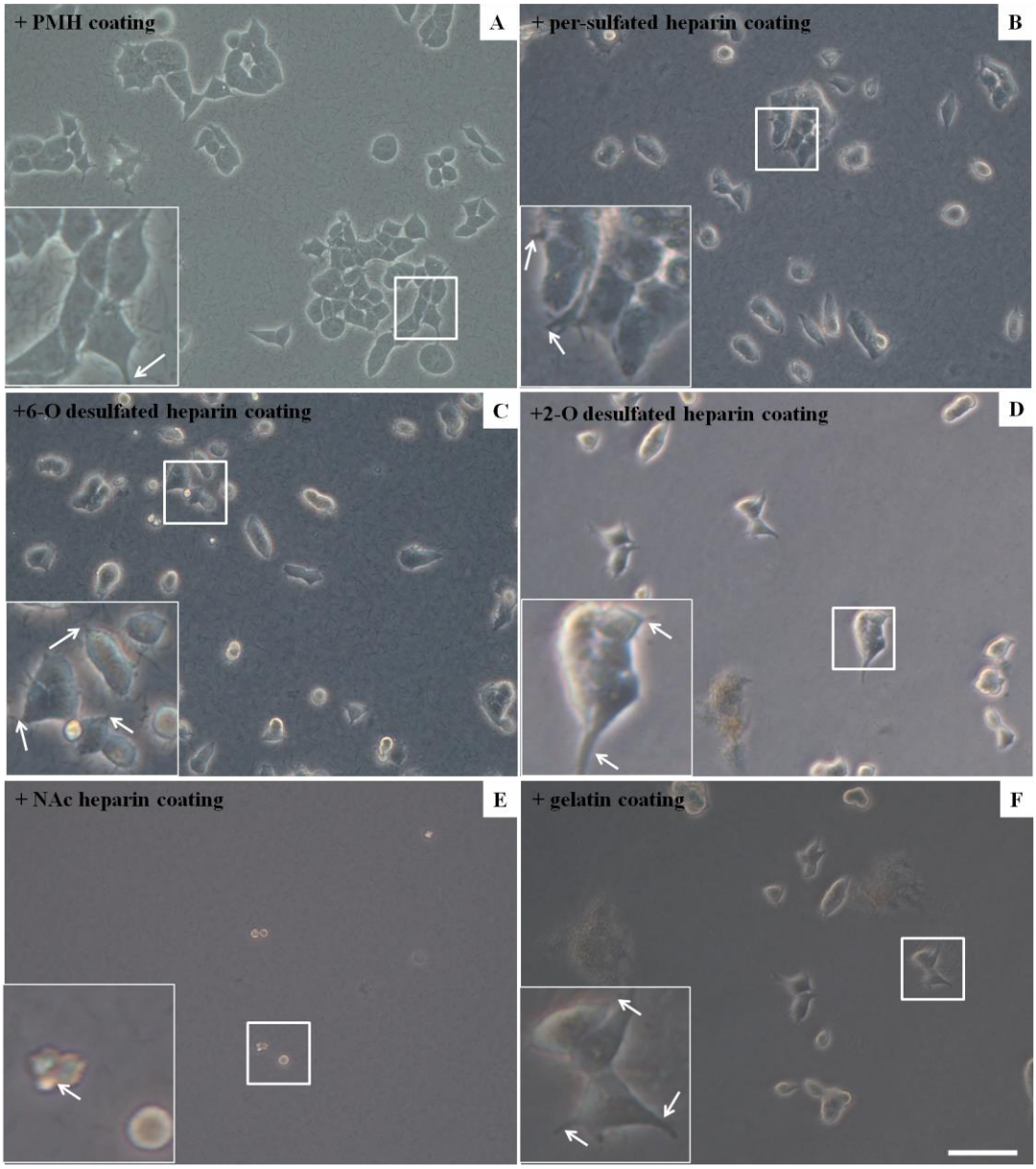

Figure 5.14 Tissue culture plastic coated with per-sulfated heparin, outperforms other heparin analogue coatings, in supporting KSC-GFP attachment and spreading. KSCs-GFP were seeded onto tissue culture plastic coated with different HS analogues; per-sulfated, 6-O desulfated, 2-O desulfated, NAc heparin, PMH, and a gelatine-coated control and allowed to attach and proliferate for 48 h, after which time morphology and spread was assessed. KSCs-GFP seeded onto per-sulfated heparin coated dishes, attached and spread displaying signs of processes and spindle-like morphology (A) (arrows), likewise for KSCs-GFP seeded onto PMH-coated dishes (B) (arrows). 6-O desulfated heparin-coating and 2-O desulfated coatings supported attachment and spreading also, highlighted by the presence of processes (C and D respectively) although less apparent spindle-like morphology. Dishes coated with NAc did not support KSC-GFP attachment and cells retained a rounded morphology (E). The experiment was repeated three times and images are representative of the cell populations. Scale bar represents 100 μm.

Tissue culture plastic coated with 6-O desulfated and 2-O desulfated heparin also displayed support of KSC-GFP attachment after 48 h, although there was less evidence of processes or elongated morphology (Figure 5.14C and D, respectively). Tissue culture plastic coated with NAc-heparin structures did not support KSC-GFP attachment; instead cells retained a rounded morphology and floated in suspension (Figure 5.14E). Investigation into proliferation of KSCs-GFP and the effect of different HS-mimetic coatings have on KSC-GFP proliferation was investigated using an MTS assay, based on metabolic activity. PMH and per-sulfated heparin coatings stimulated KSCs-GFP to proliferate at a faster rate than KSCs-GFP seeded onto gelatine-coated dishes (Figure 5.15). 6-O and 2-O desulfated heparin-coated dishes displayed comparable KSC-GFP proliferation rates, but lower than gelatine-coated dishes. In contrast, NAc-heparin coated dishes did not stimulate any KSC-GFP proliferation between 24 and 96 h (Figure 5.15).

PƐL 3D macroporous polymers were coated with the same set of synthetic HS-mimetic structures and KSCs-GFP were seeded onto the polymers using the trans-well culture system employed previously. Interaction of KSCs-GFP with the polymers was investigated using SEM, and proliferation again assessed using MTS.

SEM images of the polymers demonstrated that coating, whether with gelatine or any of the synthetic structures, altered the surface topography compared to that identified previous of the PƐL polymer alone (Figure 5.16). The most apparent change in surface topography was correlated with gelatine-coating; the distinct, spherical polymer surface was evidently covered, no doubt reducing surface area: volume. Furthermore, architecture also appeared to alter from a spherical, bead-like, porous structure to a more flattened, meshwork. Similarly for PMH-coated polymers; the existence of distinct spherical surfaces was reduced; instead the surface topography appeared more variable in heigh and overall polymer architecture seemed flattened and mesh-like (Figure 5.16). Per-sulfated, 6-O desulfated, 2-O desulfated

and NAc heparin structures appeared to induce fewer alterations in surface topography or polymer architecture. These four structures did display signs of coating the material, since the topography of the polymer appeared less homogenous when viewing the entire section, compared to polymer alone which displayed more uniformity. However on the whole, the PƐL polymers displayed spherical, bead-like topography and consistent porosity across each section (Figure 5.16).

The KSC-GFP proliferation results demonstrated that per-sulfated heparin and PMH-coated polymers supported the highest level of cell proliferation and were comparable to each other. Polymers coated with gelatine, supported steady proliferation, but at a slower rate than per-sulfated heparin-coated polymers and PMH-coated polymers. 6-O desulfated-coated polymers supported steady yet slower KSC-GFP proliferation compared to per-sulfated heparin-coated polymers for example, but higher than 2-O desulfated-coated polymers, which was relatively low. NAc heparin-coated polymers did not appear to support any proliferation up to 14 days (Figure 5.17).

Further SEM analysis was conducted of the polymers which best supported KSC-GFP proliferation (PMH, per-sulfated heparin and 6-O desulfated heparin-coated polymers). KSCs-GFP detected on the surface of polymers treated with per-sulfated structures, displayed elongated morphology typical of KSCs-GFP. Similarly but often not as obvious, KSCs-GFP detected on the surface of poly-Ɛ-lysine polymers treated with 6-O desulfated heparin-coating, displayed signs of spread, attributed to a flattened morphology (Figure 5.18).

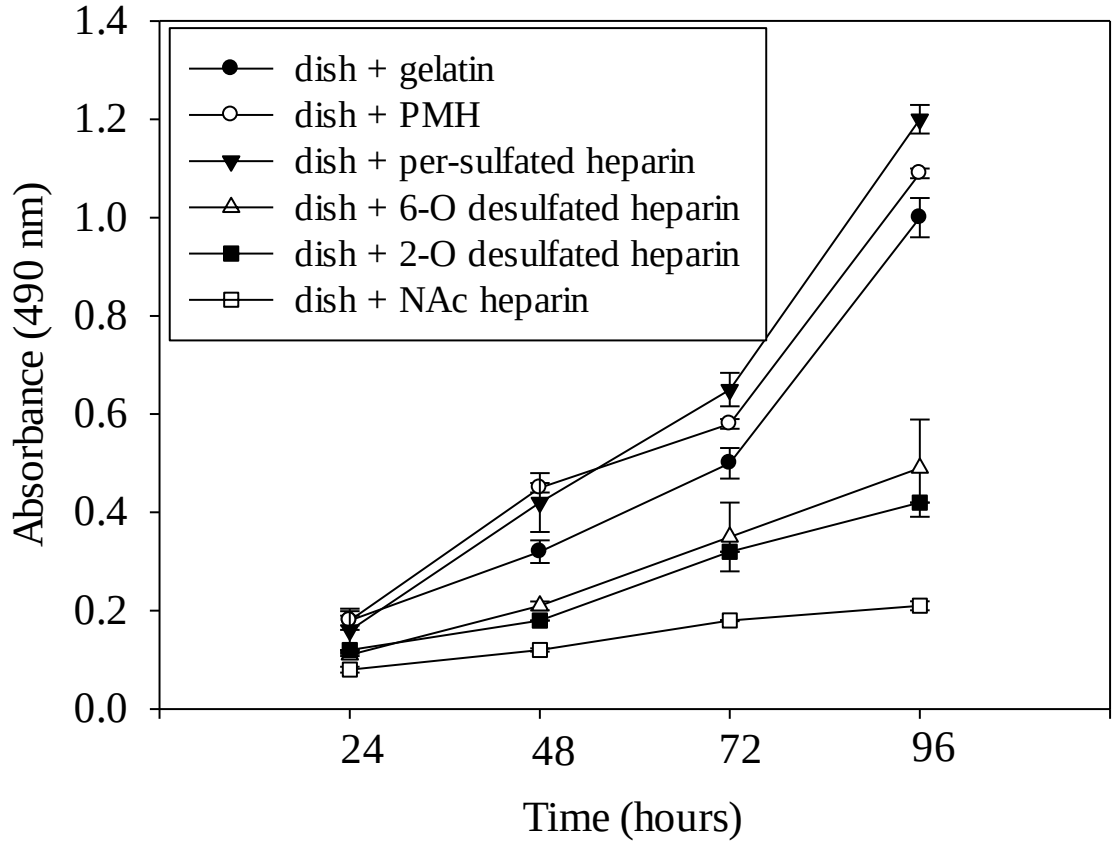

Figure 5.15 PMH and per-sulfated heparin structures absorbed to the surface of tissue culture plastic best support KSC-GFP proliferation compared to tissue culture plastic coated with 6-O and 2-O desulfated heparin or NAc heparin structures. KSCs-GFP were seeded onto tissue culture plastic coated with five different HS analogue structures and an MTS assay was used to determine KSC-GFP metabolic activity compared to gelatine-coated tissue culture plastic. Per-sulfated heparin-coated tissue culture plastic displayed the highest proliferation rate, comparable to PMH-coated dishes. 6-O desulfated heparin coatings and 2-O desulfated heparin coatings supported KSC-GFP proliferation also, at a rate comparable to gelatine-coated dishes but slower than per-sulfated heparin PMH coatings. The experiment was repeated more than three times and error bars, SEM.

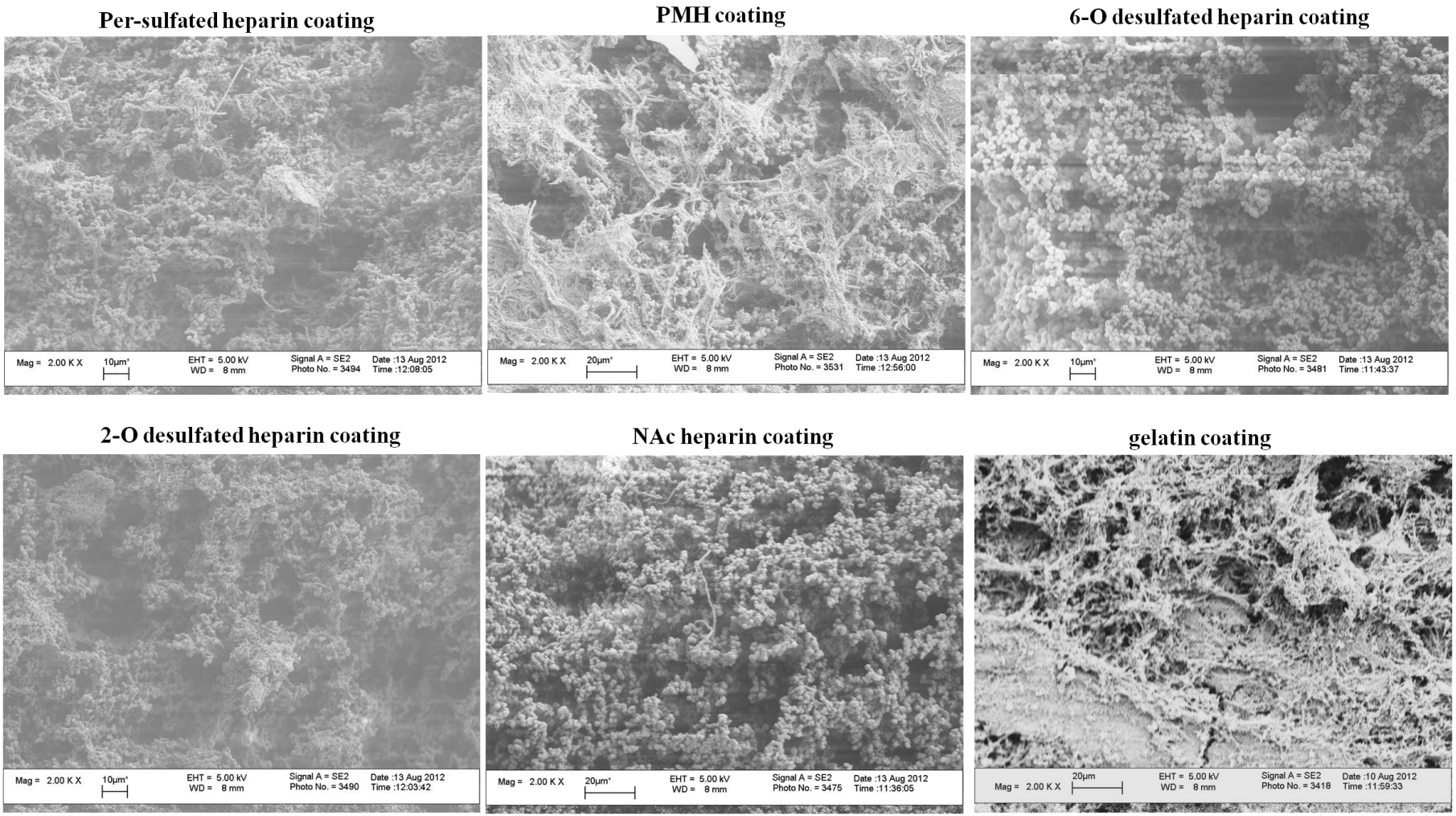

Figure 5.16 Surface topography of poly-Ɛ-lysine macroporous polymers is affected by coating with different HS-mimetic structures. PƐL macroporous polymers were synthesised and different modified heparin (HS-mimetic) structures were absorbed to the surface following 2 h incubation. Topography was analysed using SEM after standard sample preparation.

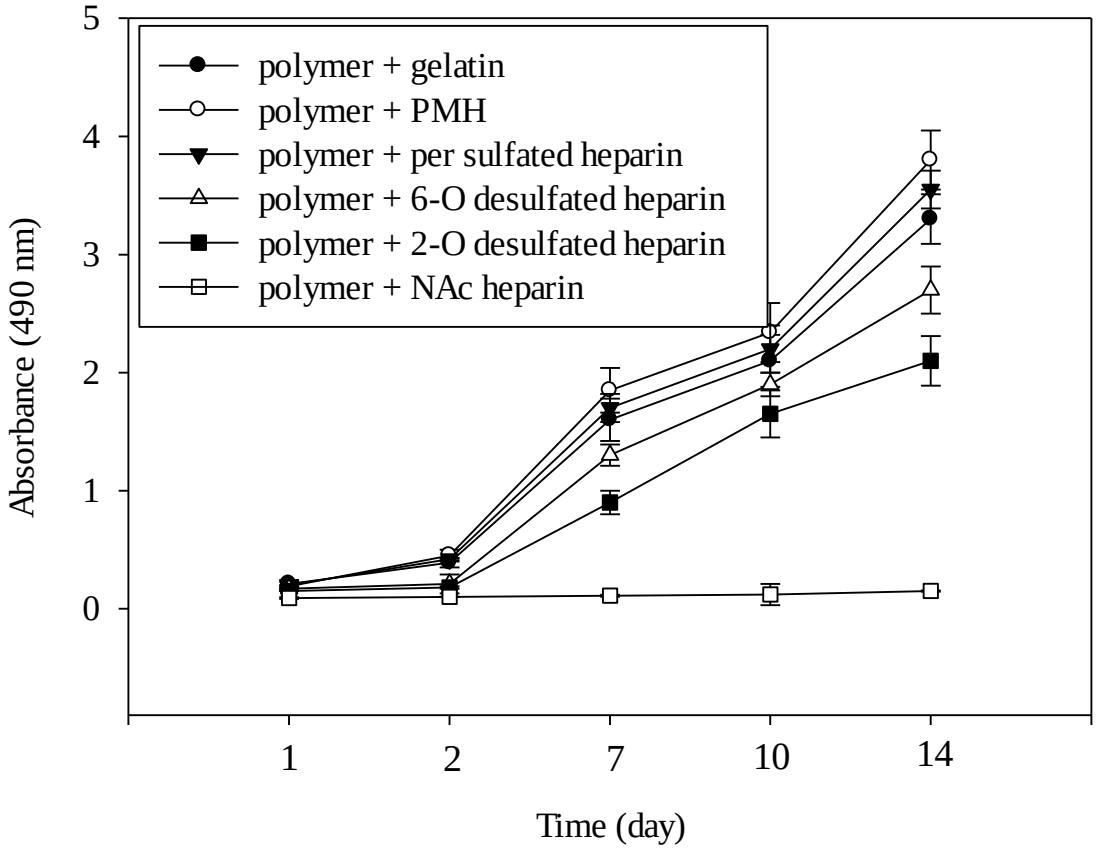

Figure 5.17 KSC-GFP proliferation on poly-Ɛ-lysine macroporous polymers altered depending on heparin structure. KSCs-GFP were seeded onto PƐL polymers after 2 h incubation with synthetic HS-mimetic heparin structures; per-sulfated, 6-O desulfated, 2-O desulfated and NAc heparin, compared to PMH and gelatine coated polymers as controls. KSC-GFP proliferation was assessed using an MTS, where metabolic activity was measured. PMH and per-sulfated heparin coatings outperformed gelatine-coated polymers, supporting faster proliferation than any other coating material. 6-O desulfated heparin-coated polymers supported more proliferation than 2-O desulfated heparin-coated polymers, but lower than per-sulfated HS. NAc heparin-coated polymers did not appear to support any proliferation up to 14 days. The experiment was repeated three times and error bars represent SEM.

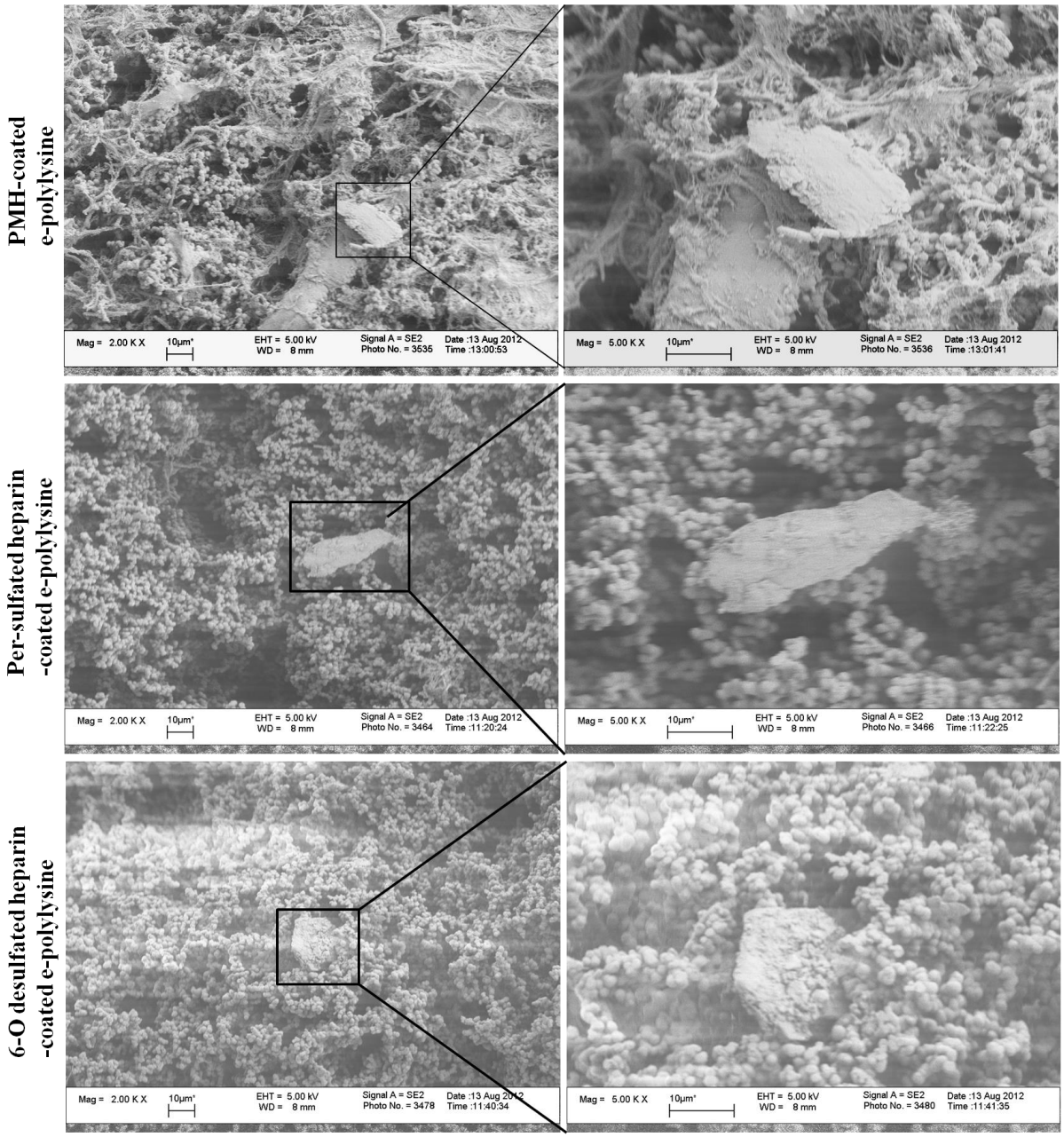

Figure 5.18 KSC-GFP-polymer interaction alters depending on the level/pattern of sulfation exhibited by the coating material; per-sulfated heparin-coated polymers support elongated KSC-GFP morphology. KSCs-GFP were seeded onto PƐL based polymers that had been coated with different synthetic heparin structures and allowed to proliferate for up to 10 days. SEM analysis was conducted in order to assess KSC-GFP morphology and interaction with polymer surface. Polymers were selected based on performance with regard to supporting the highest proliferation. Per-sulfated heparin-coating supported KSC-GFP attachment as highlighted with arrows, however, spindle-like processes are undetected. The experiment was repeated more than three times and scale bars represent 10 µm.

5.6 Discussion

The original employment of biomaterials involved petroleum-derived synthetic polymers designed to be inert without interacting with the organism (Minoura, Aiba et al. 1989), categorized by low protein absorption and weak interactions with tissues. However more recently, there has been recognition for bioactive materials and as mentioned, polymers fit this role well (Langer and Vacanti 1993; Kim and Mooney 1998; Hench and Polak 2002).

Of twelve different hydrogels synthesised using varying ratios of well established biocompatible materials (methacrylic, acrylic, PEG 360 methacrylate, PEG 526 methacrylate, 2-hydroxethyl methacrylate and M-N dimethyl acrylamide), only three displayed any evidence of supporting cell viability, adhesion or spreading. This result alone highlights the difficulties faced in identifying optimised biomaterials.

In order to assess these copolymer hydrogels, fibroblasts were initially employed. Fibroblasts represent anchorage-dependent cells, therefore adhesion and morphology not only provides indications of cell spreading behaviour, but also of polymer biocompatibility, specifically cytocompatibility. Moreover, fibroblasts are the most abundant cell in the stroma and are largely responsible for remodelling of the ECM (Grinnell 1994; Eastwood, Mudera et al. 1998).

Only methacrylic: PEG 526 methacrylate 1:1 (copolymer 3), acrylic: PEG 526 methacrylate 1:1 (copolymer 9) and acrylic: M-Ndimethylacrylamide 1:15 (copolymer 14) displayed any potential to support fibroblast adherence and expansion. Fibroblasts incubated with the remaining copolymers resulted in cells assuming a rounded morphology and were identified floating in suspension, suggesting that these polymers did not promote or support attachment. It was shown many years ago that cells settle on a favoured surface within minutes (Curtis 1964; Curtis, Forrester et al. 1983) and strong focal adhesions are seen within 24 h (van

Kooten and von Recum 1999), suggesting that these materials displayed unfavourable surface chemistries and/or topographies. Furthermore, considering, as mentioned, that fibroblast survival is dependent on adhesion, it was not surprising that of those hydrogels which caused fibroblasts to adopt a rounded unattached morphology, there was a corresponding lack of viability, measured using trypan-blue. More than 95 % of fibroblasts seeded onto hydrogel copolymers 1, 5, 6, 7, 11, 12, 13, 15 and 16 were non viable after 48 h, however, the rates of reaching complete non-viable cell populations, differed depending on the polymer surface. Where fibroblasts were identified as single floating cells (copolymers 5, 7 and 12 for example), a total unviable cell population was achieved much faster than when fibroblasts were clumped as cell aggregates initially. The instances were fibroblasts populations remained moderately viable after 24 h, were often correlated with cell aggregates. There are two forms of adhesion; cell adhesion to ECM (Harper and Juliano 1981), which is mimicked here in the case of these copolymers, or adhesion to another local cell (Harper and Juliano 1981), therefore survival of fibroblasts was perhaps prolonged via adhering to other fibroblasts.

Methacrylic: PEG 526 methacrylate 1:1 (copolymer 3), acrylic: PEG 526 methacrylate 1:1 (copolymer 9) and acrylic: M-Ndimethylacrylamide 1:15 (copolymer 14) supported KSC adhesion and cells displayed typical, elongated and fibroblast-like morphology. Fibroblast morphology has long been outlined as diverse, largely dependent on substratum (Tajima and Pinnell 1981; Tomasek, Hay et al. 1982; Olmo, Lizarbe et al. 1988), therefore it would appear that these hydrogels, which were shown to support typical fibroblast morphology, present sufficient physical and/or chemical properties, to mimic natural ECM. Acrylamide-based hydrogels have been shown to affect cardiac fibroblast morphology and adhesion, as a consequence of hydrogel stiffness and topography (Al-Haque, Miklas et al. 2012), and fibroblasts have been shown to readily polarize, characterised by long actomyosin bundles

(stress fibers) and stable edges, on rigid but not compliant acrylamides (Prager-Khoutorsky, Lichtenstein et al. 2011). Accordingly, acrylic: M-Ndimethylacrylamide 1:15 (copolymer 14), shown to support KSC elongation, could possess adequate stiffness and topographical properties, important for fibroblast polarization and response. The remaining two hydrogels shown to support KSC adhesion and spread; methacrylic: PEG 526 methacrylate 1:1 and acrylic: PEG 526 methacrylate 1:1, are similar in their building blocks; both are synthesised from PEG 526 methacrylate, and differ only in type of acrylic component (acrylic/methacrylic). PEG 526 methacrylate represents a high molecular weight component that will increase swell and has shown promise as hydrophobic drug delivery (Diramio, Kisaalita et al. 2005). However, overall analysis suggested that none of these hydrogels performed well enough to be investigated further, demonstrating the importance of selecting the correct polymer material. Wang et al., outlined precisely this, demonstrating that the choice of polymer is crucial and governs cell behaviour, showing that mesenchymal stem cells behave differently depending on material; polystyrene, polycarbonate and polyurethane stimulated distinctly different cellular responses (Wang, Ma et al.).

In this project, attention was subsequently turned to PƐL; a small homopolymer synthesised from essential amino acid L-lysine. It therefore has excellent biocompatibility and consequently is being developed in an array of biomedical applications including wound healing dressings, delivery of nanoparticles (Jin, Yu et al.) and scaffolds for 3D tissue engineering (Crompton, Goud et al. 2007). This chapter investigates more the novel acrtictecture, surface topography and cross-linking capacity of these PƐL macroporous polymers, attributed to SpeheriTech technology and novel methodology during synthesis, given that biocompatibility is already well appreciated.

SEM showed that these PƐL polymers presented a unique spherical, bead-like architecture with well-controlled porosity (Figure 5.10). It is well documented that surface topography

and polymer architecture can govern cellular behaviour, therefore porosity and the spherical nature of the polymer surface, could well underpin the cellular response identified in the work here. Alves et al., reviewed how cell behaviour can be controlled via carefully designing polymer surface properties (Alves, Pashkuleva et al.) and micro-geometries have been shown to be influential on hESC behaviour (Carlson, Florek et al.). In this chapter, mESCs appeared to congregate on the periphery of the pores and on the edges of spherical-bead like structures, and adopted an unusually rounded morphology remaining predominantly as single cells (Figure 5.18C and D). There was no evidence of cells clustering in colonies or adhering and flattening to the polymer, as one would typically identify in culture dishes, suggesting that the surface did not support this, or that the cells did not adopt this behavior given alternative cues. Similarly, in the case of KSCs-GFP seeded onto these PƐL polymers, SEM images revealed that cells nestled in the pores of the polymer and rather than spreading, as is usual for fibroblasts, and KSCs-GFP remained as single cells.

Interestingly, much research is being conducted regarding the influence of polymeric surface topographies on cell spreading, flattening and subsequent differentiation. Flattening of mesenchymal stem cells has been shown to be correlated with differentiation, according to geometric micro and nano-patterning of polymer substrates (Bucaro, Vasquez et al.; Song, Lu et al.). This is supported by another study which demonstrated that spreading of rat mesenchymal stem cells, attributed to the nanotopography of silicon columns, influenced differentiation capacity (Guvendik, Trabzon et al.), although to my knowledge, no work has been conducted with regard to mESCs specifically. Interestingly though, stiffness of a substrate (for example a stiff standard tissue culture plastic dish) has been shown to induce stress on mESCs and subsequently associated with a loss of pluripotency (Chowdhury, Li et al.). It could be that the elasticity of the PƐL, due to its hydrophobicity and swell, prevents stress-inducing cell polarization, therefore cells remain single and rounded rather than being

stimulated to flatten and potential differentiate. This suggests that the PƐL polymer is an ideal substrate for maintaining and expanding ESCs in a pluripotent (non-differentiated) state.

Aside from flattening and spreading of cells to induce differentiation, many studies have now demonstrated that surface topography can solely dictate the fate on a cell, irrespective of cell cytoskeletal shape (Chen, Villa-Diaz et al.). Mattotti et al. demonstrated that entirely synthetic PMMA substrates were able to direct the differentiation of neural progenitors using carefully patterned nanotopography (Mattotti, Alvarez et al.) in the absence of any animal-derived materials (often used in polymer bio-applications). Another study showed that roughened polymer surface topography, exploited to increase surface area: volume via solvent etching, increased the yield of human bone marrow-derived stem cells (hBMSCs) whilst stimulating controlled osteogenic differentiation, which was otherwise uncontrolled (Kumar, Waters et al.).

The response of the mESCs to the poly-Ɛ-lysine polymers identified here could potentially highlight a niche to be exploited in mESC expansion. A spherical surface cleverly generates a high surface area: volume, substantially higher than that of a flat culture dish for example, therefore expansion of mESCs in this manner could produce considerably more cells per ppopulation, whilst using the same volumes of consumables (media and growth factors supplementation for instance), than would be used when culturing mESCs on a flat, single-dimensional platform. Obviously, this would be extremely appealing commercially, since cost efficacy in the ESC field is a major factor. The use of beads and other spherical substrates with this cost-based rationale is developing in all fields of biosciences (Neurauter, Bonyhadi et al. 2007; Zhang, Zhang et al. 2009). The spherical, bead-like architecture gave rise to single mESCs often enclosed within pores and the spherical surface prevented the both mESCs and KSCs from flattening, although both cell lines did proliferate when in contact with the polymer. A rounded morphology and single-cell existence is not characteristic of

typical mESC populations however, does perhaps represent a method of expanding a pure homogenous mESC population. Currently, spontaneous differentiation is a problem in mESC cultures and hinders the isolation and expansion of pure mESC populations. Spontaneous differentiation has been shown to be induced by colony formation upon mESCs flattening (Zakany, Burg et al. 1984; Heo, Lee et al. 2005), therefore by preventing colony formation through culture with these PƐL structures, could limit spontaneous differentiation thus attaining a more pure mESC population. Many single-cell expansion systems are under investigation, with the same goal and rationale in mind – to optimise a pure cell population. One study demonstrated the use of a multi-well tissue culture plate to expand single cells; however this suffers significant inconvenience and is impractical since cell populations required dissociating and transferring to different wells over time (Greenberger, Goff et al. 2000). Taken together, the porosity and spherical, bead-like architecture could potentially represent an excellent platform for expanding single mESCs at substantially higher density than that of standard expansion methods, which are costly and limited due to spontaneous differentiation in sub-populations.

Further investigation here showed that the performance of these PƐL polymers to support KSC-GFPs could be enhanced using several different polymer modifications; a bulk material modification and a surface modification.

Bulk material modification entailed cross-linking PƐL with RGD, a well-known protein-binding motif (Ruoslahti 1996), during the polymer synthesis process. RGD has been used for several years in the biomaterials field to functionalize metals for example (Arosio, Manzoni et al.; Le Guillou-Buffello, Bareille et al. 2008) and more recently, RGD has been employed to modify biopolymers (Hersel, Dahmen et al. 2003). Examples of this include the improvement of PLGA substrates with RGD-coatings to improve in-growth of osteoblasts for bone regeneration applications (Eid, Chen et al. 2001). Similarly, the osseointegration on a

synthetic bone screw for implants, was improved using RGD coatings (Yang, He et al. 2009). In another example, RGD-coated hydrogels were shown to improve drug delivery efficacy compared to uncoated hydrogels (Chikar, Hendricks et al.) and polyurethanes engrafted with RGD motifs displayed improved adhesion and proliferation of human endothelial cells (Lin, Sun et al. 1994; Sagnella, Anderson et al. 2005). In this project, PƐL polymers cross-linked with RGD outperformed non-cross-linked polymers, since KSCs-GFP proliferated significantly more on these modified polymers, providing evidence for the importance of RGD.

A second and novel modification of these PƐL polymers entailed surface modifications using synthetic HS-mimetic compounds. PƐL coated with per-sulfated synthetic HS structures, outperformed all other coating compounds and uncoated PƐL by stimulating enhanced adherence and proliferation. Although the usage of HS and HS mimetics as a coating material is relatively unstudied, the role of heparin as a coating material for improved substrate performance is not a novel idea.

Many heparin-coated biomaterials are underpinned by the anticoagulant properties of heparin; therefore coating with heparin is often used to discourage cell adhesion, for example, in many eye-related treatments, including silicone-based intraocular implants (Fischer, Carstesen et al.) and to improve the performance of hydrogels as corneal replacements (Bourcier, Borderie et al. 1997). Heparin-coated polymer applications also include applications were a blood clot could negate the performance of the biomaterial and jeopardise the patients health, for example heparin-covered ePTFE stents for the treatment of occlusive legions in the superior femoral artery (Lensvelt, Fritschy et al.).

According to results in this chapter, the KSC-GFP response to coating materials was structure-specific, since not all coatings positively affected KSC-GFP adhesion and

proliferation; NAc-heparin coating for example, performed poorly and did not stimulate adhesion or proliferation, emphasizing the importance of sulfation for this application. Furthermore, and interestingly, per-sulfated heparin coating outperformed other compounds with regard to stimulating KSC-GFP proliferation. Collectively these results highlight the importance of ionic cell-surface interactions often exemplified by many cell-polymer investigations (Lee, Jung et al. 1994); the results suggest that in general that providing an adequate degree of sulfation is presented to the KSC-GFP cells, specific sulfation patterns may be less important. Having said that, the results indicate that the loss of specific sulfates can induce different cell responses. 2-O desulfated polymers performed the worst of all the modified heparin coatings, therefore suggesting that 2-O sulfation is important for cell adhesion. Conversely, 6-O desulfated heparin coating performed the best of the compounds with reduced sulfation, suggesting that 6-O sulfation is not required for KSC-GFP adhesion and proliferation. It is interesting to note that 6-O desulfated heparin is typically low in activity to activate signalling by heparin-dependent growth factors such as FGFs (Guimond and Turnbull 1999). This property might be exploited in maintaining ESCs in maintaining ESCs in a pluripotent state.

Since per-sulfated heparin coatings performed comparable to PMH-coatings and outperformed gelatin-coating, using these synthetic compounds could represent an attractive alternative to protein coatings. Gelatine-coatings represent the hallmark method of enhancing cell adhesion, for example a study relevant to this project showed that PƐL cross-linked with gelatin performed better than non-crosslinked PƐL in human epithelisation (Reno, Rizzi et al. 2012). Although none of the other HS-mimetic modified heparins (desulfated) outperformed gelatine-coated polymers, according to the criteria of the limited studies carried out here, they may well provide interesting compounds for manipulating other aspects of ESC behaviour, especially selective differentiation, and this remains to be explored in future studies.

6. General Discussion and Future Directions

Major findings from this project can be summarised as follows:

- The culture conditions used to expand mESCs significantly influences their developmental potential when subsequently cultured in suspension as EBs;
    - A lack of serum during 2D expansion is correlated with disrupted EEE differentiation and uncharacteristic BM in subsequent EBs
    - A lack of feeders during pre-EB culture conditions affects mESC EB cavitation
- HS-deficient mESCs were successfully expanded in 2D culture providing that serum was present, however, subsequent EB behaviour was substantially disrupted compared to normal E14 EBs
    - Soluble and cell-surface HS structures differed depending on culture conditions (those with serum and feeders displayed different HS structures)
- Poly-Ɛ-lysine represents a promising biomaterial for mESC expansion
    - PƐL was shown to support attachment and proliferation.
        - This was further enhanced by surface treatment with synthetic HS structures
        - Per-sulfated HS structures out-performed other synthetic HS structures

One caveat is that this project only investigated the behaviour of the E14 mESC line (Hooper, Hardy et al. 1987), and it is therefore possible that the observed responses of these cells to the different culture conditions are specific to this line. Every mESC line is genetically distinct, according to time of derivation and specific culture conditions used initially during derivation. Accordingly, results described throughout this project should be reproduced using several different mESC lines. E14 mESCs are a well established line, derived from the

embryo of a mouse at embryonic day 4.5 (Hooper, Hardy et al. 1987), however other mESCs are widely available, including D3 (Gossler, Doetschman et al. 1986), AB1 (McMahon and Bradley 1990), MBL-5 (Pease, Braghetta et al. 1990), EFC-3 (Nichols, Evans et al. 1990), BL/6-3 (Ledermann and Burki 1991), J1 (Li, Bestor et al. 1992), P55 (Johnson, Spiegelman et al. 1992) and TT2 (Saga, Yagi et al. 1992).

Like many ESC projects, this project has employed mESCs as a model for human embryonic stem cells (hESCs), owing to their long established history, 40 years post-derivation. Taking a wider view, although the results emphasize the requirement for serum, feeders and HS during successful mESC propagation, reproducing this data with several hESC lines is absolutely necessary before hESC-related conclusions can be made. Nonetheless, the underlying message from this project is very likely transferable to hESCs; the need for a xeno-free, standardised system for ESCs expansion is a critical if hESCs are to fulfil their potential.

Within the hESC field, depending on the laboratory and the nature of the research, expansion of these cells can occur with or without animal-derived products. Of those groups using animal products for the isolation and expansion of hESCs, problems related to downstream clinical applications are extensive. The use of serum and animal-derived products gives rise to variability in the culture system and thus presents huge challenges in long-term, robust hESC cultures. Furthermore, and perhaps more importantly, xenogenic factors used in these undefined hESC cultures may predispose hESCs towards a specific lineage, rendering their pluripotency. Ultimately, the importance of hESCs that have not contacted any animal-derived components except those of human origin is critical for the eventual drug therapy and disease treatment in humans.

Several groups and private companies are investigating the expansion of hESCs in defined animal-free culture systems. Human-derived cells have been shown to effectively replace mouse-derived fibroblasts; Richards et al., reviewed many different primary cells for the support of hESCs, of which fetal muscle, fetal skin, neonatal foreskin fibroblasts and adult human fallopian tube epithelial cells were shown to maintain hESCs over 20 passages (Richards, Fong et al. 2002). Feeder-free conditions have also been achieved using MEF-CM, although often these systems employ Matrigel or fibronectin as dish coatings (Mallon, Park et al. 2006), and in some cases additional animal-derived growth factors, FGF for example, to compensate for the lack of feeders (Amit, Shariki et al. 2004; Amit 2007). Whilst the omission/replacement of animal-derived feeder layers for hESC maintenance is becoming attainable, the omission of FBS during hESC cultures is proving more difficult, which is in agreement with results in this project. This was demonstrated by one study, which showed that the replacement of FBS with human serum was unsuccessful in maintaining hESC in culture (Richards, Tan et al. 2003) emphasizing the importance of FBS during hESC propagation, albeit via undefined mechanisms. Furthermore, serum-free hESC cultures often require the presence of a fibroblast layer, exemplified by one study which showed successful expansion of hESCs for more than 10 passages was achieved providing human placenta fibroblasts were present (Genbacev, Krtolica et al. 2005). Similarly, serum-free commercially available media (StemPro and mTeSR1) were shown to support several hESC lines for more than 10 passages, although human-derived feeder layers were required in these serum-free systems (Chin, Padmanabhan et al.).

Despite the progress being made in defining an animal-free hESC culture system, what remains unclear is the impact these systems have on the downstream differentiation capacity, which is a key emphasis of the project here. According to results in this project, pre-culture conditions for the maintenance of mESCs significantly affect the behaviour of mESCs in a

subsequent EB model. It would be interesting to identify if this is reproducible in hESCs and furthermore, the results support the views of some sceptics who suggest that exploiting hESCs in any clinical application is dangerous until the effects of prior culture conditions are known for hESCs (Mannello and Tonti 2007).

Regardless, many companies are hoping to exploit niche, by synthesizing artificial substrates (using synthetic polymers for example) to replace and mimic natural ECM proteins, and this is a goal of our CASE partner, SpheriTech. Providing we can dispel the need for animal-derived products in hESC scale-up via the employment of these synthetic substrates, which now appears feasible, hESCs offer great promise in studying development and also treating disease states (including Parkinson's, Alzheimer's, diabetes, blindness and cancers for example). RoslinCell, a regenerative-medicine based company based in Edinburgh, UK, has demonstrated the generation of clinical-grade hESCs using a xeno-free substrate, now commercially available via Invitrogen (CELLStart, Invitrogen). Currently, an array of different synthetic substrates are being investigated as alternatives (some of which have been outlined in this project), applicable to both 2D cell expansion and 3D tissue engineering application (Carletti, Motta et al.) restricted by biocompatibility, compatibility with sterilisation techniques, manufacture expense, scale-ability and efficacy in defined/xeno-free culture conditions. Hydrogels and macroporous polymers represent a large proportion of this research, and as the results in this project have suggested, substrate performance can be enhanced using chemical modifications in order to mimic protein-binding motifs, RGD for example, or to improve cell adhesion and proliferation. The latter was demonstrated with HS-based compound surface treatments, since the performance of poly-Ɛ-lysine macroporous polymers shown to support ESC and KSC attachment was enhanced further by the coating of polymers with synthetic HS-compounds.

Despite the efforts to solve the problems that surround hESCs, a controversial debate engulfs this research, largely attributed to the nature of hESCs derivation and the potential by-products, therapeutic cloning for example, and there are significant restrictions in hESC research.

hESC lines, as outlined previously, are derived from a fertilized egg that has been grown *in vitro* for 5-6 days to form a blastocyst, of which the 30-40 inner most cells (ICM) are removed and expanded *in vitro*. It is the origin of hESCs, which antagonises a 'scientists versus ethicists' debate. A classic model for this is the governing of hESC research in the USA. George W. Bush's government epitomised a 'pro-life' view and in 2001, although National Health Institute (NIH) funding for already-underway hESC research (permitted by Clinton's government in 1998) was allowed to continue, new and additional NIH funding for the derivation and long-term study of hESC lines was prohibited. This was thought by many in the science community to hinder the potential for any hESC-based theraputics. Such a bold, science-threatening, political decision, was largely based on religious views towards abortion, underpinned by the belief that an embryo has the same moral status as an adult since 'human life begins at conception', and therefore removing the ICM from a blastocyst of an aborted fetus to derive a hESC line, amounts to murder (1995; de Wert and Mummery 2003). By 2009, Obama's government had revoked these rules, supposedly 'removing barriers in hESC research' and allowing hESC to largely be governed by NIH rather than politics . Politics therefore no doubt affects hESC research, outlined by one study which showed that the rate of hESC-based publications by US-based authors specifically declined over the 2008-2010 period and accordingly, non-US authors are shown to publish more frequently and at a significantly higher rate.

Nonetheless, the first clinical trial (phase I and II) using hESCs was approved by the FDA in November 2010, for the treatment of Stargardt's Macula Dystrophy (SMD). SMD is a

hereditary disease, and a common form of macular degeneration detected in young adults. SMD is categorised by the death of retinal pigmented epithelial cells (RPEs) in the central region of the retina in the back of the eye (macula), and therefore loss of central vision persists, until eventual blindness occurs. The trial, funded by Massachusetts-based company, Advanced Cell Technology (ACT) is due to end in October 2013 and currently, two blind patients have been treated. The first report of this study is extremely positive, outlining no signs of hyperproliferation, tumourigenicity, ectopic tissue formation, or apparent rejection and encouragingly, one patient described visualising colour (Huang, McAlinden et al.; Schwartz, Hubschman et al.).

As in this clinical trial, the potential of hESCs to be used in any clinical application is governed by the FDA (or equivalent bodies in other non-US countries) and encompasses three costly, exhaustive clinical trial stages; phase I, II and III. *Phase I* exists to determine if the treatment/application is safe for the human model and typically includes low numbers of participants over relatively short time periods. *Phase II* involves more participants and seeks to determine the efficacy of the treatment whilst the final *phase III,* establishes if this new treatment is superior compared to current treatments and typically involves many thousands of participants, usually in a double-blind study more longer-term.

Several privately funded companies, unregulated by government bodies, are currently monitoring an array of other hESC-based clinical trials, all at different phases. One US-based company Geron, completed a phase I trial in October 2012, investigating the use of hESCs for spinal cord injury, where human embryonic stem cells have been directed to become neural progenitor cells (GRNOPC1). GRNOPC1 cells have been injected directly into a patient suffering with a spinal cord injury 7-14 days post injury, based on the hypothesis that these injected cells will contribute to healing. In Europe, on-going clinical trials are also underway. Glasgow University, Scotland, has been monitoring a phase I clinical trial since

June 2010, relating to the usage of a human neural stem cell line (CTX cells) derived from human fetal tissue, produced by the company ReNeuron, to treat stroke patients (Mack). All participants, disabled as a result of an ischemic stroke, have successfully been injected directly into the brain with CTX cells and a report in August 2011 outlined that no adverse effects had been observed. Furthermore, reductions in neurological impairment and spasticity were observed in all participants compared with pre-treatment. According to the success, a phase II trial is expected to begin mid-2013. Balgrist University, Zurich, Switzerland, is involved with a phase I clinical trial using human CNS stem cells (HuCNS-SCs) as a treatment for spinal-cord injury since December 2010, in conjunction with the company Stem Cells Inc.

Much of the promise of hESCs however, lie in the potential for 'personalised medicines', as a consequence of somatic nuclear cell transfer (SNCT) using hESCs (Byrne, Pedersen et al. 2007; French, Adams et al. 2008). However, the concept of 'personalised medicine' is now more recently governed by the field of induced pluirpotent stem cells (iPSCs) and interest in SNCT has therefore decreased.

iPSCs, as their name suggests, are pluripotent stem cells which have been derived from non-pluripotent stem cells and represent a favourable source of pluripotent stem cells, given that ethical issues associated with hESCs do not exist in iPSCs. In 2006, Yamanakas' laboratory at Kyoto University, Japan, optimised conditions that enabled the 'reprogramming' of murine fibroblasts to express a 'embryonic stem cell-like' fate, via forcing these adult cells to express genes important for embryionic stem cell self-renewal, initially Oct4, Sox2, Klf and c-Myc (Yamanaka and Takahashi 2006). Since then other groups have optimised the conditions for iPSCs using a combination of different embryonic stem cell genes (Takahashi, Okita et al. 2007; Yu, Vodyanik et al. 2007) and for many different species, including rat (Liao, Cui et al. 2009) and monkey (Liu, Zhu et al. 2008). The employment of iPSCs as a medical tool is

therefore extremely promising, but like hESCs, some issues still need to be addressed. Foremost, the efficacy of creating iPSCs must be greatly improved, as must the understanding of the mechanisms which govern reprogramming. However, aside from their origins, iPSCs can be categorized as hESCs, and therefore have an equally exciting future.

In conclusion, the employment of hESCs clinically undoubtably represents an area with massive potential if the science community can resolve some key issues and the political community can refrain from over-regulating this field of research (Owen-Smith, Scott et al.). However, insights into the effect of culture conditions on the downstream behaviour of mESCs as outlined in this project, is one of many concerns surrounding the usage of hESCs in the clinic. This could pave the way for iPSCs, which has just as much promise but conveniently does not harbour the burden of ethical hysteria and associated restrictions, and can practically be generated from a patients own cells.

Future directions

The results from this project, like most research, led to an array of further questions, which represent potential future directions and follow-up experimental lines, some of which include:

- Are the effects identified in the serum-free, feeder-free conditions irreversible?

Serum-free conditioned mESCs were shown in results here, to display severely uncharacteristic behavior, recognised during 2D monolayer culture but most obvious during 3D expansion in suspension culture upon the removal of LIF. For example, serum-free conditioned EBs appeared to lack the ability to transport the laminin trimer after synthesis (LamA1 was down-regulated compared to EBs conditioned in normal mESC cultures (with serum and with feeders), whilst LamB1 remained unchanged between conditions). But how is this linked to a lack of serum? Are these effects irreversible? If these cells were placed back

into normal culture conditions (i.e. in the presence of serum), would downstream self renewal, differentiation and BM functionality be rescued? If yes, a further question to confirm the link between serum and HS would be whether, if these defective mESCs are then replated back in conditions containing serum and heparitinase enzymes/chlorate-treated cells (STO feeders and/or mESCs) are the effects still rescued (via digesting soluble HS/cell surface HS)? Furthermore, medium collected from serum-free mESC cultures displayed highly sulfated HS structures (comparable to heparin) and high levels of sulfated HS were detected on the cell-surface (mESCs cultured in the presence of serum with/without feeders displayed typically low levels of low sulfated HS structrues). This raises the question; do these conditions stimulate mESCs to synthesise more highly sulfated HS, which effects subsequent mESC self renewal and differentiation? Or conversely, do these serum-free culture conditions repress the ability of the mESCs to 'fine-tune' HS structure for example by the action of Sulfs to remove 6-O-sulphation, and in fact there was a lack of *Sulf2* in serum-free conditioned mESCs. Mechanistically, it is possible that serum-free culture conditons lack adequate support for FGF-signalling, known to be crucial in mESC differentiation. This could be directly linked to inadequately sulfated species of HS, as a consequence of aberrant culture conditions.

- PMH was shown to rescue defects due to a lack of serum, how and why?

PMH, a homogenously sulfated HS-model molecule, was shown to rescue the lack of serum. What signaling pathway was this linked to; perhaps FGF signalling? One could use western blots to assess activation of FGF signaling (FGFR phosphorylation) and other downstream events, for their dependence on culture condition. ELISA could be employed also to detect activation of FGF through specific receptor dependence.

- Since PMH was shown to rescue uncharacteristic mESC phenotype (attributed to a lack of serum), one further question would be, can exogenous HS mimetics reproduce this affect?

If yes, what structures can substitute for serum and can they be produced in animal-free systems? Recent studies have shown that defined heparin/HS structures can be produced both chemically (Schworer, Zubkova et al.) and chemoenzymatically (Deangelis, Liu et al.), supporting the view that tractable production of non-animal derived heparanoids is possible.

- Poly-Ɛ-lysine was shown to support mESCs, and this action was further enhanced with synthetic HS structure surface coatings. Can this approach be optimised further?
  - Can this system be used to control and direct differentiation of ESCs and is this dependent on specific HS structures?

Overall, it is clear that the work presented here has opened up a number of avenues for potential exploitation of HS in stem cell self-renewal and differentiation, to support applications for regenerative medicine. It is hoped that in the future such applications can be realised in practice as new treatments for the benefit of patients with conditions such as Alzeimers and Parkinson's disease.

References

"Human embryonic stem cell research in the US: time for change?" Nat Cell Biol **12**(7): 627.

(1995). "The inhuman use of human beings: a statement on embryo research." First Things **49**: 17-21.

Abildgaard, U. (1968). "Highly purified antithrombin 3 with heparin cofactor activity prepared by disc electrophoresis." Scand J Clin Lab Invest **21**(1): 89-91.

Abraham, S., M. J. Riggs, et al. (2010). "Characterization of human fibroblast-derived extracellular matrix components for human pluripotent stem cell propagation." Acta Biomater **6**(12): 4622-33.

Ai, X., A. T. Do, et al. (2003). "QSulf1 remodels the 6-O sulfation states of cell surface heparan sulfate proteoglycans to promote Wnt signaling." J Cell Biol **162**(2): 341-51.

Aitola, M., P. Carlsson, et al. (2000). "Forkhead transcription factor FoxF2 is expressed in mesodermal tissues involved in epithelio-mesenchymal interactions." Dev Dyn **218**(1): 136-49.

Akerlund, M., V. Carmignac, et al. (2009). "Laminin alpha1 domains LG4-5 are essential for the complete differentiation of visceral endoderm." Cell Tissue Res **338**(1): 129-37.

Al-Haque, S., J. W. Miklas, et al. (2012). "Hydrogel Substrate Stiffness and Topography Interact to Induce Contact Guidance in Cardiac Fibroblasts." Macromol Biosci.

Allen, B. L., M. S. Filla, et al. (2001). "Role of heparan sulfate as a tissue-specific regulator of FGF-4 and FGF receptor recognition." J Cell Biol **155**(5): 845-58.

Almodovar, J., S. Bacon, et al. (2010). "Polysaccharide-based polyelectrolyte multilayer surface coatings can enhance mesenchymal stem cell response to adsorbed growth factors." Biomacromolecules **11**(10): 2629-39.

Altankov, G., F. Grinnell, et al. (1996). "Studies on the biocompatibility of materials: fibroblast reorganization of substratum-bound fibronectin on surfaces varying in wettability." J Biomed Mater Res **30**(3): 385-91.

Alves, N. M., I. Pashkuleva, et al. "Controlling cell behavior through the design of polymer surfaces." Small **6**(20): 2208-20.

Ambrosio, L., R. De Santis, et al. (1998). "Composite hydrogels for implants." Proc Inst Mech Eng H **212**(2): 93-9.

Amenta, P. S., C. C. Clark, et al. (1983). "Deposition of fibronectin and laminin in the basement membrane of the rat parietal yolk sac: immunohistochemical and biosynthetic studies." J Cell Biol **96**(1): 104-11.

Amit, M. (2007). "Feeder-layer free culture system for human embryonic stem cells." Methods Mol Biol **407**: 11-20.

Amit, M., C. Shariki, et al. (2004). "Feeder layer- and serum-free culture of human embryonic stem cells." Biol Reprod **70**(3): 837-45.

Anderson, C., S. Thorsteinsdottir, et al. (2009). "Sonic hedgehog-dependent synthesis of laminin alpha1 controls basement membrane assembly in the myotome." Development **136**(20): 3495-504.

Ang, S. L., R. A. Conlon, et al. (1994). "Positive and negative signals from mesoderm regulate the expression of mouse Otx2 in ectoderm explants." Development **120**(10): 2979-89.

Arica, M. Y., D. Tuglu, et al. (2008). "Preparation and characterization of infection-resistant antibiotics-releasing hydrogels rods of poly[hydroxyethyl methacrylate-co-(poly(ethylene glycol)-methacrylate]: biomedical application in a novel rabbit penile prosthesis model." J Biomed Mater Res B Appl Biomater **86**(1): 18-28.

Arman, E., R. Haffner-Krausz, et al. (1998). "Targeted disruption of fibroblast growth factor (FGF) receptor 2 suggests a role for FGF signaling in pregastrulation mammalian development." Proc Natl Acad Sci U S A **95**(9): 5082-7.

Arosio, D., L. Manzoni, et al. "Cyclic RGD functionalized gold nanoparticles for tumor targeting." Bioconjug Chem **22**(4): 664-72.

Artus, J., J. J. Panthier, et al. (2010). "A role for PDGF signaling in expansion of the extra-embryonic endoderm lineage of the mouse blastocyst." Development **137**(20): 3361-72.

Artus, J., A. Piliszek, et al. (2010). "The primitive endoderm lineage of the mouse blastocyst: Sequential transcription factor activation and regulation of differentiation by Sox17." Dev Biol.

Ashikari-Hada, S., H. Habuchi, et al. (2004). "Characterization of growth factor-binding structures in heparin/heparan sulfate using an octasaccharide library." J Biol Chem **279**(13): 12346-54.

Aumailley, M., L. Bruckner-Tuderman, et al. (2005). "A simplified laminin nomenclature." Matrix Biol **24**(5): 326-32.

Aumailley, M., M. Pesch, et al. (2000). "Altered synthesis of laminin 1 and absence of basement membrane component deposition in (beta)1 integrin-deficient embryoid bodies." J Cell Sci **113 Pt 2**: 259-68.

Austria, M. R. and J. R. Couchman (1991). "Enhanced assembly of basement membrane matrix by endodermal cells in response to fibronectin substrata." J Cell Sci **99 (Pt 2)**: 443-51.

Aviezer, D., M. Safran, et al. (1999). "Heparin differentially regulates the interaction of fibroblast growth factor-4 with FGF receptors 1 and 2." Biochem Biophys Res Commun **263**(3): 621-6.

Avivi, A., A. Yayon, et al. (1993). "A novel form of FGF receptor-3 using an alternative exon in the immunoglobulin domain III." FEBS Lett **330**(3): 249-52.

Baldwin, R. J., G. B. ten Dam, et al. (2008). "A developmentally regulated heparan sulfate epitope defines a subpopulation with increased blood potential during mesodermal differentiation." Stem Cells **26**(12): 3108-18.

Ballas, N., C. Grunseich, et al. (2005). "REST and its corepressors mediate plasticity of neuronal gene chromatin throughout neurogenesis." Cell **121**(4): 645-57.

Bame, K. J. (1993). "Release of heparan sulfate glycosaminoglycans from proteoglycans in Chinese hamster ovary cells does not require proteolysis of the core protein." J Biol Chem **268**(27): 19956-64.

Barrias, C. C., M. C. Martins, et al. (2009). "The correlation between the adsorption of adhesive proteins and cell behaviour on hydroxyl-methyl mixed self-assembled monolayers." Biomaterials **30**(3): 307-16.

Battaglia, C., U. Mayer, et al. (1992). "Basement-membrane heparan sulfate proteoglycan binds to laminin by its heparan sulfate chains and to nidogen by sites in the protein core." Eur J Biochem **208**(2): 359-66.

Beck, K., I. Hunter, et al. (1990). "Structure and function of laminin: anatomy of a multidomain glycoprotein." FASEB J **4**(2): 148-60.

Beddington, R. S. and E. J. Robertson (1999). "Axis development and early asymmetry in mammals." Cell **96**(2): 195-209.

Beenken, A. and M. Mohammadi (2009). "The FGF family: biology, pathophysiology and therapy." Nat Rev Drug Discov **8**(3): 235-53.

Behrendtsen, O. and Z. Werb (1997). "Metalloproteinases regulate parietal endoderm differentiating and migrating in cultured mouse embryos." Dev Dyn **208**(2): 255-65.

Bellaiche, Y., I. The, et al. (1998). "Tout-velu is a Drosophila homologue of the putative tumour suppressor EXT-1 and is needed for Hh diffusion." Nature **394**(6688): 85-8.

Bellairs, R. (1961). "Cell death in chick embryos as studied by electron microscopy." J Anat **95**(Pt 1): 54-60 3.

Benoit, D. S. and K. S. Anseth (2005). "Heparin functionalized PEG gels that modulate protein adsorption for hMSC adhesion and differentiation." Acta Biomater **1**(4): 461-70.

Bernfield, M., M. Gotte, et al. (1999). "Functions of cell surface heparan sulfate proteoglycans." Annu Rev Biochem **68**: 729-77.

Bettiol, E., L. Sartiani, et al. (2007). "Fetal bovine serum enables cardiac differentiation of human embryonic stem cells." Differentiation **75**(8): 669-81.

Bezakova, G. and M. A. Ruegg (2003). "New insights into the roles of agrin." Nat Rev Mol Cell Biol **4**(4): 295-308.

Binari, R. C., B. E. Staveley, et al. (1997). "Genetic evidence that heparin-like glycosaminoglycans are involved in wingless signaling." Development **124**(13): 2623-32.

Boeuf, H., C. Hauss, et al. (1997). "Leukemia inhibitory factor-dependent transcriptional activation in embryonic stem cells." J Cell Biol **138**(6): 1207-17.

Borgens, R. B. and D. Bohnert (2001). "Rapid recovery from spinal cord injury after subcutaneously administered polyethylene glycol." J Neurosci Res **66**(6): 1179-86.
Bourcier, T., V. Borderie, et al. (1997). "[Cultures of corneal epithelium on hydrogel for synthetic epikeratoplasty]." J Fr Ophtalmol **20**(6): 444-52.
Bourillot, P. Y., I. Aksoy, et al. (2009). "Novel STAT3 target genes exert distinct roles in the inhibition of mesoderm and endoderm differentiation in cooperation with Nanog." Stem Cells **27**(8): 1760-71.
Bourillot, P. Y. and P. Savatier "Kruppel-like transcription factors and control of pluripotency." BMC Biol **8**: 125.
Brafman, D. A., C. W. Chang, et al. (2010). "Long-term human pluripotent stem cell self-renewal on synthetic polymer surfaces." Biomaterials **31**(34): 9135-44.
Brauer, P. R., K. M. Keller, et al. (1990). "Concurrent reduction in the sulfation of heparan sulfate and basement membrane assembly in a cell model system." Development **110**(3): 805-13.
Brennan, J., D. P. Norris, et al. (2002). "Nodal activity in the node governs left-right asymmetry." Genes Dev **16**(18): 2339-44.
Brickman, Y. G., V. Nurcombe, et al. (1998). "Structural comparison of fibroblast growth factor-specific heparan sulfates derived from a growing or differentiating neuroepithelial cell line." Glycobiology **8**(5): 463-71.
Brill, G., N. Kahane, et al. (1995). "Epithelial-mesenchymal conversion of dermatome progenitors requires neural tube-derived signals: characterization of the role of Neurotrophin-3." Development **121**(8): 2583-94.
Brook, F. A. and R. L. Gardner (1997). "The origin and efficient derivation of embryonic stem cells in the mouse." Proc Natl Acad Sci U S A **94**(11): 5709-12.
Bucaro, M. A., Y. Vasquez, et al. "Fine-tuning the degree of stem cell polarization and alignment on ordered arrays of high-aspect-ratio nanopillars." ACS Nano **6**(7): 6222-30.
Buhr, N., C. Carapito, et al. (2007). "Proteome analysis of the culture environment supporting undifferentiated mouse embryonic stem and germ cell growth." Electrophoresis **28**(10): 1615-23.
Bullock, S. L., J. M. Fletcher, et al. (1998). "Renal agenesis in mice homozygous for a gene trap mutation in the gene encoding heparan sulfate 2-sulfotransferase." Genes Dev **12**(12): 1894-906.
Busse, M., A. Feta, et al. (2007). "Contribution of EXT1, EXT2, and EXTL3 to heparan sulfate chain elongation." J Biol Chem **282**(45): 32802-10.
Byrne, J. A., D. A. Pedersen, et al. (2007). "Producing primate embryonic stem cells by somatic cell nuclear transfer." Nature **450**(7169): 497-502.
Cai, K. Q., C. D. Capo-Chichi, et al. (2008). "Dynamic GATA6 expression in primitive endoderm formation and maturation in early mouse embryogenesis." Dev Dyn **237**(10): 2820-9.
Cai, L., J. Lu, et al. (2012). "Optimal poly(L-lysine) grafting density in hydrogels for promoting neural progenitor cell functions." Biomacromolecules **13**(5): 1663-74.
Cai, L., J. Lu, et al. (2012). "Promoting nerve cell functions on hydrogels grafted with poly(L-lysine)." Biomacromolecules **13**(2): 342-9.
Campbell, P., F. W. Shen, et al. (2004). "Biologic and tribologic considerations of alternative bearing surfaces." Clin Orthop Relat Res(418): 98-111.
Cano-Gauci, D. F., H. H. Song, et al. (1999). "Glypican-3-deficient mice exhibit developmental overgrowth and some of the abnormalities typical of Simpson-Golabi-Behmel syndrome." J Cell Biol **146**(1): 255-64.
Carletti, E., A. Motta, et al. "Scaffolds for tissue engineering and 3D cell culture." Methods Mol Biol **695**: 17-39.
Carlin, B., R. Jaffe, et al. (1981). "Entactin, a novel basal lamina-associated sulfated glycoprotein." J Biol Chem **256**(10): 5209-14.
Carlson, A. L., C. A. Florek, et al. "Microfibrous substrate geometry as a critical trigger for organization, self-renewal, and differentiation of human embryonic stem cells within synthetic 3-dimensional microenvironments." FASEB J **26**(8): 3240-51.
Carlsson, P., J. Presto, et al. (2008). "Heparin/heparan sulfate biosynthesis: processive formation of N-sulfated domains." J Biol Chem **283**(29): 20008-14.

Casu, B. and U. Lindahl (2001). "Structure and biological interactions of heparin and heparan sulfate." Adv Carbohydr Chem Biochem **57**: 159-206.
Chambers, I., D. Colby, et al. (2003). "Functional expression cloning of Nanog, a pluripotency sustaining factor in embryonic stem cells." Cell **113**(5): 643-55.
Chambers, I. and S. R. Tomlinson (2009). "The transcriptional foundation of pluripotency." Development **136**(14): 2311-22.
Chang, Y., L. McLandsborough, et al. (2012). "Cationic antimicrobial (epsilon-polylysine)-anionic polysaccharide (pectin) interactions: influence of polymer charge on physical stability and antimicrobial efficacy." J Agric Food Chem **60**(7): 1837-44.
Chapman, D. L., I. Agulnik, et al. (1996). "Tbx6, a mouse T-Box gene implicated in paraxial mesoderm formation at gastrulation." Dev Biol **180**(2): 534-42.
Chappard, D., C. Alexandre, et al. (1986). "Improved stability of a purified glycol methacrylate preparation: comments." Stain Technol **61**(3): 185-6.
Chappard, D., J. L. Laurent, et al. (1982). "A simple and reliable method for purifying glycol methacrylate for histopathological studies." Acta Histochem **71**(1): 95-102.
Chen, A. C., Y. L. Lee, et al. (2012). "Study of transforming growth factor alpha for the maintenance of human embryonic stem cells." Cell Tissue Res.
Chen, Q. Z., C. T. Wong, et al. (2004). "Strengthening mechanisms of bone bonding to crystalline hydroxyapatite in vivo." Biomaterials **25**(18): 4243-54.
Chen, W., L. G. Villa-Diaz, et al. "Nanotopography influences adhesion, spreading, and self-renewal of human embryonic stem cells." ACS Nano **6**(5): 4094-103.
Chen, W. Y. and G. Abatangelo (1999). "Functions of hyaluronan in wound repair." Wound Repair Regen **7**(2): 79-89.
Chen, Y., X. Li, et al. (2000). "Fibroblast growth factor (FGF) signaling through PI 3-kinase and Akt/PKB is required for embryoid body differentiation." Oncogene **19**(33): 3750-6.
Cheung, C. Y. (1997). "Vascular endothelial growth factor: possible role in fetal development and placental function." J Soc Gynecol Investig **4**(4): 169-77.
Chiao, E., P. Fisher, et al. (2002). "Overgrowth of a mouse model of the Simpson-Golabi-Behmel syndrome is independent of IGF signaling." Dev Biol **243**(1): 185-206.
Chikar, J. A., J. L. Hendricks, et al. "The use of a dual PEDOT and RGD-functionalized alginate hydrogel coating to provide sustained drug delivery and improved cochlear implant function." Biomaterials **33**(7): 1982-90.
Chin, A. C., J. Padmanabhan, et al. "Defined and serum-free media support undifferentiated human embryonic stem cell growth." Stem Cells Dev **19**(6): 753-61.
Chlupac, J., E. Filova, et al. (2009). "Blood vessel replacement: 50 years of development and tissue engineering paradigms in vascular surgery." Physiol Res **58 Suppl 2**: S119-39.
Chng, Z., L. Vallier, et al. (2011). "Activin/nodal signaling and pluripotency." Vitam Horm **85**: 39-58.
Chowdhury, F., Y. Li, et al. "Soft substrates promote homogeneous self-renewal of embryonic stem cells via downregulating cell-matrix tractions." PLoS One **5**(12): e15655.
Ciardelli, G., B. Cioni, et al. (2004). "Acrylic polymeric nanospheres for the release and recognition of molecules of clinical interest." Biosens Bioelectron **20**(6): 1083-90.
Clayton, A., J. Thomas, et al. (2001). "Cell surface heparan sulfate proteoglycans control the response of renal interstitial fibroblasts to fibroblast growth factor-2." Kidney Int **59**(6): 2084-94.
Cole, G. J. and W. Halfter (1996). "Agrin: an extracellular matrix heparan sulfate proteoglycan involved in cell interactions and synaptogenesis." Perspect Dev Neurobiol **3**(4): 359-71.
Conley, B. J., S. Ellis, et al. (2007). "BMPs regulate differentiation of a putative visceral endoderm layer within human embryonic stem-cell-derived embryoid bodies." Biochem Cell Biol **85**(1): 121-32.
Conlon, F. L., K. M. Lyons, et al. (1994). "A primary requirement for nodal in the formation and maintenance of the primitive streak in the mouse." Development **120**(7): 1919-28.
Cooper, A. R. and H. A. MacQueen (1983). "Subunits of laminin are differentially synthesized in mouse eggs and early embryos." Dev Biol **96**(2): 467-71.
Cormier, J. T., N. I. zur Nieden, et al. (2006). "Expansion of undifferentiated murine embryonic stem cells as aggregates in suspension culture bioreactors." Tissue Eng **12**(11): 3233-45.

Cornelison, D. D., S. A. Wilcox-Adelman, et al. (2004). "Essential and separable roles for Syndecan-3 and Syndecan-4 in skeletal muscle development and regeneration." Genes Dev **18**(18): 2231-6.
Corpet, D. E., G. Parnaud, et al. (2000). "Consistent and fast inhibition of colon carcinogenesis by polyethylene glycol in mice and rats given various carcinogens." Cancer Res **60**(12): 3160-4.
Costell, M., E. Gustafsson, et al. (1999). "Perlecan maintains the integrity of cartilage and some basement membranes." J Cell Biol **147**(5): 1109-22.
Coucouvanis, E. and G. R. Martin (1995). "Signals for death and survival: a two-step mechanism for cavitation in the vertebrate embryo." Cell **83**(2): 279-87.
Crompton, K. E., J. D. Goud, et al. (2007). "Polylysine-functionalised thermoresponsive chitosan hydrogel for neural tissue engineering." Biomaterials **28**(3): 441-9.
Curran, J. M., R. Chen, et al. "Nanoscale definition of substrate materials to direct human adult stem cells towards tissue specific populations." J Mater Sci Mater Med **21**(3): 1021-9.
Curtis, A. S. (1964). "The Mechanism of Adhesion of Cells to Glass. A Study by Interference Reflection Microscopy." J Cell Biol **20**: 199-215.
Curtis, A. S., J. V. Forrester, et al. (1983). "Adhesion of cells to polystyrene surfaces." J Cell Biol **97**(5 Pt 1): 1500-6.
D'Souza, S. E., M. H. Ginsberg, et al. (1991). "Arginyl-glycyl-aspartic acid (RGD): a cell adhesion motif." Trends Biochem Sci **16**(7): 246-50.
Dagalv, A., K. Holmborn, et al. (2011). "Lowered expression of heparan sulfate/heparin biosynthesis enzyme N-deacetylase/n-sulfotransferase 1 results in increased sulfation of mast cell heparin." J Biol Chem **286**(52): 44433-40.
Dalton, P. D., L. Flynn, et al. (2002). "Manufacture of poly(2-hydroxyethyl methacrylate-co-methyl methacrylate) hydrogel tubes for use as nerve guidance channels." Biomaterials **23**(18): 3843-51.
Damjanov, I., A. Damjanov, et al. (1987). Production of teratocarcinomas from embryo transplanted to extra-uterine sites. Teratocarcinomas and embryonic stem cells. E. J. Robertson. Oxford. Washington DC, IRL Press**:** 1-18.
David, G., X. M. Bai, et al. (1992). "Developmental changes in heparan sulfate expression: in situ detection with mAbs." J Cell Biol **119**(4): 961-75.
Davidson, J. A. (1993). "Characteristics of metal and ceramic total hip bearing surfaces and their effect on long-term ultra high molecular weight polyethylene wear." Clin Orthop Relat Res(294): 361-78.
Davidson, J. A. and G. Schwartz (1987). "Wear, creep, and frictional heat of femoral implant articulating surfaces and the effect on long-term performance--Part I, A review." J Biomed Mater Res **21**(A3 Suppl): 261-85.
De Felici, M., D. Farini, et al. (2009). "In or out stemness: comparing growth factor signalling in mouse embryonic stem cells and primordial germ cells." Curr Stem Cell Res Ther **4**(2): 87-97.
de Wert, G. and C. Mummery (2003). "Human embryonic stem cells: research, ethics and policy." Hum Reprod **18**(4): 672-82.
Deangelis, P. L., J. Liu, et al. "Chemoenzymatic synthesis of glycosaminoglycans: Re-creating, re-modeling and re-designing nature's longest or most complex carbohydrate chains." Glycobiology.
Delehedde, M., E. Deudon, et al. (1996). "Heparan sulfate proteoglycans play a dual role in regulating fibroblast growth factor-2 mitogenic activity in human breast cancer cells." Exp Cell Res **229**(2): 398-406.
Denker, H. W. (2004). "Early human development: new data raise important embryological and ethical questions relevant for stem cell research." Naturwissenschaften **91**(1): 1-21.
Dhoot, G. K., M. K. Gustafsson, et al. (2001). "Regulation of Wnt signaling and embryo patterning by an extracellular sulfatase." Science **293**(5535): 1663-6.
Diecke, S., A. Quiroga-Negreira, et al. (2008). "FGF2 signaling in mouse embryonic fibroblasts is crucial for self-renewal of embryonic stem cells." Cells Tissues Organs **188**(1-2): 52-61.
Dietrich, C. P., H. B. Nader, et al. (1983). "Structural differences of heparan sulfates according to the tissue and species of origin." Biochem Biophys Res Commun **111**(3): 865-71.

Diramio, J. A., W. S. Kisaalita, et al. (2005). "Poly(ethylene glycol) methacrylate/dimethacrylate hydrogels for controlled release of hydrophobic drugs." Biotechnol Prog **21**(4): 1281-8.
Dluz, S. M., S. Higashiyama, et al. (1993). "Heparin-binding epidermal growth factor-like growth factor expression in cultured fetal human vascular smooth muscle cells. Induction of mRNA levels and secretion of active mitogen." J Biol Chem **268**(24): 18330-4.
Dockter, J. L. (2000). "Sclerotome induction and differentiation." Curr Top Dev Biol **48**: 77-127.
Dockter, J. L. and C. P. Ordahl (1998). "Determination of sclerotome to the cartilage fate." Development **125**(11): 2113-24.
Doetschman, T. C., H. Eistetter, et al. (1985). "The in vitro development of blastocyst-derived embryonic stem cell lines: formation of visceral yolk sac, blood islands and myocardium." J Embryol Exp Morphol **87**: 27-45.
Donovan, P. J. and M. P. de Miguel (2003). "Turning germ cells into stem cells." Curr Opin Genet Dev **13**(5): 463-71.
dos Santos, K. S., J. F. Coelho, et al. (2006). "Synthesis and characterization of membranes obtained by graft copolymerization of 2-hydroxyethyl methacrylate and acrylic acid onto chitosan." Int J Pharm **310**(1-2): 37-45.
Douthwaite, J. A., T. S. Johnson, et al. (1999). "Effects of transforming growth factor-beta1 on renal extracellular matrix components and their regulating proteins." J Am Soc Nephrol **10**(10): 2109-19.
Dow, K. E. and R. J. Riopelle (1990). "Specific effects of ethanol on neurite-promoting proteoglycans of neuronal origin." Brain Res **508**(1): 40-5.
Dubrulle, J. and O. Pourquie (2004). "fgf8 mRNA decay establishes a gradient that couples axial elongation to patterning in the vertebrate embryo." Nature **427**(6973): 419-22.
Dudley, A. T., K. M. Lyons, et al. (1995). "A requirement for bone morphogenetic protein-7 during development of the mammalian kidney and eye." Genes Dev **9**(22): 2795-807.
Duffield, J. S., K. M. Park, et al. (2005). "Restoration of tubular epithelial cells during repair of the postischemic kidney occurs independently of bone marrow-derived stem cells." J Clin Invest **115**(7): 1743-55.
Duffy, D. M. (1990). "Silicone: a critical review." Adv Dermatol **5**: 93-107; discussion 108-9.
Duffy, D. M. (2005). "Liquid silicone for soft tissue augmentation." Dermatol Surg **31**(11 Pt 2): 1530-41.
Duncan, S. A., K. Manova, et al. (1994). "Expression of transcription factor HNF-4 in the extraembryonic endoderm, gut, and nephrogenic tissue of the developing mouse embryo: HNF-4 is a marker for primary endoderm in the implanting blastocyst." Proc Natl Acad Sci U S A **91**(16): 7598-602.
Duncan, S. A., A. Nagy, et al. (1997). "Murine gastrulation requires HNF-4 regulated gene expression in the visceral endoderm: tetraploid rescue of Hnf-4(-/-) embryos." Development **124**(2): 279-87.
Dziadek, M. (1978). "Modulation of alphafetoprotein synthesis in the early postimplantation mouse embryo." J Embryol Exp Morphol **46**: 135-46.
Dziadek, M. and R. Timpl (1985). "Expression of nidogen and laminin in basement membranes during mouse embryogenesis and in teratocarcinoma cells." Dev Biol **111**(2): 372-82.
Eastwood, M., V. C. Mudera, et al. (1998). "Effect of precise mechanical loading on fibroblast populated collagen lattices: morphological changes." Cell Motil Cytoskeleton **40**(1): 13-21.
Eid, K., E. Chen, et al. (2001). "Effect of RGD coating on osteocompatibility of PLGA-polymer disks in a rat tibial wound." J Biomed Mater Res **57**(2): 224-31.
Eiselleova, L., K. Matulka, et al. (2009). "A complex role for FGF-2 in self-renewal, survival, and adhesion of human embryonic stem cells." Stem Cells **27**(8): 1847-57.
Ekblom, P., P. Lonai, et al. (2003). "Expression and biological role of laminin-1." Matrix Biol **22**(1): 35-47.
Elling, U., C. Klasen, et al. (2006). "Murine inner cell mass-derived lineages depend on Sall4 function." Proc Natl Acad Sci U S A **103**(44): 16319-24.
Engler, A. J., S. Sen, et al. (2006). "Matrix elasticity directs stem cell lineage specification." Cell **126**(4): 677-89.
Engvall, E. (1995). "Structure and function of basement membranes." Int J Dev Biol **39**(5): 781-7.

Eom, K. D., J. S. Kim, et al. (2006). "A facile synthesis and physical properties of nano-sized dendritic alpha,epsilon-poly(L-lysine)s for the delivery of nucleic acids." J Nanosci Nanotechnol **6**(11): 3532-8.
Eom, K. D., S. M. Park, et al. (2007). "Dendritic alpha,epsilon-poly(L-lysine)s as delivery agents for antisense oligonucleotides." Pharm Res **24**(8): 1581-9.
Era, T. "Mesoderm cell development from ES cells." Methods Mol Biol **636**: 87-103.
Eriksson, A. E., L. S. Cousens, et al. (1991). "Three-dimensional structure of human basic fibroblast growth factor." Proc Natl Acad Sci U S A **88**(8): 3441-5.
Esko, J. D. and U. Lindahl (2001). "Molecular diversity of heparan sulfate." J Clin Invest **108**(2): 169-73.
Esner, M., J. Pachernik, et al. (2002). "Targeted disruption of fibroblast growth factor receptor-1 blocks maturation of visceral endoderm and cavitation in mouse embryoid bodies." Int J Dev Biol **46**(6): 817-25.
Evans, M. J. and M. H. Kaufman (1981). "Establishment in culture of pluripotential cells from mouse embryos." Nature **292**(5819): 154-6.
Evseenko, D., Y. Zhu, et al. "Mapping the first stages of mesoderm commitment during differentiation of human embryonic stem cells." Proc Natl Acad Sci U S A **107**(31): 13742-7.
Faham, S., R. E. Hileman, et al. (1996). "Heparin structure and interactions with basic fibroblast growth factor." Science **271**(5252): 1116-20.
Faham, S., R. J. Linhardt, et al. (1998). "Diversity does make a difference: fibroblast growth factor-heparin interactions." Curr Opin Struct Biol **8**(5): 578-86.
Faherty, S., M. T. Kane, et al. (2005). "Self-renewal and differentiation of mouse embryonic stem cells as measured by Oct 4 gene expression: effects of lif, serum-free medium, retinoic acid, and dbcAMP." In Vitro Cell Dev Biol Anim **41**(10): 356-63.
Farach-Carson, M. C., J. T. Hecht, et al. (2005). "Heparan sulfate proteoglycans: key players in cartilage biology." Crit Rev Eukaryot Gene Expr **15**(1): 29-48.
Fehling, H. J., G. Lacaud, et al. (2003). "Tracking mesoderm induction and its specification to the hemangioblast during embryonic stem cell differentiation." Development **130**(17): 4217-27.
Feldman, B., W. Poueymirou, et al. (1995). "Requirement of FGF-4 for postimplantation mouse development." Science **267**(5195): 246-9.
Feraud, O., N. Debili, et al. (2007). "Cavitation of embryoid bodies requires optimal oxidative phosphorylation and AIF." Cell Death Differ **14**(2): 385-7.
Feyerabend, T. B., J. P. Li, et al. (2006). "Heparan sulfate C5-epimerase is essential for heparin biosynthesis in mast cells." Nat Chem Biol **2**(4): 195-6.
Feyzi, E., F. Lustig, et al. (1997). "Characterization of heparin and heparan sulfate domains binding to the long splice variant of platelet-derived growth factor A chain." J Biol Chem **272**(9): 5518-24.
Feyzi, E., E. Trybala, et al. (1997). "Structural requirement of heparan sulfate for interaction with herpes simplex virus type 1 virions and isolated glycoprotein C." J Biol Chem **272**(40): 24850-7.
Filliers, M., K. Goossens, et al. (2012). "Gene expression profiling of pluripotency and differentiation-related markers in cat oocytes and preimplantation embryos." Reprod Fertil Dev **24**(5): 691-703.
Fischer, S., D. Carstesen, et al. "Surface-modified silicone foils for intraocular implantation." Graefes Arch Clin Exp Ophthalmol **250**(6): 823-7.
Fisher, M. C., Y. Li, et al. (2006). "Heparan sulfate proteoglycans including syndecan-3 modulate BMP activity during limb cartilage differentiation." Matrix Biol **25**(1): 27-39.
Flaim, C. J., D. Teng, et al. (2008). "Combinatorial signaling microenvironments for studying stem cell fate." Stem Cells Dev **17**(1): 29-39.
Folpe, A. L., T. Veikkola, et al. (2000). "Vascular endothelial growth factor receptor-3 (VEGFR-3): a marker of vascular tumors with presumed lymphatic differentiation, including Kaposi's sarcoma, kaposiform and Dabska-type hemangioendotheliomas, and a subset of angiosarcomas." Mod Pathol **13**(2): 180-5.
Ford-Perriss, M., S. E. Guimond, et al. (2002). "Variant heparan sulfates synthesized in developing mouse brain differentially regulate FGF signaling." Glycobiology **12**(11): 721-7.

Forsberg, E. and L. Kjellen (2001). "Heparan sulfate: lessons from knockout mice." J Clin Invest **108**(2): 175-80.
Forsberg, M., K. Holmborn, et al. (2012). "Undersulfation of heparan sulfate restricts differentiation potential of mouse embryonic stem cells." J Biol Chem **287**(14): 10853-62.
Frame, M. C. and G. J. Inman (2008). "NCAM is at the heart of reciprocal regulation of E-cadherin- and integrin-mediated adhesions via signaling modulation." Dev Cell **15**(4): 494-6.
Frankenberg, S., F. Gerbe, et al. (2011). "Primitive endoderm differentiates via a three-step mechanism involving Nanog and RTK signaling." Dev Cell **21**(6): 1005-13.
French, A. J., C. A. Adams, et al. (2008). "Development of human cloned blastocysts following somatic cell nuclear transfer with adult fibroblasts." Stem Cells **26**(2): 485-93.
Fuerer, C., S. J. Habib, et al. (2010). "A study on the interactions between heparan sulfate proteoglycans and Wnt proteins." Dev Dyn **239**(1): 184-90.
Futaki, S., Y. Hayashi, et al. (2004). "Sox7 plays crucial roles in parietal endoderm differentiation in F9 embryonal carcinoma cells through regulating Gata-4 and Gata-6 expression." Mol Cell Biol **24**(23): 10492-503.
Galliher, P. M., C. L. Cooney, et al. (1981). "Heparinase production by Flavobacterium heparinum." Appl Environ Microbiol **41**(2): 360-5.
Galvin, K. E., E. D. Travis, et al. (2010). "Nodal signaling regulates the bone morphogenic protein pluripotency pathway in mouse embryonic stem cells." J Biol Chem **285**(26): 19747-56.
Gandhi, N. S. and R. L. Mancera (2008). "The structure of glycosaminoglycans and their interactions with proteins." Chem Biol Drug Des **72**(6): 455-82.
Gardner, R. L. (1982). "Investigation of cell lineage and differentiation in the extraembryonic endoderm of the mouse embryo." J Embryol Exp Morphol **68**: 175-98.
Gautier, C., P. J. Lopez, et al. (2007). "Influence of poly-L-lysine on the biomimetic growth of silica tubes in confined media." J Colloid Interface Sci **309**(1): 44-8.
Genbacev, O., A. Krtolica, et al. (2005). "Serum-free derivation of human embryonic stem cell lines on human placental fibroblast feeders." Fertil Steril **83**(5): 1517-29.
Genethliou, N., E. Panayiotou, et al. (2009). "Spatially distinct functions of PAX6 and NKX2.2 during gliogenesis in the ventral spinal cord." Biochem Biophys Res Commun **382**(1): 69-73.
Gengrinovitch, S., B. Berman, et al. (1999). "Glypican-1 is a VEGF165 binding proteoglycan that acts as an extracellular chaperone for VEGF165." J Biol Chem **274**(16): 10816-22.
Gersdorff, N., M. Muller, et al. (2005). "Basement membrane composition in the early mouse embryo day 7." Dev Dyn **233**(3): 1140-8.
Ginis, I., Y. Luo, et al. (2004). "Differences between human and mouse embryonic stem cells." Dev Biol **269**(2): 360-80.
Gitay-Goren, H., S. Soker, et al. (1992). "The binding of vascular endothelial growth factor to its receptors is dependent on cell surface-associated heparin-like molecules." J Biol Chem **267**(9): 6093-8.
Goda, T. and K. Ishihara (2006). "Soft contact lens biomaterials from bioinspired phospholipid polymers." Expert Rev Med Devices **3**(2): 167-74.
Goetz, A. K., B. Scheffler, et al. (2006). "Temporally restricted substrate interactions direct fate and specification of neural precursors derived from embryonic stem cells." Proc Natl Acad Sci U S A **103**(29): 11063-8.
Gomes, P. B. and C. P. Dietrich (1982). "Distribution of heparin and other sulfated glycosaminoglycans in vertebrates." Comp Biochem Physiol B **73**(4): 857-63.
Gordon, P. B., G. Conn, et al. (1985). "Glycosaminoglycan production in cultures of early and late passage human endothelial cells: the influence of an anionic endothelial cell growth factor and the extracellular matrix." J Cell Physiol **125**(3): 596-607.
Gorsi, B. and S. E. Stringer (2007). "Tinkering with heparan sulfate sulfation to steer development." Trends Cell Biol **17**(4): 173-7.
Gossler, A., T. Doetschman, et al. (1986). "Transgenesis by means of blastocyst-derived embryonic stem cell lines." Proc Natl Acad Sci U S A **83**(23): 9065-9.
Goto, A., M. Aoki, et al. (2001). "alpha-, beta- or gamma-chain-specific RNA interference of laminin assembly in Drosophila Kc167 cells." Biochem J **360**(Pt 1): 167-72.

Gotoh, N., K. Manova, et al. (2005). "The docking protein FRS2alpha is an essential component of multiple fibroblast growth factor responses during early mouse development." Mol Cell Biol **25**(10): 4105-16.
Gotte, M., A. M. Joussen, et al. (2002). "Role of syndecan-1 in leukocyte-endothelial interactions in the ocular vasculature." Invest Ophthalmol Vis Sci **43**(4): 1135-41.
Grabel, L. B. and T. D. Watts (1987). "The role of extracellular matrix in the migration and differentiation of parietal endoderm from teratocarcinoma embryoid bodies." J Cell Biol **105**(1): 441-8.
Grave, B. (2000). "Localization of TGF-Bs and perlecan in mouse skull development." Ann R Australas Coll Dent Surg **15**: 352-6.
Greenberger, J. S., J. P. Goff, et al. (2000). "Expansion of hematopoietic stem cells in vitro as a model system for human tissue engineering." Orthop Clin North Am **31**(3): 499-510.
Grindley, J. C., D. R. Davidson, et al. (1995). "The role of Pax-6 in eye and nasal development." Development **121**(5): 1433-42.
Grinnell, F. (1978). "Cellular adhesiveness and extracellular substrata." Int Rev Cytol **53**: 65-144.
Grinnell, F. (1994). "Fibroblasts, myofibroblasts, and wound contraction." J Cell Biol **124**(4): 401-4.
Gritsman, K., W. S. Talbot, et al. (2000). "Nodal signaling patterns the organizer." Development **127**(5): 921-32.
Grover, G. N., J. Lam, et al. (2012). "Biocompatible Hydrogels by Oxime Click Chemistry." Biomacromolecules.
Grunert, M., V. Nurcombe, et al. (2008). "Stem cell fate decisions: the role of heparan sulfate in the control of autocrine and paracrine signals." Curr Stem Cell Res Ther **3**(1): 1-8.
Guillot, P. V., H. T. Cook, et al. (2008). "Transplantation of human fetal mesenchymal stem cells improves glomerulopathy in a collagen type I alpha 2-deficient mouse." J Pathol **214**(5): 627-36.
Guimond, S. E. and J. E. Turnbull (1999). "Fibroblast growth factor receptor signalling is dictated by specific heparan sulphate saccharides." Curr Biol **9**(22): 1343-6.
Gunatillake, P. A. and R. Adhikari (2003). "Biodegradable synthetic polymers for tissue engineering." Eur Cell Mater **5**: 1-16; discussion 16.
Guo, G., J. Yang, et al. (2009). "Klf4 reverts developmentally programmed restriction of ground state pluripotency." Development **136**(7): 1063-9.
Gustafsson, Y., J. Haag, et al. (2012). "Viability and proliferation of rat MSCs on adhesion protein-modified PET and PU scaffolds." Biomaterials **33**(32): 8094-103.
Guvendik, S., L. Trabzon, et al. "The effect of Si nano-columns in 2-D and 3-D on cellular behaviour: nanotopography-induced CaP deposition from differentiating mesenchymal stem cells." J Nanosci Nanotechnol **11**(10): 8896-902.
Hacker, U., X. Lin, et al. (1997). "The Drosophila sugarless gene modulates Wingless signaling and encodes an enzyme involved in polysaccharide biosynthesis." Development **124**(18): 3565-73.
Hacker, U., K. Nybakken, et al. (2005). "Heparan sulphate proteoglycans: the sweet side of development." Nat Rev Mol Cell Biol **6**(7): 530-41.
Hadari, Y. R., N. Gotoh, et al. (2001). "Critical role for the docking-protein FRS2 alpha in FGF receptor-mediated signal transduction pathways." Proc Natl Acad Sci U S A **98**(15): 8578-83.
Hadjantonakis, A. K., E. Pisano, et al. (2008). "Tbx6 regulates left/right patterning in mouse embryos through effects on nodal cilia and perinodal signaling." PLoS One **3**(6): e2511.
Hall, J., G. Guo, et al. (2009). "Oct4 and LIF/Stat3 additively induce Kruppel factors to sustain embryonic stem cell self-renewal." Cell Stem Cell **5**(6): 597-609.
Hamazaki, T., S. M. Kehoe, et al. (2006). "The Grb2/Mek pathway represses Nanog in murine embryonic stem cells." Mol Cell Biol **26**(20): 7539-49.
Hamazaki, T., M. Oka, et al. (2004). "Aggregation of embryonic stem cells induces Nanog repression and primitive endoderm differentiation." J Cell Sci **117**(Pt 23): 5681-6.
Harmer, N. J. (2006). "Insights into the role of heparan sulphate in fibroblast growth factor signalling." Biochem Soc Trans **34**(Pt 3): 442-5.

Harper, P. A. and R. L. Juliano (1981). "Fibronectin-independent adhesion of fibroblasts to the extracellular matrix: mediation by a high molecular weight membrane glycoprotein." J Cell Biol **91**(3 Pt 1): 647-53.
Harper, P. A. and R. L. Juliano (1981). "Two distinct mechanisms of fibroblast adhesion." Nature **290**(5802): 136-8.
Haugen, P. K., P. C. Letourneau, et al. (1992). "A cell-surface heparan sulfate proteoglycan mediates neural cell adhesion and spreading on a defined sequence from the C-terminal cell and heparin binding domain of fibronectin, FN-C/H II." J Neurosci **12**(7): 2597-608.
Hay, D. C., L. Sutherland, et al. (2004). "Oct-4 knockdown induces similar patterns of endoderm and trophoblast differentiation markers in human and mouse embryonic stem cells." Stem Cells **22**(2): 225-35.
Hayashi, Y., M. K. Furue, et al. (2007). "Integrins regulate mouse embryonic stem cell self-renewal." Stem Cells **25**(12): 3005-15.
He, W., Z. Ma, et al. (2005). "Fabrication of collagen-coated biodegradable polymer nanofiber mesh and its potential for endothelial cells growth." Biomaterials **26**(36): 7606-15.
Heath, J. K. and A. G. Smith (1988). "Regulatory factors of embryonic stem cells." J Cell Sci Suppl **10**: 257-66.
Heimke, G., S. Leyen, et al. (2002). "Knee arthoplasty: recently developed ceramics offer new solutions." Biomaterials **23**(7): 1539-51.
Helledie, T., C. Dombrowski, et al. (2011). "Heparan sulfate enhances the self-renewal and therapeutic potential of mesenchymal stem cells from human adult bone marrow." Stem Cells Dev.
Hench, L. L. and J. M. Polak (2002). "Third-generation biomedical materials." Science **295**(5557): 1014-7.
Heng, C., O. Lefebvre, et al. (2011). "Functional role of laminin alpha1 chain during cerebellum development." Cell Adh Migr **5**(6): 480-9.
Heo, J., J. S. Lee, et al. (2005). "Spontaneous differentiation of mouse embryonic stem cells in vitro: characterization by global gene expression profiles." Biochem Biophys Res Commun **332**(4): 1061-9.
Hernandez-Garcia, D., S. Castro-Obregon, et al. (2008). "Cell death activation during cavitation of embryoid bodies is mediated by hydrogen peroxide." Exp Cell Res **314**(10): 2090-9.
Herrmann, B. G. (1992). "Action of the Brachyury gene in mouse embryogenesis." Ciba Found Symp **165**: 78-86; discussion 86-91.
Herrmann, B. G. and A. Kispert (1994). "The T genes in embryogenesis." Trends Genet **10**(8): 280-6.
Hersel, U., C. Dahmen, et al. (2003). "RGD modified polymers: biomaterials for stimulated cell adhesion and beyond." Biomaterials **24**(24): 4385-415.
Hey, A. W., C. A. Browne, et al. (1987). "Fetal sheep serum contains a high molecular weight insulin-like growth factor (IGF) binding protein that is acid stable and specific for IGF-II." Endocrinology **121**(6): 1975-84.
Higuchi, Y., N. Shiraki, et al. (2010). "Synthesized basement membranes direct the differentiation of mouse embryonic stem cells into pancreatic lineages." J Cell Sci **123**(Pt 16): 2733-42.
Hinderer, U. T. (1991). "Nasal base, maxillary, and infraorbital implants--alloplastic." Clin Plast Surg **18**(1): 87-105.
Hiraki, J., T. Ichikawa, et al. (2003). "Use of ADME studies to confirm the safety of epsilon-polylysine as a preservative in food." Regul Toxicol Pharmacol **37**(2): 328-40.
Hirayama, C., M. Sakata, et al. (1999). "Preparation of poly(epsilon-lysine) adsorbents and application to selective removal of lipopolysaccharides." J Chromatogr B Biomed Sci Appl **721**(2): 187-95.
Hirsinger, E., D. Duprez, et al. (1997). "Noggin acts downstream of Wnt and Sonic Hedgehog to antagonize BMP4 in avian somite patterning." Development **124**(22): 4605-14.
Hogan, B. L., G. Horsburgh, et al. (1986). "Small eyes (Sey): a homozygous lethal mutation on chromosome 2 which affects the differentiation of both lens and nasal placodes in the mouse." J Embryol Exp Morphol **97**: 95-110.
Hogan, B. L. and R. Tilly (1981). "Cell interactions and endoderm differentiation in cultured mouse embryos." J Embryol Exp Morphol **62**: 379-94.

Holley, R. J., C. E. Pickford, et al. (2011). "Influencing hematopoietic differentiation of mouse embryonic stem cells using soluble heparin and heparan sulfate saccharides." J Biol Chem **286**(8): 6241-52.
Holmborn, K., J. Ledin, et al. (2004). "Heparan sulfate synthesized by mouse embryonic stem cells deficient in NDST1 and NDST2 is 6-O-sulfated but contains no N-sulfate groups." J Biol Chem **279**(41): 42355-8.
Holst, C. R., H. Bou-Reslan, et al. (2007). "Secreted sulfatases Sulf1 and Sulf2 have overlapping yet essential roles in mouse neonatal survival." PLoS One **2**(6): e575.
Hooper, M., K. Hardy, et al. (1987). "HPRT-deficient (Lesch-Nyhan) mouse embryos derived from germline colonization by cultured cells." Nature **326**(6110): 292-5.
Horak, D., J. Kroupova, et al. (2004). "Poly(2-hydroxyethyl methacrylate)-based slabs as a mouse embryonic stem cell support." Biomaterials **25**(22): 5249-60.
Hosseinkhani, H., M. Hosseinkhani, et al. (2008). "DNA nanoparticles encapsulated in 3D tissue-engineered scaffolds enhance osteogenic differentiation of mesenchymal stem cells." J Biomed Mater Res A **85**(1): 47-60.
Hsieh, Y. C., P. Intawicha, et al. (2011). "LIF and FGF cooperatively support stemness of rabbit embryonic stem cells derived from parthenogenetically activated embryos." Cell Reprogram **13**(3): 241-55.
Hu, Z., C. Wang, et al. (2009). "NDST1-dependent heparan sulfate regulates BMP signaling and internalization in lung development." J Cell Sci **122**(Pt 8): 1145-54.
Huang, C. C., D. H. Hall, et al. (2003). "Laminin alpha subunits and their role in C. elegans development." Development **130**(14): 3343-58.
Huang, J., C. McAlinden, et al. "Embryonic stem-cell-derived retinal pigment epithelial cells for macular degeneration." Lancet **379**(9831): 2050; author reply 2050-1.
Huang, Y. C., C. C. Huang, et al. (2007). "Surface modification and characterization of chitosan or PLGA membrane with laminin by chemical and oxygen plasma treatment for neural regeneration." J Biomed Mater Res A **82**(4): 842-51.
Huber, M., P. Heiduschka, et al. (1998). "Modification of glassy carbon surfaces with synthetic laminin-derived peptides for nerve cell attachment and neurite growth." J Biomed Mater Res **41**(2): 278-88.
Ifandi, V. and M. Al-Rubeai (2003). "Stable transfection of CHO cells with the c-myc gene results in increased proliferation rates, reduces serum dependency, and induces anchorage independence." Cytotechnology **41**(1): 1-10.
Igarashi, M., P. W. Finch, et al. (1998). "Characterization of recombinant human fibroblast growth factor (FGF)-10 reveals functional similarities with keratinocyte growth factor (FGF-7)." J Biol Chem **273**(21): 13230-5.
Inman, K. E. and K. M. Downs (2006). "Localization of Brachyury (T) in embryonic and extraembryonic tissues during mouse gastrulation." Gene Expr Patterns **6**(8): 783-93.
Inoue, S., C. P. Leblond, et al. (1983). "Ultrastructure of Reichert's membrane, a multilayered basement membrane in the parietal wall of the rat yolk sac." J Cell Biol **97**(5 Pt 1): 1524-37.
Iozzo, R. V., I. R. Cohen, et al. (1994). "The biology of perlecan: the multifaceted heparan sulphate proteoglycan of basement membranes and pericellular matrices." Biochem J **302 (Pt 3)**: 625-39.
Irie, A., H. Habuchi, et al. (2003). "Heparan sulfate is required for bone morphogenetic protein-7 signaling." Biochem Biophys Res Commun **308**(4): 858-65.
Ishiguro, K., K. Kadomatsu, et al. (2001). "Syndecan-4 deficiency increases susceptibility to kappa-carrageenan-induced renal damage." Lab Invest **81**(4): 509-16.
Ishiguro, K., K. Kadomatsu, et al. (2000). "Syndecan-4 deficiency impairs the fetal vessels in the placental labyrinth." Dev Dyn **219**(4): 539-44.
Ishihara, M., Y. Saito, et al. (2000). "Heparin-carrying polystyrene to mediate cellular attachment and growth via interaction with growth factors." J Biomed Mater Res **50**(2): 144-52.
Ito, Y., M. Kajihara, et al. (1991). "Materials for enhancing cell adhesion by immobilization of cell-adhesive peptide." J Biomed Mater Res **25**(11): 1325-37.
Ivanova, N., R. Dobrin, et al. (2006). "Dissecting self-renewal in stem cells with RNA interference." Nature **442**(7102): 533-8.

Jackson, R. A., S. Murali, et al. (2007). "Heparan sulfate regulates the anabolic activity of MC3T3-E1 preosteoblast cells by induction of Runx2." J Cell Physiol **210**(1): 38-50.
Jain, A. K., K. Allton, et al. (2012). "p53 regulates cell cycle and microRNAs to promote differentiation of human embryonic stem cells." PLoS Biol **10**(2): e1001268.
Jakeman, L. B., M. Armanini, et al. (1993). "Developmental expression of binding sites and messenger ribonucleic acid for vascular endothelial growth factor suggests a role for this protein in vasculogenesis and angiogenesis." Endocrinology **133**(2): 848-59.
James, R. G. and T. M. Schultheiss (2005). "Bmp signaling promotes intermediate mesoderm gene expression in a dose-dependent, cell-autonomous and translation-dependent manner." Dev Biol **288**(1): 113-25.
Jayabalan, M. (1995). "Sterilization and reprocessing of materials and medical devices--reusability." J Biomater Appl **10**(1): 97-112.
Jiang, J., Y. S. Chan, et al. (2008). "A core Klf circuitry regulates self-renewal of embryonic stem cells." Nat Cell Biol **10**(3): 353-60.
Jiao, X., P. C. Billings, et al. (2007). "Heparan sulfate proteoglycans (HSPGs) modulate BMP2 osteogenic bioactivity in C2C12 cells." J Biol Chem **282**(2): 1080-6.
Jin, H., Y. Yu, et al. "Delivery of MicroRNA-10b with Polylysine Nanoparticles for Inhibition of Breast Cancer Cell Wound Healing." Breast Cancer (Auckl) **6**: 9-19.
Johnson, C. E., B. E. Crawford, et al. (2007). "Essential alterations of heparan sulfate during the differentiation of embryonic stem cells to Sox1-enhanced green fluorescent protein-expressing neural progenitor cells." Stem Cells **25**(8): 1913-23.
Johnson, R. S., B. M. Spiegelman, et al. (1992). "Pleiotropic effects of a null mutation in the c-fos proto-oncogene." Cell **71**(4): 577-86.
Jokimaa, V., P. Inki, et al. (1998). "Expression of syndecan-1 in human placenta and decidua." Placenta **19**(2-3): 157-63.
Jones, C. M., M. R. Kuehn, et al. (1995). "Nodal-related signals induce axial mesoderm and dorsalize mesoderm during gastrulation." Development **121**(11): 3651-62.
Joy, A., D. M. Cohen, et al. (2011). "Control of surface chemistry, substrate stiffness, and cell function in a novel terpolymer methacrylate library." Langmuir **27**(5): 1891-9.
Joza, N., S. A. Susin, et al. (2001). "Essential role of the mitochondrial apoptosis-inducing factor in programmed cell death." Nature **410**(6828): 549-54.
Jozefczuk, J., K. Drews, et al. (2012). "Preparation of mouse embryonic fibroblast cells suitable for culturing human embryonic and induced pluripotent stem cells." J Vis Exp(64).
Kadlecova, Z., L. Baldi, et al. (2012). "Comparative Study on the In Vitro Cytotoxicity of Linear, Dendritic, and Hyperbranched Polylysine Analogues." Biomacromolecules.
Kaksonen, M., I. Pavlov, et al. (2002). "Syndecan-3-deficient mice exhibit enhanced LTP and impaired hippocampus-dependent memory." Mol Cell Neurosci **21**(1): 158-72.
Kale, S., A. Karihaloo, et al. (2003). "Bone marrow stem cells contribute to repair of the ischemically injured renal tubule." J Clin Invest **112**(1): 42-9.
Kallunki, P. and K. Tryggvason (1992). "Human basement membrane heparan sulfate proteoglycan core protein: a 467-kD protein containing multiple domains resembling elements of the low density lipoprotein receptor, laminin, neural cell adhesion molecules, and epidermal growth factor." J Cell Biol **116**(2): 559-71.
Kamimura, K., M. Fujise, et al. (2001). "Drosophila heparan sulfate 6-O-sulfotransferase (dHS6ST) gene. Structure, expression, and function in the formation of the tracheal system." J Biol Chem **276**(20): 17014-21.
Kan, M., F. Wang, et al. (1993). "An essential heparin-binding domain in the fibroblast growth factor receptor kinase." Science **259**(5103): 1918-21.
Kardestuncer, T., M. B. McCarthy, et al. (2006). "RGD-tethered silk substrate stimulates the differentiation of human tendon cells." Clin Orthop Relat Res **448**: 234-9.
Kashyap, V., N. C. Rezende, et al. (2009). "Regulation of stem cell pluripotency and differentiation involves a mutual regulatory circuit of the NANOG, OCT4, and SOX2 pluripotency transcription factors with polycomb repressive complexes and stem cell microRNAs." Stem Cells Dev **18**(7): 1093-108.

Kaufmann, T. J., M. E. Jensen, et al. (2002). "Cardiovascular effects of polymethylmethacrylate use in percutaneous vertebroplasty." AJNR Am J Neuroradiol **23**(4): 601-4.
Keller, G. M. (1995). "In vitro differentiation of embryonic stem cells." Curr Opin Cell Biol **7**(6): 862-9.
Kim, B. S. and D. J. Mooney (1998). "Development of biocompatible synthetic extracellular matrices for tissue engineering." Trends Biotechnol **16**(5): 224-30.
Kim, G. H., G. R. Lee, et al. (2012). "Overexpression of bone morphogenetic protein 4 in STO fibroblast feeder cells represses the proliferation of mouse embryonic stem cells in vitro." Exp Mol Med **44**(7): 457-63.
Kim, P. T. and C. J. Ong (2012). "Differentiation of definitive endoderm from mouse embryonic stem cells." Results Probl Cell Differ **55**: 303-19.
Kishigami, S. and Y. Mishina (2005). "BMP signaling and early embryonic patterning." Cytokine Growth Factor Rev **16**(3): 265-78.
Kispert, A. and B. G. Herrmann (1994). "Immunohistochemical analysis of the Brachyury protein in wild-type and mutant mouse embryos." Dev Biol **161**(1): 179-93.
Kjellen, L. (2003). "Glucosaminyl N-deacetylase/N-sulphotransferases in heparan sulphate biosynthesis and biology." Biochem Soc Trans **31**(2): 340-2.
Klagsbrun, M. (1990). "The affinity of fibroblast growth factors (FGFs) for heparin; FGF-heparan sulfate interactions in cells and extracellular matrix." Curr Opin Cell Biol **2**(5): 857-63.
Kleinman, H. K., F. B. Cannon, et al. (1985). "Biological activities of laminin." J Cell Biochem **27**(4): 317-25.
Knospel, F., R. K. Schindler, et al. (2010). "Optimization of a serum-free culture medium for mouse embryonic stem cells using design of experiments (DoE) methodology." Cytotechnology **62**(6): 557-71.
Koschwanez, H. E. and E. Broadbent "The use of wound healing assessment methods in psychological studies: a review and recommendations." Br J Health Psychol **16**(Pt 1): 1-32.
Kraushaar, D. C., Y. Yamaguchi, et al. (2010). "Heparan sulfate is required for embryonic stem cells to exit from self-renewal." J Biol Chem **285**(8): 5907-16.
Kreuger, J., P. Jemth, et al. (2005). "Fibroblast growth factors share binding sites in heparan sulphate." Biochem J **389**(Pt 1): 145-50.
Kroger, S. and J. E. Schroder (2002). "Agrin in the developing CNS: new roles for a synapse organizer." News Physiol Sci **17**: 207-12.
Krtolica, A., O. Genbacev, et al. (2007). "Disruption of apical-basal polarity of human embryonic stem cells enhances hematoendothelial differentiation." Stem Cells **25**(9): 2215-23.
Kruithof-de Julio, M., M. J. Alvarez, et al. (2011). "Regulation of extra-embryonic endoderm stem cell differentiation by Nodal and Cripto signaling." Development **138**(18): 3885-95.
Kubo, A., K. Shinozaki, et al. (2004). "Development of definitive endoderm from embryonic stem cells in culture." Development **131**(7): 1651-62.
Kumagai, C., T. Kadowaki, et al. (1997). "Disulfide-bonding between Drosophila laminin beta and gamma chains is essential for alpha chain to form alpha betagamma trimer." FEBS Lett **412**(1): 211-6.
Kumar, G., M. S. Waters, et al. "Freeform fabricated scaffolds with roughened struts that enhance both stem cell proliferation and differentiation by controlling cell shape." Biomaterials **33**(16): 4022-30.
Kunath, T., M. K. Saba-El-Leil, et al. (2007). "FGF stimulation of the Erk1/2 signalling cascade triggers transition of pluripotent embryonic stem cells from self-renewal to lineage commitment." Development **134**(16): 2895-902.
Labosky, P. A., D. P. Barlow, et al. (1994). "Mouse embryonic germ (EG) cell lines: transmission through the germline and differences in the methylation imprint of insulin-like growth factor 2 receptor (Igf2r) gene compared with embryonic stem (ES) cell lines." Development **120**(11): 3197-204.
Lai, B. F., Y. Zou, et al. (2010). "The influence of poly-N-[(2,2-dimethyl-1,3-dioxolane)methyl]acrylamide on fibrin polymerization, cross-linking and clot structure." Biomaterials **31**(22): 5749-58.

Lai, J. P., J. R. Chien, et al. (2004). "hSulf1 Sulfatase promotes apoptosis of hepatocellular cancer cells by decreasing heparin-binding growth factor signaling." Gastroenterology **126**(1): 231-48.
Lamanna, W. C., M. A. Frese, et al. (2008). "Sulf loss influences N-, 2-O-, and 6-O-sulfation of multiple heparan sulfate proteoglycans and modulates fibroblast growth factor signaling." J Biol Chem **283**(41): 27724-35.
Langer, R. and J. P. Vacanti (1993). "Tissue engineering." Science **260**(5110): 920-6.
Lanner, F., K. L. Lee, et al. (2010). "Heparan sulfation-dependent fibroblast growth factor signaling maintains embryonic stem cells primed for differentiation in a heterogeneous state." Stem Cells **28**(2): 191-200.
Lanner, F. and J. Rossant (2010). "The role of FGF/Erk signaling in pluripotent cells." Development **137**(20): 3351-60.
Laurent, T. (1989). "The biology of hyaluronan. Introduction." Ciba Found Symp **143**: 1-20.
Lawrence, P. A., P. Johnston, et al. (1994). "Wingless can bring about a mesoderm-to-ectoderm induction in Drosophila embryos." Development **120**(12): 3355-9.
Lawson, K. A., N. R. Dunn, et al. (1999). "Bmp4 is required for the generation of primordial germ cells in the mouse embryo." Genes Dev **13**(4): 424-36.
Lawson, K. A., J. J. Meneses, et al. (1991). "Clonal analysis of epiblast fate during germ layer formation in the mouse embryo." Development **113**(3): 891-911.
Lazzeri, E., C. Crescioli, et al. (2007). "Regenerative potential of embryonic renal multipotent progenitors in acute renal failure." J Am Soc Nephrol **18**(12): 3128-38.
Le Guillou-Buffello, D., R. Bareille, et al. (2008). "Additive effect of RGD coating to functionalized titanium surfaces on human osteoprogenitor cell adhesion and spreading." Tissue Eng Part A **14**(8): 1445-55.
LeBaron, R. G., A. Hook, et al. (1989). "Binding of heparan sulfate to type V collagen. A mechanism of cell-substrate adhesion." J Biol Chem **264**(14): 7950-6.
LeBleu, V. S., B. Macdonald, et al. (2007). "Structure and function of basement membranes." Exp Biol Med (Maywood) **232**(9): 1121-9.
Ledermann, B. and K. Burki (1991). "Establishment of a germ-line competent C57BL/6 embryonic stem cell line." Exp Cell Res **197**(2): 254-8.
Lee, J. H., H. W. Jung, et al. (1994). "Cell behaviour on polymer surfaces with different functional groups." Biomaterials **15**(9): 705-11.
Lees, J. G., S. A. Lim, et al. (2007). "Transplantation of 3D scaffolds seeded with human embryonic stem cells: biological features of surrogate tissue and teratoma-forming potential." Regen Med **2**(3): 289-300.
Lehembre, F., M. Yilmaz, et al. (2008). "NCAM-induced focal adhesion assembly: a functional switch upon loss of E-cadherin." EMBO J **27**(19): 2603-15.
Lehtonen, E., V. P. Lehto, et al. (1983). "Parietal and visceral endoderm differ in their expression of intermediate filaments." EMBO J **2**(7): 1023-8.
Leivo, I. and E. Engvall (1988). "Merosin, a protein specific for basement membranes of Schwann cells, striated muscle, and trophoblast, is expressed late in nerve and muscle development." Proc Natl Acad Sci U S A **85**(5): 1544-8.
Lensvelt, M. M., W. M. Fritschy, et al. "Results of heparin-bonded ePTFE-covered stents for chronic occlusive superficial femoral artery disease." J Vasc Surg **56**(1): 118-25.
Levenstein, M. E., W. T. Berggren, et al. (2008). "Secreted proteoglycans directly mediate human embryonic stem cell-basic fibroblast growth factor 2 interactions critical for proliferation." Stem Cells **26**(12): 3099-107.
Levenstein, M. E., T. E. Ludwig, et al. (2006). "Basic fibroblast growth factor support of human embryonic stem cell self-renewal." Stem Cells **24**(3): 568-74.
Levey, A. S., R. Atkins, et al. (2007). "Chronic kidney disease as a global public health problem: approaches and initiatives - a position statement from Kidney Disease Improving Global Outcomes." Kidney Int **72**(3): 247-59.
Li, E., T. H. Bestor, et al. (1992). "Targeted mutation of the DNA methyltransferase gene results in embryonic lethality." Cell **69**(6): 915-26.

Li, H. S., J. M. Yang, et al. (1994). "Pax-6 is first expressed in a region of ectoderm anterior to the early neural plate: implications for stepwise determination of the lens." Dev Biol **162**(1): 181-94.
Li, J., G. Wang, et al. (2007). "MEK/ERK signaling contributes to the maintenance of human embryonic stem cell self-renewal." Differentiation **75**(4): 299-307.
Li, L., E. Arman, et al. (2004). "Distinct GATA6- and laminin-dependent mechanisms regulate endodermal and ectodermal embryonic stem cell fates." Development **131**(21): 5277-86.
Li, L., L. Sun, et al. (2010). "Stk40 links the pluripotency factor Oct4 to the Erk/MAPK pathway and controls extraembryonic endoderm differentiation." Proc Natl Acad Sci U S A **107**(4): 1402-7.
Li, M., T. Cui, et al. (2005). "Comparison of selective attachment and growth of smooth muscle cells on gelatin- and fibronectin-coated micropatterns." J Nanosci Nanotechnol **5**(11): 1809-15.
Li, M., D. K. Mills, et al. (2005). "Cellular response to gelatin- and fibronectin-coated multilayer polyelectrolyte nanofilms." IEEE Trans Nanobioscience **4**(2): 170-9.
Li, S., D. Edgar, et al. (2003). "The role of laminin in embryonic cell polarization and tissue organization." Dev Cell **4**(5): 613-24.
Li, X., Y. Chen, et al. (2001). "Fibroblast growth factor signaling and basement membrane assembly are connected during epithelial morphogenesis of the embryoid body." J Cell Biol **153**(4): 811-22.
Li, Z. and Y. G. Chen (2012). "Fine-tune of intrinsic ERK activity by extrinsic BMP signaling in mouse embryonic stem cells." Protein Cell **3**(6): 401-4.
Lianguzova, M. S., I. A. Chuykin, et al. (2007). "Phosphoinositide 3-kinase inhibitor LY294002 but not serum withdrawal suppresses proliferation of murine embryonic stem cells." Cell Biol Int **31**(4): 330-7.
Liao, J., C. Cui, et al. (2009). "Generation of induced pluripotent stem cell lines from adult rat cells." Cell Stem Cell **4**(1): 11-5.
Lim, J. W. and A. Bodnar (2002). "Proteome analysis of conditioned medium from mouse embryonic fibroblast feeder layers which support the growth of human embryonic stem cells." Proteomics **2**(9): 1187-203.
Lin, F. (2006). "Stem cells in kidney regeneration following acute renal injury." Pediatr Res **59**(4 Pt 2): 74R-8R.
Lin, F., K. Cordes, et al. (2003). "Hematopoietic stem cells contribute to the regeneration of renal tubules after renal ischemia-reperfusion injury in mice." J Am Soc Nephrol **14**(5): 1188-99.
Lin, F., A. Moran, et al. (2005). "Intrarenal cells, not bone marrow-derived cells, are the major source for regeneration in postischemic kidney." J Clin Invest **115**(7): 1756-64.
Lin, H. B., W. Sun, et al. (1994). "Synthesis, surface, and cell-adhesion properties of polyurethanes containing covalently grafted RGD-peptides." J Biomed Mater Res **28**(3): 329-42.
Lin, X., E. M. Buff, et al. (1999). "Heparan sulfate proteoglycans are essential for FGF receptor signaling during Drosophila embryonic development." Development **126**(17): 3715-23.
Lin, X., G. Wei, et al. (2000). "Disruption of gastrulation and heparan sulfate biosynthesis in EXT1-deficient mice." Dev Biol **224**(2): 299-311.
Lind, T., F. Tufaro, et al. (1998). "The putative tumor suppressors EXT1 and EXT2 are glycosyltransferases required for the biosynthesis of heparan sulfate." J Biol Chem **273**(41): 26265-8.
Lindahl, B. and U. Lindahl (1997). "Amyloid-specific heparan sulfate from human liver and spleen." J Biol Chem **272**(42): 26091-4.
Lindblom, A., I. Carlstedt, et al. (1989). "Identification of the core proteins in proteoglycans synthesized by vascular endothelial cells." Biochem J **261**(1): 145-53.
Linhardt, R. J., J. E. Turnbull, et al. (1990). "Examination of the substrate specificity of heparin and heparan sulfate lyases." Biochemistry **29**(10): 2611-7.
Liotta, L. A., C. N. Rao, et al. (1986). "Biochemical interactions of tumor cells with the basement membrane." Annu Rev Biochem **55**: 1037-57.
Lipscombe, R. J., A. M. Nakhoul, et al. (1998). "Interleukin-5 binds to heparin/heparan sulfate. A model for an interaction with extracellular matrix." J Leukoc Biol **63**(3): 342-50.

Liu, H., F. Zhu, et al. (2008). "Generation of induced pluripotent stem cells from adult rhesus monkey fibroblasts." Cell Stem Cell **3**(6): 587-90.
Liu, Y., X. Wang, et al. "A synthetic substrate to support early mesodermal differentiation of human embryonic stem cells." Biomaterials **32**(32): 8058-66.
Long, S. F., S. Clarke, et al. (2003). "Controlled biological response on blends of a phosphorylcholine-based copolymer with poly(butyl methacrylate)." Biomaterials **24**(23): 4115-21.
Lopes, C. C., C. P. Dietrich, et al. (2006). "Specific structural features of syndecans and heparan sulfate chains are needed for cell signaling." Braz J Med Biol Res **39**(2): 157-67.
Lowe, L. A., S. Yamada, et al. (2001). "Genetic dissection of nodal function in patterning the mouse embryo." Development **128**(10): 1831-43.
Luders, F., H. Segawa, et al. (2003). "Slalom encodes an adenosine 3'-phosphate 5'-phosphosulfate transporter essential for development in Drosophila." EMBO J **22**(14): 3635-44.
Luikart, S. D., C. A. Maniglia, et al. (1990). "A heparan sulfate-containing fraction of bone marrow stroma induces maturation of HL-60 cells in vitro." Cancer Res **50**(12): 3781-5.
Lum, D. H., J. Tan, et al. (2007). "Gene trap disruption of the mouse heparan sulfate 6-O-endosulfatase gene, Sulf2." Mol Cell Biol **27**(2): 678-88.
Luo, G., C. Hofmann, et al. (1995). "BMP-7 is an inducer of nephrogenesis, and is also required for eye development and skeletal patterning." Genes Dev **9**(22): 2808-20.
Lutz, J. F. and Z. Zarafshani (2008). "Efficient construction of therapeutics, bioconjugates, biomaterials and bioactive surfaces using azide-alkyne "click" chemistry." Adv Drug Deliv Rev **60**(9): 958-70.
Lyon, M., J. A. Deakin, et al. (1994). "Liver heparan sulfate structure. A novel molecular design." J Biol Chem **269**(15): 11208-15.
Lyon, M., J. A. Deakin, et al. (1998). "Hepatocyte growth factor/scatter factor binds with high affinity to dermatan sulfate." J Biol Chem **273**(1): 271-8.
M.P.Matise, W. A., A.L.Joyner, Ed. (2000). Gene Targeting, a practical approach. The Practical Approach Series, Oxford University Press.
Ma, Z., Z. Mao, et al. (2007). "Surface modification and property analysis of biomedical polymers used for tissue engineering." Colloids Surf B Biointerfaces **60**(2): 137-57.
Maccarana, M., Y. Sakura, et al. (1996). "Domain structure of heparan sulfates from bovine organs." J Biol Chem **271**(30): 17804-10.
Maciel, J., M. I. Oliveira, et al. (2012). "The effect of adsorbed fibronectin and osteopontin on macrophage adhesion and morphology on hydrophilic and hydrophobic model surfaces." Acta Biomater **8**(10): 3669-77.
Mack, G. S. "ReNeuron and StemCells get green light for neural stem cell trials." Nat Biotechnol **29**(2): 95-7.
Maeshima, A., S. Yamashita, et al. (2003). "Identification of renal progenitor-like tubular cells that participate in the regeneration processes of the kidney." J Am Soc Nephrol **14**(12): 3138-46.
Mahalingam, Y., J. T. Gallagher, et al. (2007). "Cellular adhesion responses to the heparin-binding (HepII) domain of fibronectin require heparan sulfate with specific properties." J Biol Chem **282**(5): 3221-30.
Mahmood, A., L. Harkness, et al. (2010). "Enhanced differentiation of human embryonic stem cells to mesenchymal progenitors by inhibition of TGF-beta/activin/nodal signaling using SB-431542." J Bone Miner Res **25**(6): 1216-33.
Mahoney, Z. X., T. S. Stappenbeck, et al. (2008). "Laminin alpha 5 influences the architecture of the mouse small intestine mucosa." J Cell Sci **121**(Pt 15): 2493-502.
Makadia, H. K. and S. J. Siegel (2011). "Poly Lactic-co-Glycolic Acid (PLGA) as Biodegradable Controlled Drug Delivery Carrier." Polymers (Basel) **3**(3): 1377-1397.
Mallon, B. S., K. Y. Park, et al. (2006). "Toward xeno-free culture of human embryonic stem cells." Int J Biochem Cell Biol **38**(7): 1063-75.
Mannello, F. and G. A. Tonti (2007). "Concise review: no breakthroughs for human mesenchymal and embryonic stem cell culture: conditioned medium, feeder layer, or feeder-free; medium with fetal calf serum, human serum, or enriched plasma; serum-free, serum replacement

nonconditioned medium, or ad hoc formula? All that glitters is not gold!" Stem Cells **25**(7): 1603-9.
Marchetto, M. C., K. J. Brennand, et al. "Induced pluripotent stem cells (iPSCs) and neurological disease modeling: progress and promises." Hum Mol Genet **20**(R2): R109-15.
Marneros, A. G. and B. R. Olsen (2005). "Physiological role of collagen XVIII and endostatin." FASEB J **19**(7): 716-28.
Maroudas, N. G. (1977). "Sulphonated polystyrene as an optimal substratum for the adhesion and spreading of mesenchymal cells in monovalent and divalent saline solutions." J Cell Physiol **90**(3): 511-9.
Martin-Bermudo, M. D. and N. H. Brown (1999). "Uncoupling integrin adhesion and signaling: the betaPS cytoplasmic domain is sufficient to regulate gene expression in the Drosophila embryo." Genes Dev **13**(6): 729-39.
Martin, G. R. (1981). "Isolation of a pluripotent cell line from early mouse embryos cultured in medium conditioned by teratocarcinoma stem cells." Proc Natl Acad Sci U S A **78**(12): 7634-8.
Martin, G. R. and R. Timpl (1987). "Laminin and other basement membrane components." Annu Rev Cell Biol **3**: 57-85.
Martinez-Hernandez, A. and P. S. Amenta (1983). "The basement membrane in pathology." Lab Invest **48**(6): 656-77.
Masui, S., Y. Nakatake, et al. (2007). "Pluripotency governed by Sox2 via regulation of Oct3/4 expression in mouse embryonic stem cells." Nat Cell Biol **9**(6): 625-35.
Matsuda, T., T. Nakamura, et al. (1999). "STAT3 activation is sufficient to maintain an undifferentiated state of mouse embryonic stem cells." EMBO J **18**(15): 4261-9.
Matsui, C., C. K. Wang, et al. (1995). "The assembly of laminin-5 subunits." J Biol Chem **270**(40): 23496-503.
Mattotti, M., Z. Alvarez, et al. "Inducing functional radial glia-like progenitors from cortical astrocyte cultures using micropatterned PMMA." Biomaterials **33**(6): 1759-70.
Mayer, U., E. Kohfeldt, et al. (1998). "Structural and genetic analysis of laminin-nidogen interaction." Ann N Y Acad Sci **857**: 130-42.
Mazzocca, A. D., G. Trainer, et al. (2012). "Biologic enhancement of a common arthroscopic suture." Arthroscopy **28**(3): 390-6.
McCormick, C., G. Duncan, et al. (2000). "The putative tumor suppressors EXT1 and EXT2 form a stable complex that accumulates in the Golgi apparatus and catalyzes the synthesis of heparan sulfate." Proc Natl Acad Sci U S A **97**(2): 668-73.
McCormick, C., Y. Leduc, et al. (1998). "The putative tumour suppressor EXT1 alters the expression of cell-surface heparan sulfate." Nat Genet **19**(2): 158-61.
McKeehan, W. L., F. Wang, et al. (1998). "The heparan sulfate-fibroblast growth factor family: diversity of structure and function." Prog Nucleic Acid Res Mol Biol **59**: 135-76.
McMahon, A. P. and A. Bradley (1990). "The Wnt-1 (int-1) proto-oncogene is required for development of a large region of the mouse brain." Cell **62**(6): 1073-85.
Medeiros, G. F., A. Mendes, et al. (2000). "Distribution of sulfated glycosaminoglycans in the animal kingdom: widespread occurrence of heparin-like compounds in invertebrates." Biochim Biophys Acta **1475**(3): 287-94.
Medvedev, S. P., A. I. Shevchenko, et al. (2008). "[OCT4 and NANOG are the key genes in the system of pluripotency maintenance in mammalian cells]." Genetika **44**(12): 1589-608.
Mei, Y., J. Hollister-Lock, et al. (2010). "A high throughput micro-array system of polymer surfaces for the manipulation of primary pancreatic islet cells." Biomaterials **31**(34): 8989-95.
Mercier, F. and E. Arikawa-Hirasawa (2011). "Heparan sulfate niche for cell proliferation in the adult brain." Neurosci Lett.
Messana, J. M., N. S. Hwang, et al. (2008). "Size of the embryoid body influences chondrogenesis of mouse embryonic stem cells." J Tissue Eng Regen Med **2**(8): 499-506.
Miki, T., S. Y. Yasuda, et al. (2011). "Wnt/beta-catenin signaling in embryonic stem cell self-renewal and somatic cell reprogramming." Stem Cell Rev **7**(4): 836-46.
Miller, K. L. and D. O. Clegg "Glucosamine and chondroitin sulfate." Rheum Dis Clin North Am **37**(1): 103-18.

Miner, J. H., C. Li, et al. (2004). "Compositional and structural requirements for laminin and basement membranes during mouse embryo implantation and gastrulation." Development **131**(10): 2247-56.
Miner, J. H. and P. D. Yurchenco (2004). "Laminin functions in tissue morphogenesis." Annu Rev Cell Dev Biol **20**: 255-84.
Minoura, N., S. Aiba, et al. (1989). "The interaction of cultured cells with membranes composed of random and block copolypeptides." J Biomed Mater Res **23**(2): 267-79.
Mishina, Y. (2003). "Function of bone morphogenetic protein signaling during mouse development." Front Biosci **8**: d855-69.
Mitsui, K., Y. Tokuzawa, et al. (2003). "The homeoprotein Nanog is required for maintenance of pluripotency in mouse epiblast and ES cells." Cell **113**(5): 631-42.
Miyazawa, K., M. Shinozaki, et al. (2002). "Two major Smad pathways in TGF-beta superfamily signalling." Genes Cells **7**(12): 1191-204.
Mohammadi, M., S. K. Olsen, et al. (2005). "A protein canyon in the FGF-FGF receptor dimer selects from an a la carte menu of heparan sulfate motifs." Curr Opin Struct Biol **15**(5): 506-16.
Molkentin, J. D. (2000). "The zinc finger-containing transcription factors GATA-4, -5, and -6. Ubiquitously expressed regulators of tissue-specific gene expression." J Biol Chem **275**(50): 38949-52.
Montgomery, R. I., K. Lidholt, et al. (1992). "Stable heparin-producing cell lines derived from the Furth murine mastocytoma." Proc Natl Acad Sci U S A **89**(23): 11327-31.
Moreau, J. F., D. D. Donaldson, et al. (1988). "Leukaemia inhibitory factor is identical to the myeloid growth factor human interleukin for DA cells." Nature **336**(6200): 690-2.
Morigi, M., B. Imberti, et al. (2004). "Mesenchymal stem cells are renotropic, helping to repair the kidney and improve function in acute renal failure." J Am Soc Nephrol **15**(7): 1794-804.
Morimoto-Tomita, M., K. Uchimura, et al. (2002). "Cloning and characterization of two extracellular heparin-degrading endosulfatases in mice and humans." J Biol Chem **277**(51): 49175-85.
Morita, A., E. Sugimoto, et al. (1985). "Post-translational assembly and glycosylation of laminin subunits in parietal endoderm-like F9 cells." Biochem J **229**(1): 259-64.
Morrisey, E. E., Z. Tang, et al. (1998). "GATA6 regulates HNF4 and is required for differentiation of visceral endoderm in the mouse embryo." Genes Dev **12**(22): 3579-90.
Mountford, P., J. Nichols, et al. (1998). "Maintenance of pluripotential embryonic stem cells by stem cell selection." Reprod Fertil Dev **10**(7-8): 527-33.
Mourier, P. A. and C. Viskov (2004). "Chromatographic analysis and sequencing approach of heparin oligosaccharides using cetyltrimethylammonium dynamically coated stationary phases." Anal Biochem **332**(2): 299-313.
Mulloy, B. and C. C. Rider (2006). "Cytokines and proteoglycans: an introductory overview." Biochem Soc Trans **34**(Pt 3): 409-13.
Mummery, C. L., T. A. van Achterberg, et al. (1991). "Visceral-endoderm-like cell lines induce differentiation of murine P19 embryonal carcinoma cells." Differentiation **46**(1): 51-60.
Mundy, C., T. Yasuda, et al. (2011). "Synovial joint formation requires local Ext1 expression and heparan sulfate production in developing mouse embryo limbs and spine." Dev Biol **351**(1): 70-81.
Murakami, A., H. Shen, et al. (2004). "SOX7 and GATA-4 are competitive activators of Fgf-3 transcription." J Biol Chem **279**(27): 28564-73.
Murakami, R., T. Okumura, et al. (2005). "GATA factors as key regulatory molecules in the development of Drosophila endoderm." Dev Growth Differ **47**(9): 581-9.
Murali, S., K. J. Manton, et al. (2009). "Purification and characterization of heparan sulfate from human primary osteoblasts." J Cell Biochem **108**(5): 1132-42.
Murdoch, A. D., B. Liu, et al. (1994). "Widespread expression of perlecan proteoglycan in basement membranes and extracellular matrices of human tissues as detected by a novel monoclonal antibody against domain III and by in situ hybridization." J Histochem Cytochem **42**(2): 239-49.
Murray, P. and D. Edgar (2000). "Regulation of programmed cell death by basement membranes in embryonic development." J Cell Biol **150**(5): 1215-21.

Murray, P. and D. Edgar (2001). "The regulation of embryonic stem cell differentiation by leukaemia inhibitory factor (LIF)." Differentiation **68**(4-5): 227-34.
Murugan, R., P. Molnar, et al. (2009). "Biomaterial Surface patterning of self assembled monolayers for controlling neuronal cell behavior." Int J Biomed Eng Technol **2**(2): 104-134.
Naimy, H., N. Leymarie, et al. "Screening for anticoagulant heparan sulfate octasaccharides and fine structure characterization using tandem mass spectrometry." Biochemistry **49**(17): 3743-52.
Nairn, A. V., A. Kinoshita-Toyoda, et al. (2007). "Glycomics of proteoglycan biosynthesis in murine embryonic stem cell differentiation." J Proteome Res **6**(11): 4374-87.
Nakajima, M., T. Ishimuro, et al. (2007). "Combinatorial protein display for the cell-based screening of biomaterials that direct neural stem cell differentiation." Biomaterials **28**(6): 1048-60.
Nakanishi, M., A. Kurisaki, et al. (2009). "Directed induction of anterior and posterior primitive streak by Wnt from embryonic stem cells cultured in a chemically defined serum-free medium." FASEB J **23**(1): 114-22.
Nakano, T., H. Kodama, et al. (1994). "Generation of lymphohematopoietic cells from embryonic stem cells in culture." Science **265**(5175): 1098-101.
Natori, S. H. and K. Kurita (2007). "Blood cell separation using amphiphilic copolymers containing N,N-dimethylacrylamide." J Biomed Mater Res B Appl Biomater **81**(2): 419-26.
Navaratnam, V. (1991). "Organisation and reorganisation of blood vessels in embryonic development." Eye (Lond) **5 (Pt 2)**: 147-50.
Neurauter, A. A., M. Bonyhadi, et al. (2007). "Cell isolation and expansion using Dynabeads." Adv Biochem Eng Biotechnol **106**: 41-73.
Nguyen, N. M., Y. Bai, et al. (2002). "Laminin alpha-chain expression and basement membrane formation by MLE-15 respiratory epithelial cells." Am J Physiol Lung Cell Mol Physiol **282**(5): L1004-11.
Ni, J., M. Takehara, et al. (2010). "Identification of activity related amino acid mutations of a GH9 termite cellulase." Bioresour Technol **101**(16): 6438-43.
Nichol, J. W., S. T. Koshy, et al. (2010). "Cell-laden microengineered gelatin methacrylate hydrogels." Biomaterials **31**(21): 5536-44.
Nichols, J., E. P. Evans, et al. (1990). "Establishment of germ-line-competent embryonic stem (ES) cells using differentiation inhibiting activity." Development **110**(4): 1341-8.
Nichols, J., B. Zevnik, et al. (1998). "Formation of pluripotent stem cells in the mammalian embryo depends on the POU transcription factor Oct4." Cell **95**(3): 379-91.
Nicolson, P. C. and J. Vogt (2001). "Soft contact lens polymers: an evolution." Biomaterials **22**(24): 3273-83.
Niimi, T., Y. Hayashi, et al. (2004). "SOX7 and SOX17 regulate the parietal endoderm-specific enhancer activity of mouse laminin alpha1 gene." J Biol Chem **279**(36): 38055-61.
Nishikawa, S. I., S. Nishikawa, et al. (1998). "Progressive lineage analysis by cell sorting and culture identifies FLK1+VE-cadherin+ cells at a diverging point of endothelial and hemopoietic lineages." Development **125**(9): 1747-57.
Niwa, H. (2001). "Molecular mechanism to maintain stem cell renewal of ES cells." Cell Struct Funct **26**(3): 137-48.
Niwa, H. (2007). "How is pluripotency determined and maintained?" Development **134**(4): 635-46.
Niwa, H., T. Burdon, et al. (1998). "Self-renewal of pluripotent embryonic stem cells is mediated via activation of STAT3." Genes Dev **12**(13): 2048-60.
Niwa, H., J. Miyazaki, et al. (2000). "Quantitative expression of Oct-3/4 defines differentiation, dedifferentiation or self-renewal of ES cells." Nat Genet **24**(4): 372-6.
Niwa, H., K. Ogawa, et al. (2009). "A parallel circuit of LIF signalling pathways maintains pluripotency of mouse ES cells." Nature **460**(7251): 118-22.
Nurcombe, V. and S. M. Cool (2007). "Heparan sulfate control of proliferation and differentiation in the stem cell niche." Crit Rev Eukaryot Gene Expr **17**(2): 159-71.
Ogawa, K., A. Saito, et al. (2007). "Activin-Nodal signaling is involved in propagation of mouse embryonic stem cells." J Cell Sci **120**(Pt 1): 55-65.
Okada, M., S. Nadanaka, et al. "Biosynthesis of heparan sulfate in EXT1-deficient cells." Biochem J **428**(3): 463-71.

Okumura, T., A. Matsumoto, et al. (2005). "An endoderm-specific GATA factor gene, dGATAe, is required for the terminal differentiation of the Drosophila endoderm." Dev Biol **278**(2): 576-86.
Olmo, N., M. A. Lizarbe, et al. (1988). "Cell morphology, proliferation and collagen synthesis of human fibroblasts cultured on sepiolite-collagen complexes." J Biomed Mater Res **22**(4): 257-70.
Opferman, J. T. and S. J. Korsmeyer (2003). "Apoptosis in the development and maintenance of the immune system." Nat Immunol **4**(5): 410-5.
Ori, A., M. C. Wilkinson, et al. (2008). "The heparanome and regulation of cell function: structures, functions and challenges." Front Biosci **13**: 4309-38.
Orilall, M. C. and U. Wiesner (2011). "Block copolymer based composition and morphology control in nanostructured hybrid materials for energy conversion and storage: solar cells, batteries, and fuel cells." Chem Soc Rev **40**(2): 520-35.
Orkin, S. H., J. Wang, et al. (2008). "The transcriptional network controlling pluripotency in ES cells." Cold Spring Harb Symp Quant Biol **73**: 195-202.
Orkin, S. H., J. Wang, et al. (2008). "The Transcriptional Network Controlling Pluripotency in ES Cells." Cold Spring Harb Symp Quant Biol.
Ornitz, D. M. (2000). "FGFs, heparan sulfate and FGFRs: complex interactions essential for development." Bioessays **22**(2): 108-12.
Ornitz, D. M. and N. Itoh (2001). "Fibroblast growth factors." Genome Biol **2**(3): REVIEWS3005.
Owen-Smith, J., C. T. Scott, et al. "Democracy is working." J Policy Anal Manage **31**(3): 726-8.
Ozkurt, Z. and E. Kazazoglu "Zirconia dental implants: a literature review." J Oral Implantol **37**(3): 367-76.
Paca, A., C. A. Seguin, et al. (2012). "BMP signaling induces visceral endoderm differentiation of XEN cells and parietal endoderm." Dev Biol **361**(1): 90-102.
Paine-Saunders, S., B. L. Viviano, et al. (2000). "glypican-3 controls cellular responses to Bmp4 in limb patterning and skeletal development." Dev Biol **225**(1): 179-87.
Palacio, M., S. Schricker, et al. (2010). "Morphology and protein adsorption characteristics of block copolymer surfaces." J Microsc **240**(3): 239-48.
Pallerla, S. R., Y. Pan, et al. (2007). "Heparan sulfate Ndst1 gene function variably regulates multiple signaling pathways during mouse development." Dev Dyn **236**(2): 556-63.
Parisi, S., F. Passaro, et al. (2008). "Klf5 is involved in self-renewal of mouse embryonic stem cells." J Cell Sci **121**(Pt 16): 2629-34.
Park, H., X. Guo, et al. (2009). "Effect of swelling ratio of injectable hydrogel composites on chondrogenic differentiation of encapsulated rabbit marrow mesenchymal stem cells in vitro." Biomacromolecules **10**(3): 541-6.
Park, J. H., R. Olivares-Navarrete, et al. (2012). "Use of polyelectrolyte thin films to modulate osteoblast response to microstructured titanium surfaces." Biomaterials **33**(21): 5267-77.
Park, P. W., G. B. Pier, et al. (2001). "Exploitation of syndecan-1 shedding by Pseudomonas aeruginosa enhances virulence." Nature **411**(6833): 98-102.
Patel, V. N., S. M. Knox, et al. (2007). "Heparanase cleavage of perlecan heparan sulfate modulates FGF10 activity during ex vivo submandibular gland branching morphogenesis." Development **134**(23): 4177-86.
Patterson, P. H. (1994). "Leukemia inhibitory factor, a cytokine at the interface between neurobiology and immunology." Proc Natl Acad Sci U S A **91**(17): 7833-5.
Paulsson, M. (1992). "Basement membrane proteins: structure, assembly, and cellular interactions." Crit Rev Biochem Mol Biol **27**(1-2): 93-127.
Pease, S., P. Braghetta, et al. (1990). "Isolation of embryonic stem (ES) cells in media supplemented with recombinant leukemia inhibitory factor (LIF)." Dev Biol **141**(2): 344-52.
Peck, M., D. Gebhart, et al. "The evolution of vascular tissue engineering and current state of the art." Cells Tissues Organs **195**(1-2): 144-58.
Pellegrini, L. (2001). "Role of heparan sulfate in fibroblast growth factor signalling: a structural view." Curr Opin Struct Biol **11**(5): 629-34.
Pempe, E. H., T. C. Burch, et al. (2012). "Substrate specificity of 6-O-endosulfatase (Sulf-2) and its implications in synthesizing anticoagulant heparan sulfate." Glycobiology **22**(10): 1353-62.

Perrimon, N. and M. Bernfield (2000). "Specificities of heparan sulphate proteoglycans in developmental processes." Nature **404**(6779): 725-8.
Pesce, M. and H. R. Scholer (2001). "Oct-4: gatekeeper in the beginnings of mammalian development." Stem Cells **19**(4): 271-8.
Petitou, M., B. Casu, et al. (2003). "1976-1983, a critical period in the history of heparin: the discovery of the antithrombin binding site." Biochimie **85**(1-2): 83-9.
Piccolo, S., Y. Sasai, et al. (1996). "Dorsoventral patterning in Xenopus: inhibition of ventral signals by direct binding of chordin to BMP-4." Cell **86**(4): 589-98.
Pickford, C. E., R. J. Holley, et al. (2011). "Specific glycosaminoglycans modulate neural specification of mouse embryonic stem cells." Stem Cells **29**(4): 629-40.
Pierschbacher, M. D. and E. Ruoslahti (1984). "Cell attachment activity of fibronectin can be duplicated by small synthetic fragments of the molecule." Nature **309**(5963): 30-3.
Pierschbacher, M. D. and E. Ruoslahti (1984). "Variants of the cell recognition site of fibronectin that retain attachment-promoting activity." Proc Natl Acad Sci U S A **81**(19): 5985-8.
Pikas, D. S., I. Eriksson, et al. (2000). "Overexpression of different isoforms of glucosaminyl N-deacetylase/N-sulfotransferase results in distinct heparan sulfate N-sulfation patterns." Biochemistry **39**(15): 4552-8.
Plotnikov, A. N., A. V. Eliseenkova, et al. (2001). "Crystal structure of fibroblast growth factor 9 reveals regions implicated in dimerization and autoinhibition." J Biol Chem **276**(6): 4322-9.
Plotnikov, A. N., J. Schlessinger, et al. (1999). "Structural basis for FGF receptor dimerization and activation." Cell **98**(5): 641-50.
Porter, A. E., T. Buckland, et al. (2006). "The structure of the bond between bone and porous silicon-substituted hydroxyapatite bioceramic implants." J Biomed Mater Res A **78**(1): 25-33.
Powell, A. K., D. G. Fernig, et al. (2002). "Fibroblast growth factor receptors 1 and 2 interact differently with heparin/heparan sulfate. Implications for dynamic assembly of a ternary signaling complex." J Biol Chem **277**(32): 28554-63.
Powell, A. K., E. A. Yates, et al. (2004). "Interactions of heparin/heparan sulfate with proteins: appraisal of structural factors and experimental approaches." Glycobiology **14**(4): 17R-30R.
Prager-Khoutorsky, M., A. Lichtenstein, et al. (2011). "Fibroblast polarization is a matrix-rigidity-dependent process controlled by focal adhesion mechanosensing." Nat Cell Biol **13**(12): 1457-65.
Presto, J., M. Thuveson, et al. (2008). "Heparan sulfate biosynthesis enzymes EXT1 and EXT2 affect NDST1 expression and heparan sulfate sulfation." Proc Natl Acad Sci U S A **105**(12): 4751-6.
Prowse, A. B., L. R. McQuade, et al. (2007). "Identification of potential pluripotency determinants for human embryonic stem cells following proteomic analysis of human and mouse fibroblast conditioned media." J Proteome Res **6**(9): 3796-807.
Prowse, A. B., L. R. McQuade, et al. (2005). "A proteome analysis of conditioned media from human neonatal fibroblasts used in the maintenance of human embryonic stem cells." Proteomics **5**(4): 978-89.
Prydz, K. and K. T. Dalen (2000). "Synthesis and sorting of proteoglycans." J Cell Sci **113 Pt 2**: 193-205.
Pye, D. A., R. R. Vives, et al. (1998). "Heparan sulfate oligosaccharides require 6-O-sulfation for promotion of basic fibroblast growth factor mitogenic activity." J Biol Chem **273**(36): 22936-42.
Qi, X., T. G. Li, et al. (2004). "BMP4 supports self-renewal of embryonic stem cells by inhibiting mitogen-activated protein kinase pathways." Proc Natl Acad Sci U S A **101**(16): 6027-32.
Qiao, D., K. Meyer, et al. (2003). "Heparan sulfate proteoglycans as regulators of fibroblast growth factor-2 signaling in brain endothelial cells. Specific role for glypican-1 in glioma angiogenesis." J Biol Chem **278**(18): 16045-53.
Quinn, C. P., C. P. Pathak, et al. (1995). "Photo-crosslinked copolymers of 2-hydroxyethyl methacrylate, poly(ethylene glycol) tetra-acrylate and ethylene dimethacrylate for improving biocompatibility of biosensors." Biomaterials **16**(5): 389-96.
Quiring, R., U. Walldorf, et al. (1994). "Homology of the eyeless gene of Drosophila to the Small eye gene in mice and Aniridia in humans." Science **265**(5173): 785-9.

Rabenstein, D. L. (2002). "Heparin and heparan sulfate: structure and function." Nat Prod Rep **19**(3): 312-31.
Rahmoune, H., P. S. Rudland, et al. (1998). "Hepatocyte growth factor/scatter factor has distinct classes of binding site in heparan sulfate from mammary cells." Biochemistry **37**(17): 6003-8.
Ralston, A. and J. Rossant (2005). "Genetic regulation of stem cell origins in the mouse embryo." Clin Genet **68**(2): 106-12.
Ramalho-Santos, M., S. Yoon, et al. (2002). ""Stemness": transcriptional profiling of embryonic and adult stem cells." Science **298**(5593): 597-600.
Raman, R., V. Sasisekharan, et al. (2005). "Structural insights into biological roles of protein-glycosaminoglycan interactions." Chem Biol **12**(3): 267-77.
Rao, S. S. and J. O. Winter (2009). "Adhesion molecule-modified biomaterials for neural tissue engineering." Front Neuroeng **2**: 6.
Rapraeger, A. C. (1995). "In the clutches of proteoglycans: how does heparan sulfate regulate FGF binding?" Chem Biol **2**(10): 645-9.
Ratanavaraporn, J. and Y. Tabata (2012). "Enhanced osteogenic activity of bone morphogenetic protein-2 by 2-O-desulfated heparin." Acta Biomater **8**(1): 173-82.
Rauch, M. F., M. Michaud, et al. (2008). "Co-culture of primary neural progenitor and endothelial cells in a macroporous gel promotes stable vascular networks in vivo." J Biomater Sci Polym Ed **19**(11): 1469-85.
Reichenberger, M. A., A. Stoff, et al. (2007). "Polymethylmethacrylate for managing frontal bone deformities." Aesthetic Plast Surg **31**(4): 397-400.
Reno, F., M. Rizzi, et al. (2012). "Gelatin-based anionic hydrogel as biocompatible substrate for human keratinocyte growth." J Mater Sci Mater Med **23**(2): 565-71.
Resnick, J. L., L. S. Bixler, et al. (1992). "Long-term proliferation of mouse primordial germ cells in culture." Nature **359**(6395): 550-1.
Reuss, B. and O. von Bohlen und Halbach (2003). "Fibroblast growth factors and their receptors in the central nervous system." Cell Tissue Res **313**(2): 139-57.
Reya, T., A. W. Duncan, et al. (2003). "A role for Wnt signalling in self-renewal of haematopoietic stem cells." Nature **423**(6938): 409-14.
Richards, M., C. Y. Fong, et al. (2002). "Human feeders support prolonged undifferentiated growth of human inner cell masses and embryonic stem cells." Nat Biotechnol **20**(9): 933-6.
Richards, M., S. Tan, et al. (2003). "Comparative evaluation of various human feeders for prolonged undifferentiated growth of human embryonic stem cells." Stem Cells **21**(5): 546-56.
Rider, C. C. (2006). "Heparin/heparan sulphate binding in the TGF-beta cytokine superfamily." Biochem Soc Trans **34**(Pt 3): 458-60.
Ringvall, M. and L. Kjellen (2010). "Mice deficient in heparan sulfate N-deacetylase/N-sulfotransferase 1." Prog Mol Biol Transl Sci **93**: 35-58.
Riopelle, R. J. and K. E. Dow (1990). "Functional interactions of neuronal heparan sulphate proteoglycans with laminin." Brain Res **525**(1): 92-100.
Robertson, E. (1987). Embryo-derived stem cell lines in: Robertson, EJ (Ed) Teratocarcinomas and embryonic stem cells; a practical approach. Oxford.
Robinson, C. J. and S. E. Stringer (2001). "The splice variants of vascular endothelial growth factor (VEGF) and their receptors." J Cell Sci **114**(Pt 5): 853-65.
Robinson, J. and D. Gospodarowicz (1983). "Glycosaminoglycans synthesized by cultured bovine corneal endothelial cells." J Cell Physiol **117**(3): 368-76.
Roden, L., S. Ananth, et al. (1992). "Heparin--an introduction." Adv Exp Med Biol **313**: 1-20.
Rohde, L. H., M. J. Janatpore, et al. (1998). "Complementary expression of HIP, a cell-surface heparan sulfate binding protein, and perlecan at the human fetal-maternal interface." Biol Reprod **58**(4): 1075-83.
Rolny, C., D. Spillmann, et al. (2002). "Heparin amplifies platelet-derived growth factor (PDGF)-BB-induced PDGF alpha -receptor but not PDGF beta -receptor tyrosine phosphorylation in heparan sulfate-deficient cells. Effects on signal transduction and biological responses." J Biol Chem **277**(22): 19315-21.

Romero-Lanman, E. E., S. Pavlovic, et al. (2012). "Id1 maintains embryonic stem cell self-renewal by up-regulation of Nanog and repression of Brachyury expression." Stem Cells Dev **21**(3): 384-93.
Ruoslahti, E. (1996). "RGD and other recognition sequences for integrins." Annu Rev Cell Dev Biol **12**: 697-715.
Rykova, V. I. and E. V. Grigorieva (1998). "Proteoglycan composition in cell nuclei of mouse hepatoma." Biochemistry (Mosc) **63**(11): 1271-6.
Saga, Y., T. Yagi, et al. (1992). "Mice develop normally without tenascin." Genes Dev **6**(10): 1821-31.
Sagnella, S., E. Anderson, et al. (2005). "Human endothelial cell interaction with biomimetic surfactant polymers containing Peptide ligands from the heparin binding domain of fibronectin." Tissue Eng **11**(1-2): 226-36.
Saha, K., Y. Mei, et al. (2011). "Surface-engineered substrates for improved human pluripotent stem cell culture under fully defined conditions." Proc Natl Acad Sci U S A **108**(46): 18714-9.
Saijoh, Y., S. Oki, et al. (2003). "Left-right patterning of the mouse lateral plate requires nodal produced in the node." Dev Biol **256**(1): 160-72.
Sakaki-Yumoto, M., C. Kobayashi, et al. (2006). "The murine homolog of SALL4, a causative gene in Okihiro syndrome, is essential for embryonic stem cell proliferation, and cooperates with Sall1 in anorectal, heart, brain and kidney development." Development **133**(15): 3005-13.
Salmivirta, M., F. Safaiyan, et al. (1998). "Differentiation-associated modulation of heparan sulfate structure and function in CaCo-2 colon carcinoma cells." Glycobiology **8**(10): 1029-36.
San Martin, B. and M. Bate (2001). "Hindgut visceral mesoderm requires an ectodermal template for normal development in Drosophila." Development **128**(2): 233-42.
San Martin, S., M. Soto-Suazo, et al. (2004). "Perlecan and syndecan-4 in uterine tissues during the early pregnancy in mice." Am J Reprod Immunol **52**(1): 53-9.
Sanchez, L. A., R. A. Wain, et al. (1997). "Endovascular grafting for aortoiliac occlusive disease." Semin Vasc Surg **10**(4): 297-309.
Sanchez, M. P., I. Silos-Santiago, et al. (1996). "Renal agenesis and the absence of enteric neurons in mice lacking GDNF." Nature **382**(6586): 70-3.
Saranya, N., S. Saravanan, et al. "Enhanced osteoblast adhesion on polymeric nano-scaffolds for bone tissue engineering." J Biomed Nanotechnol **7**(2): 238-44.
Sasaki, N., K. Okishio, et al. (2008). "Heparan sulfate regulates self-renewal and pluripotency of embryonic stem cells." J Biol Chem **283**(6): 3594-606.
Sasaki, T., E. Forsberg, et al. (1998). "Deficiency of beta 1 integrins in teratoma interferes with basement membrane assembly and laminin-1 expression." Exp Cell Res **238**(1): 70-81.
Sasisekharan, R. and G. Venkataraman (2000). "Heparin and heparan sulfate: biosynthesis, structure and function." Curr Opin Chem Biol **4**(6): 626-31.
Sato, N., L. Meijer, et al. (2004). "Maintenance of pluripotency in human and mouse embryonic stem cells through activation of Wnt signaling by a pharmacological GSK-3-specific inhibitor." Nat Med **10**(1): 55-63.
Saunders, J. W., Jr. (1966). "Death in embryonic systems." Science **154**(3749): 604-12.
Scheele, S., M. Falk, et al. (2005). "Laminin alpha1 globular domains 4-5 induce fetal development but are not vital for embryonic basement membrane assembly." Proc Natl Acad Sci U S A **102**(5): 1502-6.
Schofield, K. P., J. T. Gallagher, et al. (1999). "Expression of proteoglycan core proteins in human bone marrow stroma." Biochem J **343 Pt 3**: 663-8.
Schricker, S., M. Palacio, et al. (2010). "Synthesis and morphological characterization of block copolymers for improved biomaterials." Ultramicroscopy **110**(6): 639-49.
Schulz, H., R. Kolde, et al. (2009). "The FunGenES database: a genomics resource for mouse embryonic stem cell differentiation." PLoS One **4**(9): e6804.
Schwartz, S. D., J. P. Hubschman, et al. "Embryonic stem cell trials for macular degeneration: a preliminary report." Lancet **379**(9817): 713-20.
Schworer, R., O. V. Zubkova, et al. "Synthesis of a Targeted Library of Heparan Sulfate Hexa- to Dodecasaccharides as Inhibitors of beta-Secretase: Potential Therapeutics for Alzheimer's Disease." Chemistry.

Sedita, J., K. Izvolsky, et al. (2004). "Differential expression of heparan sulfate 6-O-sulfotransferase isoforms in the mouse embryo suggests distinctive roles during organogenesis." Dev Dyn **231**(4): 782-94.
Seppinen, L. and T. Pihlajaniemi "The multiple functions of collagen XVIII in development and disease." Matrix Biol **30**(2): 83-92.
Serls, A. E., S. Doherty, et al. (2005). "Different thresholds of fibroblast growth factors pattern the ventral foregut into liver and lung." Development **132**(1): 35-47.
Shah, M. M., H. Sakurai, et al. (2011). "Growth factor-dependent branching of the ureteric bud is modulated by selective 6-O sulfation of heparan sulfate." Dev Biol **356**(1): 19-27.
Shah, M. M., H. Sakurai, et al. (2010). "Hs2st mediated kidney mesenchyme induction regulates early ureteric bud branching." Dev Biol **339**(2): 354-65.
Shah, M. M., J. B. Tee, et al. (2009). "The instructive role of metanephric mesenchyme in ureteric bud patterning, sculpting, and maturation and its potential ability to buffer ureteric bud branching defects." Am J Physiol Renal Physiol **297**(5): F1330-41.
Shen, M. M. and P. Leder (1992). "Leukemia inhibitory factor is expressed by the preimplantation uterus and selectively blocks primitive ectoderm formation in vitro." Proc Natl Acad Sci U S A **89**(17): 8240-4.
Sheng, G. and C. D. Stern (1999). "Gata2 and Gata3: novel markers for early embryonic polarity and for non-neural ectoderm in the chick embryo." Mech Dev **87**(1-2): 213-6.
Shi, G., F. Gao, et al. (2011). "The regulatory role of histone deacetylase inhibitors in Fgf4 expression is dependent on the differentiation state of pluripotent stem cells." J Cell Physiol **226**(12): 3190-6.
Shi, M., C. Q. Xie, et al. (2005). "[Preliminary proteome analysis of mouse embryonic fibroblast conditioned medium]." Zhong Nan Da Xue Xue Bao Yi Xue Ban **30**(1): 11-5.
Shimokawa, K., C. Kimura-Yoshida, et al. (2011). "Cell surface heparan sulfate chains regulate local reception of FGF signaling in the mouse embryo." Dev Cell **21**(2): 257-72.
Shukla, D., J. Liu, et al. (1999). "A novel role for 3-O-sulfated heparan sulfate in herpes simplex virus 1 entry." Cell **99**(1): 13-22.
Silva, J., J. Nichols, et al. (2009). "Nanog is the gateway to the pluripotent ground state." Cell **138**(4): 722-37.
Silva, J. and A. Smith (2008). "Capturing pluripotency." Cell **132**(4): 532-6.
Simo, P., F. Bouziges, et al. (1992). "Dual and asynchronous deposition of laminin chains at the epithelial-mesenchymal interface in the gut." Gastroenterology **102**(6): 1835-45.
Simon, M. C. (1995). "Gotta have GATA." Nat Genet **11**(1): 9-11.
Singh, A. M., T. Hamazaki, et al. (2007). "A heterogeneous expression pattern for Nanog in embryonic stem cells." Stem Cells **25**(10): 2534-42.
Singh, S. K., M. N. Kagalwala, et al. (2008). "REST maintains self-renewal and pluripotency of embryonic stem cells." Nature **453**(7192): 223-7.
Sirard, C., J. L. de la Pompa, et al. (1998). "The tumor suppressor gene Smad4/Dpc4 is required for gastrulation and later for anterior development of the mouse embryo." Genes Dev **12**(1): 107-19.
Sladek, F. M. (1994). "Orphan receptor HNF-4 and liver-specific gene expression." Receptor **4**(1): 64.
Sladowski, D., I. Grabska-Liberek, et al. (2008). "An evaluation of sterilisation processes." Altern Lab Anim **36**(5): 585-90.
Smith, A. G. (2001). "Embryo-derived stem cells: of mice and men." Annu Rev Cell Dev Biol **17**: 435-62.
Smith, A. G., J. K. Heath, et al. (1988). "Inhibition of pluripotential embryonic stem cell differentiation by purified polypeptides." Nature **336**(6200): 688-90.
Smith, K. and S. Dalton (2010). "Myc transcription factors: key regulators behind establishment and maintenance of pluripotency." Regen Med **5**(6): 947-59.
Smith, K. K. and S. Strickland (1981). "Structural components and characteristics of Reichert's membrane, an extra-embryonic basement membrane." J Biol Chem **256**(9): 4654-61.
Smith, K. N., A. M. Singh, et al. (2010). "Myc represses primitive endoderm differentiation in pluripotent stem cells." Cell Stem Cell **7**(3): 343-54.

Smith, R. A., K. Meade, et al. (2011). "Glycosaminoglycans as regulators of stem cell differentiation." Biochem Soc Trans **39**(1): 383-7.
Smyth, N., H. S. Vatansever, et al. (1999). "Absence of basement membranes after targeting the LAMC1 gene results in embryonic lethality due to failure of endoderm differentiation." J Cell Biol **144**(1): 151-60.
Sokol, S. Y. (2011). "Maintaining embryonic stem cell pluripotency with Wnt signaling." Development **138**(20): 4341-50.
Song, W., H. Lu, et al. "Adipogenic differentiation of individual mesenchymal stem cell on different geometric micropatterns." Langmuir **27**(10): 6155-62.
Soria, B., E. Roche, et al. (2000). "Insulin-secreting cells derived from embryonic stem cells normalize glycemia in streptozotocin-induced diabetic mice." Diabetes **49**(2): 157-62.
Spear, B. T. and S. M. Tilghman (1990). "Role of alpha-fetoprotein regulatory elements in transcriptional activation in transient heterokaryons." Mol Cell Biol **10**(10): 5047-54.
Specks, U., U. Mayer, et al. (1992). "Structure of recombinant N-terminal globule of type VI collagen alpha 3 chain and its binding to heparin and hyaluronan." EMBO J **11**(12): 4281-90.
Sperinde, G. V. and M. A. Nugent (2000). "Mechanisms of fibroblast growth factor 2 intracellular processing: a kinetic analysis of the role of heparan sulfate proteoglycans." Biochemistry **39**(13): 3788-96.
Sprague, L., M. Muccioli, et al. (2011). "The interplay between surfaces and soluble factors define the immunologic and angiogenic properties of myeloid dendritic cells." BMC Immunol **12**: 35.
Steinemann, S. G. (1998). "Titanium--the material of choice?" Periodontol 2000 **17**: 7-21.
Sterneckert, J., S. Hoing, et al. (2012). "Concise review: Oct4 and more: the reprogramming expressway." Stem Cells **30**(1): 15-21.
Stevens, L. C. (1970). "The development of transplantable teratocarcinomas from intratesticular grafts of pre- and postimplantation mouse embryos." Dev Biol **21**(3): 364-82.
Stewart, C. L., I. Gadi, et al. (1994). "Stem cells from primordial germ cells can reenter the germ line." Dev Biol **161**(2): 626-8.
Stickens, D., B. M. Zak, et al. (2005). "Mice deficient in Ext2 lack heparan sulfate and develop exostoses." Development **132**(22): 5055-68.
Stokes, K. and K. Cobian (1982). "Polyether polyurethanes for implantable pacemaker leads." Biomaterials **3**(4): 225-31.
Stone, G. W., S. G. Ellis, et al. (2004). "A polymer-based, paclitaxel-eluting stent in patients with coronary artery disease." N Engl J Med **350**(3): 221-31.
Stoykova, A. and P. Gruss (1994). "Roles of Pax-genes in developing and adult brain as suggested by expression patterns." J Neurosci **14**(3 Pt 2): 1395-412.
Strigini, M. and S. M. Cohen (1999). "Formation of morphogen gradients in the Drosophila wing." Semin Cell Dev Biol **10**(3): 335-44.
Struszczyk, M. H., P. Bednarek, et al. (2002). "Synthetic vascular prostheses." Polim Med **32**(1-2): 13-22.
Sugaya, N., H. Habuchi, et al. (2008). "6-O-sulfation of heparan sulfate differentially regulates various fibroblast growth factor-dependent signalings in culture." J Biol Chem **283**(16): 10366-76.
Sun, H. and W. K. Shi (1998). "[Expression of LIF gene during early development of mouse embryo]." Shi Yan Sheng Wu Xue Bao **31**(1): 105-9.
Sun, Y., Z. Huang, et al. (2012). "Surface coating as a key parameter in engineering neuronal network structures in vitro." Biointerphases **7**(1-4): 29.
Suwinska, A. and M. A. Ciemerych (2011). "Factors regulating pluripotency and differentiation in early mammalian embryos and embryo-derived stem cells." Vitam Horm **87**: 1-37.
Tajima, S. and S. R. Pinnell (1981). "Collagen synthesis by human skin fibroblasts in culture: studies of fibroblasts explanted from papillary and reticular dermis." J Invest Dermatol **77**(5): 410-2.
Takahashi, K., K. Okita, et al. (2007). "Induction of pluripotent stem cells from fibroblast cultures." Nat Protoc **2**(12): 3081-9.
Talbot, N. C., W. O. Sparks, et al. (2012). "Quantitative and semiquantitative immunoassay of growth factors and cytokines in the conditioned medium of STO and CF-1 mouse feeder cells." In Vitro Cell Dev Biol Anim **48**(1): 1-11.

Tamura, K., B. Hua, et al. (2005). "Stress response gene ATF3 is a target of c-myc in serum-induced cell proliferation." EMBO J **24**(14): 2590-601.
Tao, H., R. Rao, et al. (2005). "Cytokine-induced stable neuronal differentiation of human bone marrow mesenchymal stem cells in a serum/feeder cell-free condition." Dev Growth Differ **47**(6): 423-33.
Tashiro, K., G. C. Sephel, et al. (1991). "The RGD containing site of the mouse laminin A chain is active for cell attachment, spreading, migration and neurite outgrowth." J Cell Physiol **146**(3): 451-9.
Taubenberger, A. V., M. A. Woodruff, et al. (2010). "The effect of unlocking RGD-motifs in collagen I on pre-osteoblast adhesion and differentiation." Biomaterials **31**(10): 2827-35.
Thomas, G., A. Clayton, et al. (2003). "Structural and functional changes in heparan sulfate proteoglycan expression associated with the myofibroblastic phenotype." Am J Pathol **162**(3): 977-89.
Thompson, S. M., M. G. Connell, et al. (2011). "Structure and epitope distribution of heparan sulfate is disrupted in experimental lung hypoplasia: a glycobiological epigenetic cause for malformation?" BMC Dev Biol **11**: 38.
Thomson, J. A., J. Itskovitz-Eldor, et al. (1998). "Embryonic stem cell lines derived from human blastocysts." Science **282**(5391): 1145-7.
Tian, W. M., S. P. Hou, et al. (2005). "Hyaluronic acid-poly-D-lysine-based three-dimensional hydrogel for traumatic brain injury." Tissue Eng **11**(3-4): 513-25.
Timpl, R. and J. C. Brown (1996). "Supramolecular assembly of basement membranes." Bioessays **18**(2): 123-32.
Timpl, R., S. Fujiwara, et al. (1984). "Laminin, proteoglycan, nidogen and collagen IV: structural models and molecular interactions." Ciba Found Symp **108**: 25-43.
Tollefsen, D. M. "Vascular dermatan sulfate and heparin cofactor II." Prog Mol Biol Transl Sci **93**: 351-72.
Tomasek, J. J., E. D. Hay, et al. (1982). "Collagen modulates cell shape and cytoskeleton of embryonic corneal and fibroma fibroblasts: distribution of actin, alpha-actinin, and myosin." Dev Biol **92**(1): 107-22.
Tomasi, T. B., Jr. (1977). "Structure and function of alpha-fetoprotein." Annu Rev Med **28**: 453-65.
Torres, J., J. Prieto, et al. "Efficient differentiation of embryonic stem cells into mesodermal precursors by BMP, retinoic acid and Notch signalling." PLoS One **7**(4): e36405.
Tosatti, S., Z. Schwartz, et al. (2004). "RGD-containing peptide GCRGYGRGDSPG reduces enhancement of osteoblast differentiation by poly(L-lysine)-graft-poly(ethylene glycol)-coated titanium surfaces." J Biomed Mater Res A **68**(3): 458-72.
Toyoda, H., A. Kinoshita-Toyoda, et al. (2000). "Structural analysis of glycosaminoglycans in Drosophila and Caenorhabditis elegans and demonstration that tout-velu, a Drosophila gene related to EXT tumor suppressors, affects heparan sulfate in vivo." J Biol Chem **275**(4): 2269-75.
Trowbridge, J. M. and R. L. Gallo (2002). "Dermatan sulfate: new functions from an old glycosaminoglycan." Glycobiology **12**(9): 117R-25R.
Trowbridge, J. M., J. A. Rudisill, et al. (2002). "Dermatan sulfate binds and potentiates activity of keratinocyte growth factor (FGF-7)." J Biol Chem **277**(45): 42815-20.
Tumova, S., A. Woods, et al. (2000). "Heparan sulfate proteoglycans on the cell surface: versatile coordinators of cellular functions." Int J Biochem Cell Biol **32**(3): 269-88.
Turkson, J., D. Ryan, et al. (2001). "Phosphotyrosyl peptides block Stat3-mediated DNA binding activity, gene regulation, and cell transformation." J Biol Chem **276**(48): 45443-55.
Turnbull, J., A. Powell, et al. (2001). "Heparan sulfate: decoding a dynamic multifunctional cell regulator." Trends Cell Biol **11**(2): 75-82.
Turnbull, J. E. and J. T. Gallagher (1991). "Sequence analysis of heparan sulphate indicates defined location of N-sulphated glucosamine and iduronate 2-sulphate residues proximal to the protein-linkage region." Biochem J **277 (Pt 2)**: 297-303.
Tweden, K. S., H. Harasaki, et al. (1995). "Accelerated healing of cardiovascular textiles promoted by an RGD peptide." J Heart Valve Dis **4 Suppl 1**: S90-7.

Tzu, J. and M. P. Marinkovich (2008). "Bridging structure with function: structural, regulatory, and developmental role of laminins." Int J Biochem Cell Biol **40**(2): 199-214.
Uematsu, K., K. Hattori, et al. (2005). "Cartilage regeneration using mesenchymal stem cells and a three-dimensional poly-lactic-glycolic acid (PLGA) scaffold." Biomaterials **26**(20): 4273-9.
Uhlman, D. L., D. L. Mooradian, et al. (1990). "The effect of transforming growth factor-beta 1 on glycosaminoglycan production by human marrow cultures." Exp Hematol **18**(10): 1121-5.
Urbano, J. M., C. N. Torgler, et al. (2009). "Drosophila laminins act as key regulators of basement membrane assembly and morphogenesis." Development **136**(24): 4165-76.
Urist, M. R. (1965). "Bone: formation by autoinduction." Science **150**(3698): 893-9.
Uygun, B. E., S. E. Stojsih, et al. (2009). "Effects of immobilized glycosaminoglycans on the proliferation and differentiation of mesenchymal stem cells." Tissue Eng Part A **15**(11): 3499-512.
van den Born, J., K. Salmivirta, et al. (2005). "Novel heparan sulfate structures revealed by monoclonal antibodies." J Biol Chem **280**(21): 20516-23.
Van Hoof, D., A. J. Heck, et al. (2008). "Proteomics and human embryonic stem cells." Stem Cell Res **1**(3): 169-82.
van Kooten, T. G. and A. F. von Recum (1999). "Cell adhesion to textured silicone surfaces: the influence of time of adhesion and texture on focal contact and fibronectin fibril formation." Tissue Eng **5**(3): 223-40.
VandeVondele, S., J. Voros, et al. (2003). "RGD-grafted poly-L-lysine-graft-(polyethylene glycol) copolymers block non-specific protein adsorption while promoting cell adhesion." Biotechnol Bioeng **82**(7): 784-90.
Veikkola, T., M. Karkkainen, et al. (2000). "Regulation of angiogenesis via vascular endothelial growth factor receptors." Cancer Res **60**(2): 203-12.
Viviano, B. L., S. Paine-Saunders, et al. (2004). "Domain-specific modification of heparan sulfate by Qsulf1 modulates the binding of the bone morphogenetic protein antagonist Noggin." J Biol Chem **279**(7): 5604-11.
Vlodavsky, I., O. Goldshmidt, et al. (2002). "Mammalian heparanase: involvement in cancer metastasis, angiogenesis and normal development." Semin Cancer Biol **12**(2): 121-9.
Vlodavsky, I., N. Ilan, et al. (2007). "Heparanase: structure, biological functions, and inhibition by heparin-derived mimetics of heparan sulfate." Curr Pharm Des **13**(20): 2057-73.
Vongchan, P., M. Warda, et al. (2005). "Structural characterization of human liver heparan sulfate." Biochim Biophys Acta **1721**(1-3): 1-8.
Walther, C. and P. Gruss (1991). "Pax-6, a murine paired box gene, is expressed in the developing CNS." Development **113**(4): 1435-49.
Walther, C., J. L. Guenet, et al. (1991). "Pax: a murine multigene family of paired box-containing genes." Genomics **11**(2): 424-34.
Wang, S., X. Ai, et al. (2004). "QSulf1, a heparan sulfate 6-O-endosulfatase, inhibits fibroblast growth factor signaling in mesoderm induction and angiogenesis." Proc Natl Acad Sci U S A **101**(14): 4833-8.
Wang, W., N. Ma, et al. "The influence of polymer scaffolds on cellular behaviour of bone marrow derived human mesenchymal stem cells." Clin Hemorheol Microcirc.
Wang, Y., J. L. Smedberg, et al. (2011). "Ectopic expression of GATA6 bypasses requirement for Grb2 in primitive endoderm formation." Dev Dyn **240**(3): 566-76.
Wang, Y. X., J. L. Robertson, et al. (2004). "Effects of the chemical structure and the surface properties of polymeric biomaterials on their biocompatibility." Pharm Res **21**(8): 1362-73.
Ward, G. M., P. L. Knox, et al. (1977). "Beef production options and requirements for fossil fuel." Science **198**(4314): 265-71.
Warda, M., W. Mao, et al. (2003). "Turkey intestine as a commercial source of heparin? Comparative structural studies of intestinal avian and mammalian glycosaminoglycans." Comp Biochem Physiol B Biochem Mol Biol **134**(1): 189-97.
Warda, M., T. Toida, et al. (2006). "Isolation and characterization of heparan sulfate from various murine tissues." Glycoconj J **23**(7-8): 555-63.
Wells, J. M. and D. A. Melton (1999). "Vertebrate endoderm development." Annu Rev Cell Dev Biol **15**: 393-410.

Westphal, V., S. Murch, et al. (2000). "Reduced heparan sulfate accumulation in enterocytes contributes to protein-losing enteropathy in a congenital disorder of glycosylation." Am J Pathol **157**(6): 1917-25.
Wheeler, J. C., J. A. Woods, et al. (1996). "Evolution of hydrogel polymers as contact lenses, surface coatings, dressings, and drug delivery systems." J Long Term Eff Med Implants **6**(3-4): 207-17.
Whitelock, J. M. and R. V. Iozzo (2005). "Heparan sulfate: a complex polymer charged with biological activity." Chem Rev **105**(7): 2745-64.
Wilder, P. J., D. Kelly, et al. (1997). "Inactivation of the FGF-4 gene in embryonic stem cells alters the growth and/or the survival of their early differentiated progeny." Dev Biol **192**(2): 614-29.
Wiles, M. V. and B. M. Johansson (1999). "Embryonic stem cell development in a chemically defined medium." Exp Cell Res **247**(1): 241-8.
Wilkinson, D. G., S. Bhatt, et al. (1990). "Expression pattern of the mouse T gene and its role in mesoderm formation." Nature **343**(6259): 657-9.
Williams, D. (2003). "Revisiting the definition of biocompatibility." Med Device Technol **14**(8): 10-3.
Williams, K. J. and I. V. Fuki (1997). "Cell-surface heparan sulfate proteoglycans: dynamic molecules mediating ligand catabolism." Curr Opin Lipidol **8**(5): 253-62.
Williams, R. L., D. J. Hilton, et al. (1988). "Myeloid leukaemia inhibitory factor maintains the developmental potential of embryonic stem cells." Nature **336**(6200): 684-7.
Wilm, B., R. G. James, et al. (2004). "The forkhead genes, Foxc1 and Foxc2, regulate paraxial versus intermediate mesoderm cell fate." Dev Biol **271**(1): 176-89.
Winnier, G., M. Blessing, et al. (1995). "Bone morphogenetic protein-4 is required for mesoderm formation and patterning in the mouse." Genes Dev **9**(17): 2105-16.
Wischerhoff, E., K. Uhlig, et al. (2008). "Controlled cell adhesion on PEG-based switchable surfaces." Angew Chem Int Ed Engl **47**(30): 5666-8.
Wojtowicz, A. M., A. Shekaran, et al. (2010). "Coating of biomaterial scaffolds with the collagen-mimetic peptide GFOGER for bone defect repair." Biomaterials **31**(9): 2574-82.
Wu, Z. L., L. Zhang, et al. (2003). "The involvement of heparan sulfate (HS) in FGF1/HS/FGFR1 signaling complex." J Biol Chem **278**(19): 17121-9.
Xu, D., D. Song, et al. (2007). "Mutational study of heparan sulfate 2-O-sulfotransferase and chondroitin sulfate 2-O-sulfotransferase." J Biol Chem **282**(11): 8356-67.
Xu, J., S. B. Lim, et al. (2012). "ZO-1 Regulates Erk, Smad1/5/8, Smad2, and RhoA Activities to Modulate Self-Renewal and Differentiation of Mouse Embryonic Stem Cells." Stem Cells **30**(9): 1885-900.
Xu, J., P. W. Park, et al. (2005). "Endogenous attenuation of allergic lung inflammation by syndecan-1." J Immunol **174**(9): 5758-65.
Yamaguchi, S., H. Kimura, et al. (2005). "Nanog expression in mouse germ cell development." Gene Expr Patterns **5**(5): 639-46.
Yamanaka, K., N. Kito, et al. (2010). "Mechanism of epsilon-poly-L-lysine production and accumulation revealed by identification and analysis of an epsilon-poly-L-lysine-degrading enzyme." Appl Environ Microbiol **76**(17): 5669-75.
Yamanaka, S. and K. Takahashi (2006). "[Induction of pluripotent stem cells from mouse fibroblast cultures]." Tanpakushitsu Kakusan Koso **51**(15): 2346-51.
Yamane, T., S. J. Dylla, et al. (2005). "Enforced Bcl-2 expression overrides serum and feeder cell requirements for mouse embryonic stem cell self-renewal." Proc Natl Acad Sci U S A **102**(9): 3312-7.
Yan, G., Y. Fukabori, et al. (1993). "Exon switching and activation of stromal and embryonic fibroblast growth factor (FGF)-FGF receptor genes in prostate epithelial cells accompany stromal independence and malignancy." Mol Cell Biol **13**(8): 4513-22.
Yang, G. L., F. M. He, et al. (2009). "In vivo evaluation of bone-bonding ability of RGD-coated porous implant using layer-by-layer electrostatic self-assembly." J Biomed Mater Res A **90**(1): 175-85.
Yang, J. J., Y. M. Chen, et al. (2010). "Spontaneous redifferentiation of dedifferentiated human articular chondrocytes on hydrogel surfaces." Tissue Eng Part A **16**(8): 2529-40.

Yang, X., C. Li, et al. (1998). "The tumor suppressor SMAD4/DPC4 is essential for epiblast proliferation and mesoderm induction in mice." Proc Natl Acad Sci U S A **95**(7): 3667-72.
Yang, Y., S. Y. Zhang, et al. (2001). "Glomerular extracellular matrix and growth factors in diffuse mesangial sclerosis." Pediatr Nephrol **16**(5): 429-38.
Yasuda, S. Y., N. Tsuneyoshi, et al. (2006). "NANOG maintains self-renewal of primate ES cells in the absence of a feeder layer." Genes Cells **11**(9): 1115-23.
Yates, E. A., S. E. Guimond, et al. (2004). "Highly diverse heparan sulfate analogue libraries: providing access to expanded areas of sequence space for bioactivity screening." J Med Chem **47**(1): 277-80.
Ying, Q. L., J. Nichols, et al. (2003). "BMP induction of Id proteins suppresses differentiation and sustains embryonic stem cell self-renewal in collaboration with STAT3." Cell **115**(3): 281-92.
Ying, Q. L., J. Wray, et al. (2008). "The ground state of embryonic stem cell self-renewal." Nature **453**(7194): 519-23.
Ying, Y. and G. Q. Zhao (2001). "Cooperation of endoderm-derived BMP2 and extraembryonic ectoderm-derived BMP4 in primordial germ cell generation in the mouse." Dev Biol **232**(2): 484-92.
Yu, H., Y. Huang, et al. (2010). "Synthesis and characterization of novel antimicrobial emulsifiers from epsilon-polylysine." J Agric Food Chem **58**(2): 1290-5.
Yu, J., M. A. Vodyanik, et al. (2007). "Induced pluripotent stem cell lines derived from human somatic cells." Science **318**(5858): 1917-20.
Yuan, H., N. Corbi, et al. (1995). "Developmental-specific activity of the FGF-4 enhancer requires the synergistic action of Sox2 and Oct-3." Genes Dev **9**(21): 2635-45.
Yue, X., X. Li, et al. (2008). "Transforming growth factor-beta1 induces heparan sulfate 6-O-endosulfatase 1 expression in vitro and in vivo." J Biol Chem **283**(29): 20397-407.
Yurchenco, P. D., Y. S. Cheng, et al. (1990). "Heparin modulation of laminin polymerization." J Biol Chem **265**(7): 3981-91.
Yurchenco, P. D., Y. Quan, et al. (1997). "The alpha chain of laminin-1 is independently secreted and drives secretion of its beta- and gamma-chain partners." Proc Natl Acad Sci U S A **94**(19): 10189-94.
Yurchenco, P. D., E. C. Tsilibary, et al. (1986). "Models for the self-assembly of basement membrane." J Histochem Cytochem **34**(1): 93-102.
Zakany, J., K. Burg, et al. (1984). "Spontaneous differentiation in the colonies of a nullipotent embryonal carcinoma cell line (F9)." Differentiation **27**(2): 146-51.
Zeng, X., T. Miura, et al. (2004). "Properties of pluripotent human embryonic stem cells BG01 and BG02." Stem Cells **22**(3): 292-312.
Zhang, F., Z. Zhang, et al. (2009). "Compositional analysis of heparin/heparan sulfate interacting with fibroblast growth factor.fibroblast growth factor receptor complexes." Biochemistry **48**(35): 8379-86.
Zhang, H. and A. Bradley (1996). "Mice deficient for BMP2 are nonviable and have defects in amnion/chorion and cardiac development." Development **122**(10): 2977-86.
Zhang, J., A. Skardal, et al. (2008). "Engineered extracellular matrices with cleavable crosslinkers for cell expansion and easy cell recovery." Biomaterials **29**(34): 4521-31.
Zhang, L. (2010). "Glycosaminoglycan (GAG) biosynthesis and GAG-binding proteins." Prog Mol Biol Transl Sci **93**: 1-17.
Zhang, W., S. Duan, et al. "Converted neural cells: induced to a cure?" Protein Cell **3**(2): 91-7.
Zhang, Y., X. Feng, et al. (2011). "[Biosynthesis of epsilon-poly-L-lysine--a review]." Wei Sheng Wu Xue Bao **51**(10): 1291-6.
Zhang, Y., Z. Zhang, et al. (2009). "Solution-processed microwires of phthalocyanine copper(II) derivative with excellent conductivity." Langmuir **25**(11): 6045-8.
Zhou, C., P. Li, et al. (2011). "A photopolymerized antimicrobial hydrogel coating derived from epsilon-poly-L-lysine." Biomaterials **32**(11): 2704-12.
Zhou, J., D. A. Khodakov, et al. "Surface modification for PDMS-based microfluidic devices." Electrophoresis **33**(1): 89-104.
Zimmerman, L. B., J. M. De Jesus-Escobar, et al. (1996). "The Spemann organizer signal noggin binds and inactivates bone morphogenetic protein 4." Cell **86**(4): 599-606.

Zon, L. I., C. Mather, et al. (1991). "Expression of GATA-binding proteins during embryonic development in Xenopus laevis." Proc Natl Acad Sci U S A **88**(23): 10642-6.

Appendices

Appendix I

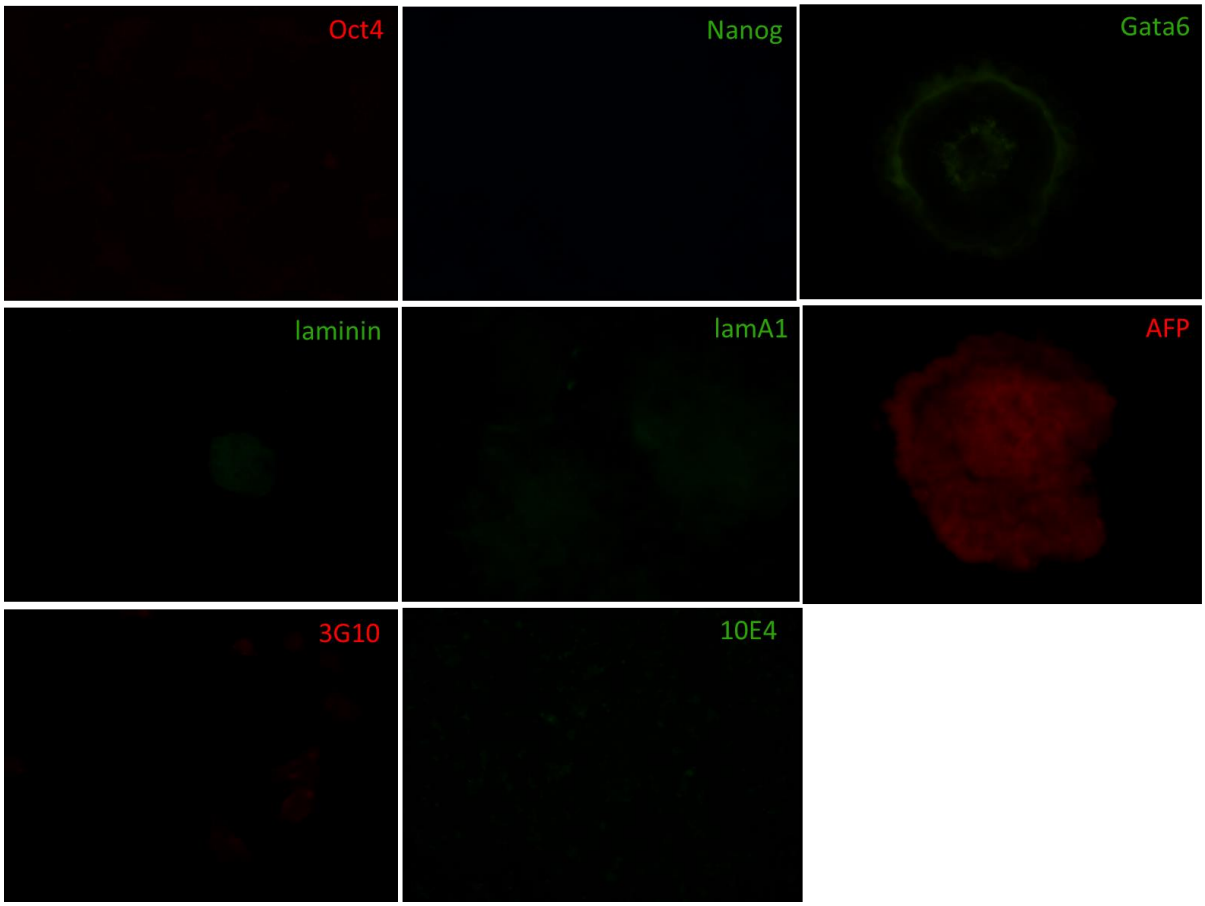

Figure A1. Negative controls for all antibodies used throughout this project. Primary antibody controls for Oct4, Nanog, Gata6, laminin, LamA1, AFP, 3G10 and 10E4.

Appendix II

Table A1. Details of primers used throughout this project for RT-qPCR

Gene		*Primer Sequence*	*Amplicon size (bp)*	*Temp C/cycle number*	*Source*
Pluripotency					
Oct4	F	5'TGGAGACTTTGCAGCCTGAG3'	188	56/33	
	R	5 CTTCAGCAGCTTGGCAAACTG3'			
Endoderm					
GATA6	F	5'CAAGATGAATGGCCTCAGCAG3'		64/33	
	R	5'TGGTGGTGGTGTGACAGTTGG3'			
AFP	F	5'ACATGAGTGTCTGCTGGCAC3'	461	63/33	
	R	5'AGCGAGTTTCCTTGGCAACAC3'			
Mesoderm					
Bry	F	5'CATCGGAACAGCTCTCCAACCTAT3'			
	R	5'GTGGGCTGGCGTTATGACTCA3'			
Foxc1	F	5'TCAGAGCGGAAATTGTAGGA3'	226	58/33	
	R	5'GTATTTGTTCATGTGCCAACTC3'			
Tbx6	F	5'GCCTCCTTCCGATTTCCT3'	141	62/33	
	R	5'CATCCCGCTCCCTCTTAC3'			
Ectoderm					
Pax6	F	5'GAGAAGAGAAGAGAAATGAGGAAGGAGA3'	201	63/33	
	R	5'ATGGGTTGGCAAAGCACTGTACG3'			
Basement membrane					
Lam-111	F				
	R				
LamA1	F				
	R				
LamB1	F				
	R				
HS biosynthetic enzymes					
EXT1	F				
	R				
EXT2	F				
	R				
NDST1	F				
	R				
Sulf1	F				
	R				
Sulf2	F				
	R				
Reference					
GAPDH	F	5'TGAAGCAGGCATCTGAGGG3'	102	56/33	
	R	5'CGAAGGTGGAAGAGTGGGAG3'			